

Trifluoromethyl ketones: Potential insecticides towards *Anopheles gambiae*

Eugene Camerino

Thesis submitted to the faculty of the Virginia Polytechnic Institute and State University in
partial fulfillment of the requirements for the degree of

Master of Science

In

Chemistry

Paul R. Carlier, (Chairman)

David G. I. Kingston

Webster L. Santos

December 10th 2012

Blacksburg, VA

Keywords: acetylcholinesterase inhibitors, acetylcholine, transition-state analogues,
trifluoromethyl ketones, insecticides, mosquitocides

Copyright Eugene Camerino

Trifluoromethyl ketones: Potential insecticides towards *Anopheles gambiae*

Eugene Camerino

ABSTRACT

Malaria continues to cause significant mortality in sub-Saharan Africa and elsewhere, and existing vector control measures are being threatened by growing resistance to pyrethroid insecticides. With the goal of developing new human-safe, resistance-breaking insecticides we have explored several classes of acetylcholinesterase inhibitors. In vitro assay studies have shown that trifluoromethyl ketones (TFK's) are potent inhibitors of *An. gambiae* AChE (AgAChE), that inhibit the enzyme by making a covalent adduct with the catalytic serine of the enzyme. However research in the Carlier group has shown that trifluoromethyl ketones bearing benzene and pyrazole cores have shown very little toxicity to *An. gambiae*, perhaps due to hydration and rapid clearance.

Focus was directed towards synthesis of oximes, oxime ethers, and hydrazones as potential prodrugs to prevent immediate hydration and reach the central nervous system. The synthesis of various oximes, oxime ethers, and hydrazones has been shown to give compounds toxic to *Anopheles gambiae* within 3- to 4- fold of the toxicity of propoxur. However, thus far we have not been able to link the toxicity of these compounds to a cholinergic mechanism. Pre-incubation studies suggest that significant hydrolysis of these compounds to TFKs does not occur or 22 h at pH 7.7 or 5.5.

Future work will be directed towards TFKs that have better pharmacokinetic properties. Work will also be directed at synthesis of oxime and hydrazone TFK isosteres to determine the mechanism of action of these compounds.

Acknowledgements

I would like to start by expressing my utmost gratitude to my adviser Dr. Paul R. Carlier. Throughout this entire process, he has been my role model. He has been extremely patient with me throughout this entire process. There were times that seemed difficult and sometimes impossible but his perseverance never wavered. His knowledge about science is something of which I admired and wish to mimic. Without his guidance, I do not think that I would have gotten as far as I would have. I also appreciate his inquisitive nature about my project. I am now able to appreciate why he asked questions about every aspect of my project and because of that it has made me more knowledgeable. I would also like to thank the members of my advisory committee, Dr. Santos and Dr. Kingston, for the knowledge and experiences that they imparted to me during this journey.

I would like to thank my colleagues in the Carlier group, Dr. Dawn Wong, Dr. Ming Ma, Dr. Josh Hartsel, Dr. Qiao Hong Chen, Dr. Ming Gao, Dr. Derek Craft, Ms. Astha, Ms. Stephanie Antolak, and Ms. Rachel Davis, for all the help that they offered to me these past 3 years. I would like to acknowledge all the help that Dr. Dawn Wong gave to me with the assay studies that she performed which was pivotal in understanding the project. Also, many thanks for the discussions with Ms. Astha about synthesis and an understanding of the medicinal chemistry aspects of my project.

I would also like to thank my parents, Arturo and Carmina Mateo, for raising me with the passion to be successful in life. Without the lessons that they taught me, I know that I would not be the person that I am today. My good friends also kept me sane throughout these past few years, and for that I thank them. I would lastly like to thank my girlfriend Emily for pushing me throughout this semester. She drove me to better myself and to write this thesis when times were tough.

Dedication

To my father Arturo and mother Carmina for always telling me to reach for the stars and to dream big.

Table of contents

Chapter 1: Malaria and Utilizing Acetylcholinesterase as an Insecticidal Target.....	1
1.1 Introduction	1
1.2 Malaria.....	1
1.2.2 Malaria control.....	1
1.3 Acetylcholinesterase and Alzheimer’s disease.....	3
1.3.1 Alzheimer’s disease.....	4
1.3.1.1 Acetylcholine.....	5
1.3.2 Acetylcholinesterase.....	5
1.3.3 Inhibitors of acetylcholinesterase.....	7
1.3.4 How acetylcholinesterase inhibitors bind.....	7
1.3.5 AChE inhibitors used in the treatment of Alzheimer’s disease.....	7
1.3.5.1 Basic Amines.....	7
1.3.5.2 Carbamates.....	8
1.3.5.3 Trifluoromethyl ketones (TFKs).....	9
1.3.6 Inhibitors of AChE used as insecticides.....	11
1.3.6.1 Insecticides-Carbamates.....	11
1.3.6.2 Insecticides-Organophosphates.....	12
1.3.6.3 Insecticides-Basic Amines.....	13
1.3.6.4 Insecticides-Trifluoromethyl Ketones (TFKs).....	14
1.4 References for Chapter 1.....	16
Chapter 2: The pharmacology and toxicology of potential trifluoromethyl ketone insecticides.....	21
2.1 Design and synthesis of TFKs.....	21
2.1.1 Synthesis of Inhibitors.....	22
2.1.2 In vitro assays	24
2.1.3 Mosquito toxicity assay.....	28
2.2 Design, synthesis and discussion of prodrug of TFKs.....	31
2.2.1 Structure design of prodrugs.....	31
2.2.2 Synthesis of prodrugs.....	32
2.2.3 Toxicology evaluation of prodrugs.....	37
2.2.4 In vitro assay results.....	40
2.3 Future Work.....	42
2.4 References for Chapter 2.....	46
Chapter 3: Experimental.....	48
3.1 General.....	48
3.2 Procedures.....	48
3.3 Enzyme assay and determination of IC ₅₀ values.....	79
3.4 Mosquito toxicity assay.....	80
3.5 References for Chapter 3.....	81
Appendix.....	82

List of Schemes

Scheme 1-1: In the case of the carbamate, the active serine readily binds to the carbamate but its slow to dissociate from serine.....	9
Scheme 1-2: While organophosphates can competitively inhibit AChE, the loss of an alkyl group through “aging” results in an inactivation of AChE.....	12
Scheme 1-3: While reactive, the TFK can be attacked by two nucleophiles.....	15
Scheme 2-1: Synthesis of the TFKs with different ring cores	24
Scheme 2-2: The Ellman assay test used to determine AChE activity using ATCh and DTNB.....	25
Scheme 2-3: In the body, TFKs can undergo hydration from water to form the geminal diol.....	31
Scheme 2-4: The proposed scheme of the prodrugs.....	41
Scheme 2-5: All oxime derivatives appeared to be a single diastereomer by ¹ H and ¹⁹ F NMR spectroscopy unless noted.....	42
Scheme 2-6: All oxime derivatives appeared to be a single diastereomer by ¹ H and ¹⁹ F NMR spectroscopy unless noted	43
Scheme 2-7: Synthesis of 2-4a with the corresponding hydrazines.....	44
Scheme 2-8: Synthesis of 2-5c-f with the corresponding hydrazines.....	45
Scheme 2-9: Proposed scheme for the synthesis of oxime and hydrazones.....	53

List of Figures

Figure 1-1: Compounds that are used to minimize human/ mosquito interaction; permethrin, deltamethrin, DDT and DEET.....	3
Figure 1-2: Drugs that are FDA approved for Alzheimer’s whose method of action is based on the cholinergic hypothesis.....	4
Figure 1-3: Acetylcholine, a neurotransmitter in the CNS.....	5
Figure 1-4: A collection of amino acids consisting of glutamate, histidine, and serine are responsible of AChE binding to ACh.....	6
Figure 1-5: Tacrine, a well-known inhibitor of AChE.....	8
Figure 1-6: As the TFK is attacked, the resulting intermediate is stabilized in the oxyanion pocket by hydrogen bonding.....	10
Figure 1-7: Examples of TFKs that inhibit AChE.....	10
Figure 1-8: Examples of carbamate insecticides.....	12
Figure 1-9: OPs that have been used as commercial pesticides.....	13
Figure 2-1: Our optimized compounds for our study along with the lead TFK (2-1) that demonstrated potency towards AChE.....	21
Figure 2-2: Representation of the <i>Tc</i> AChE/ 2-1 complex (RCSB ID: 1HBJ)	21
Figure 2-3: An inhibition response curve of 2-4a with <i>h</i> AChE (in blue) and WT AChE (in black).....	25
Figure 2-4: Two compounds that contain the hydrazone functional group.....	45

List of Tables

Table 2-1: IC₅₀ values of different TFKs with the corresponding type of AChE.....27

Table 2-2: Mosquito values with phenyl and pyrazole core TFKs.....30

Table 2-3: Toxicity studies results on the carious oximes (**2-5** through **2-7**) via tarsal contact toxicity.....38

Table 2-4: Toxicity results via tarsal contact assay for various hydrazones that were synthesized39

Table 2-5: Compounds of interest, **2-6e**, **2-11a**, and **2-12a**, were compared to propoxur for toxicity.....40

Table 2-6: In vitro assays were performed on **2-6c**, an oxime.....41

Table 2-7: IC₅₀ studies were performed on **2-6c** and **2-9e** at pH 5-5 and 7-7 to determine whether hydrolysis occurs.....42

List of Abbreviations

ACh- Acetylcholine

AChE- Acetylcholinesterase

BBB- Blood-brain barrier

DDT- Dichlorodiphenyltrichloroethane

DEET- N, N-diethyl-meta-toluamide

DTNB- 5,5'-dithiobis-2-nitrobenzoate

IRS- Indoor residual spraying

ITN- Insecticide treated nets

OP- Organophosphate

OPIDN- Organophosphate induced delayed neuropathy

TFK- Trifluoromethyl ketones

Chapter 1: Malaria and Utilizing Acetylcholinesterase as an Insecticidal Target

1.1 Introduction

Malaria, an example of a vector borne disease, continues to endure as a global health issue in numerous parts of the world, commonly tropical regions.¹⁻³ According to the World Health Organization (WHO) as of 2011, malaria has killed upwards of 655,000 people annually.² Malaria primarily affects third world countries such as Africa, due to factors such as formidable climates, insecticide resistant mosquitoes, continued movement of refugees, and poor immune systems caused by impoverished conditions.¹

1.2 Malaria

Malaria is an illness caused by a parasitic protozoan carried by mosquitoes.¹ Mosquitoes are not the source of the parasite but they are the carrier of the parasite from one infected human to a non-infected human.³ Because only female mosquitoes need to blood feed, the female mosquitoes are solely responsible for transmission of the parasite.⁴ The journey for the parasite starts when it enters the mosquito during a blood meal. It then undergoes a complex life cycle where it can multiply within the mosquito.¹ When an infected mosquito bites a human during the subsequent blood meal, the parasites are released into the bloodstream in the form of sporozites.³ They then travel to the liver to multiply into merozoites. Once multiplied, they attack the host's red blood cells, at which time the infected host suffers from symptoms ranging from fever, headache, muscle pain, and vomiting. The onset of symptoms of malaria infection can range as to when they occur.⁵

1.2.1 Malaria Control

In order to reduce the spread of malaria, one of two things needs to be done. One way would be to eradicate the parasite that is responsible for the malaria disease. If that can't be done then

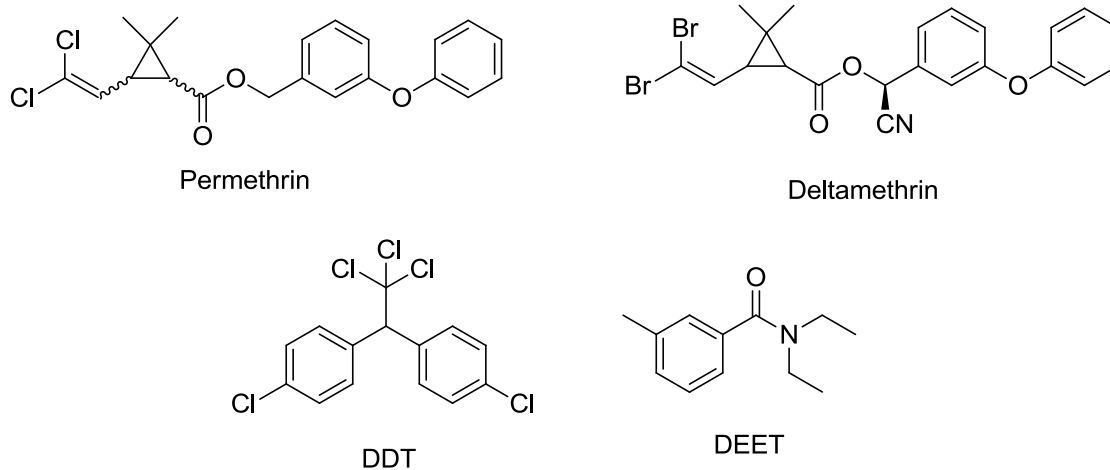
another way would be to control the vector population, which is responsible for the transmission of the disease. The main focus of this paper will be on controlling the disease from a vector perspective.

One of the ways to control the vector population was through *N, N*-diethyl-3-methylbenzamide, also known as DEET (Figure 1-1).⁶ DEET acts as a repellent to prevent mosquitoes from biting a person. The initial hypothesis was that DEET interfered with the mosquito's ability to detect lactic acid.⁷ Syed and associates challenged this idea and suggested that mosquitoes directly avoid the DEET chemical.⁷

Aside from repellents, insecticides are another means to reduce mosquito-human interaction. Pyrethroids are one class of insecticides that are effective in combating mosquitoes.⁸⁻⁹ The pyrethroids (i.e. permethrin and deltamethrin, Figure 1-1) works by tampering with the sodium gated channels, leaving them open causing an influx of sodium ions into the membrane which results in paralysis.⁹ The resulting synaptic disturbances in the mosquitoes and can ultimately lead to its death. While effective and nontoxic to humans, knockdown resistance to pyrethroids is emerging due to reduced sensitivity to these compounds.⁸⁻⁹

The most widely used insecticide prior to the 1990's was dichlorodiphenyltrichloroethane (DDT) (Figure 1-1).¹⁰ While very potent towards *Anopheles* initially and cheap to produce, emerging resistance and human toxicity effects were reported in the 1970's and 80's by Brown, Pal, and Fontaine.¹⁰ Due to the negative side effects such as genotoxicity and disruption of the endocrine system, the WHO urged other countries to stop using DDT in the early 1980's. However, this decision was reversed in 2006 when the WHO authorized the use of DDT again but only for indoor residual spraying (IRS), a method where dilute concentrations of the insecticide are sprayed on surfaces inside homes.¹⁰⁻¹¹ Insecticide treated nets (ITN) is an example of how these insecticides can be safely and effectively used to reduce malaria transmission.¹² Using both ITN and IRS in combination has proved effective in reducing malaria cases.¹²

Figure 1-1: Compounds that are used to minimize human/ mosquito interaction; permethrin, deltamethrin, DDT, and DEET.



Current methods of controlling the vector population are not as effective as they initially were due to problems such as emerging resistance with pyrethroids and environmental safety with DDT.¹⁰ One possible solution is to reinvestigate acetylcholinesterase (AChE) enzyme inhibitors that were previously used in agriculture and IRS towards vector mosquitoes. An attempt towards developing more human safe AChE inhibitors may prove beneficial towards applying these insecticides on ITN's.

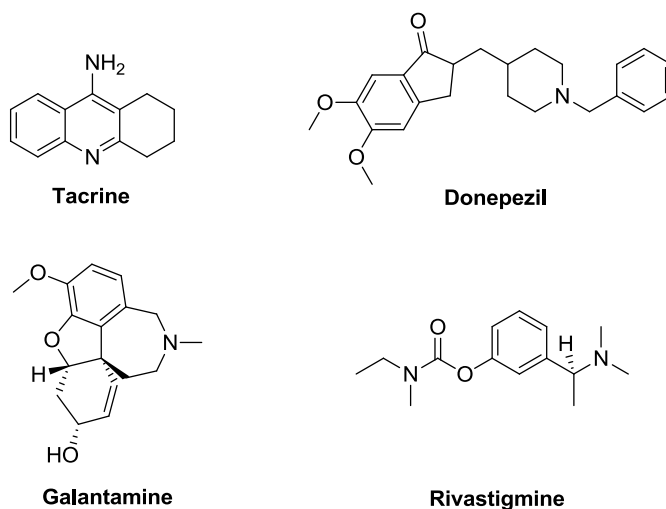
1.3 Acetylcholinesterase and Alzheimer's disease

As mentioned above, the AChE enzyme is exploited as an insecticidal target. Interestingly enough, the mechanism of action used as insecticides are also possessed by memory-enhancing drugs used to treat Alzheimer's disease.¹³ These therapeutic drugs that are used to treat Alzheimer's disease became an inspiration for the Carlier group for their use as insecticides. The transition from therapeutics to insecticides will be further discussed in detail below.

1.3.1 Alzheimer's disease

Alzheimer's disease, named after its discoverer in 1906, is characterized as a neurodegenerative disease that affects brain function.¹⁴ Diseases of this nature typically results in the death of neurons in the central nervous system.¹⁵ Alzheimer's is the leading cause of death in the elderly, only behind heart disease, cancer, and stroke.¹⁴ Due to weaker immune systems, people over the age of 50 are more susceptible to brain disorders with symptoms such as loss of or trouble recalling memory, judgment, decision making, and learning.^{14, 16-17}

Figure 1-2: Drugs that are FDA approved for Alzheimer's whose method of action is based on the cholinergic hypothesis.

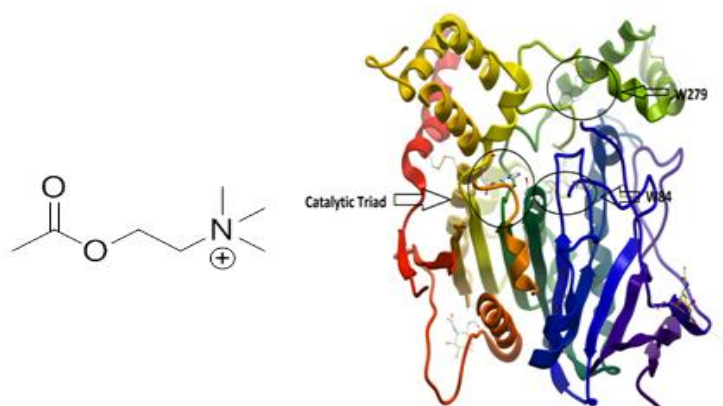


Even with the information that is currently known about Alzheimer's disease, the origin of the disease is unknown and only the symptoms can be treated at this time.^{13-14, 18} The accepted symptomatic premise for Alzheimer's is the cholinergic hypothesis, stating that the memory loss and cognitive dysfunction are linked to a deficiency of acetylcholine in the brain and central nervous system.^{13-14, 17-18} While several therapeutic strategies have been proposed, the cholinergic hypothesis underlies 4 of the 5 drugs currently approved by the FDA to treat AD (Figure 1-2).¹⁶

1.3.1.1 Acetylcholine

Acetylcholine (ACh), shown in Figure 1-3, is a neurotransmitter located throughout the central nervous system.¹⁶ The majority of acetylcholine produced in the body is stored in the basal forebrain.¹⁷ It is responsible for many functions in the body such as eye activity, brain blood flow, cerebral cortical development, sleep-wake cycle and motor functions.^{16-17, 19}

Figure 1-3: Acetylcholine, a neurotransmitter in the CNS. Acetylcholinesterase, an enzyme, has the role of hydrolyzing acetylcholine in the body. The ribbon model of *Torpedo Californica*-AChE (Tc) is shown above (PDB ID: 1EA5). The locations of the catalytic triad, and Trp in the active and peripheral site are shown. Credit for production goes to Dr. Dawn Wong.



1.3.2 Acetylcholinesterase

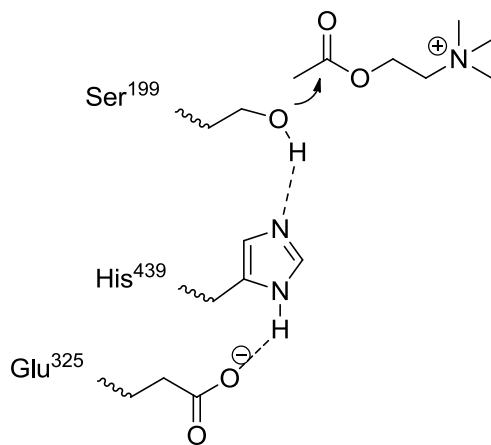
AChE is an enzyme that is predominantly responsible for the hydrolysis of the ACh neurotransmitter and for ending cholinergic transmission at synapses in the central nervous system for both humans and insects (Figure 1-3).²⁰ One suggested method to increase ACh levels was to inject the patient with ACh. While logical, that was not effective due to rapid hydrolysis and poor permeability through the blood brain barrier (BBB).²¹ One effective method in the treatment of Alzheimer's disease is to inhibit the enzyme AChE, to allow a buildup of acetylcholine according to the cholinergic hypothesis.⁶

^{13-14, 16-18, 20} The cholinergic hypothesis states that Alzheimer's disease is characterized by lowered ACh levels in the body, leading to cognitive decline.¹³ Since the first x-ray crystal structure in 1991, a better understanding of how the enzyme works has been attained.²⁰

The enzyme contains 12 beta-strands on the inside and 14 alpha helices on the outside.¹⁴ In addition, there are 4 distinct subsites that together comprise the catalytic site: the choline binding site, the catalytic triad, the oxyanion hole and the acyl pocket.²⁰ Each region, while distinct, contributes for the hydrolysis of acetylcholine. The choline binding site has a cation-pi interaction with the quaternary ammonium group keeping acetylcholine in place.

An acyl pocket in the catalytic site also keeps acetylcholine in place via hydrophobic interactions with the methyl of the acyl group. Because serine is not nucleophilic enough by itself, a charge-relay mechanism by a collection of three amino acids (catalytic triad) is needed for the nucleophilic attack by serine to ACh. When ACh is attacked, the resulting oxyanion is stabilized by hydrogen bonding by Ala²⁰⁰, Gly¹¹⁹, and Gly¹¹⁸ in what is called the oxyanion hole.

Figure 1-4: A collection of amino acids consisting of glutamate, histidine, and serine are responsible of AChE binding to ACh.



1.3.3 Inhibitors of Acetylcholinesterase

1.3.4 How acetylcholinesterase inhibitors bind

Inhibitors of AChE bind to AChE to prevent the hydrolysis of ACh.^{20, 22} Inhibitors can accomplish this through various means by binding reversibly, irreversibly, and pseudo-irreversibly to the enzyme.^{13-14, 18, 20} Inhibition of AChE should partially increase the amount of ACh in the synapse.^{14, 17}

1.3.5 AChE inhibitors used in the treatment of Alzheimer's disease

AChE inhibitors have been effective in improving cerebral blood flow in patients in the early stages of AD by vasodilation, in addition to increasing ACh levels in the body, which is part of the cholinergic –vascular hypothesis.¹⁷⁻¹⁸ In vitro studies done by Nordberg and Svenson showed that acetylcholine levels taken from an autopsy in AD patients were increased with cholinesterase inhibitors such as physostigmine and tacrine.¹³ While effective, the inhibitors can only slow the progressive symptomology of the disease, giving only mild improvements in terms of motor function and cognition.^{13, 17} They cannot stop the progression of neurodegeneration in patients with AD.¹⁴

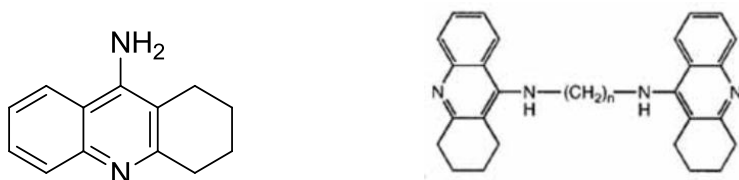
1.3.5.1 Basic Amines

One structural class of inhibitors used as AD therapeutics consists of basic amines.^{13-14, 22} These reversible inhibitors are protonated at physiological pH and bind noncovalently in the catalytic active site through an interaction with Trp⁸⁴ in the choline binding site, like that of the quaternary amine in ACh, but do not bind to the active Ser²⁰⁰ residue.²³

Tacrine, a well-known inhibitor of AChE shown in Figure 1-5, can bind to the catalytic active site through pi-pi stacking with Trp⁸⁴ in the active site or can also bind to a lesser extent to Trp²⁷⁹ of the peripheral site.²³ Tacrine unfortunately had negative side effects such as low bioavailability and hepatotoxicity.¹³⁻¹⁴ Tacrine dimers were then created to see how they fared as a new derivative. First

created by Pang, the Carlier group collaborated with Pang in which they systematically modified the tether length and peripheral site ligand.^{14, 24-25} They successfully synthesized Bis(n)-tacrine ligands where n is a varying number of methylene groups, while Bis(7)-tacrine was a potent and selective inhibitor of AChE which also exhibited low toxicity compared with the corresponding monomeric tacrine derivative (Figure 1-5).

Figure 1-5: Tacrine, a well-known inhibitor of AChE. A collaboration between Pang and Carlier groups explored potent AChE inhibitors in the form of Bis(n)-tacrines.



Galantamine, an FDA approved reversible inhibitor of AChE, also doubles as an allosteric ligand to nicotinic receptors (Figure 1-2).^{13, 22} Studies done on inhibition with galantamine show that while it is a selective inhibitor of AChE compared to butyrylcholinesterase, it may also produce therapeutic effects with diseases such as schizophrenia, major depression, bipolar disorder, and alcohol abuse.²² Studies done by Nordberg showed no liver toxicity associated with Galantamine but symptoms such as nausea, diarrhea, and cramps were reported.¹³

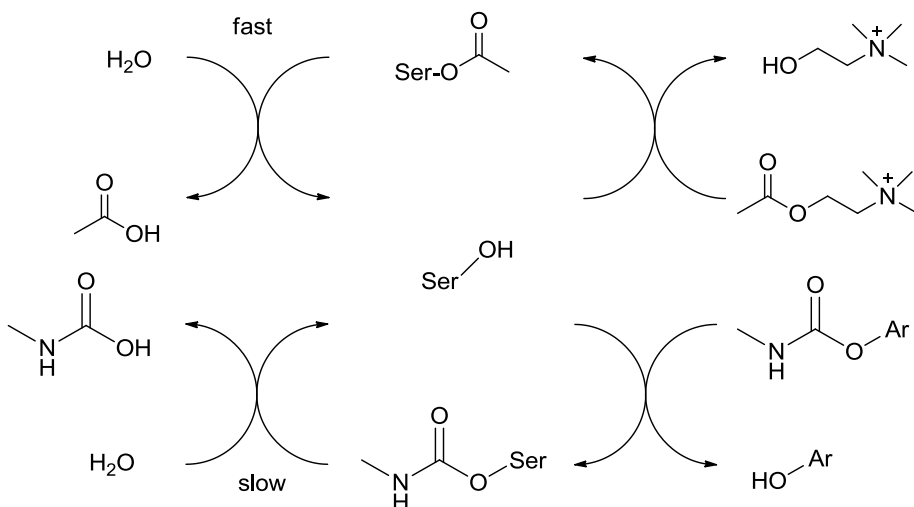
Donepezil is a piperidine based reversible inhibitor of AChE that has mixed inhibition (Figure 1-2).^{13, 26} In 1996, the FDA approved the use of Donepezil for cognitive dysfunction in AD patients.²⁶ The main side effects of it as a therapeutic were primarily nausea and vomiting.^{13, 26}

1.3.5.2 Carbamates

A substrate analogue of ACh, the carbamate group mimics the acetylcholine molecule and the Ser²⁰⁰ from AChE attacks the carbamate group in a nucleophilic fashion (Scheme 1-1).²⁷ Following reaction with ACh, the acetylated serine readily undergoes hydrolysis to regenerate the enzyme. But in

the case of the carbamoylated serine, slow hydrolysis is observed, possibly due to the reduced electrophilicity of the carbamate carbonyl.²⁷ The slow hydrolysis results in a buildup of ACh which may produce a therapeutic effect (Scheme 1-1).

Scheme 1-1: In the case of the carbamate, the active serine readily binds to the carbamate but it is slow to dissociate from serine.



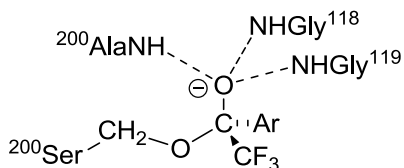
Rivastigmine has been approved by the Food and Drug Administration as an Alzheimer's therapeutic (Figure 1-2).²⁸ This carbamate is known as a dual inhibitor since it can inhibit AChE and Butylcholinesterase (BuChE).²⁸ In addition to serving as a therapeutic in AD, this carbamate is used to improve behavior and cognition in patients with Huntington's disease suffering from apathy.²⁹

1.3.5.3 Trifluoromethyl ketones (TFK's)

A less explored class of AChE inhibitors is the trifluoromethyl ketone species.³⁰ Their defining features are the three fluorines that replace the methyl group in ketones. They behave as transition state analogues, forming a tetrahedral adduct with the serine of AChE. They are reversible, potent inhibitors due to the fact that the trifluoromethyl group makes the ketone carbon more electrophilic, allowing for nucleophilic attack by the active serine in AChE. This attachment results in the formation of

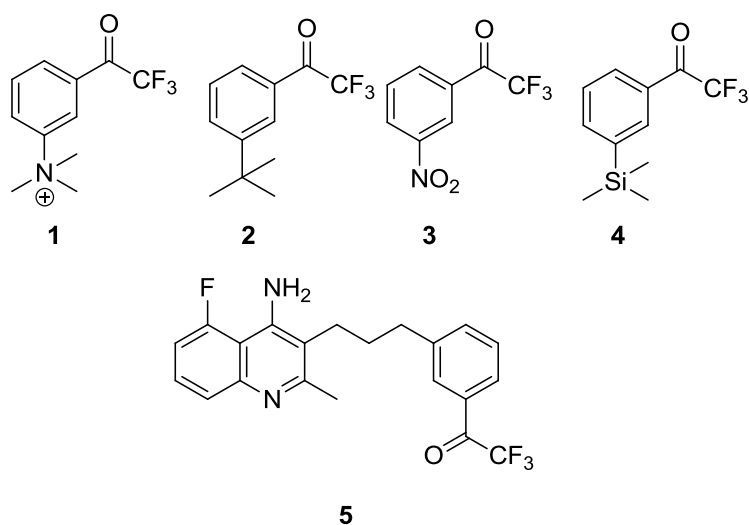
a stable, charged tetrahedral hemiketal adduct with the oxyanion being further stabilized in the oxyanion pocket (Figure 1-6).³⁰⁻³¹

Figure 1-6: As the TFK is attacked, the resulting intermediate is stabilized in the oxyanion pocket by hydrogen bonding.



Measurements done on *Torpedo californica* AChE inhibition for trimethylammonio trifluoroacetophenone, **1**, gave an IC₅₀ value of 1.3 nM (Figure 1-7).³² Hornsperger reported that because of the potent inhibition with this compound, more analogs of these compounds would be investigated as therapeutics towards AD.³⁰ Extensive research on this class of compounds as AD therapeutics was done in the 1980's but given the market success of Aricept (donepezil) and Razadyne (Galantamine), industry has apparently had little interest in developing new AChE inhibitor-based therapies.

Figure 1-7: Example of TFKs that inhibit AChE.



The TFK which attracted the most preclinical interest in the 1980's and 1990's was Zifrosilone (4), also known as MDL 73,745 (Figure 1-7).³³ In the 1990's, studies performed by Zhu via injections into rats tested the potential of AChE inhibition by Zifrosilone.³⁴ Cutler also tested whether zifrosilone was potent and the results from both scientists showed that zifrosilone was indeed a potent inhibitor of AChE. Symptomatic hypertension caused by zifrosilone may be one factor that decreased interest in zifrosilone.³⁵

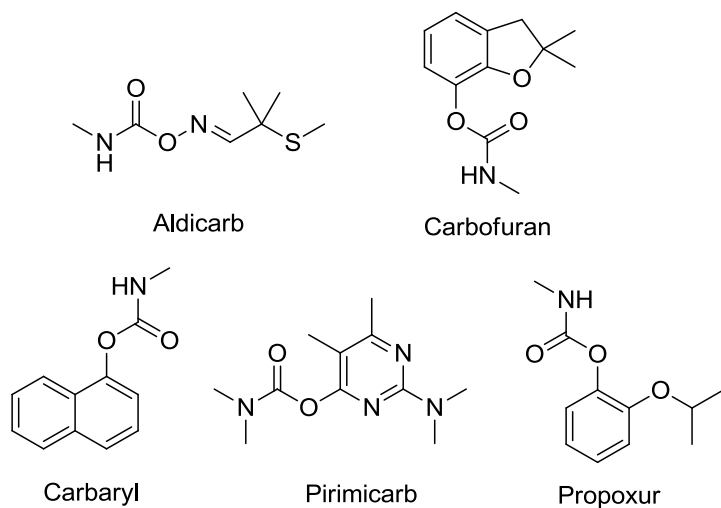
1.3.6 Inhibitors of AChE used as insecticides

Attention has been drawn towards AChE inhibitor-based insecticides for the past 50 years due to the realization that significant AChE inhibition is lethal.^{6, 20, 26} Ideally, the inhibitor used towards insecticides need to be selective towards insects to reduce human toxicity during exposure.²⁰ If such compounds could be developed, they could be deployed on insecticide-treated nets to reduce malaria transmission by *Anopheles gambiae*.^{12, 20}

1.3.6.1 Insecticides-Carbamates

Along with their use as AD therapeutics, carbamates are used as insecticides/pesticides.²⁰ These compounds include: aldicarb, carbofuran, pirimicarb, propoxur, and carbaryl (shown in Figure 1-8). Like AD therapeutics, the insecticidal carbamates inhibit AChE, but with an intent to inundate synapses with ACh, resulting in death. When used as pesticides, human toxicity becomes an issue. Research at this time is directed towards making a more species selective carbamate towards *Anopheles gambiae*. The Carlier group has successfully made derivatives of propoxur that show a 530:1 selectivity of mosquito to human AChE.³⁶

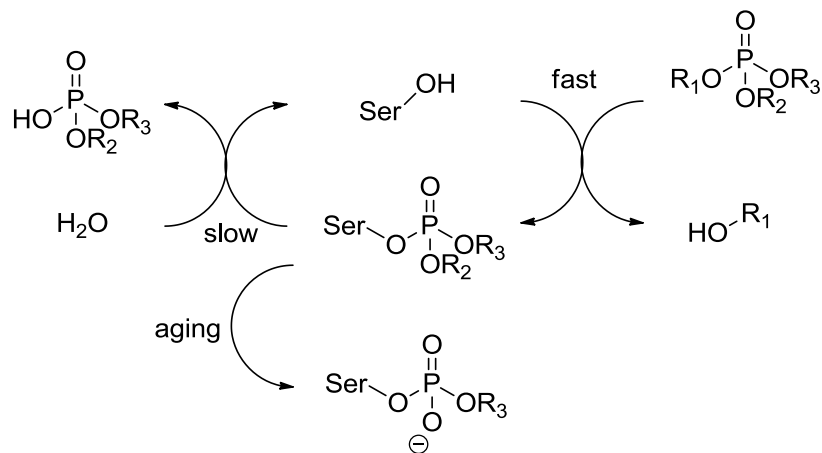
Figure 1-8: Examples of carbamate insecticides.



1.3.6.2 Insecticides- Organophosphates

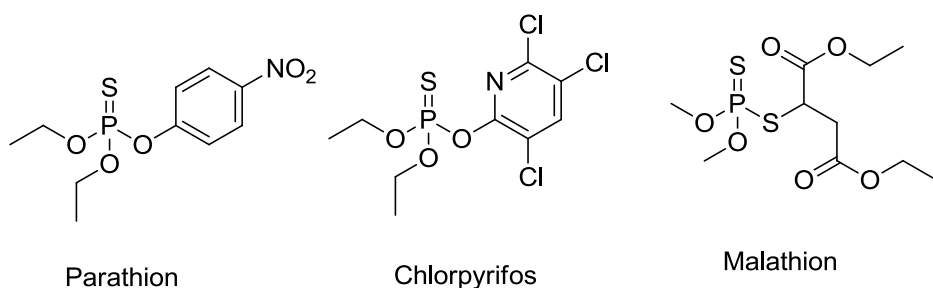
Like carbamates, organophosphates (OPs) have been reviewed as a possible candidate for pesticides. OPs share the same AChE inhibition mechanism like carbamates in which serine attacks the electrophilic phosphorus (Scheme 1-2).³⁷⁻³⁹ The rate of hydrolysis shown for organophosphates (hours to days) was slower compared to carbamates (minutes to hours).²⁶

Scheme 1-2: While organophosphates can competitively inhibit AChE, the loss of an alkyl group through "aging" results in an inactivation of AChE.



As an AD therapeutic, OP's were poor candidates due to the acute toxicity by inhibition of AChE in people.³⁸ OP's have the potential to be excellent candidates as insecticides/pesticides and some have been used in agriculture such as parathion, malathion, and chlorpyrifos (Figure 1-9). But acute toxicity in humans account for more than 50% of poisoning cases associated with pesticides with 10% of those cases resulting in death.^{26, 37, 40} Short term effects such as hyperglycemia, lacrimation, and salivation have been observed.⁴⁰⁻⁴¹ Long term exposure can have negative effects on the metabolism of carbohydrates and degradation of neurons leading to organophosphate induced delayed neuropathy (OPIDN).⁴⁰ Organs such as the pancreas, liver, and brain have been shown to be affected by OP pesticides by affecting processes like glycolysis, and gluconeogenesis and glycogenesis.⁴⁰ Long term effects are due to the irreversible binding process of aging that occurs in which the loss of an alkyl group occurs and the resulting anion deactivates AChE because of its resulting stability (Scheme 1-2).^{26, 40} These drawbacks have decreased the use of OPs as pesticides in agriculture. In addition, OP's have not been approved on ITNs but some have been used in IRS (Figure 1-9).

Figure 1-9: OPs that have been used as commercial pesticides.



1.3.6.3 Insecticides- Basic amines

As mentioned previously, basic amines like tacrine can be potent inhibitors of *hAChE*.¹³ However, collaborative research of the Carrier and Bloomquist groups have shown that even very potent basic amine inhibitors of *AgAChE* show very low contact toxicity to *Anopheles gambiae*. One potential

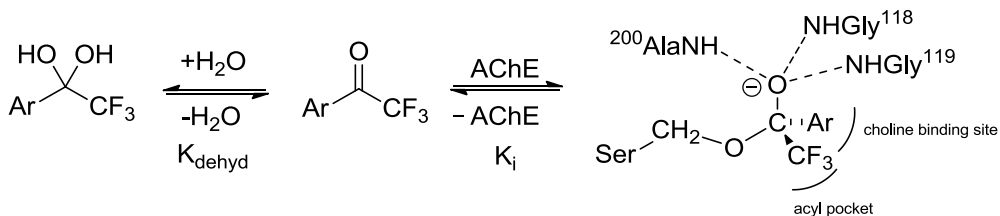
reason is that maybe the insecticide cannot pass through the mosquito's exoskeleton or cuticle. Another possible explanation may be that it can enter into the body of the mosquito, but is not able to cross the BBB. This may be attributed to the basic nature of the amines and their tendency to be in the protonated form rather than the unprotonated form. With no insecticide in the system, there is no way to inhibit AChE.

1.3.6.4 Insecticides- Trifluoromethyl Ketones (TFK's)

There is a need to develop new classes of AChE based insecticides. Basic amines lack insecticidal activity and organophosphates have the danger of causing OPIDN in humans. Currently approved carbamates have too much potency against human AChE to be safely used on ITNs. Current research in the Carrier group is directed at more human safe carbamates but a possible parallel strategy is to explore TFKs. TFKs show promise because they haven't been explored as much which allows for more open chemical space.

Being transition state analogues, compounds that favor a tetrahedral adduct make for better inhibitors due to their ability to mimic the enzyme substrate transition state.⁴² As mentioned previously, they are potent inhibitors of AChE because of increased electrophilicity at the carbonyl carbon due to the addition of fluorines (Figure 1-7).³² Other halogens were considered and while halogens affected the rate of nucleophilic attack by water, steric hindrance was believed to prevent direct interaction with the active site on AChE with other halogens other than fluorine.⁴³ With its increased electrophilicity, the ketone in vivo is in equilibrium with the geminal diol form (Scheme 1-3). The resulting geminal diol formed by attack of water is should be a poor inhibitor of AChE. The TFK's reactivity is a double edged sword because the increased electrophilicity is such a distinctive feature of these ketones.⁴⁴ But the extent of hydration is also important because it indicates how susceptible the TFK is to attack by the Ser²⁰⁰.

Scheme 1-3: While reactive, the TFK can be attacked by two nucleophiles. The normal manner would be attack by Serine to give the stabilized intermediate. Because of abundance, water can also be a source of nucleophilic attack to give a diol, a poor inhibitor of AChE. Due to the fit of the inhibitor in the binding pocket, changes with the aryl substituent should not affect K_{dehyd} and K_i identically.



At present, possible TFK insecticides lack insecticidal potential due to hurdles that must first be identified and then overcome. The hydrated form of the TFK could present pharmacokinetic problems.⁴⁴ Hypothetically in the diol form, glucuronidation could occur with the addition of UDP-glucuronic acid potentially making it more water soluble and excretion of the compound may occur faster.⁴⁵ Lipophilicity is another hurdle that must be overcome to make successful TFK's. For these drugs to be successful, as with any CNS drugs, they must pass through the BBB.⁴⁶ **1** cannot penetrate the barrier due to the positive charge on nitrogen while the other variations can potentially pass through the BBB (Figure 1-9). A balance must be made between trying to make the molecule lipophilic and small enough to penetrate the barrier, but without sacrificing potency.

A better understanding is necessary before the transition from TFKs as therapeutics to insecticides can be made. As with drug discovery, a good approach to developing insecticides is to observe what other scientists have done to see what has been done before instead of random syntheses of TFKs. The next chapter will focus on the rationale of the TFK design and evaluation of toxicity and bind of these lead compounds.

References for chapter 1:

1. Mueller, A. K., *et al.*, Invasion of mosquito salivary glands by malaria parasites: prerequisites and defense strategies. *Int. J. Parasit.* **2010**, *40*, 1229-1235.
2. World Malaria Report. *The World Health Organization* **2011**.
3. Bousema, T. B. T.; Drakeley, C., Epidemiology and infectivity of plasmodium falciparum and plasmodium vivax gametocytes in relation to malaria control and elimination. *Clin. Microbiol. Rev.* **2011**, *24*, 377.
4. Raghavendra, K., *et al.*, Malaria vector control: from past to future. *Parasitol. Res.* **2011**, *108*, 757-779.
5. NIH website. <http://www.ncbi.nlm.nih.gov/pubmedhealth/PMH0001646/> (accessed 12/10/10).
6. Corbel, V., *et al.*, Evidence for inhibition of cholinesterases in insect and mammalian nervous systems by the insect repellent deet. *BMC Biol.* **2009**, *7*, 47.
7. Syed, Z.; Leal, W. S., Mosquitoes smell and avoid the insect repellent DEET. *Proc. Natl. Acad. Sci. U. S. A.* **2008**, *105*, 13598-13603.
8. Enayati, A. A.; Hemingway, J., Pyrethroid insecticide resistance and treated bednets efficacy in malaria control. *Pestic. Biochem. Physiol.* **2006**, *84*, 116-126.
9. Soderlund, D. M., *et al.*, Mechanisms of pyrethroid neurotoxicity: implications for cumulative risk assessment. *Toxicology* **2002**, *171*, 3-59.
10. Walker, K., Cost-comparison of DDT and alternative insecticides for malaria control. *Med. Vet. Entomol.* **2000**, *14*, 345-354.
11. Palmer <http://www.who.int/mediacentre/news/releases/2006/pr50/en/> (accessed 12/10/10).
12. Okumu, F. O.; Moore, S. J., Combining indoor residual spraying and insecticide-treated nets for malaria control in Africa: a review of possible outcomes and an outline of suggestions for the future. *Malar. J.* **2011**, *10*.

13. Nordberg, A.; Svensson, A. L., Cholinesterase inhibitors in the treatment of alzheimer's disease - a comparison of tolerability and pharmacology. *Drug Saf.* **1998**, *19*, 465-480.
14. Li, W. M., *et al.*, East meets west in the search for Alzheimer's therapeutics - novel dimeric inhibitors from tacrine and huperzine a. *Curr. Alzheimer Res.* **2007**, *4*, 386-396.
15. Park, S. Y., Potential therapeutic agents against Alzheimer's disease from natural sources. *Arch. Pharm. Res.* **2010**, *33*, 1589-1609.
16. Schliebs, R.; Arendt, T., The cholinergic system in aging and neuronal degeneration. *Behav. Brain Res.* **2011**, *221*, 555-563.
17. Van Beek, A.; Claassen, J., The cerebrovascular role of the cholinergic neural system in Alzheimer's disease. *Behav. Brain Res.* **2011**, *221*, 537-542.
18. Scarpini, E., *et al.*, Treatment of Alzheimer's disease: current status and new perspectives. *Lancet Neurol.* **2003**, *2*, 539-547.
19. Hicks, D., *et al.*, Membrane targeting, shedding and protein interactions of brain acetylcholinesterase. *J. Neurochem.* **2011**, *116*, 742-746.
20. Carlier, P. R., *et al.*, Towards a species-selective acetylcholinesterase inhibitor to control the mosquito vector of malaria, *Anopheles gambiae*. *Chem.-Biol. Interact.* **2008**, *175*, 368-375.
21. Cannon, J., *Pharmacology for Chemists*. second ed.; New York, 1999; p 272.
22. Ago, Y., *et al.*, Pharmacological aspects of the acetylcholinesterase inhibitor galantamine. *J. Pharmacol. Sci.* **2011**, *116*, 6-17.
23. Rydberg, E. H., *et al.*, Complexes of alkylene-linked tacrine dimers with torpedo californica acetylcholinesterase: binding of bis(5)-tacrine produces a dramatic rearrangement in the active-site gorge. *J. Med. Chem.* **2006**, *49*, 5491-5500.

24. Pang, Y. P., *et al.*, Synthesis of alkylene linked bis-THA and alkylene linked benzyl-THA as highly potent and selective inhibitors and molecular probes of acetylcholinesterase. *J. Chem. Soc.-Perkin Trans. 1* **1997**, 171-176.
25. Du, D. M.; Carlier, P. R., Development of bivalent acetylcholinesterase inhibitors as potential therapeutic drugs for Alzheimer's disease. *Curr. Pharm. Design* **2004**, *10*, 3141-3156.
26. Gupta, *Toxicology of organophosphate & carbamate compounds*. Elsevier: London, 2006; Vol. 1, p 763.
27. Rosman, Y., *et al.*, Carbamate poisoning: treatment recommendations in the setting of a mass casualties event. *Am. J. Emerg. Med.* **2009**, *27*, 1117-1124.
28. Patyar, S., *et al.*, Dual inhibition: a novel promising pharmacological approach for different disease conditions. *J. Pharm. Pharmacol.* **2011**, *63*, 459-471.
29. Krishnamoorthy, A.; Craufurd, D., Treatment of apathy in Huntington's disease and other movement disorders. *Curr. Treat. Options Neurol.* **2011**, *13*, 508-519.
30. Hornsperger, J. M., *et al.*, Trimethylsilylated trifluoromethyl ketones, a novel class of acetylcholinesterase inhibitors - biochemical and pharmacological profile of MDL-73,745. *Biochem. Soc. Trans.* **1994**, *22*, 758-763.
31. Gelb, M. H., *et al.*, Fluoro ketone inhibitors of hydrolytic enzymes. *Biochemistry* **1985**, *24*, 1813-1817.
32. Nair, H. K., *et al.*, m-(N,N,N-Trimethylammonio)trifluoroacetophenone - a femtomolar inhibitor of acetylcholinesterase. *J. Am. Chem. Soc.* **1993**, *115*, 9939-9941.
33. Wolf, R. A., Process research on the preparation of 1-(3-trimethylsilylphenyl)-2,2,2-trifluoroethanone by a friedel-crafts acylation reaction. *Org. Process Res. Dev.* **2008**, *12*, 23-29.
34. Zhu, X. D., *et al.*, Effect of MDL-73,745 on acetylcholine and biogenic-amine levels in rat cortex. *Eur. J. Pharmacol.* **1995**, *276*, 93-99.

35. Cutler, N. R., *et al.*, Acetylcholinesterase inhibition by zifrosilone - pharmacokinetics and pharmacodynamics. *Clin. Pharmacol. Ther.* **1995**, *58*, 54-61.
36. Hartsel, J. A., *et al.*, Re-engineering aryl methylcarbamates to confer high selectivity for inhibition of *Anopheles gambiae* versus human acetylcholinesterase. *Bioorg. Med. Chem. Lett.* **2012**, *22*, 4593-4598.
37. Eyer, P., *et al.*, Paradox findings may challenge orthodox reasoning in acute organophosphate poisoning. *Chem.-Biol. Interact.* **2010**, *187*, 270-278.
38. Lorke, D. E., *et al.*, Pretreatment for acute exposure to diisopropylfluorophosphate: in vivo efficacy of various acetylcholinesterase inhibitors. *J. Appl. Toxicol.* **2011**, *31*, 515-523.
39. Fukuto, Mechanism of Action of Organophosphorus and Carbamate Insecticides. *Environ. Health Perspect.* **1990**, *87*, 245-254.
40. Karami-Mohajeri, S.; Abdollahi, M., Toxic influence of organophosphate, carbamate, and organochlorine pesticides on cellular metabolism of lipids, proteins, and carbohydrates: a systematic review. *Hum. Exp. Toxicol.* **2011**, *30*, 1119-1140.
41. Jokanovic, M., *et al.*, Organophosphate induced delayed polyneuropathy in man: an overview. *Clin. Neurol. Neurosurg.* **2011**, *113*, 7-10.
42. Rayo, J., *et al.*, Reactivity versus steric effects in fluorinated ketones as esterase inhibitors: a quantum mechanical and molecular dynamics study. *J. Mol. Model.* **2010**, *16*, 1753-1764.
43. Brodbeck, U., *et al.*, Fluorinated aldehydes and ketones acting as quasi-substrate inhibitors of acetylcholinesterase. *Biochim. Biophys. Acta* **1979**, *567*, 357-369.
44. Wheelock, C. E., *et al.*, Use of ab initio calculations to predict the biological potency of carboxylesterase inhibitors. *J. Med. Chem.* **2002**, *45*, 5576-5593.
45. Rais, R., *et al.*, Pharmacokinetics of Oral D-Serine in D-Amino Acid Oxidase Knockout Mice. *Drug Metab. Dispos.* **2012**, *40*, 2067-2073.

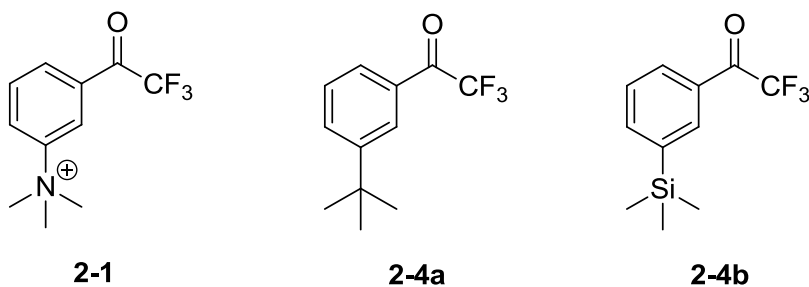
46. Rubin, L. L.; Staddon, J. M., The cell biology of the blood-brain barrier. *Annu. Rev. Neurosci.* **1999**, *22*, 11-28.

Chapter 2: The pharmacology and toxicology of potential trifluoromethyl ketone insecticides

2.1 Design and Synthesis of TFKs

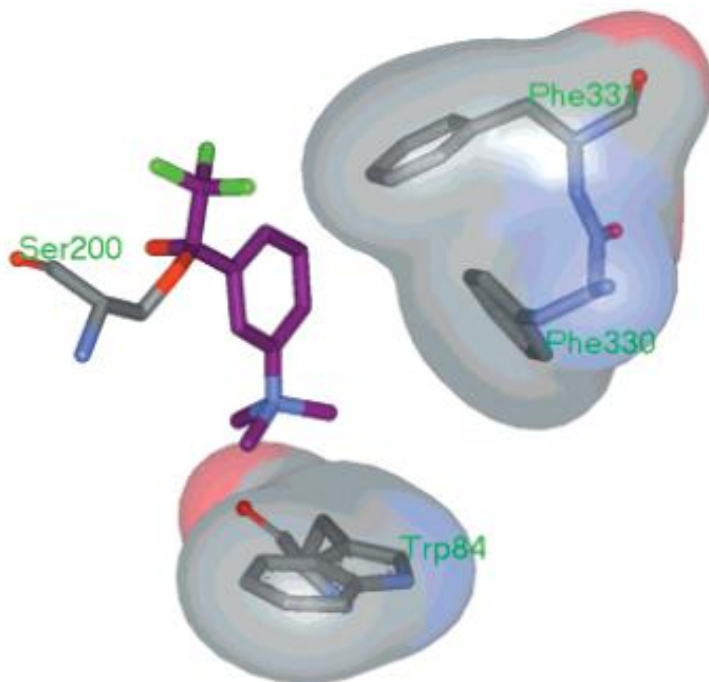
A good starting point for our design of insecticidal TFKs as mentioned in the previous chapter was **2-4a** (Figure 2-1). The structure of **2-4a** is a modification of **2-1**, a known potent inhibitor of AChE.¹⁻² In the 1970's, Brodbeck reported that **2-1** inhibited *Electrophorus electricus* (*Ee*) AChE with a nanomolar concentration of inhibitor.³ Inhibitor **2-1** has been studied using AChE from various species. Quinn was able to successfully crystallize **2-1** in *Torpedo californica* (*Tc*) AChE (RCSB ID: 1HBJ) and show potency for **2-1** in both *Tc*-AChE and *Ee*-AChE considering that the majority of the inhibitor is in the inactive diol form.^{1,4} If one calculates the k_i value for **2-1** based on the amount of free ketone (not 1,1-diol) present at equilibrium, the value falls in the single digit femtomolar range.¹ **2-1** has also been crystallized in mouse AChE (PDB ID: 2H9Y).⁵

Figure 2-1: Our optimized compounds for our study along with the lead TFK (2-1) that demonstrated potency towards AChE.



The x-ray crystal structures provide good insight as to why **2-1** has great binding affinity towards AChE. A favorable cation-pi interaction between the quaternary ammonium and the Trp⁸⁴ residue of AChE is evident (Figure 2-2), keeping the inhibitor in place.⁶ In addition, the incorporation of a benzene ring provides a more rigid conformation which allows for an enhanced interaction in the enzyme pocket.⁶

Figure 2-2: Representation of the TcAChE/2-1 complex (RCSB ID: 1HBJ). Key interactions include an electrostatic interaction of the quaternary ammonium of 2-1 with the indole ring of Trp⁸⁴ and pi-pi interaction with the benzene rings of 2-1 and Phe³³¹ and Phe³³⁰.⁶⁻⁷ Reprinted with permission from Doucet-Personeni, C.; Bentley, P. D.; Fletcher, R. J.; Kinkaid, A.; Kryger, G.; Pirard, B.; Taylor, A.; Taylor, R.; Taylor, J.; Viner, R.; Silman, I.; Sussman, J. L.; Greenblatt, H. M.; Lewis, T., A structure-based design approach to the development of novel, reversible AChE inhibitors. *J. Med. Chem.* 2001, 44, 3203-3215. Copyright 2012 American Chemical Society.



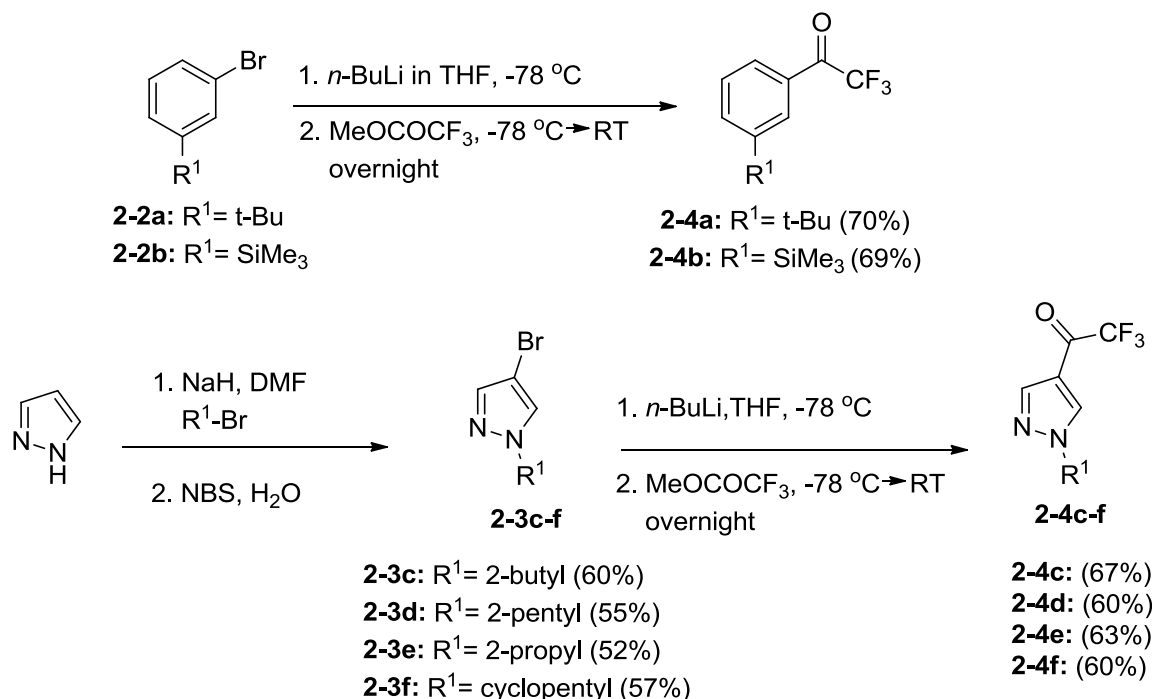
While **2-1** has been shown to be a potent inhibitor, it does not have acceptable pharmacokinetic properties for an insecticide.^{1,8} The charged ammonium moiety, while placing the compound in position for serine to bind, would not be able to penetrate the blood brain barrier (BBB) into the central nervous system (CNS) where the enzyme is located. A potential modification (**2-4a, b**) may prove beneficial toward its pharmacokinetic properties and also keep it in position like **2-1** did (Figure 2-2).

2.1.1 Synthesis of Inhibitors

Compound **2-4a** was synthesized using a literature procedure of a metal-halogen exchange reaction with *n*-butyl lithium and 3-bromo-*tert*butylbenzene (**2-2a**) in 70% yield (Scheme 1).¹⁻² Another

modification from the optimized structure was the change of the quaternary center nitrogen to silicon. This TFK was mentioned in Chapter 1 as Zifrosilone (**2-4b**), a potential TFK therapeutic. Zifrosilone was remade to test its insecticidal ability as a reference. Following the literature procedure, **2-4b** was synthesized in 69% yield, similar to **2-4a** (Scheme 2-1).¹ TLC analysis did not indicate residual starting material, or formation of by-products. We believe that volatility of the products **2-4a** and **2-4b** is responsible for the lower than desired yields.

Scheme 2-1: Synthesis of the TFKs with different core rings.



Another modification of our starting compound was changing the ring core of the inhibitor to allow a better fit in the enzyme-binding pocket.⁹ The inspiration originated from previous research in the Carrier group to design insecticidal AChE inhibitors for mosquitoes which had a G119S resistance mutation.⁹ The oxyanion hole of the G119S mutated enzyme is reduced in size due to a change from a glycine to a serine. Traditional phenyl ring containing carbamates show low potency owing to the reduced active site volume. Thus a smaller ring size was tested and proved successful in delivering the

inhibitor into the binding pocket.⁹ The synthesis of the pyrazole-4-yl TFKs was completed in 3 steps (Scheme 2). Pyrazole was deprotonated with sodium hydride and alkylated with the corresponding bromoalkane ($R^1\text{-Br}$), then brominated with N-bromosuccinimide to give bromides **2-3c-f** in yields ranging from 52% to 60% over 2 reactions (Scheme 2-1). Metal-halogen exchange and trapping with $\text{CF}_3\text{CO}_2\text{Me}$ (as with **2-4a, b**) gave yields ranging from 60% to 67% (Scheme 2-1).¹ As with **2-4a** and **b**, volatility issues were seen and the yields could not be improved.

2.1.2 In vitro assays

Inhibition of AChE by the various TFKs was determined by using the Ellman assay, performed by Dr. Dawn Wong of the Carrier group to determine IC_{50} values. The Ellman assay has been used for decades to measure cholinesterase activity.¹⁰ Instead of acetylcholine, a satisfactory substitute in the form of acetylthiocholine (ATCh) is used. The principle is to measure the amount of thiocholine produced as acetylthiocholine is hydrolyzed.¹⁰ Thiocholine can then react with 5-dithiobis-2-nitrobenzoate (DTNB) to produce 2-nitrosulfidobenzoate which gives off a yellow color which can be detected at 405nm (Scheme 2-2). The assay is performed at various concentrations of inhibitor in order to produce an inhibition response curve (Figure 2-3). Inhibition potency can be measured by calculating the IC_{50} value, the concentration of inhibitor needed to give 50% activity of the enzyme.

Scheme 2-2: The Ellman assay test used to determine AChE activity using ATCh and DTNB. Activity is measured by absorbance of the leaving group formed by ATCh and DTNB.

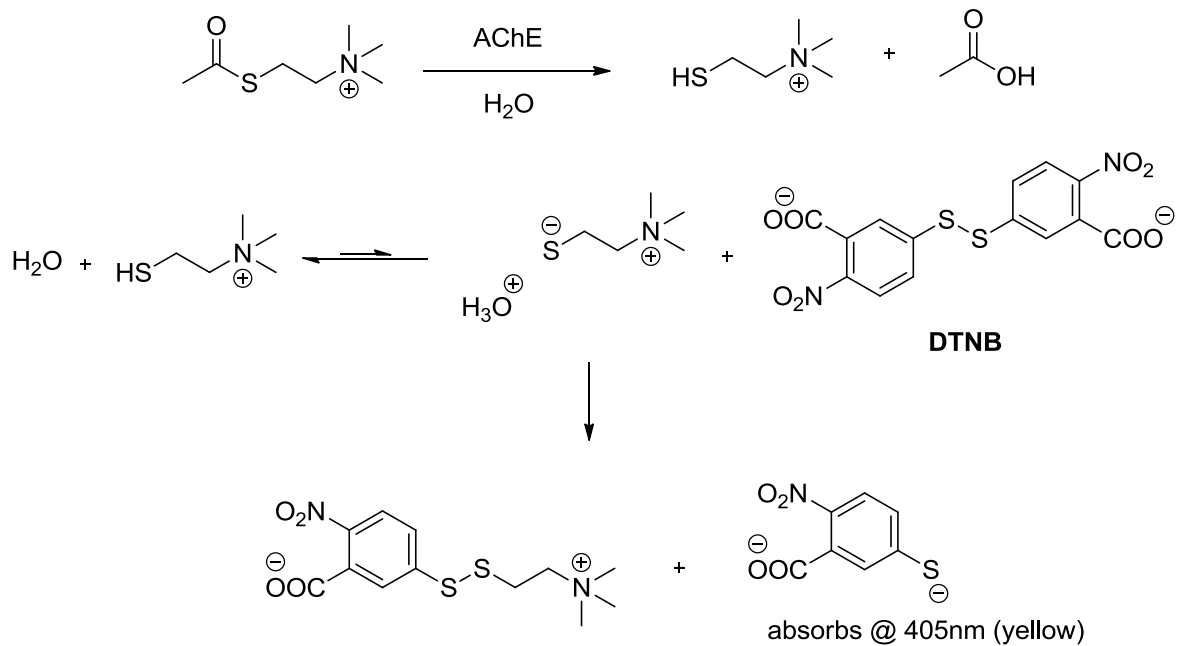
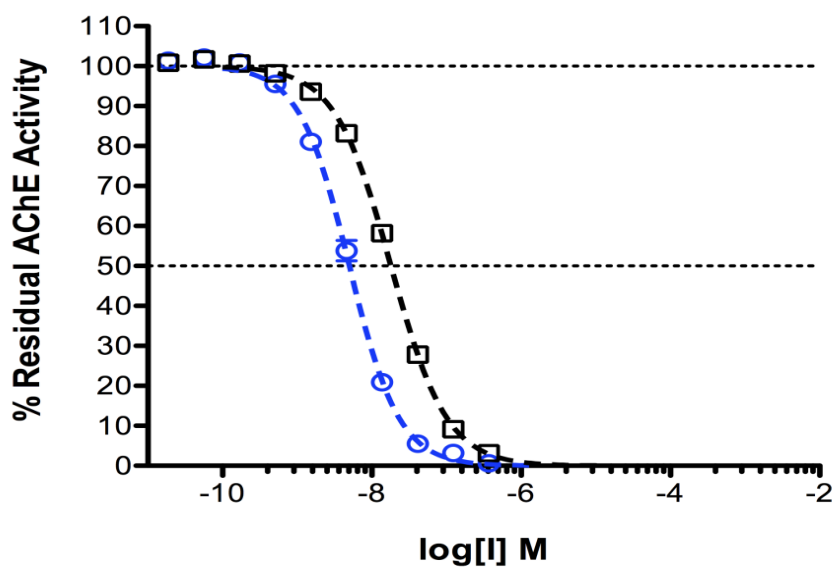


Figure 2-3: An inhibition response curve of 2-4a with *h*AChE (in blue) and WT AChE (in black). The activity of the enzyme was taken at various concentrations of inhibitor. Note that activity was taken at 10 different concentrations to obtain an IC_{50} value.



The Ellman assay was performed at pH 7.8 and inhibitory activity was measured following incubation for 10, 20, and 60 min before the addition of ACh and DTNB. The three types of enzymes that were used were human AChE (*hAChE*) purchased from Sigma-Aldrich, recombinant wild type *An. gambiae* AChE (*rAgAChE*) made by Dr. Jianyong Li, a collaborator with the Carlier group at Virginia Tech Department of Biochemistry, and homogenate *An. gambiae* (*AghmgAChE*). The use of the two different types of mosquito AChE stemmed from earlier research performed in the Carlier group.⁹ A series of carbamates was examined and the inactivation rate constants (k_i) observed for both *rAgAChE* and *AghmgAChE* showed excellent correlation, even though *AghmgAChE* contains other proteins that could interact with the carbamate.⁹ In the case of the TFK, the *AghmgAChE* values can initially serve as a reference because the values should be similar to *rAgAChE*. If the IC_{50} value in *AghmgAChE* is higher than *rAgAChE*, it may suggest that there is a protein or enzyme in the *AghmgAChE* that may be consuming the TFK and not allowing it to inhibit AChE.

Among all the TFKs, **2-4c** and **2-4f** show the best potency towards all three types of AChE (Table 2-1). **2-4c** had IC_{50} values of 8.8 nM for *hAChE*, 1.5 nM for *rAgAChE*, and 1.6 nM for *AghmgAChE* after a 60 min incubation time. **2-4f** showed potency that was similar to **2-4c** with values of 6.1 nM for *hAChE*, 1.5 nM for *rAgAChE*, and 1.7 nM for *AghmgAChE* after a 60 min incubation time. The low nanomolar values may suggest that the 2-butyl branch for **2-4c** and cyclopentyl branch for **2-4f** has the best fit in the binding pocket. The increase of a carbon going from **2-4c** to the 2-pentyl derivative for **2-4d** may show that **2-4d** can't fit into the binding pocket as easily with IC_{50} values of 38.2 nM for *hAChE*, 9.3 nM for *rAgAChE*, and 8.4 nM for *AghmgAChE* after a 60 min incubation. While **2-4f** and **2-4d** have the same number of carbons, the restricted conformation of **2-4f** may allow for a better fit in the active site. The reduction of the butyl chain to an isopropyl chain in the case of **2-4e** shows an increase of IC_{50} with values of 121 nM for *hAChE*, 285 nM for *rAgAChE*, and 250 nM for *AghmgAChE*. The 2-butyl chain may have more interactions and be a better fit in the binding pocket than the smaller isopropyl chain.

Table 2-1: IC₅₀ values of different TFK with the corresponding type of AChE. ^aError estimated as ± 10%.

Entry	Compound (incubation time)	Core structure	<i>h</i> AChE IC ₅₀ (nM)	<i>rAg</i> AChE IC ₅₀ (nM)	<i>Aghmg</i> AChE IC ₅₀ (nM)
1	2-4a (10 min)	phenyl	14 ± 1	51 ± 6	54 ± 7
2	2-4a (60 min)	phenyl	4.9 ± .9	ND	18.2 ± 3.1
3	2-4b (10 min)	phenyl	290 ± 30 ^a	850 ± 90 ^a	1040 ± 100 ^a
4	2-4b (60 min)	phenyl	93 ± 9 ^a	257 ± 26 ^a	352 ± 35 ^a
5	2-4c (10 min)	pyrazol-4-yl	6.5 ± 0.2	2.5 ± 0.1	2.5 ± 0.1
6	2-4c (60 min)	pyrazol-4-yl	8.8 ± 0.3	1.5 ± 0.1	1.6 ± 0.1
7	2-4d (10 min)	pyrazol-4-yl	29.1 ± 0.7	19.6 ± 0.4	17.3 ± 0.4
8	2-4d (60 min)	pyrazol-4-yl	38.2 ± 0.9	9.3 ± 0.3	8.4 ± 0.2
9	2-4e (10 min)	pyrazol-4-yl	77 ± 2	142 ± 5	139 ± 4
10	2-4e (60 min)	pyrazol-4-yl	121 ± 3	285 ± 7	250 ± 10
11	2-4e (17 h)	pyrazol-4-yl	167 ± 7	380 ± 10	365 ± 9
12	2-4f (10 min)	pyrazol-4-yl	5.2 ± 0.2	2.9 ± 0.1	2.7 ± 0.1
13	2-4f (60 min)	pyrazol-4-yl	6.1 ± 0.2	1.5 ± 0.1	1.7 ± 0.1

Time dependent inhibition was observed with **2-4a** and **2-4b** for all 3 types of AChE used (Table 2-1, Entry 1 & 2). With a 10 min incubation time, **2-4a** had IC₅₀ values of 14 nM for *h*AChE, 51 nM for *rAg*AChE, and 54 nM for *Aghmg*AChE (Table 2-1, Entry 1). Increasing the incubation time to 60 min, **2-4a** had IC₅₀ values of 4.9 nM for *h*AChE, and 18.2 nM for *Aghmg*AChE (Table 2-1, Entry 2). The IC₅₀ values for **2-4b** decreased from 290 nM to 93 for *h*AChE, 850 nM to 257 nM for *rAg*AChE, and 1,040 nM to 352 nM for *Aghmg*AChE by increasing the incubation time from 10 to 60 min (Table 2-1, Entry 3 & 4). Time dependent inhibition with mosquito AChE was observed with **2-4c**, **2-4d**, and **2-4f** (Table 2-1, Entry 5-8,12,13). With 10 min incubation, **2-4c** gave IC₅₀ values of 2.5 nM (*rAg*AChE) and 2.5 nM (*Aghmg*AChE),

2-4d gave IC₅₀ values of 19.6 nM (*rAgAChE*) and 17.3 nM (*AghmgAChE*) and **2-4f** gave values of 2.9 nM (*rAgAChE*) and 2.7 nM (*AghmgAChE*) (Table 2-1, Entry 5 & 12). It is of interest to note that any of the IC₅₀ values at each incubation time for *rAgAChE* and *AghmgAChE* did not change significantly for any of the compounds tested. The lack of significant change of the values may indicate that there is not a protein or enzyme in the mosquito that is consuming the TFK. **2-4e** was the only compound to show an increase of IC₅₀ with increasing incubation time (Table 2-1, Entry 9-11). The IC₅₀ increased from 77 nM to 167 nM for *hAChE* and 142 nM to 380 nM for *rAgAChE* going from 10 min incubation to 17 h. This may be attributed to a reduced molecular weight shown with **2-4e** compared to the other compounds (Table 2-2).

For *hAChE*, **2-4a**, **c**, and **f** all indicate single digit nanomolar IC₅₀ values towards all types of AChE (Table 2-1). For *AgAChE*, only the pyrazol-4-yl TFKs (**2-4c** and **f**) show excellent potency. Excellent selectivity was not displayed by any compound towards *AgAChE*, but the best selectivity is seen with **2-4c** with a 6-fold selectivity towards *Ag* over *hAChE*.

The IC₅₀ values suggest that **2-4a**, **c**, and **f** are potent inhibitors of AChE (Table 2-1). The values furthermore suggest that all of the inhibitors except compound **2-4e** are time dependent inhibitors of *AgAChE*. An additional test that is used to assess the compounds is the mosquito toxicity assay. This is a more valuable method to determine the toxicity towards the target, *Anopheles gambiae*.

2.1.3 Mosquito toxicity assay

The mosquito toxicity assay test is the essential test to establish insecticidal potency of our compounds. The protocol of testing is regulated by the World Health Organization (WHO) to ensure quality results that can be repeated.¹¹ For the paper assay, protocol dictates that batches of mosquitoes, female between 2-5 days old, are exposed to a filter paper that has been pretreated with the compound.¹¹ The mosquitos are then exposed to the chemical on filter paper for an hour and after

that period of time they are transferred into a dark chamber without compound for 24 h and mortality is recorded.¹¹ The test is done in replicates to ensure precision. In addition, topical application assays of these potential mosquitocides can be used to determine LD₅₀ values. The tests are performed from a literature procedure in which mosquitoes are anesthetized on ice and application of a 0.2 µL solution of TFK in ethanol is placed on the dorsal thorax of the mosquito.¹² These tests were performed by members of the Bloomquist Group at the University of Florida.

When the mosquito toxicity assay was performed on **2-4a**, the results were not promising (Table 2-2, Entry 1). Compound **2-4a** showed no mortality at the highest concentration of 1 mg/mL. Compound **2-4b** showed only a slight improvement with 10% mortality observed (Table 2-2, Entry 2). Modification of the ring showed an increase in mosquito toxicity (Table 2-2, Entry 3-6). All of the pyrazol-4-yl TFKs had mortality values of at least 30%. Compound **2-4c** with the 2-butyl chain had 30% mortality at 1 mg/mL (Table 2-2, Entry 3). Increasing the number of carbons improved toxicity as shown with a 90% mortality for the 2-pentyl branch of **2-4d** (Table 2-2, Entry 4) and the cyclopentyl branch of **2-4f** (Table 2-2, Entry 6). Similarly, a decrease in the number of carbons resulted in lower toxicity with a 20% mortality for the isopropyl branch of **2-4e** (Table 2-2, Entry 5).

One reason for the increased toxicity of the pyrazole-4-yl TFKs may be due to the ClogP, calculated log partition coefficient (Table 2-2). Compounds **2-4c-f** with the pyrazole core is less lipophilic than its phenyl core counterparts (Table 2-2, Entry 3-6). If we compare the ClogP of our compounds with propoxur (1.65), a carbamate insecticide, we can see that the pyrazol-4-yl TFKs has a ClogP closer to that of propoxur than that of the phenyl core TFKs (Table 2-2). The increased ClogP of **2-4a** (3.97) and **b** (4.72) compared to **2-4c** (1.91), **d** (2.44), **e** (1.38), and **f** (2.01) may make the compounds too lipophilic and get stuck in the BBB and decrease insecticidal activity (Table 2-2).

Within the pyrazol-4-yl series, molecular weight can correlate with toxicity (Table 2-2). The isopropyl derivative (**2-4e**) with its reduced molecular weight makes it more volatile than the other compounds and less of the compound may be on the filter paper to get on the mosquito. Starting with the pyrazole-4-yl TFK that weighs the least, **2-4e**, we see a 20% mortality rate. If we increase the molecular weight, **2-4c** shows 30% mortality, **2-4f** having 40% mortality, and **2-4d** having 90% toxicity. While **2-4d** and **2-4f** have the same molecular weight, the increased lipophilic character of **2-4d** may give a better pharmacokinetic profile to better travel into the CNS.

Table 2-2: Mortality values with phenyl and pyrazole core TFKs. Molecular weight (MW) and clogP may be factors that influence toxicity.

Entry	Compound	Core structure	Mortality @ 1 mg/ mL	MW	clogP ^a
1	2-4a	phenyl	0%	230.23	3.97
2	2-4b	phenyl	10%	246.30	4.72
3	2-4c	pyrazole	30%	220.19	1.91
4	2-4d	pyrazole	90%	234.22	2.44
5	2-4e	pyrazole	20%	206.17	1.38
6	2-4f	pyrazole	40%	232.20	2.01
7	propoxur	phenyl	100%	209.24	1.65

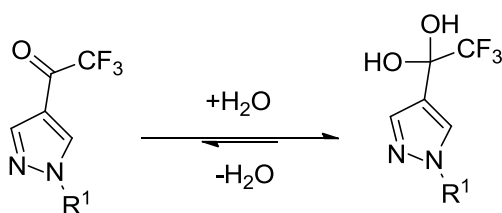
^aCalculated with ChemDraw v. 12.0

Testing of enzyme inhibition potency and mosquito toxicity is essential in insecticide development. The compounds that will be developed need to show potency towards AgAChE, but also need to have the necessary pharmacokinetic characteristics to be able to penetrate the cuticle/ BBB to act on AChE, in the mosquito CNS. One modification involved changing the quaternary carbon to silicon and the result improved mortality slightly.¹³⁻¹⁴ Another was to change the ring size to see how toxicity was affected and that proved more successful in increasing mortality.⁹ The in vitro assays performed do not necessarily correlate with the toxicity values observed. If potent, the inhibitor may not have the

desirable pharmacokinetic properties needed to produce toxicity in the mosquito. Other properties need to be taken into account such as MW and clogP ,¹⁵

A lack of TFK insecticidal activity may also be attributed to the increased electrophilic character of the carbonyl carbon. Previous studies suggest that the TFK is majority hydrated in aqueous medium, which may affect insecticidal activity (Scheme 2-3).¹

Scheme 2-3: In the body, TFK's can undergo hydration from water to form the geminal diol. The diol is not a good inhibitor of AChE due to the loss of the carbonyl.



Modifications of the TFKs are needed in order to achieve better contact toxicity. The new molecules that were made need to address and fix the potential problems that the previous TFKs had: cuticle penetration problems and hydration. A solution could be to possibly mask the TFKs in the form of prodrugs. Initially inactive, the prodrug may have better characteristics towards cuticle penetration and be robust enough to make it into the BBB and then hydrolyze in the CNS to become the TFK to inhibit AChE.

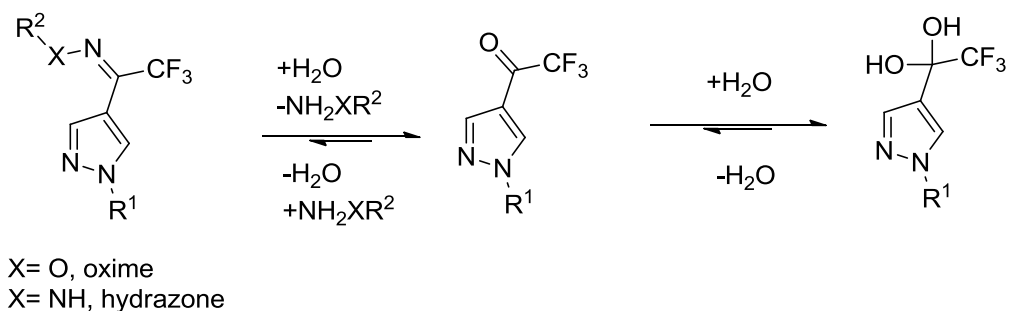
2.2 Design, synthesis and discussion of prodrugs of TFKs

2.2.1 Structure design of prodrugs

The candidates that were used as potential prodrugs for the TFKs were oximes and hydrazones. The oxime functional group, with its reduced electrophilicity, will hopefully be robust enough to resist being hydrolyzed by water until reaching the CNS (Scheme 2-4). In addition to oximes, synthesis of hydrazones was planned. Hydrazones are very similar to oximes structurally and mechanistically. Both

are shown to hydrolyze at pHs ranging from 3-8, but hydrazones consistently hydrolyze faster than oximes.¹⁶ This may prove to be advantageous due to the mosquito hemolymph being slightly acidic and may help to catalyze hydrolysis. The drug delivery properties could potentially be improved by changing the alkyl groups on the oximes/hydrazones.

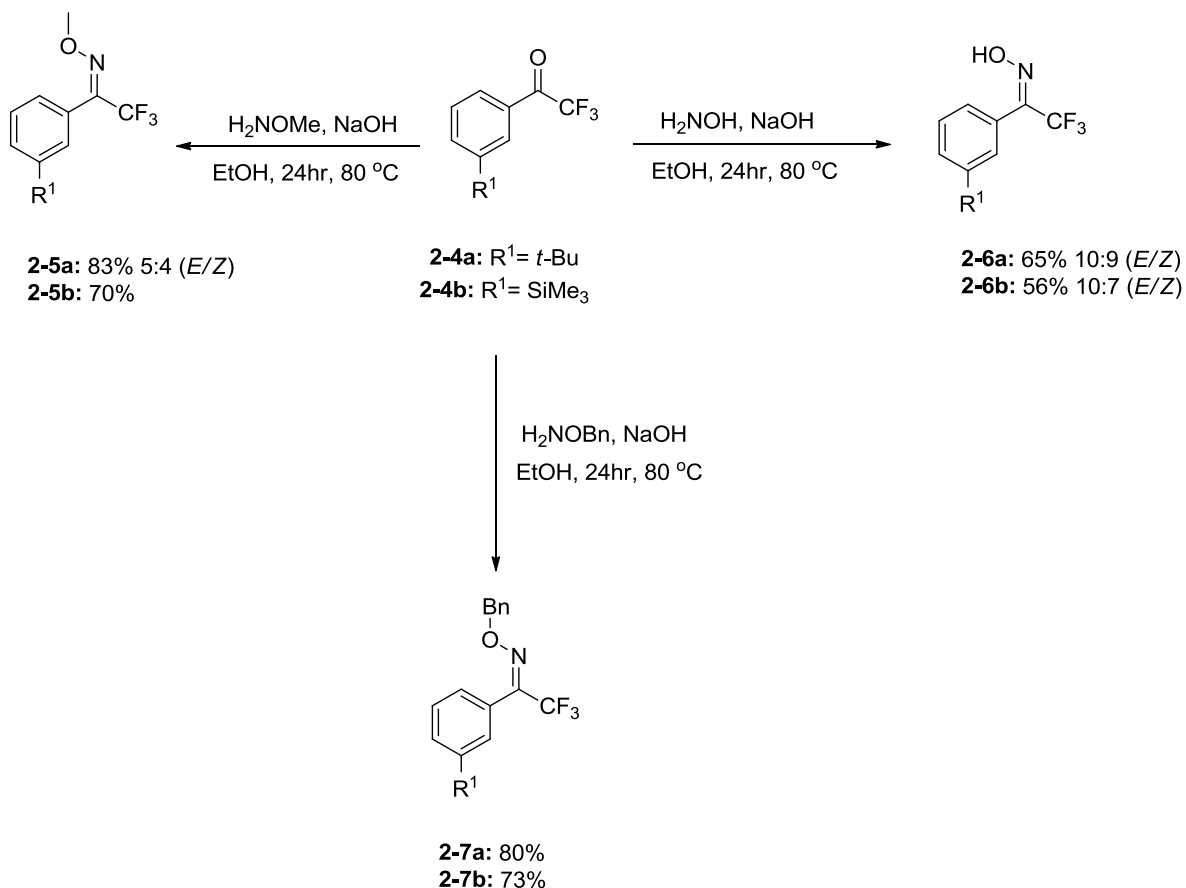
Scheme 2-4: The proposed scheme of the prodrugs. The prodrug can be hydrolyzed back into the TFK where it can go back into the oxime/hydrazine or hydrate into the diol.



2.2.2 Synthesis of prodrugs

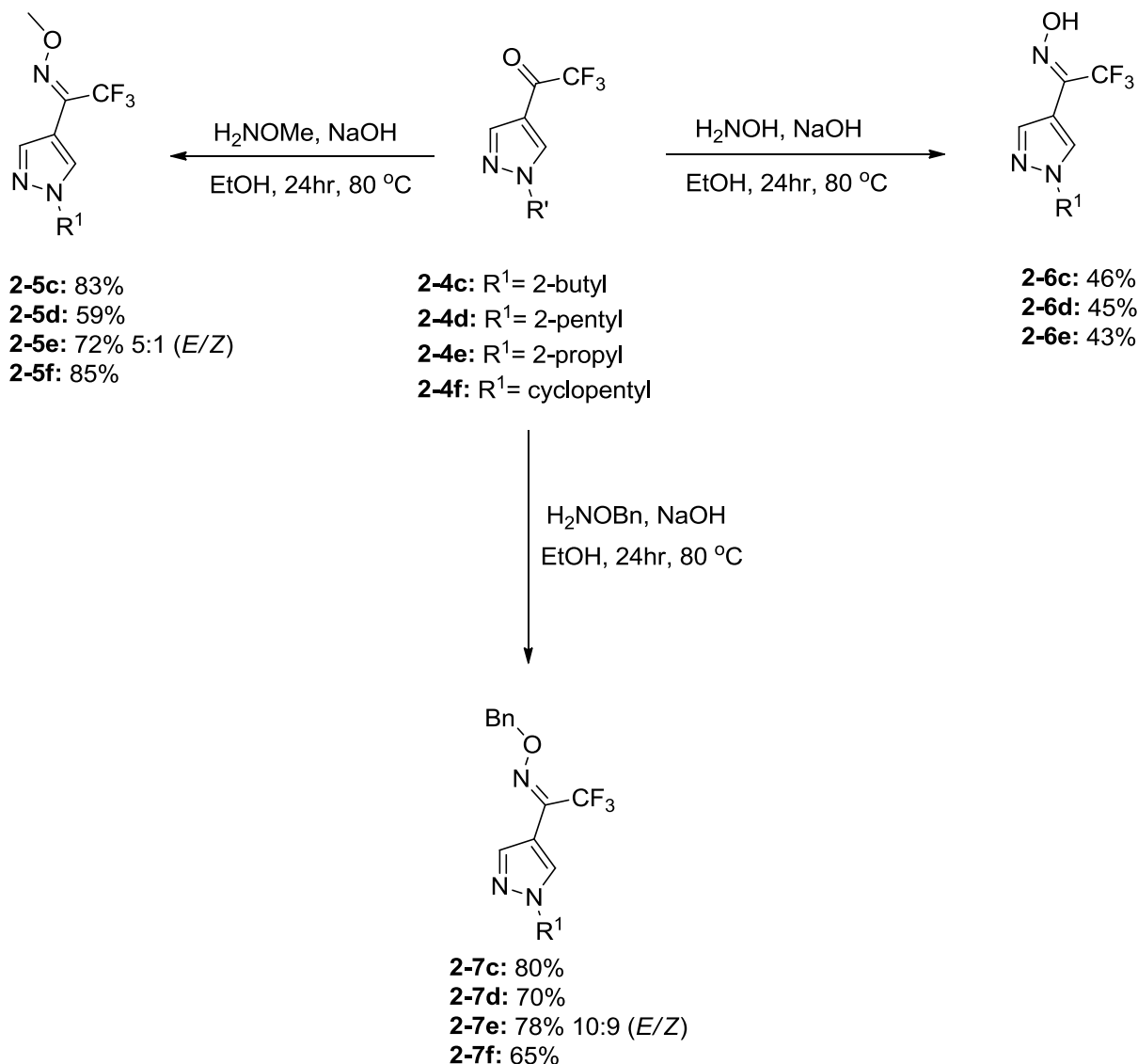
The synthesis of the oximes and oxime ethers was accomplished by refluxing TFKs with the oxime or oxime ether salt and sodium hydroxide in ethanol for 24 h to afford the product in 43% to 85% yield (Schemes 2-5 & 2-6). The phenyl core TFKs (**2-4a, b**) yielded the corresponding oxime and oxime ethers in moderate to good yields (Scheme 2-5). The methyl and benzyl oxime ether (**2-5a-b, 2-7a-b**) gave the best yields due to going to completion and giving a single product. The formation of the oxime, while proceeding to completion, gave side products that ultimately lowered the yield. It is of note to mention that **2-5a, 2-6a, b** and **2-7** furnished the final product as a set of diastereomers.

Scheme 2-5: All oxime derivatives appeared to be a single diastereomer by ^1H and ^{19}F NMR spectroscopy unless noted. Assignment of (*E*)-configuration to the major or sole isomer is arbitrary in each case.



The same trend was observed for the synthesis of the pyrazole-4-yl derivatives. The previously described procedure afforded the various oxime and oxime ethers of various chain lengths in moderate to good yield (Scheme 2-6). As in the case of **2-4a**, and **b**, oximes **2-6c-e** were formed in lower yields than oxime ethers **2-5c-f** and **2-7c-f**. The appearance of an impurity may be the cause of lower yields. For the most part except compound **2-5d**, the formation of the methyl and benzyl oxime ether proceeded with yields greater than 70%. In contrast with the phenyl core series, only **2-5e** and **2-7e** produced diastereomeric mixtures.

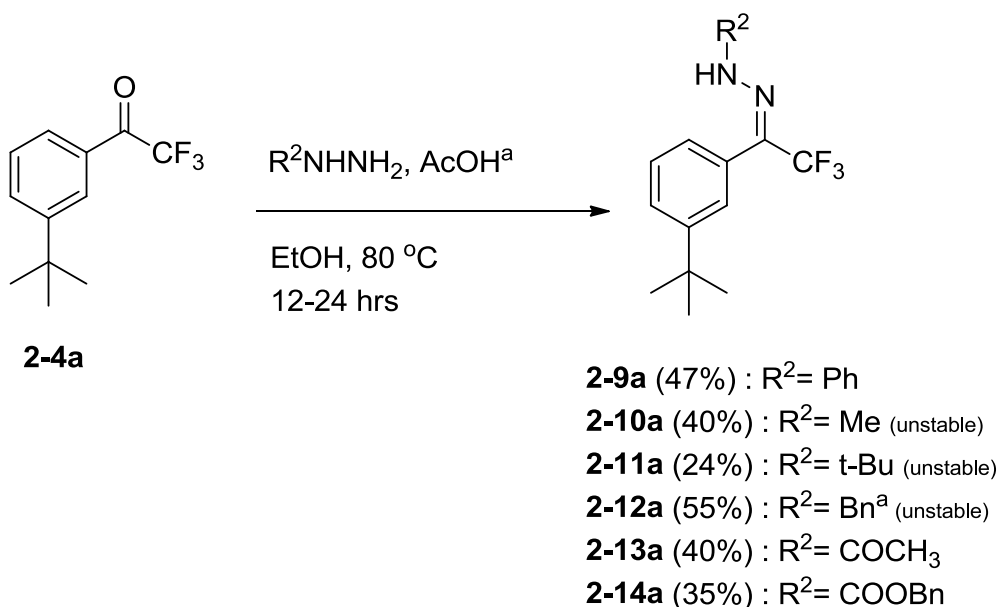
Scheme 2-6: All oxime derivatives appeared to be a single diastereomer by ^1H and ^{19}F NMR spectroscopy unless noted. Assignment of (*E*)-configuration to the major or sole isomer is arbitrary in each case.



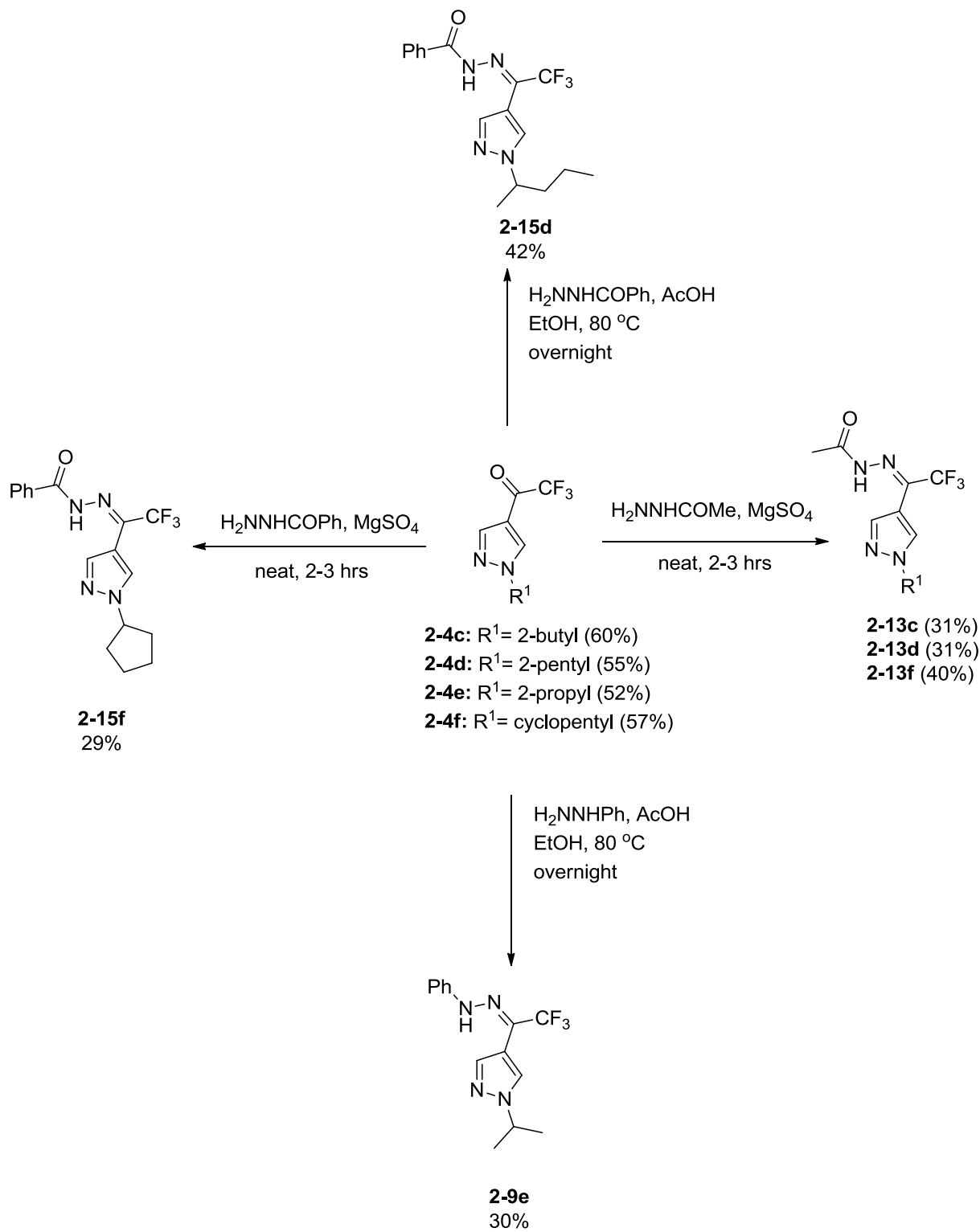
The synthesis of hydrazones primarily followed the scheme previously shown for oxime formation (Scheme 2-7). The TFK was mixed with the hydrazine in ethanol with a catalytic amount of acetic acid to afford the corresponding hydrazones ranging in 29-65% yield. The syntheses of the some hydrazones were problematic. When making the methyl hydrazone (**2-10a**), a 40% yield was obtained. Multiple spots were seen after a week-long period after purification of the methyl hydrazone. A distinct color change was also observed from clear to bright yellow. At this point we do not know what the

nature of this decomposition is, but the same problem was noted for *t*-butyl hydrazone **2-11a** and benzyl hydrazone **2-12a**. The same phenomenon also occurred during the formation of the methyl hydrazones within the pyrazol-4-yl series but on a much shorter timescale (1 day). The rapid decomposition prevented testing of the pyrazole-4-yl methyl hydrazones for insecticidal activity and assay studies. While the majority of the hydrazones yielded liquids, some of the hydrazones came out as solids (**2-9e**, **2-13c-f**, and **2-15f**). Low solubility and scaling down the reported literature may have resulted in lower yields seen for these compounds.¹⁶

Scheme 2-7: Synthesis of 2-4a with the corresponding hydrazones. ^aFor **2-12a**, $\text{BnNHNH}_2 \cdot \text{HCl}$ was used and NaOAc was used instead of AcOH . Assignment of (*E*)-configuration to the major or sole isomer is arbitrary in each case.



Scheme 2-8: Synthesis of 2-5c-f with the corresponding hydrazines. Assignment of (*E*)-configuration to the major or sole isomer is arbitrary in each case.

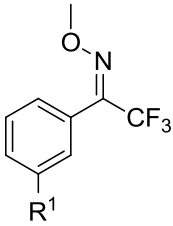
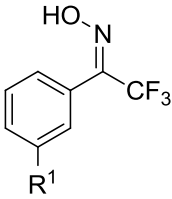
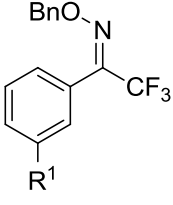
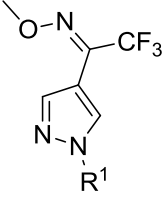
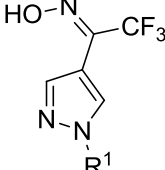
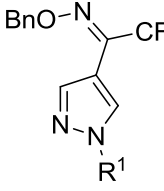


2.2.3 Toxicity evaluation of prodrugs

We decided to examine the mosquito toxicity of the prodrugs before assessment of their inhibition potency to AChE. If a compound proves to be nontoxic to *An. gambiae*, there would be no reason to further investigate it. On the other hand, toxicity shown towards *An. gambiae* may indicate that the prodrug strategy was successful. Pharmacological studies from that point can confirm whether the compounds go through a cholinergic mechanism or if the compounds kill the mosquitoes through another mechanism.

As shown in Table 2-3, the results indicate that as a whole, the pyrazole-4-yl oximes and oxime ethers (**2-5c** through **2-7f**) were more toxic than the phenyl core series. The most toxic phenyl oxime derivative was **2-7a** with 40% toxicity at 1 mg/mL while almost half of the pyrazole-4-yl oxime/ oxime ether derivatives showed at least 80% mortality at the same concentration. Within the pyrazole-4-yl series, the oxime/ oxime ethers that bear the isopropyl branch (**2-5e**, **2-6e**, and **2-7e**) showed the most toxicity. **2-5e** was shown to have 90% mortality; **2-6e** and **2-7e** both had 100% mortality at 1 mg/mL. The most toxic of the three types of oxime/ oxime ethers were the benzyl oxime ethers with two compounds (**2-7d**, **2-7e**) showing 100% toxicity at 1 mg/mL. The benzyl oxime ethers may be showing greater mortality due to increased lipophilicity leading to better delivery through the cuticle or BBB.

Table 2-3: Toxicity studies results on the various oximes (2-5 through 2-7) via tarsal contact toxicity.^a

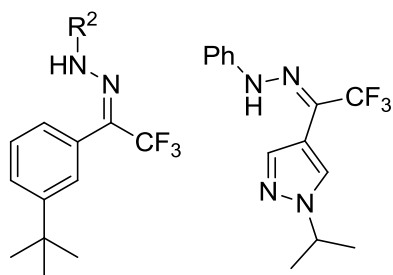
			Toxicity (% mortality @ 1 mg/mL)			
Compound	2-5	2-6	2-7			
			a	30%	20%	40%
2-5a: R ¹ = <i>t</i> -Bu 2-5b: R ¹ = SiMe ₃	2-6a: R ¹ = <i>t</i> -Bu 2-6b: R ¹ = SiMe ₃	2-7a: R ¹ = <i>t</i> -Bu 2-7b: R ¹ = SiMe ₃	b	0%	10%	0%
			c	0%	80%	ND
			d	30%	50%	100%
			e	90%	100%	100%
			F	10%	ND	0%
2-5c: R ¹ = 2-butyl 2-5d: R ¹ = 2-pentyl 2-5e: R ¹ = isopropyl 2-5f: R ¹ = cyclopentyl	2-6c: R ¹ = 2-butyl 2-6d: R ¹ = 2-pentyl 2-6e: R ¹ = isopropyl 2-6f: R ¹ = cyclopentyl	2-7c: R ¹ = 2-butyl 2-7d: R ¹ = 2-pentyl 2-7e: R ¹ = isopropyl 2-7f: R ¹ = cyclopentyl	^a WHO filter paper protocol was followed. ¹¹			

After synthesis, the resulting hydrazones were also tested to determine whether they were toxic (Table 2-4). Compared with oximes, more of the hydrazones showed more toxicity and mortality towards *Anopheles gambiae*. The phenyl hydrazone (**2-9a**) showed 90% mortality at 1 mg/mL. Reducing the size of the core resulted in a loss of toxicity to 30% (**2-9e**). Modification of the phenyl group to various alkyl groups resulted in no general trend of toxicity. Altering the phenyl group (**2-9a**) to a methyl (**2-10a**) and *tert*-butyl (**2-11a**) group resulted in 100% mortality. Increasing the phenyl group to a benzyl group (**2-12a**) resulted in a decrease in mortality to 30%. Addition of an acyl group could not produce the same toxicity of **2-10a** and **2-11a**. The highest toxicity observed for any acyl hydrazone was **2-15d** with 50% mortality. Changing the reagent from acetylhydrazide to benzhydrazide showed toxicity comparable to **2-10a** and **2-11a**. **2-15f** presented 100% mortality while **2-15d** showed 80% mortality.

Table 2-4: Toxicity results via tarsal contact assay^a for various hydrazones that were synthesized.

Compound	Toxicity (% mortality @ 1 mg/mL)
2-9a	90%
2-9e	30%
2-10a	100%
2-11a	100%
2-12a	30%
2-13a	10%
2-13c	20%
2-13d	50%
2-13f	20%
2-14a	40%
2-15d	80%
2-15f	100%

^aWHO filter paper protocol was followed



2-9a: R²= Ph

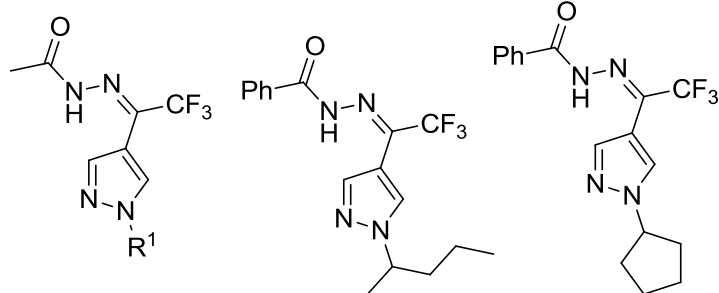
2-10a: R²= Me

2-11a: R²= *t*-Bu

2-12a: R²= Bn

2-13a: R²= COCH₃

2-14a: R²= COOBn



2-13c: R¹= 2-butyl

2-13d: R¹= 2-pentyl

2-13f: R¹= cyclopentyl

Two of the hydrazones and an oxime, **2-6e**, **2-10a** and **2-11a**, were some of the first prodrugs to display 100% mortality which garnered interest in further studies with these compounds. Additional concentrations with the paper assay produced LC₅₀ values of 106 µg/mL for **2-6e**, 83 µg/mL for **2-10a**, 73 µg/mL for **2-11a**, and propoxur, a carbamate insecticide used as a reference had LC₅₀ value 39 µg/mL (Table 2-5). The amount to kill 50% of the mosquitoes topically was investigated and LD₅₀ values were obtained for resulting in a LD₅₀ of 12 ng/ mosquito for **2-6e**, 11 ng/ mosquito for **2-10a**, and 10.2 ng/ mosquito for **2-11a**. Though not as toxic as propoxur, the data is promising towards synthesizing compounds toxic to *An. gambiae*.

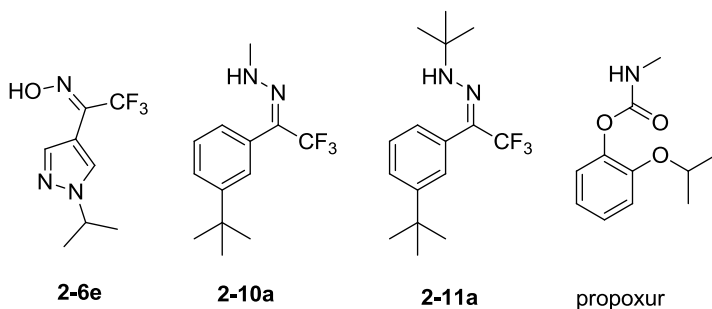


Table 2-5: Compounds of interest, 2-6e, 2-11a and 2-12a, were compared to propoxur for toxicity.

	2-6e	2-10a	2-11a	propoxur
Paper assay	83	73	39	
LC ₅₀ (µg/mL)				
Topical LD ₅₀ (ng/mosquito)	11	10.2	3.2	

To ascertain whether the toxicity of these compounds was cholinergic, or arose from interfering with another target, we investigated their AChE inhibition properties.

2.2.4 In vitro assay results

In order to have an idea of the mechanism of action of these mosquitocides, AChE inhibition assays were performed on an oxime (**2-6c**) that showed contact toxicity towards *Anopheles Gambiae* (80% mortality @ 1 mg/mL, Table 3). Low IC₅₀ values would suggest that the prodrug was hydrolyzing in the mosquito and the enzyme was inhibited by the active TFK form.

Table 2-6: In vitro assays were performed on 2-6c, an oxime. 2-4c is also displayed as a reference.

Compound	Incubation time	AgAChE IC ₅₀ (nM)	hAChE IC ₅₀ (nM)
2-4c	10	2.5 ± 0.1	6.5 ± 0.2
2-4c	60	1.5 ± 0.2	8.8 ± 0.3
2-6c	10	7,000 ± 2,000	30,000 ± 100
2-6c	60	4,900 ± 300	60,000 ± 40,000

As shown in Table 2-6, the free trifluoromethyl ketone (**2-4c**) shows potency towards AChE in the nanomolar range, but the oxime prodrug (**2-6c**) shows an IC₅₀ value in the micromolar range (Table 2-6). Ideally the prodrug should have an IC₅₀ value very similar to **2-4c** assuming hydrolysis. The IC₅₀ value of 7 μM for **2-6c** at 10 min incubation for AgAChE suggest that the oxime is a poor inhibitor of AChE. Giving only a slightly lower IC₅₀ value after a 60 minute preincubation indicates that hydrolysis to the TFK is a very slow; if indeed it occurs at all. A compound that shows toxicity towards *Anopheles gambiae* but no hydrolysis might suggest that the oxime itself is acting as a poor AChE inhibitor. Due to oximes being hydrolyzed faster under acidic conditions, IC₅₀ studies were done under more acidic conditions to more accurately mimic the mosquito hemolymph with a pH of 6.7.¹⁶

To determine whether prodrug hydrolysis was accelerated under acidic conditions, the inhibitor was incubated in a pH 5.5 buffer before combining with enzyme at pH 7.7 (Table 2-7). For the oxime (**2-6c**), incubating under neutral conditions gave an IC₅₀ value of 7.5 μM for AgAChE with an incubation of 10 min (Entry 1, Table 2-7)). Increasing the incubation time to 68 min showed a decrease to 4.7 μM. After 22 hr, the IC₅₀ increased to 8.5 μM. Decreasing the pH to 5.5, gave an IC₅₀ value of 17 μM after a 10 min preincubation time. Increasing the preincubation time to 20 h gives an IC₅₀ value of 14 μM for AgAChE, suggesting that hydrolysis is not occurring even under acidic conditions. The same can also be observed for **2-6c** with hAChE and increasing incubation time and varying pH. Giving an IC₅₀ value of

30 μM at 10 min at pH 7, increasing the incubation time to 22 h at the same pH shows no significant decrease in IC_{50} within error with an IC_{50} value of 20 μM (Entry 4).

Table 2-7: IC_{50} studies were performed on 2-6c and 2-9e at pH 5.5 and 7.7 to determine whether hydrolysis occurs. (Note that concentrations in μM .)

Entry	Compound	Incubation time	pH	<i>AgAChE</i> IC_{50} (μM)	<i>hAChE</i> IC_{50} (μM)
1	2-6c	10 min	7.7	7.5 ± 0.4	30 ± 3
2		30 min		15 ± 6	20 ± 10
3		68 min		4.7 ± 2	60 ± 40
4		22 h		8.5 ± 0.3	20 ± 10
5		10 min	5.5	17.0 ± 0.9	40 ± 9
6		20 h		14.9 ± 0.9	20 ± 3
7	2-9e	10 min	7.7	28 ± 4	9 ± 1
8		60 min		>10	19 ± 2
9		17 h		40 ± 10	7.3 ± 0.5
10		10 min	5.5	>10	>10
11		31 min		>10	>10
12		60 min		>10	>10
13		22 h		36 ± 6	8.4 ± 0.2

The hydrazone (**2-9e**) that was tested performed similarly to **2-6c**. For *AgAChE*, we see that with a 10 min incubation under neutral conditions gives an IC_{50} value of 28 μM (Entry 7, Table 2-7). Increasing the incubation time to 17 h did not decrease the IC_{50} value but rather increased the IC_{50} value to 40 μM (Entry 9, Table 2-7). Lowering the pH to 5.5 and increasing incubation time for entries 10-13 still shows IC_{50} values greater than 10 μM . With *hAChE*, we see that varying the incubation time from 10 min (Entry 7, Table 2-7) to 17 h (Entry 9, Table 2-7), causes no significant change in IC_{50} . Decreasing the

pH to 5.5 did not help to hydrolyze with IC_{50} value $>10 \mu\text{M}$ after 10 min incubation (Entry 10, Table 2-7) and $8.4 \mu\text{M}$ after 22h incubation (Entry 13, Table 2-7).

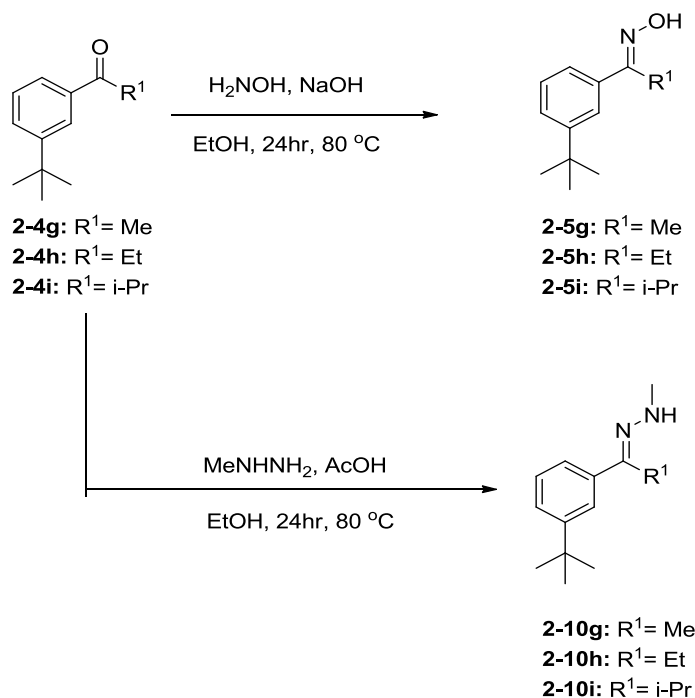
These results with oxime **2-6e** and phenyl hydrazone **2-9e** show that even incubation of the oxime/hydrazone in an acidic buffer for up to 22 h does not improve AChE inhibition (Table 2-7, Entries 1-13). Thus aqueous hydrolysis of these compounds to the TFK cannot account for their mosquito toxicity. One possibility is that the oxime/hydrazone is utilizing another mechanism of action targeting another enzyme or receptor in the mosquito. To address this issue, a new approach must be made.

2.3 Future Work

The synthesis of various oximes, oxime ethers, and hydrazones have shown to be significantly toxic to *An. gambiae* to within 3- to 4- fold of the toxicity of propoxur. However, thus far we have not been able to link the toxicity of these compounds to a cholinergic mechanism. Pre-incubation studies suggest that significant hydrolysis of these compounds to TFKs does not occur or 22 h at pH 7.7 or 5.5.

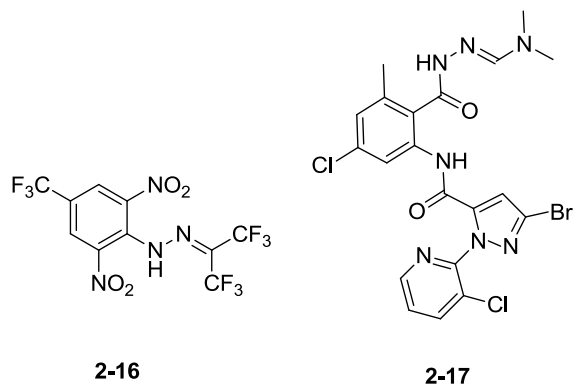
With this information, two hypotheses can be made. The first hypothesis is that the compounds are not transformed into the active TFK and are toxic due to some other mechanism. The second is that conversion of these compounds to TFKs does happen *in vivo* through an unidentified enzyme and toxicity is the consequence of potent AChE inhibition. In order to discriminate between these hypotheses, we plan to synthesize oximes and hydrazones, wherein the CF_3 functional group is replaced by CH_3 , CH_2CH_3 and $\text{CH}(\text{CH}_3)_2$. We chose these three substituents because the size of the CF_3 group is believed to be somewhere between that of the CH_2CH_3 and $\text{CH}(\text{CH}_3)_2$ (Scheme 2-9).

Scheme 2-9: Proposed scheme for the synthesis of oximes and hydrazones. Previously used procedures for the formation of the oximes/ hydrazones for the TFKs can be used here also to synthesize the corresponding oxime/ hydrazones.



After testing of these new synthesized compounds, one of two things can be hypothesized. If the CF₃ isosteres (e.g. **2-4g**, **2-5g**, **2-10g**) are toxic to *An. gambiae*, a prodrug mechanism can be eliminated. **2-4g** is expected to be a poor inhibitor of AChE due to reduced electrophilicity but will be tested in conjunction to the prodrugs. We could then explore the possibility that toxicity is due to some other mode of action. The hydrazone functional group has been used in pesticide design for decades ranging from uncouplers of oxidative phosphorylation¹⁷ (**2-16**, Figure 2-4) to ryanodine receptor activators¹⁸⁻¹⁹ (**2-17**, Figure 2-4) If the prodrugs do not have a cholinergic mechanism, it may be working at the sites previously mentioned. Collaboration with agrochemical companies may help to elucidate the mechanism of these compounds.

Figure 2-4: Two compounds that contain the hydrazone functional group. 2-16 was tested as an uncoupler of oxidative phosphorylation and 2-17 was tested as a ryanodine receptor activator.



If the compounds are not toxic to *An. gambiae*, we cannot necessarily eliminate the previous hypothesis. Toxicity may have arisen from the oxime/hydrazone functional group in addition to the CF_3 group. Again, further investigation will likely require collaboration with a chemical company.

2.4 References for Chapter 2

1. Nair, H. K., *et al.*, m-(N,N,N-Trimethylammonio)trifluoroacetophenone - a femtomolar inhibitor of acetylcholinesterase. *J. Am. Chem. Soc.* **1993**, *115*, 9939-9941.
2. Nair, H. K.; Quinn, D. M., m-alkyl alpha,alpha,alpha-trifluoroacetophenones - a new class of potent transition-state analog inhibitors of acetylcholinesterase. *Bioorg. Med. Chem. Lett.* **1993**, *3*, 2619-2622.
3. Brodbeck, U., *et al.*, Fluorinated aldehydes and ketones acting as quasi-substrate inhibitors of acetylcholinesterase. *Biochim. Biophys. Acta* **1979**, *567*, 357-369.
4. Harel, M., *et al.*, The X-ray structure of a transition state analog complex reveals the molecular origins of the catalytic power and substrate specificity of acetylcholinesterase. *J. Am. Chem. Soc.* **1996**, *118*, 2340-2346.
5. Bourne, Y., *et al.*, Substrate and product trafficking through the active center gorge of acetylcholinesterase analyzed by crystallography and equilibrium binding. *J. Biol. Chem.* **2006**, *281*, 29256-29267.
6. Nair, H. K., *et al.*, Molecular recognition in acetylcholinesterase catalysis - free-energy correlations for substrate turnover and inhibition by trifluoro ketone transition-state analogs. *Biochemistry* **1994**, *33*, 8566-8576.
7. Doucet-Personeni, C., *et al.*, A structure-based design approach to the development of novel, reversible AChE inhibitors. *J. Med. Chem.* **2001**, *44*, 3203-3215.
8. Pajouhesh, H., Medicinal chemical properties of successful central nervous system drugs. *Amer. Soc. Exper. Neuro.* **2005**, *2*, 541-553.
9. Wong, D. M. L., J.; Chen, Q.-H.; Han, Q.; Mutunga, J. M.; Wysinski, A.; Anderson, T. D.; Ding, H.; Carpenetti, T. L.; Verma, A.; Islam, R.; Paulson, S. L.; Lam, P. C. H.; Totrov, M.; Bloomquist, J. R.; Carlier, P.

R., Select small core structure carbamates exhibit high contact toxicity to "carbamate-resistant" strain malaria mosquitoes, *Anopheles gambiae* (Akron). *PLOS one* **2012**.

10. Ellman, G., A new and rapid colorimetric determination of acetylcholinesterase activity. *Biochem. Pharmacol.* **1961**, *7*, 88-95.

11. Organization, W. H., Guidelines for testing mosquito adulticides for indoor residual spraying and treatment of mosquito nets. **2006**.

12. Pridgeon, J. W., *et al.*, Susceptibility of *Aedes aegypti*, *Culex quinquefasciatus* say, and *Anopheles quadrimaculatus* say to 19 pesticides with different modes of action. *J. Med. Entomol.* **2008**, *45*, 82-87.

13. Aberman, A., *et al.*, Silicon-Compounds as Substrates and Inhibitors of Acetylcholinesterase. *Biochim. Biophys. Acta* **1984**, *791*, 278-280.

14. Sieburth, S. M., *et al.*, New Insecticides by Replacement of Carbon by Other Group-IV Elements. *Pest. Sci.* **1990**, *29*, 215-225.

15. Wong, D. M., *et. al.*, Aryl methylcarbamates: potency and selectivity towards wild-type and carbamate-insensitive (G119S) *anopheles gambiae* acetylcholinesterase, and toxicity to G3 Strain *An. gambiae*. *Chem.-Biol. Interact.* **2012**.

16. Kalia, J.; Raines, R. T., Hydrolytic stability of hydrazones and oximes. *Angew. Chem. Int. Ed.* **2008**, *47*, 7523-7526.

17. Holan, G.; Smith, D. R. J., A new selective insecticidal uncoupler of oxidative-phosphorylation. *Experientia* **1986**, *42*, 558-560.

18. Wu, J., *et al.*, Design, synthesis and insecticidal activities of novel pyrazole amides containing hydrazone substructures. *Pest Manag. Sci.* **2012**, *68*, 801-810.

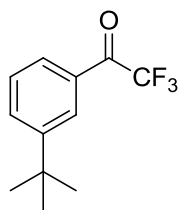
19. Aggarwal, N., *et al.*, Synthesis of Nalidixic Acid Based Hydrazones as Novel Pesticides. *J. Agric. Food Chem.* **2010**, *58*, 3056-3061.

Chapter 3: Experimental

3.1 General

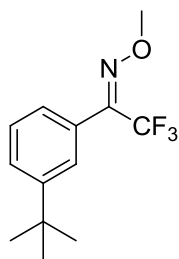
NMR spectra were performed on a Varian Inova-400 (400 MHz) or a JEOL EclipsePlus-500 (500 MHz). ^{13}C NMR spectra were correspondingly recorded at 101 MHz or 126 MHz. ^{19}F NMR spectra were correspondingly recorded at 376 MHz or 471 MHz. Chemical shifts for ^1H and ^{13}C are presented in ppm against tetramethylsilane with an internal standard as a reference and ^{19}F NMR used hexafluorobenzene as a reference. Deuterated solvents were purchased from Cambridge Isotope Laboratories. The following abbreviations are used to show coupling in the spectra: s (singlet), d (doublet), t (triplet), q (quartet), qt (quintet), bs (broad singlet), and m (multiplet). High resolution mass spectroscopy (HRMS) was performed on an Agilent 6220 LC/MS time-of-flight mass spectrometer using either electrospray ionization (ESI) or extracted ion chromatogram (EIC). Column chromatography was performed by using flash grade silica gel (SiO_2 , 32-63 μm). Thin layer chromatography (TLC) was performed on EMD silica gel 60 F₂₅₄ plates. Compounds prepared for enzyme or mosquito bioassay were >95% pure as judged by ^1H and ^{19}F NMR.

3.2 Procedures



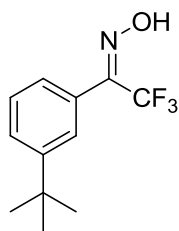
1-(3-(*tert*-butyl)phenyl)-2,2,2-trifluoroethanone (2-4a) : The literature procedure was followed.¹ 1-bromo-3-(*tert*-butyl)benzene (1.0 g, 4.7 mmol) was dissolved in dry THF at -78 °C under nitrogen and was stirred for 10 min. *n*-BuLi (2.5 M in hexanes, 2.0 mL, 4.9 mmol) was added drop wise to the solution was stirred for 2 h at -78 °C. After two hours, methyl trifluoroacetate (0.52 mL, 5.6 mmol) was added drop wise and stirred for 30 min at -78 °C. The solution was then allowed to warm up to room

temperature and let stir for overnight. The mixture was then quenched with NH_4Cl (20 mL) and extracted with ether (50 mL), and dried over MgSO_4 . After concentration in vacuo (note: remove shortly after the ether is removed, because the compound is quite volatile), the residue was purified with flash chromatography over silica gel (hexane: ether = 98:2) to yield the product as a yellow liquid in 61% yield (0.65 g). ^1H NMR (500 MHz, DMSO-d_6) δ 8.04 (s, 1H), 7.99 (d, $J = 7.9$ Hz, 1H), 7.92 (d, $J = 7.9$ Hz, 1H), 7.67 (t, $J = 7.9$ Hz, 1H), 1.37 (s, 9H); ^{13}C NMR (126 MHz, DMSO-d_6) δ 180.85 (q, $^2J_{\text{CF}} = 34$ Hz), 153.05, 134.50, 130.39, 130.05, 128.23, 126.72, 117.37 (q, $^1J_{\text{CF}} = 292$ Hz), 35.58, 31.64; ^{19}F NMR (376 MHz, CDCl_3) δ -74.37; HRMS (Mixed EIC) m/z calcd for $\text{C}_{12}\text{H}_{13}\text{F}_3\text{O}$ [M] 230.0918, found 230.0921.

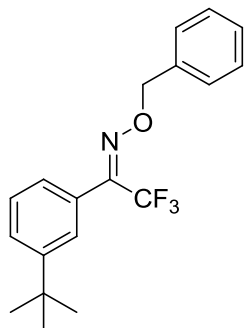


1-(3-(tert-butyl)phenyl)-2,2,2-trifluoroethanone O-methyl oxime (2-5a): A standard literature procedure for oxime ether synthesis was followed.² O-methylhydroxylamine hydrochloride (0.24 g, 2.6 mmol) and sodium hydroxide (0.12 g, 2.9 mmol) was dissolved in ethanol (7 mL). A solution of **2-4a** (0.20 g, .87 mmol) in ethanol (2 mL) was added into the mixture. The resulting white suspension was refluxed overnight then concentrated in vacuo, extracted with dichloromethane (40 mL) and water (20 mL). The dichloromethane fraction was dried with MgSO_4 and concentrated in vacuo. The residue was purified using flash chromatography on silica gel (hexane : ethyl acetate = 98:2) to yield the product as diastereomers as a yellow liquid in 97% yield (0.246 g). ^1H NMR (500 MHz, DMSO-d_6) δ 7.59 (t, $J = 9.1$ Hz, 1H), 7.47-7.43 (m, 2H), 7.29 (d, $J = 7.5$ Hz, 1H), 4.03 (s, 3H), 1.30 (s, 9H); ^{13}C NMR (126 MHz, DMSO-d_6) δ 151.14, 145.87, 145.71, 145.61, 145.48, 129.03, 128.47, 128.42, 127.51, 127.48, 125.87, 125.55,

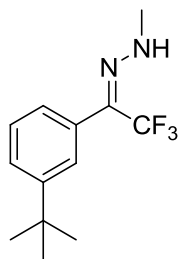
124.88, 124.74, 124.33, 121.52, 119.34, 119.12, 116.88, 63.97, 63.58, 34.47, 34.46, 30.88, 30.87, the doubling of numerous resonances suggests an *E/Z* isomer mixture; ^{19}F NMR (376 MHz, CDCl_3) δ -65.43, -69.34 *E/Z* isomers in a 5 : 4 ratio; HRMS (Mixed EIC) m/z calcd for $\text{C}_{13}\text{H}_{17}\text{F}_3\text{NO}$ $[\text{M}+\text{H}]^+$ 260.1262, found 260.1263.



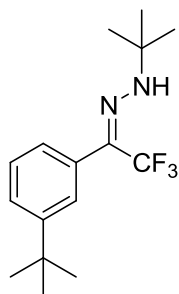
1-(3-(tert-butyl)phenyl)-2,2,2-trifluoroethanone oxime (2-6a): A standard literature procedure for oxime synthesis was followed.² Hydroxylamine hydrochloride (0.18 g, 2.6 mmol) and sodium hydroxide (0.10 g, 2.6 mmol) was dissolved in ethanol (7 mL). A solution of **2-4a** (0.20 g, 0.87 mmol) in ethanol (2 mL) was added into the mixture. The resulting white suspension was refluxed overnight then concentrated in vacuo, extracted with dichloromethane (40 mL) and water (20 mL). The dichloromethane fraction was dried with MgSO_4 and concentrated in vacuo. The residue was purified using flash chromatography on silica gel (hexane: ethyl acetate = 98:2) to yield the product as diastereomers as a clear liquid in 85% yield (0.18 g). ^1H NMR (500 MHz, DMSO-d_6) δ 12.87 (s, 1H), 7.61 – 7.55 (m, 1H), 7.47 (d, $J = 7.9$ Hz, 1H), 7.46 – 7.41 (m, 1H), 7.35 – 7.27 (m, 1H), 1.32 (s, 9H); ^{13}C NMR (126 MHz, DMSO-d_6) δ 150.98, 150.90, 145.14, 145.07, 144.89, 144.84, 130.13, 128.32, 128.29, 127.05, 126.88, 126.44, 125.60, 125.30, 124.93, 124.78, 122.22, 120.04, 119.59, 117.34, 66.97, 64.87, 34.43, 34.42, 30.91, the doubling of numerous resonances suggests an *E/Z* isomer mixture; ^{19}F NMR (376 MHz, CDCl_3) δ -65.51, -69.20, *E/Z* isomers in a 10:9 ratio; HRMS (Mixed EIC) m/z calcd for $\text{C}_{12}\text{H}_{14}\text{F}_3\text{NO}$ $[\text{M}-\text{H}]^-$ 244.0949, found 244.0947.



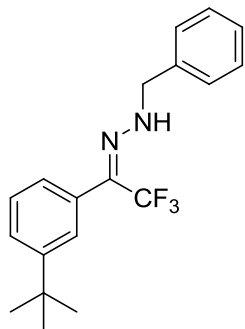
1-(3-(tert-butyl)phenyl)-2,2,2-trifluoroethane O-benzyl oxime (2-7a): A standard literature procedure for oxime ether synthesis was followed.² O-benzylhydroxylamine hydrochloride (0.42 g, 2.6 mmol) and sodium hydroxide (0.10 g, 2.6 mmol) was dissolved in ethanol (7 mL). A solution of **2-4a** (0.20 g, 0.87 mmol) in ethanol (2 mL) was added into the mixture. The resulting white suspension was refluxed overnight then concentrated in vacuo, extracted with dichloromethane (40 mL) and water (20 mL). The dichloromethane fraction was dried with MgSO₄ and concentrated in vacuo. The residue was purified using flash chromatography on silica gel (hexane : ethyl acetate = 99.5:0.5) to yield the product as a clear liquid in 39% yield (0.113 g). ¹H NMR (500 MHz, CDCl₃) δ 7.51 – 7.43 (m, 2H), 7.39 – 7.30 (m, 6H), 7.26 (m, 1H), 5.24 (s, 2H), 1.29 (s, 9H); ¹³C NMR (126 MHz, CDCl₃) δ 151.20, 146.92 (q, ²J_{CF} = 32 Hz), 136.38, 128.44, 128.31, 128.23, 128.07, 127.28, 126.51, 125.86, 125.51, 120.65 (q, ¹J_{CF} = 276 Hz), 77.99, 34.75, 31.15; ¹⁹F NMR (376 MHz, cdcl₃) δ -69.08; HRMS (Mixed EIC) *m/z* calcd for C₁₉H₂₀F₃NO [M+H]⁺ 336.1575, found 336.1585.



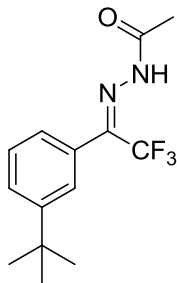
1-(1-(3-(tert-butyl)phenyl)-2,2,2-trifluoroethylidene)-2-methylhydrazine (2-10a): A standard literature procedure for hydrazone synthesis was followed.³ A solution of **2-4a** (0.2g, 0.869 mmol) and ethanol (7 mL) was made at room temperature. Methylhydrazine (0.04 g, 0.95 mmol) and 4 drops of acetic acid were then added and refluxed for overnight. The mixture was then extracted with water (20 mL) and ether (40 mL). The ether fraction was dried with MgSO₄ followed by concentration in vacuo. The residue was purified using flash chromatography over silica gel (hexane: ether = 19:1) to furnish the product in 45% yield (0.099 g). Note that the flash column has to be done relatively quickly due to decomposition of product. ¹H (500 MHz, CDCl₃) δ 7.48 (ddd, *J* = 8.0, 2.0, 1.2 Hz, 1H), 7.42 (t, 7.7, 1H), 7.33 (s, 1H), 7.14 (d, *J* = 7.7 Hz, 1H), 5.78 – 5.68 (m, 1H), 3.06 – 3.02 (m, 3H), 1.33 (s, 9H); ¹³C NMR (126 MHz, CDCl₃) δ 152.66, 130.88 (q, ²*J*_{CF} = 34 Hz), 129.12, 127.41, 127.00, 125.91, 125.73, 121.50 (q, ¹*J*_{CF} = 272 Hz), 37.49, 34.85, 31.22; ¹⁹F (471 MHz, CDCl₃, C₆F₆) δ -74.37; HRMS (Mixed EIC) *m/z* calcd for C₁₃H₁₈F₃N₂ [M+H]⁺ 259.1422, found 259.1424.



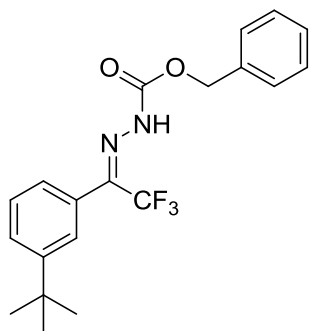
1-(tert-butyl)-2-(1-(3-(tert-butyl)phenyl)-2,2,2-trifluoroethylidene)hydrazine (2-11a): A standard literature procedure for hydrazone synthesis was followed.³ A solution of **2-4a** (0.2 g, 0.869 mmol) and ethanol (7 mL) was made at room temperature. *Tert*-butylhydrazine hydrochloride (0.12 g, 0.95 mmol) and sodium acetate (0.07g, 0.95 mmol) were added and refluxed for overnight. The mixture was then extracted with water (20 mL) and ether (40 mL). The ether fraction was dried with MgSO₄ followed by concentration in vacuo. The residue was purified using flash chromatography over silica gel (hexane: ether = 99.5: 0.5) to furnish the product as a colorless liquid in 19% yield (0.049 g). Note that the flash column has to be done relatively quickly due to decomposition of product. ¹H (500 MHz, CDCl₃) δ 7.48 – 7.45 (m, 1H), 7.42 (t, *J* = 7.5 Hz, 1H), 7.34 (s, 1H), 7.14 (d, *J* = 7.5 Hz, 1H), 5.72 (s, 1H), 1.33 (s, 9H), 1.18 (s, 9H); ¹³C NMR (126 MHz, CDCl₃) δ 152.44, 130.30 (q, ²*J*_{CF} = 34 Hz), 129.15, 127.69, 126.63, 125.83, 125.82, 121.66 (q, ¹*J*_{CF} = 272 Hz), 54.24, 34.84, 31.21, 28.47; ¹⁹F (471 MHz, CDCl₃, C₆F₆) δ -69.07; HRMS (Mixed EIC) *m/z* calcd for C₁₆H₂₄F₃N₂ [M+H]⁺ 301.1892, found 301.1911.



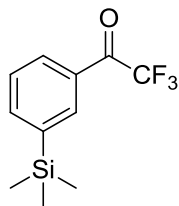
1-benzyl-2-(1-(3-(tert-butyl)phenyl)-2,2,2-trifluoroethylidene)hydrazine (2-12a): A standard literature procedure for hydrazone synthesis was followed.⁴ A solution of **2-4a** (0.2 g, 0.869 mmol) and ethanol (7 mL) was made at room temperature. Benzylhydrazine hydrochloride (0.19 g, 0.95 mmol) and sodium acetate (0.16 g, 1.95 mmol) were added and refluxed for overnight. The mixture was then extracted with water (20 mL) and ether (40 mL). The ether fraction was dried with MgSO₄ followed by concentration in vacuo. The residue was purified using flash chromatography over silica gel (hexane: ether = 4: 1) to furnish the product as a colorless liquid in 28% yield (0.08 g). Note that the flash column has to be done relatively quickly due to decomposition of product. ¹H (400 MHz, CDCl₃) δ 7.48 – 7.21 (m, 8H), 7.12 (d, *J* = 7.4 Hz, 1H), 6.05 (t, *J* = 5.1 Hz, 1H), 4.49 (d, *J* = 5.1 Hz, 2H), 1.29 (s, 9H); ¹³C NMR (101 MHz, cdcl₃) δ 152.65, 138.33, 131.87 (q, ²*J*_{CF} = 34 Hz), 129.26, 128.63, 127.79, 127.56, 127.32, 127.06, 125.79, 125.64, 121.45 (q, ¹*J*_{CF} = 270 Hz), 54.76, 34.81, 31.16; ¹⁹F (376 MHz, CDCl₃, C₆F₆) -71.25; HRMS (Mixed ESI) *m/z* calcd for C₁₉H₂₂F₃N₂ [M+H]⁺ 335.1735, found 335.1757.



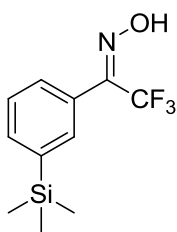
N'-(1-(3-(tert-butyl)phenyl)-2,2,2-trifluoroethylidene)acetohydrazide (2-13a): A standard literature procedure for hydrazone synthesis was followed.³ A solution of **2-4a** (0.2 g, 0.869 mmol) and ethanol (7 mL) was made at room temperature. Acetylhydrazide (0.07 g, 0.95 mmol) and 4 drops of acetic acid were then added and refluxed for overnight. The mixture was then extracted with water (20 mL) and ether (40 mL). The ether fraction was dried with MgSO₄ followed by concentration in vacuo. The residue was purified using flash chromatography over silica gel (hexane: ether = 4:1) to furnish the product in 15% (0.037 g). Note that the flash column has to be done relatively quickly due to decomposition of product. ¹H (500 MHz, CDCl₃) δ 8.46 (s, 1H), 7.58 (ddd, *J* = 8.0, 1.9, 1.1 Hz, 1H), 7.47 (t, *J* = 7.8 Hz, 1H), 7.28 (s, 1H), 7.10 (d, *J* = 7.8 Hz, 1H), 2.37 (s, 3H), 1.34 (s, 9H); ¹³C NMR (126 MHz, CDCl₃) δ 173.12, 139.14 (q, ²*J*_{CF} = 35 Hz), 129.71, 128.52, 125.45, 125.24, 124.85, 120.34 (q, ¹*J*_{CF} = 275 Hz), 34.97, 31.15, 20.28; ¹⁹F (471 MHz, CDCl₃, C₆F₆) δ -71.45; HRMS (ESI) *m/z* calcd for C₁₄H₂₁F₃N₃O [M+NH₄]⁺ 304.1637, found 304.1647.



Benzyl 2-(1-(3-(tert-butyl)phenyl)-2,2,2-trifluoroethylidene)hydrazinecarboxylate (2-14a): A standard literature procedure for hydrazone synthesis was followed.³ A solution of **2-4a** (0.2 g, 0.869 mmol) and ethanol (7 mL) was made at room temperature. Benzyl carbazate (0.19 g, 1.12 mmol) and 4 drops of acetic acid were then added and refluxed for overnight. The mixture was then extracted with water (20 mL) and ether (40 mL). The ether fraction was dried with MgSO_4 followed by concentration in vacuo. The residue was purified using flash chromatography over silica gel (hexane: ether = 4:1) to furnish the product in 10% yield (0.04 g). Note flash column has to be done relatively fast due to decomposition of product. ^1H NMR (500 MHz, CDCl_3) δ 8.05 (s, 1H), 7.57 (ddd, J = 8.0, 2.0, 1.1 Hz, 1H), 7.51 – 7.42 (m, 1H), 7.41 – 7.31 (m, 5H), 7.29 (s, 1H), 7.10 (d, J = 7.5 Hz, 1H), 5.25 (s, 2H), 1.33 (s, 9H); ^{13}C NMR (126 MHz, CDCl_3) δ 152.40, 134.09, 128.68, 127.68, 127.65 (b), 127.45, 124.51, 124.15, 123.87, 122.61, 120.43, 118.25, 67.25, 33.96, 30.13; ^{19}F NMR (376 MHz, CDCl_3) δ -71.30; HRMS (ESI) m/z calcd for $\text{C}_{20}\text{H}_{25}\text{F}_3\text{N}_3\text{O}_2$ $[\text{M}+\text{NH}_4]^+$ 396.1899, found 396.1924.

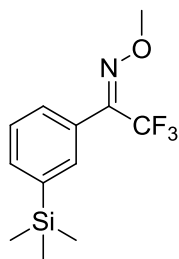


2,2,2-trifluoro-1-(3-(trimethylsilyl)phenyl)ethanone (2-4b): The literature procedure was followed.¹ **2-4b** (1.0 g, 4.4 mmol) was dissolved in dry THF at -78 °C under nitrogen and was stirred for 10 min. *n*-BuLi (2.5 M in hexanes, 1.8 mL, 4.6 mmol) was added dropwise to the solution was stirred for 2 h at -78 °C. After two hours, methyl trifluoroacetate (0.52 mL, 5.2 mmol) was added dropwise and stirred for 30 min at -78 °C. The solution was then allowed to warm up to room temperature and let stir for overnight. The mixture was then quenched with NH₄Cl (20 mL) and extracted with ether (50 mL), and dried over MgSO₄. After concentration in vacuo (note: remove shortly after the ether is removed, because the compound is quite volatile), the residue was purified with flash chromatography over silica gel (hexane: ether = 98:2) to yield the product as a liquid in 71% yield (0.727 g). ¹H NMR (500 MHz, CDCl₃) δ 8.21 (s, 1H), 8.03 (d, *J* = 7.3 Hz, 1H), 7.85 (d, *J* = 7.3 Hz, 1H), 7.53 (t, *J* = 7.3 Hz, 1H), 0.32 (s, 9H); ¹³C NMR (126 MHz, CDCl₃) δ 181.08 (q, ²*J*_{CF} = 35 Hz), 142.49, 140.51, 134.96, 130.53, 129.42, 128.49, 116.41 q, (¹*J*_{CF} = 292 Hz), -1.20; ¹⁹F NMR (376 MHz, CDCl₃) δ -77.99; For reasons that we do not understand, this known compound did not give a successful mass spectrum under ESI conditions.



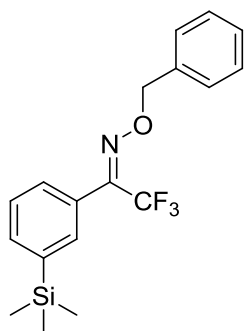
2,2,2-trifluoro-1-(3-(trimethylsilyl)phenyl)ethanone oxime (2-6b): A standard literature procedure for oxime synthesis was followed.² Hydroxylamine hydrochloride (0.17 g, 2.4 mmol) and sodium hydroxide (0.10 g, 2.6 mmol) was dissolved in ethanol (7 mL). A solution of **2-4b** (0.20 g, 0.81 mmol) in ethanol (2 mL) was added into the mixture. The resulting white suspension was refluxed overnight then concentrated in vacuo, extracted with dichloromethane (40 mL) and water (20 mL). The dichloromethane fraction was dried with MgSO₄ and concentrated in vacuo. The residue was purified

using flash chromatography on silica gel (hexane : ethyl acetate = 9:1) to yield the product as diastereomers as a clear liquid in 35% yield (0.74 g). ^1H NMR (500 MHz, CDCl_3) δ 9.62 (d, J = 107.2 Hz, 1H), 7.73 – 7.27 (m, 4H), 0.28 (d, J = 4.1 Hz, 9H); ^{13}C NMR (126 MHz, CDCl_3) δ 148.75, 148.59, 148.50, 148.40, 148.33, 148.26, 148.07, 148.02, 147.81, 141.54, 141.43, 135.66, 135.42, 133.27, 133.17, 129.54, 129.05, 128.82, 127.96, 127.94, 125.65, 124.09, 121.90, 119.72, 119.67, 117.42, 115.17, -1.16, the doubling of numerous resonances suggests an *E/Z* isomer mixture; ^{19}F NMR (376 MHz, CDCl_3) δ -65.50, -69.87, *E/Z* isomers in a 10 : 7 ratio; HRMS (Mixed EIC) m/z calcd for $\text{C}_{22}\text{H}_{29}\text{F}_6\text{N}_2\text{O}_2\text{Si}_2$ $[\text{2M}+\text{H}]^+$ 523.1672, found 523.1696.

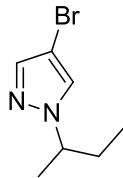


2,2,2-trifluoro-1-(3-(trimethylsilyl)phenyl)ethanone O-methyl oxime (2-5b): A standard literature procedure for oxime ether synthesis was followed.² O-methylhydroxylamine hydrochloride (0.20 g, 2.4 mmol) and sodium hydroxide (0.10 g, 2.9 mmol) was dissolved in ethanol (7 mL). A solution of **2-4b** (0.20 g, 0.81 mmol) in ethanol (2 mL) was added into the mixture. The resulting white suspension was refluxed overnight then concentrated in vacuo, extracted with dichloromethane (40 mL) and water (20 mL). The dichloromethane fraction was dried with MgSO_4 and concentrated in vacuo. The residue was purified using flash chromatography on silica gel (hexane: ethyl acetate = 99:1) to yield the product as diastereomers as a clear liquid in 64% yield (0.144 g). ^1H NMR (500 MHz, CDCl_3) δ 7.34 – 7.25 (m, 4H), 4.04 (s, 3H), 0.23 (s, 9H); ^{13}C NMR (126 MHz, CDCl_3) δ 147.46, 147.21, 146.95, 146.70, 141.12, 136.56, 135.36, 133.74, 128.94, 128.69, 128.55, 128.49, 127.91, 126.57, 124.22, 122.04, 119.85, 117.66, 78.26, -1.13, -1.16, the doubling of numerous resonances suggests an *E/Z* isomer mixture; ^{19}F NMR (376 MHz,

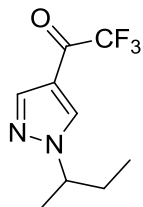
CDCl_3) δ -65.45, -69.11, *E/Z* isomers in a ratio ; HRMS (Mixed EIC) *m/z* calcd for $\text{C}_{12}\text{H}_{17}\text{F}_3\text{NOSi}$ $[\text{M}+\text{H}]^+$ 276.1031, found 276.1027.



2,2,2-trifluoro-1-(3-(trimethylsilyl)phenyl)ethanone O-benzyl oxime (2-7b): A standard literature procedure for oxime ether synthesis was followed.² O-benzylhydroxylamine hydrochloride (0.387 g, 2.4 mmol) and sodium hydroxide (0.10 g, 2.4 mmol) was dissolved in ethanol (7 mL). A solution of **2-4b** (0.20 g, .81 mmol) in ethanol (2 mL) was added into the mixture. The resulting white suspension was refluxed overnight then concentrated in vacuo, extracted with dichloromethane (40 mL) and water (20 mL). The dichloromethane fraction was dried with MgSO_4 and concentrated in vacuo. The residue was purified using flash chromatography on silica gel (hexane : ethyl acetate = 9:1) to yield the product as diastereomers as a clear liquid in 73% yield (0.207 g). ^1H NMR (400 MHz, CDCl_3) δ 7.61 (s, 1H), 7.55 (dt, *J* = 7.2, 1.2 Hz, 1H), 7.42 (d, *J* = 7.8 Hz, 1H), 7.39 – 7.34 (m, 1H), 7.33 – 7.25 (m, 5H), 5.21 (s, 2H), 0.27 (s, 9H); ^{13}C NMR (101 MHz, CDCl_3) δ 147.09, 147.07, 146.77, 146.47, 146.45, 146.17, 146.13, 141.10, 141.06, 135.18, 135.01, 133.05, 128.94, 128.77, 127.69, 127.67, 126.36, 124.72, 122.59, 121.99, 119.78, 119.26, 116.97, 116.53, 114.16, 63.87, 63.53, -1.30, -1.33, the doubling of numerous resonances suggests an *E/Z* isomer mixture; ^{19}F NMR (376 MHz, CDCl_3) δ -65.46, -69.42, *E/Z* isomers in a ; HRMS (ESI) *m/z* calcd for $\text{C}_{18}\text{H}_{21}\text{F}_3\text{NOSi}$ $[\text{M}+\text{H}]^+$ 352.1345, found 352.1353.

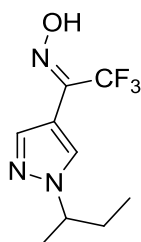


4-bromo-1-(sec-butyl)-1H-pyrazole (2-3c): To a solution of sodium hydride (60% dispersion in mineral oil, 0.73g 19.1 mmol) in DMF (8 mL), a solution of pyrazole (1 g, 14.7 mmol) in DMF (2 mL) was added drop wise. The solution was then warmed to room temperature for 2 hours to which 2-bromobutane (2.1 mL, 22.1 mmol) was then added drop wise and stirred for overnight. The resulting mixture was extracted with ether (40 mL) and brine (20 mL) and dried with MgSO_4 . The ether layer was concentrated in vacuo to furnish the residue. The residue was mixed in water (20 mL) and NBS (3.12 g, 17.5 mmol) was added. TLC was used to detect progression of reaction. After 2 hours, the mixture was extracted with DCM (50 mL) and dried with MgSO_4 . The residue was purified using flash chromatography on silica gel (hexane : ethyl acetate = 4:1) to yield the product as a clear liquid in 45% yield (1.6 g). ^1H NMR (500 MHz, CDCl_3) δ 8.26 (s, 1H), 8.07 (s, 1H), 4.40 – 4.32 (m, 1H), 1.99-1.90 (m, 1H), 1.88-1.80 (m, 1H), 1.52 (d, $J = 6.8$ Hz, 3H), 0.84 (t, $J = 7.4$ Hz, 3H); ^{13}C NMR (101 MHz, CDCl_3) δ 140.65, 131.43, 113.57, 61.01, 29.45, 20.43, 10.33.



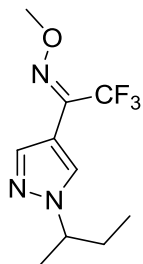
1-(1-(sec-butyl)-1H-pyrazol-4-yl)-2,2,2-trifluoroethanone (2-4c): A standard literature procedure for TFK synthesis was followed.¹ **2-3c** (1.0 g, 5.0 mmol) was dissolved in dry THF (15 mL) at -78°C under nitrogen and was stirred for 10 min. *n*-BuLi (2.5 M in hexanes, 2.1 mL, 5.2 mmol) was added dropwise to

the solution was stirred for 2 hours at -78 °C. After two hours, methyl trifluoroacetate (0.5 mL, 6.0 mmol) was added dropwise and stirred for 30 min at -78 °C. The solution was then allowed to warm up to room temperature and let stir for overnight. The mixture was then quenched with NH₄Cl (20 mL) and extracted with ether (50 mL), and dried over MgSO₄. After concentration in vacuo (note: remove shortly after the ether is removed, because the compound is quite volatile), the residue was purified with flash chromatography over silica gel (hexane: ether = 98:2) to yield the product as a clear liquid in 67% yield (0.74 g). ¹H NMR (500 MHz, CDCl₃) δ 8.08 (d, *J* = 9.0 Hz, 2H), 4.29 (dq, *J* = 13.3, 6.7 Hz, 1H), 1.96 (dp, *J* = 15.1, 7.7 Hz, 1H), 1.84 (dq, *J* = 13.8, 7.4 Hz, 1H), 1.55 (d, *J* = 6.8 Hz, 3H), 0.84 (t, *J* = 7.4 Hz, 3H); ¹³C NMR (101 MHz, CDCl₃) δ 174.53 (q, ²*J*_{CF} = 37 Hz), 141.65, 132.56, , 115.77, 116.45 (q, ¹*J*_{CF} = 291 Hz), 61.11, 29.69, 20.48, 10.34; ¹⁹F NMR (376 MHz, CDCl₃) δ -77.99; HRMS (Mixed EIC) *m/z* calcd for C₉H₁₂F₃N₂O [M+H]⁺ 221.0901, found 221.0897.

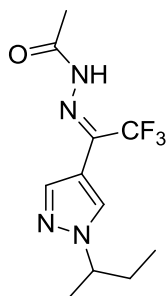


1-(1-(sec-butyl)-1H-pyrazol-4-yl)-2,2,2-trifluoroethanone oxime (2-6c): A standard literature procedure for oxime synthesis was followed.² Hydroxylamine hydrochloride (0.38 g, 5.5 mmol) and sodium hydroxide (0.22 g, 5.5 mmol) was dissolved in ethanol (7 mL). A solution of **2-4c** (0.40 g, 1.8 mmol) in ethanol (2 mL) was added into the mixture. The resulting white suspension was refluxed overnight then concentrated in vacuo, extracted with dichloromethane (40 mL) and water (20 mL). The dichloromethane fraction was dried with MgSO₄ and concentrated in vacuo. The residue was purified using flash chromatography on silica gel (hexane : ethyl acetate = 17:3) to yield the product as a white solid in 26% yield (0.113 g). ¹H NMR (400 MHz, CDCl₃) δ 9.06 (s, 1H), 8.20 (s, 1H), 8.01 (s, 1H), 4.28 (s,

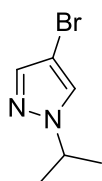
1H), 2.03 – 1.90 (m, 1H), 1.89 – 1.75 (m, 1H), 1.53 (d, 3H), 0.84 (t, 3H); ¹³C NMR (101 MHz, CDCl₃) δ 139.76, 131.01, 122.39, 119.66, 106.94, 60.51, 29.92, 20.69, 10.49; ¹⁹F NMR (376 MHz, CDCl₃) δ -69.26; HRMS (ESI) *m/z* calcd for C₉H₁₃F₃N₃O [M+H]⁺ 236.1010, found 236.1001.



1-(1-(sec-butyl)-1H-pyrazol-4-yl)-2,2,2-trifluoroethanone O-methyl oxime (2-5c): A standard literature procedure for oxime ether synthesis was followed.² O-methylhydroxylamine hydrochloride (0.46 g, 5.5 mmol) and sodium hydroxide (0.2 g, 5.5 mmol) was dissolved in ethanol (10 mL). A solution of **2-4c** (0.40 g, 1.8 mmol) in ethanol (5 mL) was added into the mixture. The resulting white suspension was refluxed overnight then concentrated in vacuo, extracted with dichloromethane (40 mL) and water (20 mL). The dichloromethane fraction was dried with MgSO₄ and concentrated in vacuo. The residue was purified using flash chromatography on silica gel (hexane : ethyl acetate = 99:1) to yield the product as a clear liquid in 77% yield (0.348 g). ¹H NMR (500 MHz, CDCl₃-d) δ 8.06 (s, 1H), 7.94 (s, 1H), 4.49 – 4.18 (m, 1H), 4.14 (s, 3H), 2.10 – 1.87 (m, 1H), 1.81 (dq, *J* = 14.8, 7.4, 5.9 Hz, 1H), 1.52 (d, *J* = 6.8 Hz, 3H), 0.83 (t, *J* = 7.4 Hz, 3H); ¹³C NMR (126 MHz, CDCl₃) δ 139.81, 139.16, 130.61, 120.98 (q, ¹*J*_{CF} = 275 Hz), 107.46, 63.67, 60.45, 29.93, 20.71, 10.51; ¹⁹F NMR (471 MHz, CDCl₃) δ -68.95; HRMS (Mixed EIC) *m/z* calcd for C₁₀H₁₅F₃N₃O [M+H]⁺ 250.1167, found 250.1159.

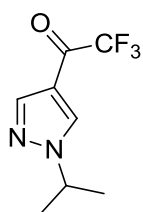


N'-(1-(1-(sec-butyl)-1H-pyrazol-4-yl)-2,2,2-trifluoroethylidene)acetohydrazide (2-13c): A standard literature procedure for hydrazone synthesis was followed.⁵ A neat mixture of 2-4c (0.1 g, .45 mmol) and acetylhydrazide (0.034 g, 0.45 mmol) were combined at 0 °C for 25 minutes. It was brought to room temperature and left for an additional 90 minutes. MgSO₄ was then added to the mixture and left for 15 minutes following washing with ether, THF, and hexane. Concentration of the solvents in vacuo furnished the product in 36% (0.045 g) with no further purification needed. ¹H NMR (500 MHz, Acetone-d₆) δ 9.08 (s, 1H), 8.57 (s, 1H), 8.12 (s, 1H), 4.58 – 4.41 (m, 1H), 2.88 (s, 3H), 2.02 – 1.81 (m, 2H), 1.54 (d, *J* = 6.7 Hz, 3H), 0.80 (t, *J* = 7.4 Hz, 3H); ¹³C NMR (126 MHz, Acetone-d₆) δ 174.86 (q, ²*J*_{CF} = 36 Hz), 172.65, 149.30, 142.05, 134.99, 116.11, 117.35 (q, ¹*J*_{CF} = 290 Hz), 61.64, 20.78, 20.60, 10.63; ¹⁹F NMR (471 MHz, Acetone-d₆) δ -75.95; HRMS (Mixed EIC) *m/z* calcd for C₁₀H₁₂F₃N₂O [M+H]⁺ 233.0902, found 233.0898.



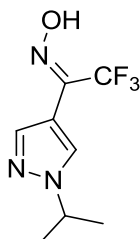
4-bromo-1-isopropyl-1H-pyrazole (2-3e): To a solution of sodium hydride (60% dispersion in mineral oil, 0.76 g 19.1 mmol) in DMF (8 mL), a solution of pyrazole (1.0 g, 14.7 mmol) in DMF (2 mL) was added drop wise. The solution was then warmed to room temperature for 2 hours to which 2-bromopropane (2.1 mL, 22.0 mmol) was then added drop wise and stirred for overnight. The resulting mixture was

extracted with ether (40 mL) and brine (20 mL) and dried with MgSO_4 . The ether layer was concentrated in vacuo to furnish the residue. The residue was mixed in water (20 mL) and NBS (2.6 g, 17.5 mmol) was added. TLC was used to detect progression of reaction. After 2 hours, the mixture was extracted with DCM (50 mL) and dried with MgSO_4 . The residue was purified using flash chromatography on silica gel (hexane : ethyl acetate = 4:1) to yield the product as a clear liquid in 49% yield (1.34 g). ^1H NMR (500 MHz, CDCl_3) δ 8.26 (s, 1H), 8.07 (s, 1H), 4.63 – 4.52 (m, 1H), 1.62 (d, J = 6.7 Hz, 6H); ^{13}C NMR (126 MHz, CDCl_3) δ 140.53, 130.42, 119.94, 63.98, 22.81.

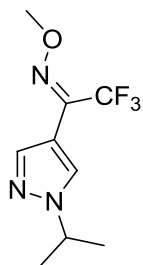


2,2-trifluoro-1-(1-isopropyl-1H-pyrazol-4-yl)ethanone (2-4e): A standard literature procedure for TFK synthesis was followed.¹ 2-2e (1.3 g, 7.1 mmol) was dissolved in dry THF (15 mL) at $-78\text{ }^\circ\text{C}$ under nitrogen and was stirred for 10 min. *n*-BuLi (2.5 M in hexanes, 2.96 mL, 7.4 mmol) was added drop wise to the solution was stirred for 2 h at $-78\text{ }^\circ\text{C}$. After two hours, methyl trifluoroacetate (0.85 mL, 8.5 mmol) was added drop wise and stirred for 30 min at $-78\text{ }^\circ\text{C}$. The solution was then allowed to warm up to room temperature and let stir for overnight. The mixture was then quenched with NH_4Cl (20 mL) and extracted with ether (50 mL), and dried over MgSO_4 . After concentration in vacuo (note: remove shortly after the ether is removed, because the compound is quite volatile), the residue was purified with flash chromatography over silica gel (hexane: ether = 98:2) to yield the product as a liquid in 63% yield (0.922 g). ^1H NMR (500 MHz, CDCl_3) δ 8.10 (s, 1H), 8.08 (s, 1H), 4.63 – 4.52 (m, 1H), 1.57 (d, J = 6.7 Hz, 6H); ^{13}C NMR (126 MHz, CDCl_3) δ 174.42 (q, $^2J_{\text{CF}}$ = 37 Hz), 141.57, 131.65, 116.51 (q, $^1J_{\text{CF}}$ = 291 Hz), 115.94, 55.04,

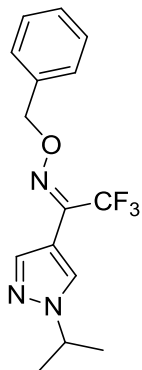
22.55; ^{19}F NMR (471 MHz, CDCl_3) δ -78.00; HRMS (Mixed EIC) m/z calcd for $\text{C}_9\text{H}_{13}\text{F}_3\text{N}_3\text{O}$ $[\text{M}+\text{H}]^+$ 236.1011, found 236.0998.



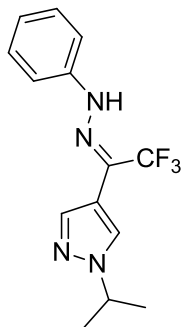
2,2,2-trifluoro-1-(1-(pentan-2-yl)-1H-pyrazol-4-yl)ethanone (6e): A standard literature procedure for oxime synthesis was followed.² Hydroxylamine hydrochloride (0.20 g, 2.9 mmol) and sodium hydroxide (0.12 g, 2.9 mmol) was dissolved in ethanol (7 mL). A solution of **2-4e** (0.20 g, 1.0 mmol) in ethanol (2 mL) was added into the mixture. The resulting white suspension was refluxed overnight then concentrated in vacuo, extracted with dichloromethane (40 mL) and water (20 mL). The dichloromethane fraction was dried with MgSO_4 and concentrated in vacuo. The residue was purified using flash chromatography on silica gel (hexane : ethyl acetate = 4:1) to yield the product as a white solid in 36% yield (0.045 g). ^1H NMR (500 MHz, CDCl_3) δ 8.10 (s, 1H), 8.31 (s, 1H), 7.81 (s, 1H), 4.63 – 4.52 (m, 1H), 1.57 (d, J = 6.7 Hz, 6H); ^{13}C NMR (126 MHz, CDCl_3) δ 140.01 (q, $^2J_{\text{CF}}$ = 32 Hz), 139.65, 131.17, 122.61 (q, $^1J_{\text{CF}}$ = 274 Hz), 108.01, 54.90, 22.86; ^{19}F NMR (471 MHz, CDCl_3) δ -78.00; HRMS (ESI) m/z calcd for $\text{C}_8\text{H}_{11}\text{F}_3\text{N}_3\text{O}$ $[\text{M}+\text{H}]^+$ 222.0854, found 222.0843.



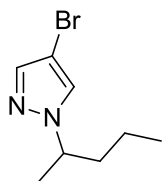
2,2,2-trifluoro-1-(1-isopropyl-1H-pyrazol-4-yl)ethanone O-methyl oxime (2-5e): A standard literature procedure for oxime ether synthesis was followed.² O-methylhydroxylamine hydrochloride (0.24 g, 2.9 mmol) and sodium hydroxide (0.12 g, 2.9 mmol) was dissolved in ethanol (7 mL). A solution of **2-4e** (0.20 g, 1.0 mmol) in ethanol (2 mL) was added into the mixture. The resulting white suspension was refluxed overnight then concentrated in vacuo, extracted with dichloromethane (40 mL) and water (20 mL). The dichloromethane fraction was dried with MgSO₄ and concentrated in vacuo. The residue was purified using flash chromatography on silica gel (hexane : ethyl acetate = 9:1) to yield the product as diastereomers as a clear liquid in 35% yield (0.10 g). ¹H NMR (500 MHz, CDCl₃) δ 8.37 – 7.56 (m, 2H), 4.81 – 4.39 (m, 1H), 4.09 (s, 3H), 1.54 (d, *J* = 6.7 Hz, 6H); ¹³C NMR (126 MHz, CDCl₃) δ 139.74, 139.73, 138.87 (q, ²*J*_{CF} = 32 Hz), 138.02, 129.72, 121.48 (q, ¹*J*_{CF} = 275 Hz), 107.58, 63.67, 54.34, 54.27, 22.76, 22.73, the doubling of numerous resonances suggests an *E/Z* isomer mixture; ¹⁹F NMR (471 MHz, CDCl₃) δ -67.12, -68.96, *E/Z* isomers in a 5 : 1 ratio ; HRMS (ESI) *m/z* calcd for C₉H₁₃F₃N₃O [M+H]⁺ 236.1010, found 236.1001.



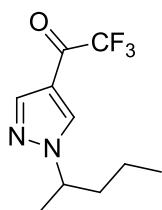
2,2-trifluoro-1-(1-isopropyl-1H-pyrazol-4-yl)ethanone O-benzyl oxime (2-7e): A standard literature procedure for oxime ether synthesis was followed.² O-benzylhydroxylamine hydrochloride (0.46 g, 2.9 mmol) and sodium hydroxide (0.12 g, 2.9 mmol) was dissolved in ethanol (7 mL). A solution of **2-4e** (0.20 g, 1.0 mmol) in ethanol (2 mL) was added into the mixture. The resulting white suspension was refluxed overnight then concentrated in vacuo, extracted with dichloromethane (40 mL) and water (20 mL). The dichloromethane fraction was dried with MgSO₄ and concentrated in vacuo. The residue was purified using flash chromatography on silica gel (hexane : ethyl acetate = 49:1) to yield the product as diastereomers as a clear liquid in 73% yield (0.21 g). ¹H NMR (500 MHz, CDCl₃) δ 8.27 – 7.55 (s, 2H), 7.49 – 7.28 (m, 5H), 5.31 (s, 2H), 4.48 (pd, *J* = 6.7, 1.8 Hz, 1H), 1.50 (dd, *J* = 7.5, 6.7 Hz, 6H); ¹³C NMR (126 MHz, CDCl₃) δ 140.47, 140.02, 139.40, 139.15, 138.14, 136.87, 136.29, 128.58, 128.42, 128.37, 128.03, 127.88, 126.60, 78.29, 77.81, 54.27, 54.26, 22.76, 22.68, the doubling of numerous resonances suggests an *E/Z* isomer mixture; ¹⁹F NMR (471 MHz, CDCl₃) δ -67.11, -68.85, *E/Z* isomers in a 10 : 9 ratio; HRMS (Mixed ESI) *m/z* calcd for C₁₅H₁₇F₃N₃O [M+H]⁺ 312.1324, found 312.1318.



1-isopropyl-4-(2,2,2-trifluoro-1-(2-phenylhydrazono)ethyl)-1H-pyrazole (2-9e): A standard literature procedure for hydrazone synthesis was followed.³ A solution of **2-4e** (0.20 g, 0.97 mmol) and ethanol (7 mL) was made at room temperature. Phenylhydrazine (0.11 g, 0.97 mmol) and 4 drops of acetic acid were then added and refluxed for overnight. The mixture was then extracted with water (20 mL) and ether (40 mL). The ether fraction was dried with MgSO₄ followed by concentration in vacuo. The residue was purified using flash chromatography over silica gel (hexane: ether = 7: 3) to furnish the product in 53% (0.152 g). Note that the flash column has to be done relatively quickly due to decomposition of product. ¹H (500 MHz, CDCl₃) δ 8.10 (s, 1H), 7.83 (s, 1H), 7.68 (s, 1H), 7.29 (dd, *J* = 8.5, 7.5 Hz, 2H), 7.18 – 7.09 (m, 2H), 6.96 (t, *J* = 7.4 Hz, 1H), 4.59 (p, *J* = 6.7 Hz, 1H), 1.58 (d, *J* = 6.7 Hz, 6H); ¹³C NMR (126 MHz, CDCl₃) δ 143.42, 138.04, 129.32, 126.87, 125.16 (q, ²*J*_{CF} = 35 Hz), 121.88, 121.61 (q, ¹*J*_{CF} = 273 Hz), 113.8, 106.79, 54.59, 22.73; ¹⁹F (471 MHz, CDCl₃, C₆F₆) δ -70.55; HRMS (Mixed ESI) *m/z* calcd for C₁₄H₁₆F₃N₄ [M+H]⁺ 297.1327, found 297.1327.

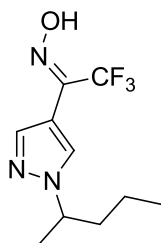


4-bromo-1-(pentan-2-yl)-1H-pyrazole (2-3d): To a solution of sodium hydride (60% dispersion in mineral oil, 1.5 g 38.2 mmol) in DMF (8 mL), a solution of pyrazole (2.0 g, 29.2 mmol) in DMF (2 mL) was added drop wise. The solution was then warmed to room temperature for 2 hours to which 2-bromopentane (5.5 mL, 44.1 mmol) was then added drop wise and stirred for overnight. The resulting mixture was extracted with ether (40 mL) and brine (20 mL) and dried with MgSO₄. The ether layer was concentrated in vacuo to furnish the residue. The residue was mixed in water (20 mL) and NBS (5.2 g, 29.2 mmol) was added. TLC was used to detect progression of reaction. After 2 hours, the mixture was extracted with DCM (50 mL) and dried with MgSO₄. The residue was purified using flash chromatography on silica gel (hexane : ethyl acetate = 4:1) to yield the product as a clear liquid in 55% yield (3.5 g). ¹H NMR (500 MHz, CDCl₃) δ 8.27 (s, 1H), 8.07 (s, 1H), 4.47 – 4.31 (m, 1H), 1.97-1.90 (m, 1H), 1.79-1.72 (m, 1H), 1.54 (d, *J* = 6.8 Hz, 3H), 1.33 – 1.11 (m, 2H), 0.92 (t, *J* = 7.4 Hz, 3H); ¹³C NMR (126 MHz, CDCl₃) δ 140.54, 139.56 130.25, 59.01, 38.36, 20.92, 19.21, 13.57.



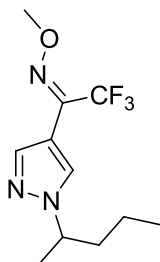
2,2,2-trifluoro-1-(1-(pentan-2-yl)-1H-pyrazol-4-yl)ethanone (2-4d): A standard literature procedure for TFK synthesis was followed.¹ 2-2d (3.5 g, 16.1 mmol) was dissolved in dry THF (15 mL) at -78 °C under nitrogen and was stirred for 10 min. *n*-BuLi (2.5 M in hexanes, 6.7 mL, 16.9 mmol) was added drop wise to the solution was stirred for 2 hours at -78 °C. After two hours, methyl trifluoroacetate (1.94 mL, 19.3

mmol) was added drop wise and stirred for 30 min at -78°C . The solution was then allowed to warm up to room temperature and let stir for overnight. The mixture was then quenched with NH_4Cl (20 mL) and extracted with ether (50 mL), and dried over MgSO_4 . After concentration in vacuo (note: remove shortly after the ether is removed, because the compound is quite volatile), the residue was purified with flash chromatography over silica gel (hexane: ether = 98:2) to yield the product as a liquid in 60% yield (2.26 g). ^1H NMR (500 MHz, CDCl_3) δ 8.08 (d, $J = 5.7$ Hz, 2H), 4.47 – 4.31 (m, 1H), 1.97-1.90 (m, 1H), 1.79-1.72 (m, 1H), 1.54 (d, $J = 6.8$ Hz, 3H), 1.33 – 1.11 (m, 2H), 0.92 (t, $J = 7.4$ Hz, 3H); ^{13}C NMR (126 MHz, CDCl_3) δ 174.61 (q, $^2J_{\text{CF}} = 37$ Hz), 141.62, 132.51, 116.54 (q, $^1J_{\text{CF}} = 291$ Hz), 115.86, 59.52, 38.73, 20.98, 19.22, 13.58; ^{19}F NMR (376 MHz, CDCl_3) δ -77.99; HRMS (Mixed EIC) m/z calcd for $\text{C}_{10}\text{H}_{14}\text{F}_3\text{N}_2\text{O}$ $[\text{M}+\text{H}]^+$ 235.1058, found 235.1052.

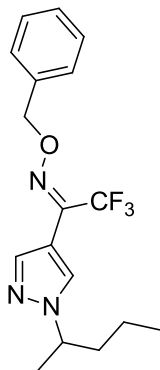


2,2,2-trifluoro-1-(1-(pentan-2-yl)-1H-pyrazol-4-yl)ethanone oxime (2-6d): A standard literature procedure for oxime synthesis was followed.² Hydroxylamine hydrochloride (0.36 g, 5.1 mmol) and sodium hydroxide (0.21 g, 5.1 mmol) was dissolved in ethanol (10 mL). A solution of **2-4e** (0.20 g, 1.0 mmol) in ethanol (5 mL) was added into the mixture. The resulting white suspension was refluxed overnight then concentrated in vacuo, extracted with dichloromethane (40 mL) and water (20 mL). The dichloromethane fraction was dried with MgSO_4 and concentrated in vacuo. The residue was purified using flash chromatography on silica gel (hexane : ethyl acetate = 9:1) to yield the product as a brown solid in 10% yield (0.04 g). ^1H NMR (500 MHz, CDCl_3) δ 10.30 (s, 1H), 8.25 (s, 1H), 8.03 (s, 1H), 4.52 –

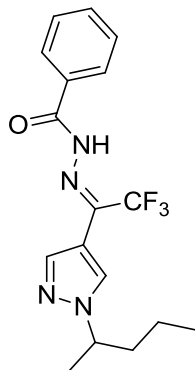
4.33 (m, 1H), 1.79-1.72 (m, 2H), 1.54 (d, $J = 6.8$ Hz, 3H), 1.38 – 1.12 (m, 2H), 0.91 (t, $J = 7.4$ Hz, 3H); ^{13}C NMR (126 MHz, CDCl_3) δ 140.03(q, $^2J_{\text{CF}} = 32$ Hz), 139.62, 131.00, 121.11(q, $^1J_{\text{CF}} = 275$ Hz), 107.15, 58.90, 38.92, 21.10, 19.27, 13.61; ^{19}F NMR (471 MHz, CDCl_3) δ -69.27; HRMS (ESI) m/z calcd for $\text{C}_{10}\text{H}_{15}\text{F}_3\text{N}_3\text{O}$ $[\text{M}+\text{H}]^+$ 250.1167, found 250.1165.



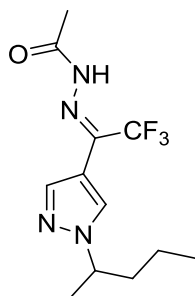
2,2,2-trifluoro-1-(1-(pentan-2-yl)-1H-pyrazol-4-yl)ethanone O-methyl oxime (2-5d): A standard literature procedure for oxime ether synthesis was followed.² O-methylhydroxylamine hydrochloride (0.32 g, 3.8 mmol) and sodium hydroxide (0.15 g, 3.5 mmol) was dissolved in ethanol (7 mL). A solution of **2-4d** (0.30 g, 1.3 mmol) in ethanol (2 mL) was added into the mixture. The resulting white suspension was refluxed overnight then concentrated in vacuo, extracted with dichloromethane (40 mL) and water (20 mL). The dichloromethane fraction was dried with MgSO_4 and concentrated in vacuo. The residue was purified using flash chromatography on silica gel (hexane : ethyl acetate = 39:1) to yield the product as a clear oil in 80% yield (0.27 g). ^1H NMR (500 MHz, CDCl_3) δ 8.06 (s, 1H), 7.94 (s, 1H), 4.52 – 4.24 (m, 1H), 4.13 (s, 3H), 2.15 – 1.82 (m, 1H), 1.73 (ddt, $J = 13.8, 10.1, 5.8$ Hz, 1H), 1.51 (d, $J = 6.8$ Hz, 3H), 1.37 – 1.07 (m, 2H), 0.90 (t, $J = 7.4$ Hz, 3H); ^{13}C NMR (126 MHz, CDCl_3) δ 139.73, 138.91(q, $^2J_{\text{CF}} = 32$ Hz), 130.54, 120.96(q, $^1J_{\text{CF}} = 275$ Hz), 107.46, 63.66, 58.76, 38.93, 21.12, 19.29, 13.62; ^{19}F NMR (471 MHz, CDCl_3) δ -68.93; HRMS (ESI) m/z calcd for $\text{C}_{11}\text{H}_{17}\text{F}_3\text{N}_3\text{O}$ $[\text{M}+\text{H}]^+$ 264.1323, found 264.1317.



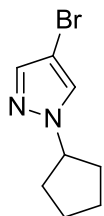
2,2,2-trifluoro-1-(1-(pentan-2-yl)-1H-pyrazol-4-yl)ethanone O-benzyl oxime (2-7d): A standard literature procedure for oxime ether synthesis was followed.² O-benzylhydroxylamine hydrochloride (0.613 g, 3.8 mmol) and sodium hydroxide (0.15 g, 3.5 mmol) was dissolved in ethanol (7 mL). A solution of **2-4d** (0.30 g, 1.3 mmol) in ethanol (5 mL) was added into the mixture. The resulting white suspension was refluxed overnight then concentrated in vacuo, extracted with dichloromethane (40 mL) and water (20 mL). The dichloromethane fraction was dried with MgSO₄ and concentrated in vacuo. The residue was purified using flash chromatography on silica gel (hexane : ethyl acetate = 9:1) to yield the product as a clear oil in 50% yield (0.21 g). ¹H NMR (500 MHz, CDCl₃) δ 8.01 (s, 1H), 7.96 (s, 1H), 7.56 – 7.29 (m, 5H), 5.34 (s, 2H), 4.50 – 4.19 (m, 1H), 2.05 – 1.80 (m, 1H), 1.68 (ddt, *J* = 13.8, 10.0, 5.8 Hz, 1H), 1.47 (d, *J* = 6.8 Hz, 3H), 1.29 – 1.06 (m, 2H), 0.87 (t, *J* = 7.3 Hz, 3H); ¹³C NMR (126 MHz, CDCl₃) δ 140.00, 139.30 (q, ²*J*_{CF} = 32 Hz), 136.29, 130.58, 128.57, 128.40, 128.37, 121.12 (q, ¹*J*_{CF} = 276 Hz), 107.54, 78.29, 58.67, 38.88, 21.07, 19.23, 13.60; ¹⁹F NMR (471 MHz, CDCl₃) δ -68.84; HRMS (ESI) *m/z* calcd for C₁₇H₂₁F₃N₃O [M+H]⁺ 340.1637, found 340.1636.



N'-(2,2,2-trifluoro-1-(1-(pentan-2-yl)-1H-pyrazol-4-yl)ethylidene)benzohydrazide (2-15d): A standard literature procedure for hydrazone synthesis was followed.⁵ A solution of benzhydrazide(0.13 g, 0.94 mmol) and THF(3 mL) was made. To this solution, **2-4d** (0.2 g, 0.85 mmol) and a drop of concentrated HCl was added. The resulting mixture was then stirred for overnight at room temperature. Precipitate that was formed was filtered out with THF (5 mL), ether (5 ml) and pentane (5 mL). Crystals crashed out of the solution and was collected without further purification in 15% (0.045 g) yield. ¹H (500 MHz, CDCl₃) δ 8.08 (d, *J* = 3.4 Hz, 2H), 8.01 (s, 1H), 7.80 – 7.74 (m, 2H), 7.55 – 7.48 (m, 1H), 7.43 (ddd, *J* = 8.1, 6.7, 1.1 Hz, 2H), 4.46 – 4.34 (m, 1H), 1.99 – 1.86 (m, 1H), 1.81 – 1.69 (m, 1H), 1.54 (d, *J* = 6.7 Hz, 3H), 1.26 – 1.16 (m, 2H), 0.91 (t, *J* = 7.4 Hz, 3H); ¹³C NMR (126 MHz, CDCl₃) δ 174.56 (q, ²*J*_{CF} = 37 Hz), 168.66, 141.55, 132.67, 132.52, 131.79, 128.67, 126.88, 116.75(q, ¹*J*_{CF} = 230 Hz), 115.78, 59.45, 38.64, 20.89, 19.14, 13.50; ¹⁹F NMR (471 MHz) -78.01 ; HRMS (Mixed EIC) *m/z* calcd for C₁₇H₂₀F₃N₄O [M+H]⁺ 353.1589, found 353.1600.

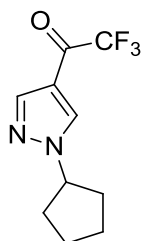


N'-(2,2,2-trifluoro-1-(1-(pentan-2-yl)-1H-pyrazol-4-yl)ethylidene)acetohydrazide (2-13d): A standard literature procedure for hydrazone synthesis was followed.⁵ A neat mixture of **2-4d** (0.2 g, 0.85 mmol) and acetylhydrazide (0.06 g, 0.45 mmol) were combined at 0 °C for 25 minutes. It was brought to room temperature and left for an additional 90 minutes. MgSO₄ was then added to the mixture and left for 15 minutes following washing with ether (5 mL), THF (5 mL), and hexane (5 mL). Concentration of the solvents in vacuo furnished the product in 36% (0.045 g) with no further purification needed. ¹H NMR (500 MHz, Acetone-d₆) δ 8.95 (s, 1H), 8.56 (s, 1H), 8.10 (s, 1H), 4.75 – 4.49 (m, 1H), 2.81 (s, 3H), 1.99-1.94 (m, 1H), 1.84-1.76 (m, 1H), 1.53 (d, *J* = 6.7 Hz, 3H), 1.32 – 1.20 (m, 1H), 1.20 – 1.07 (m, 1H), 0.89 (t, *J* = 7.4 Hz, 3H); ¹³C NMR (126 MHz, Acetone-d₆) δ 174.6 (q, ²*J*_{CF} = 37 Hz), 170.97, 142.01, 134.87, 122.91, 116.45 (q, ¹*J*_{CF} = 290 Hz), 115.80, 59.97, 39.17, 21.20, 20.58, 19.84, 13.81; ¹⁹F NMR (376 MHz, CDCl₃) δ -78.00; HRMS (Mixed EIC) *m/z* calcd for C₁₀H₁₄F₃N₂O [M+H]⁺ 235.1058, found 235.1050.



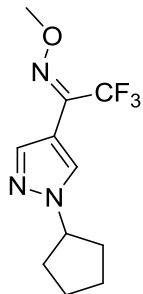
4-bromo-1-cyclopentyl-1H-pyrazole (2-3f): To a solution of sodium hydride (60% dispersion in mineral oil, 1.5 g, 38.2 mmol) in DMF (8 mL), a solution of pyrazole (2.0 g, 29.2 mmol) in DMF (2 mL) was added drop wise. The solution was then warmed to room temperature for 2 hours to which

bromocyclopentane (4.7 mL, 44.1 mmol) was then added drop wise and stirred for overnight. The resulting mixture was extracted with ether (40 mL) and brine (20 mL) and dried with MgSO₄. The ether layer was concentrated in vacuo to furnish the residue. The residue was mixed in water (20 mL) and NBS (5.2 g, 29.2 mmol) was added. TLC was used to detect progression of reaction. After 2 hours, the mixture was extracted with DCM (50 mL) and dried with MgSO₄. The residue was purified using flash chromatography on silica gel (hexane : ethyl acetate = 4:1) to yield the product as a clear liquid in 55% yield (3.5 g). ¹H NMR (500 MHz, CDCl₃) δ 8.05 (s, 1H), 7.97 (s, 1H), 4.65 (p, *J* = 7.1 Hz, 1H), 2.28 – 2.17 (m, 2H), 2.12 – 1.99 (m, 2H), 1.97 – 1.88 (m, 2H), 1.82 – 1.70 (m, 2H); ¹³C NMR (126 MHz, CDCl₃) δ 141.41, 132.15, 114.83, 63.90, 32.97, 24.10.

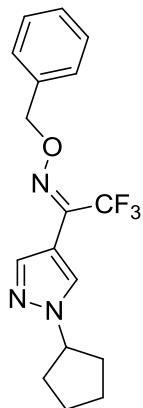


1-(1-cyclopentyl-1H-pyrazol-4-yl)-2,2,2-trifluoroethanone (2-4f): A standard literature procedure for TFK synthesis was followed.¹ **2-2f** (2.4 g, 16.4 mmol) was dissolved in dry THF (15 mL) at -78 °C under nitrogen and was stirred for 10 min. *n*-BuLi (2.5 M in hexanes, 4.6 mL, 17.5 mmol) was added drop wise to the solution was stirred for 2 hours at -78 °C. After two hours, methyl trifluoroacetate (1.31 mL, 19.9 mmol) was added drop wise and stirred for 30 min at -78 °C. The solution was then allowed to warm up to room temperature and let stir for overnight. The mixture was then quenched with NH₄Cl (20 mL) and extracted with ether (50 mL), and dried over MgSO₄. After concentration in vacuo (note: remove shortly after the ether is removed, because the compound is quite volatile), the residue was purified with flash chromatography over silica gel (hexane: ether = 98:2) to yield the product as a liquid in 52% yield (1.97

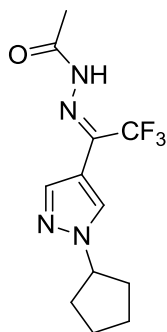
g). ^1H NMR (500 MHz, CDCl_3) δ 8.10 (s, 1H), 8.08 (s, 1H), 4.71 (p, $J = 7.1$ Hz, 1H), 2.29 – 2.17 (m, 2H), 2.11 – 1.99 (m, 2H), 1.97 – 1.86 (m, 2H), 1.82 – 1.70 (m, 2H); ^{13}C NMR (126 MHz, CDCl_3) δ 174.55 (q, $^2J_{\text{CF}} = 37$ Hz), 141.74, 132.69, 115.33, 116.47 (q, $^1J_{\text{CF}} = 290$ Hz), 64.00, 32.97, 24.10; ^{19}F NMR (376 MHz, CDCl_3) δ -78.00; HRMS (Mixed EIC) m/z calcd for $\text{C}_{10}\text{H}_{12}\text{F}_3\text{N}_2\text{O}$ $[\text{M}+\text{H}]^+$ 233.0902, found 233.0895.



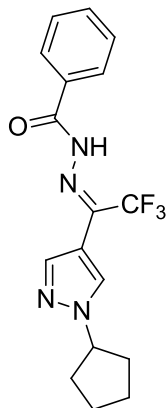
1-(1-cyclopentyl-1H-pyrazol-4-yl)-2,2,2-trifluoroethanone O-methyl oxime (2-5f): A standard literature procedure for oxime ether synthesis was followed.² O-methylhydroxylamine hydrochloride (0.11 g, 1.2 mmol) and sodium hydroxide (0.05 g, 1.3 mmol) was dissolved in ethanol (7 mL). A solution of **2-4f** (0.1 g, .43 mmol) in ethanol (2 mL) was added into the mixture. The resulting white suspension was refluxed overnight then concentrated in vacuo, extracted with dichloromethane (40 mL) and water (20 mL). The dichloromethane fraction was dried with MgSO_4 and concentrated in vacuo. The residue was purified using flash chromatography on silica gel (hexane : ethyl acetate = 19:1) to yield the product as a clear oil in 40% yield (0.45 g). ^1H NMR (400 MHz, CDCl_3) δ 8.10 (s, 1H), 7.93 (s, 1H), 4.67 (p, $J = 7.2$ Hz, 1H), 2.31 – 2.11 (m, 2H), 2.10 – 1.98 (m, 2H), 1.96 – 1.84 (m, 2H), 1.79 – 1.68 (m, 2H); ^{13}C NMR (101 MHz, CDCl_3) δ 139.86 (q, $^3J_{\text{CF}} = 2$ Hz), 138.85 (q, $^2J_{\text{CF}} = 32$ Hz), 130.80, 121.43 (q, $^1J_{\text{CF}} = 276$ Hz), 107.52, 63.65, 63.37, 32.97, 24.14; ^{19}F NMR (471 MHz, CDCl_3) δ -68.99; HRMS (Mixed EIC) m/z calcd for $\text{C}_{11}\text{H}_{15}\text{F}_3\text{N}_3\text{O}$ $[\text{M}+\text{H}]^+$ 262.1167, found 262.1170.



1-(1-cyclopentyl-1H-pyrazol-4-yl)-2,2,2-trifluoroethanone O-benzyl oxime (2-7f): A standard literature procedure for oxime ether synthesis was followed.² O-benzylhydroxylamine hydrochloride (0.21 g, 1.3 mmol) and sodium hydroxide (0.05 g, 1.3 mmol) was dissolved in ethanol (7 mL). A solution of **2-4f** (0.10 g, 0.43 mmol) in ethanol (5 mL) was added into the mixture. The resulting white suspension was refluxed overnight then concentrated in vacuo, extracted with dichloromethane (40 mL) and water (20 mL). The dichloromethane fraction was dried with MgSO₄ and concentrated in vacuo. The residue was purified using flash chromatography on silica gel (hexane : ethyl acetate = 4:1) to yield the product as a clear oil in 60% yield (0.87 g). ¹H NMR (400 MHz, CDCl₃) δ 8.05 (s, 1H), 7.95 (s, 1H), 7.51 – 7.32 (m, 5H), 5.34 (s, 2H), 4.63 (p, *J* = 7.0 Hz, 1H), 2.20 – 2.08 (m, 2H), 2.04 – 1.93 (m, 2H), 1.90 – 1.78 (m, 2H), 1.76 – 1.63 (m, 2H); ¹³C NMR (101 MHz, CDCl₃) δ 140.08 (q, ³*J*_{CF} = 2 Hz), 139.30 (q, ²*J*_{CF} = 32 Hz), 139.10, 136.20, 130.87, 130.85, 128.58, 128.41, 128.40, 121.05 (q, ¹*J*_{CF} = 275 Hz), 107.61, 78.28, 63.35, 32.96, 24.11; ¹⁹F NMR (471 MHz, CDCl₃) δ -68.96; HRMS (Mixed EIC) *m/z* calcd for C₁₇H₁₉F₃N₃O [M+H]⁺ 338.1480, found 338.1489.



N'-(1-(1-cyclopentyl-1H-pyrazol-4-yl)-2,2,2-trifluoroethylidene)acetohydrazide (2-13f): A standard literature procedure for hydrazone synthesis was followed.⁵ A neat mixture of **2-4f** (0.1 g, 0.43 mmol) and acetylhydrazide (0.03 g, 0.45 mmol) were combined at 0 °C for 25 minutes. It was brought to room temperature and left for an additional 90 minutes. MgSO₄ was then added to the mixture and left for 15 minutes following washing with ether (5 mL), THF (5 mL), and hexane (5 mL). Concentration of the solvents in vacuo furnished the product in 12% (0.015 g) with no further purification needed. ¹H NMR (500 MHz, Acetone-d₆) δ 8.99 (s, 1H), 8.55 (s, 1H), 8.10 (s, 1H), 5.04 – 4.80 (m, 1H), 2.85 (s, 3H), 2.27 – 2.16 (m, 2H), 2.12 – 2.03 (m, 2H), 1.96 – 1.84 (m, 2H), 1.80 – 1.67 (m, 2H); ¹³C NMR (126 MHz, Acetone-d₆) δ 174.77, 172.51, 149.16, 142.11, 134.94, 117.52 (q, ²J_{CF} = 295 Hz), 64.54, 33.52, 24.93, 20.60; ¹⁹F NMR (471 MHz, CDCl₃) δ -71.23; HRMS (Mixed EIC) *m/z* calcd for C₁₂H₁₆F₃N₄O [M+H]⁺ 289.1276, found 289.1281.



N'-(1-(1-cyclopentyl-1H-pyrazol-4-yl)-2,2,2-trifluoroethylidene)benzohydrazide (2-15f): A standard literature procedure for hydrazone synthesis was followed.⁵ A neat mixture of **2-4f** (0.1 g, 0.43 mmol) and acetylhydrazide (0.06 g, 0.43 mmol) were combined at 0 °C for 25 minutes. It was brought to room temperature and left for an additional 90 minutes. MgSO₄ was then added to the mixture and left for 15 minutes following washing with ether (5 mL), THF (5 mL), and hexane (5 mL). Concentration of the solvents in vacuo furnished the product in 26% (0.039 g) with no further purification needed. ¹H NMR (500 MHz, Acetone-d₆) δ 9.77 (s, 1H), 8.56 (s, 1H), 8.10 (s, 1H), 7.56-7.43 (m, 5H), 5.04 – 4.82 (m, 1H), 2.25 – 2.15 (m, 2H), 2.12 – 2.02 (m, 2H), 1.94 – 1.85 (m, 2H), 1.79 – 1.68 (m, 2H); ¹³C NMR (126 MHz, Acetone-d₆) δ 174.75 (q, ²J_{CF} = 35 Hz), 163.88, 142.13, 135.48, 134.98, 132.00, 129.10, 128.35, 117.29 (q, ¹J_{CF} = 291 Hz), 116.36, 64.52, 33.51, 24.93; ¹⁹F NMR (471 MHz, Acetone-d₆) δ -75.95; HRMS (Mixed EIC) *m/z* calcd for C₁₇H₁₈F₃N₄O [M+H]⁺ 351.1433, found 351.1429.

3.3 Enzyme assay and determination of IC₅₀ Values

Enzyme inhibition assays were performed by Dr. Dawn Wong using the Ellman assay from a published procedure. The hAChE (lyophilized powder, Sigma C1682, T-molecular form) was diluted with buffer (0.1 M sodium phosphate buffer containing 0.02% NaN₃ (w/v), pH 7.7) @ 25 °C containing 1 mg/mL bovine serum albumin and stored at -80 °C. The *Aghmg* and WT AChE were diluted in buffer (0.1 M

phosphate buffer containing 0.02% NaN_3 (w/v), pH 7.7 at 25 °C), 1 mg/mL bovine serum albumin, and 0.3% Triton X-100.

3.4 Mosquito toxicity assay

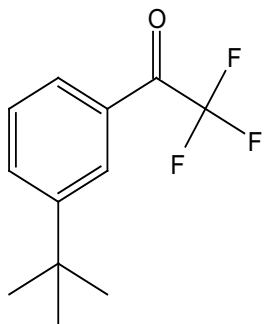
Female mosquitos (3-5 days old) were used for the mosquito toxicity assay. The tarsal contact assays were in accordance with the 2006 WHO recommendation.⁶ The filter paper was pretreated with 2.0 mL of the TFK solution and let to dry for overnight. The mosquitoes were then exposed to the filter paper and knockdown was recorded. After an hour, they were transferred to a holding tube and given sugar water (10% w/v). The mortality of the mosquitoes was recorded after 24hrs. LC_{50} values were determined by using various concentrations.⁷

Topical application assays were performed based a literature procedure in which mosquitoes are anesthetized on ice and application of a 0.2 μL solution of TFK in ethanol is placed on the dorsal thorax of the mosquito.⁸ These tests were performed by members of the Bloomquist Group at the University of Florida.

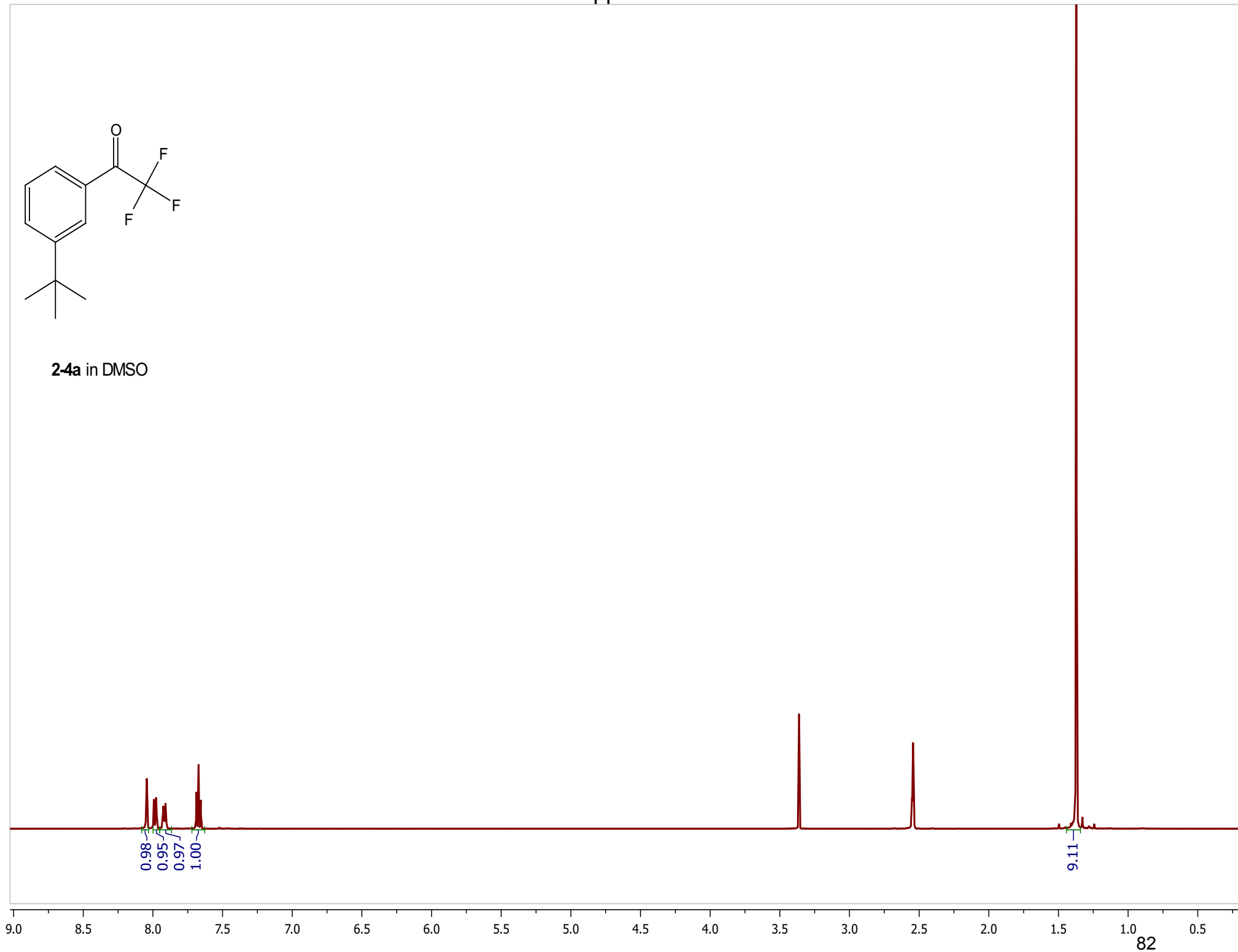
3.5 References for Chapter 3

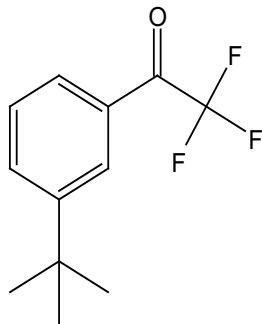
1. Nair, H. K.; Quinn, D. M., m-alkyl alpha,alpha,alpha-trifluoroacetophenones - a new class of potent transition-state analog inhibitors of acetylcholinesterase. *Bioorg. Med. Chem. Lett.* **1993**, *3*, 2619-2622.
2. Ruah, S., et. al., Indolyl cycloalkylcarboxamide compounds as modulators of ATP-binding cassette transporters and their preparation, pharmaceutical compositions and use in the treatment of diseases. *U.S Pat. Appl. Publ.* **2009**.
3. Michellys, P., et. al., Preparation of tetraline and tetrahydroquinoline derivatives as hepatocyte nuclear factor 4 α modulators. *PCT Int. Appl.* **2005**.
4. Duffy, J., Preparation of spiro-isoxazoline compounds as SSTR5 antagonists *PCT Int. Appl.* **2011**.
5. Kalia, J.; Raines, R. T., Hydrolytic stability of hydrazones and oximes. *Angew. Chem. Int. Ed.* **2008**, *47*, 7523-7526.
6. Organization, W. H. Guidelines for testing mosquito adulticides for indoor residual spraying and treatment of mosquito nets 2006.
7. Wong, D. M. L., J.; Chen, Q.-H.; Han, Q.; Mutunga, J. M.; Wysinski, A.; Anderson, T. D.; Ding, H.; Carpenetti, T. L.; Verma, A.; Islam, R.; Paulson, S. L.; Lam, P. C. H.; Totrov, M.; Bloomquist, J. R.; Carlier, P. R., Select small core structure carbamates exhibit high contact toxicity to "carbamate-resistant" strain malaria mosquitoes, *Anopheles gambiae* (Akron). *PLOS one* **2012**.
8. Pridgeon, J. W., et al., Susceptibility of *Aedes aegypti*, *Culex quinquefasciatus* say, and *Anopheles quadrimaculatus* say to 19 pesticides with different modes of action. *J. Med. Entomol.* **2008**, *45*, 82-87.

Appendix



2-4a in DMSO





2-4a in DMSO

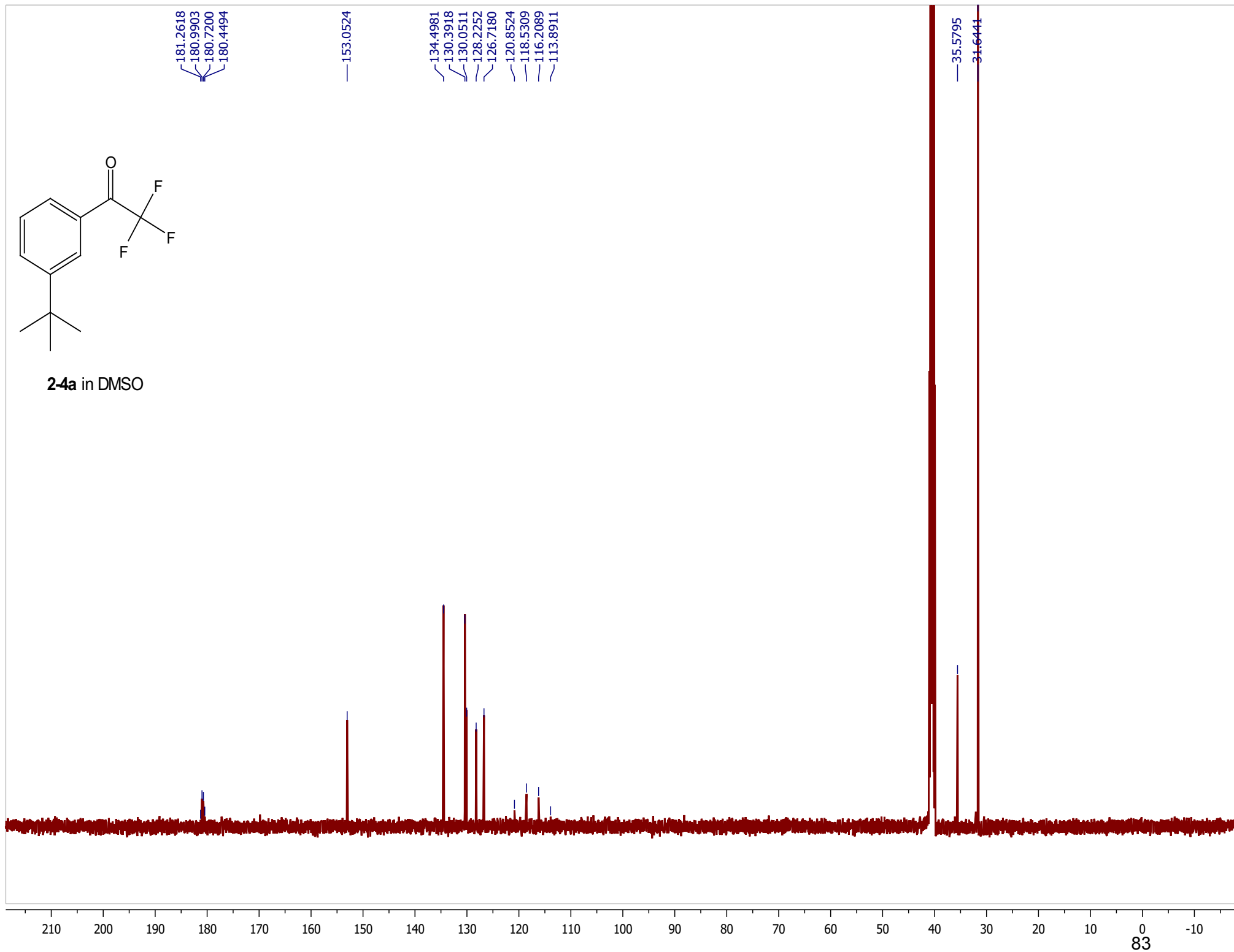
181.2618
180.9903
180.7200
180.4494

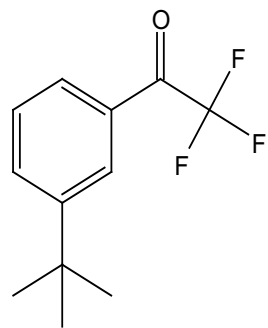
153.0524

134.4981
130.3918
130.0511
128.2252
126.7180
120.8524
118.5309
116.2089
113.8911

35.5795

31.6411

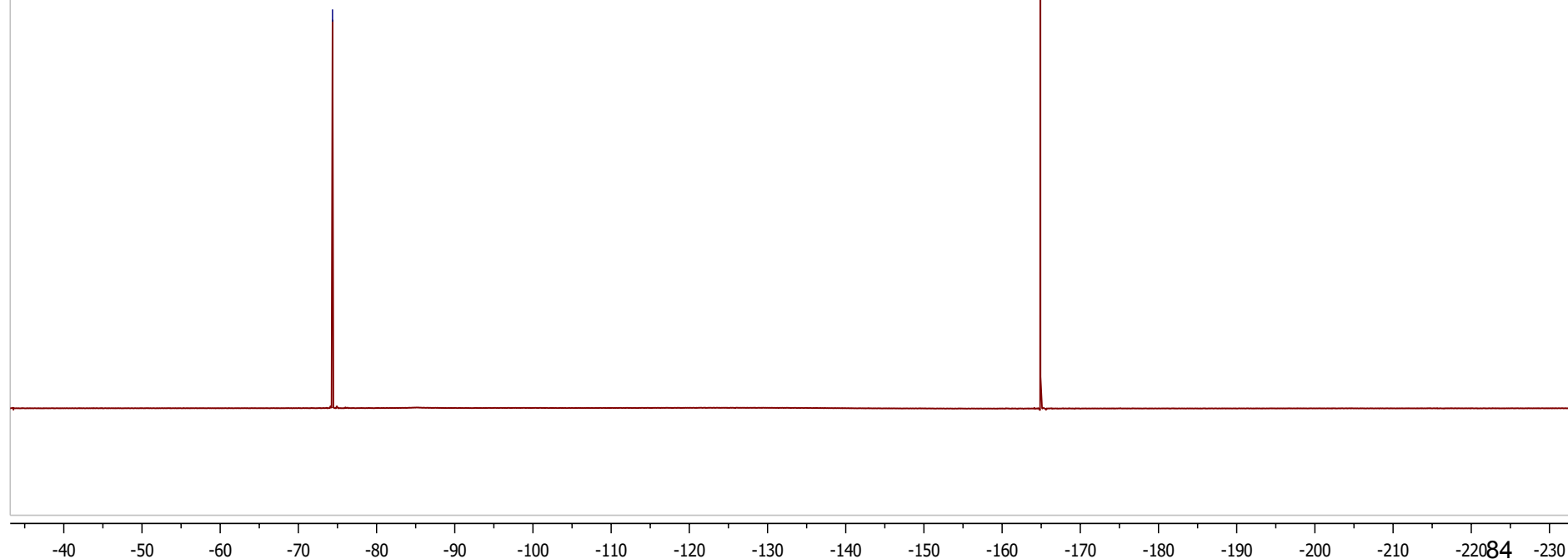


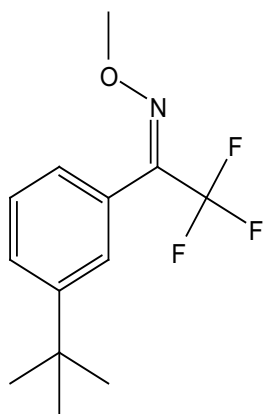


2-4a in CDCl₃

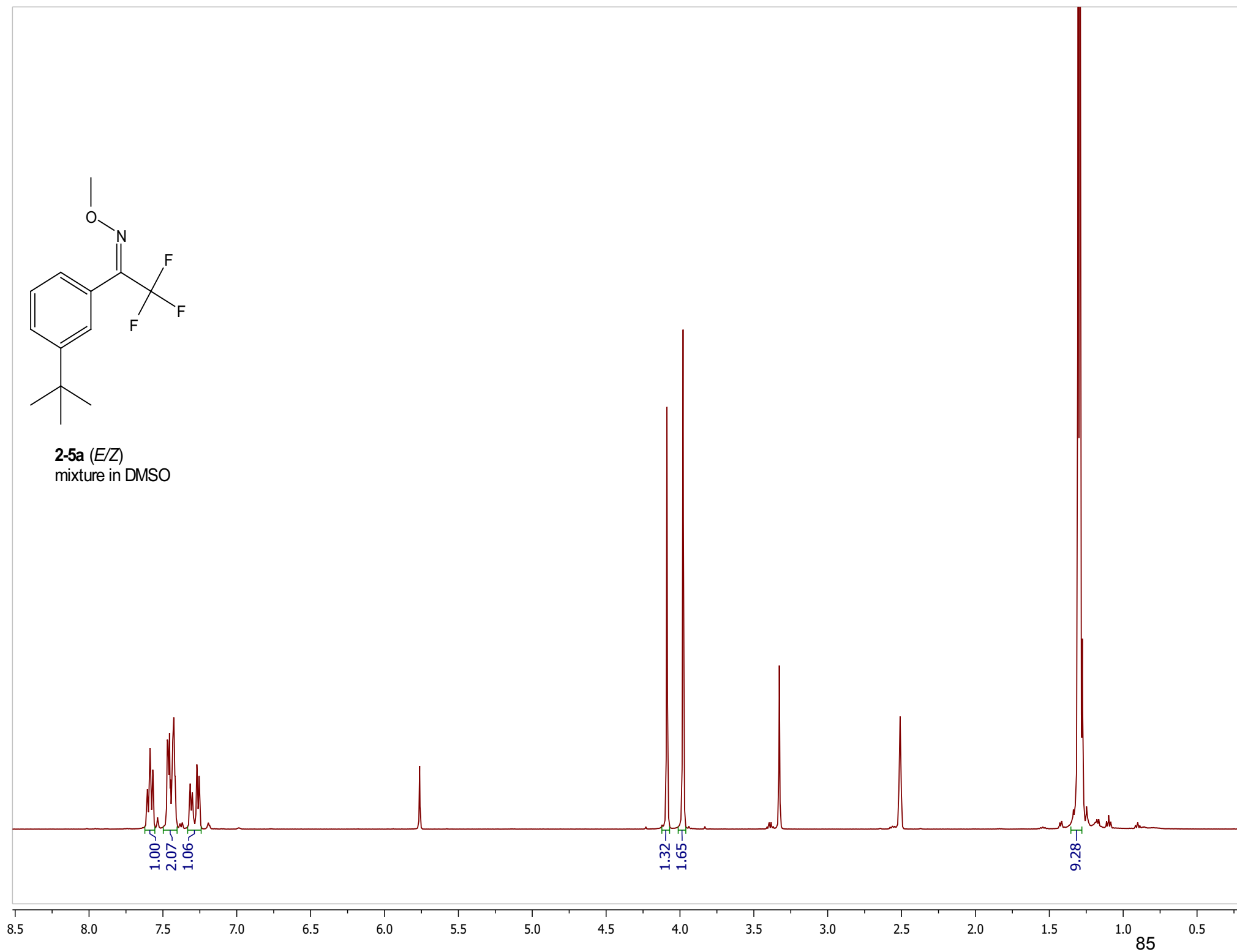
-74.3673

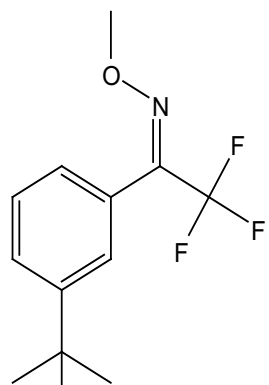
-164.8995



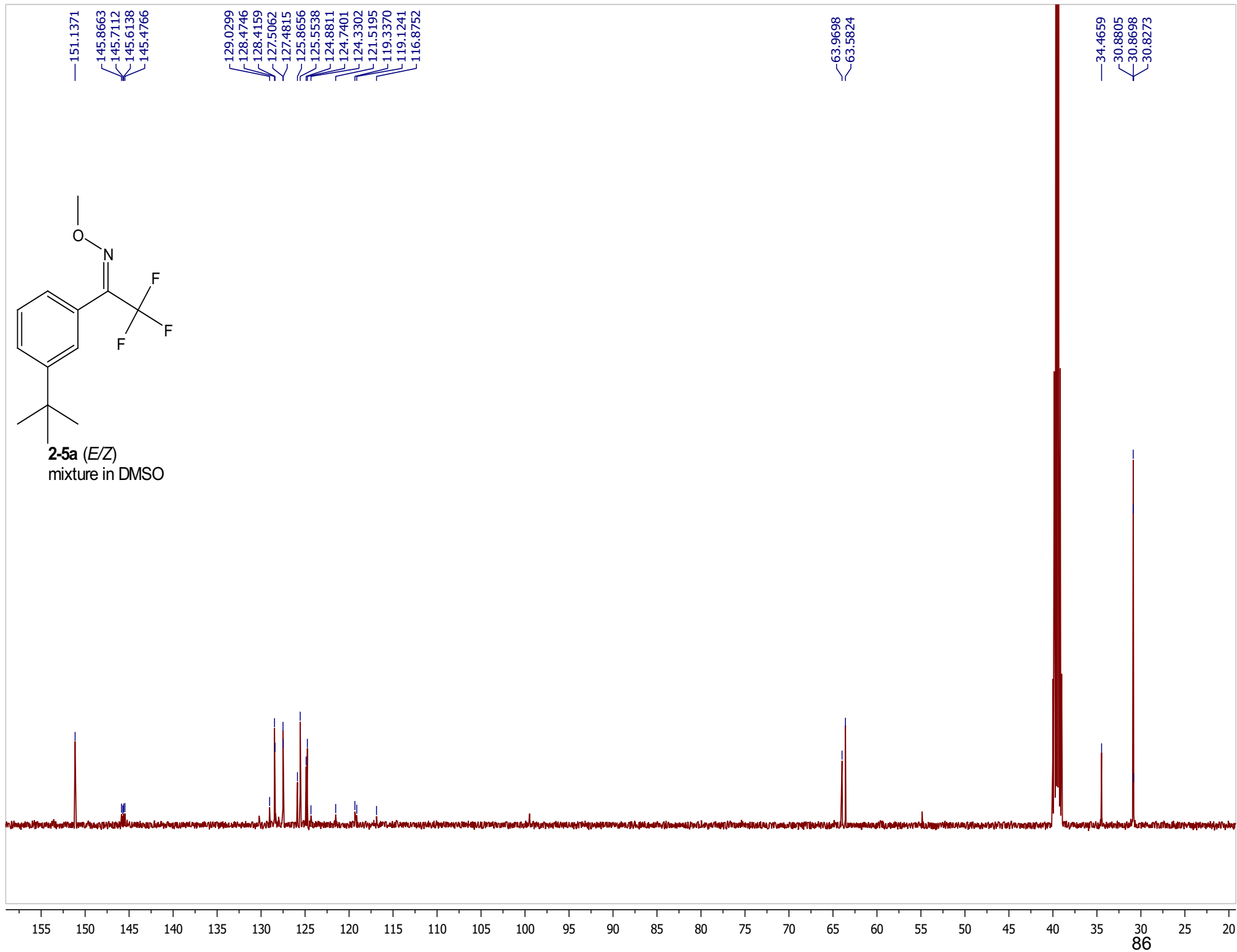


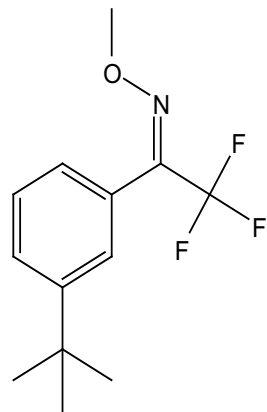
2-5a (*E/Z*)
mixture in DMSO





2-5a (*E/Z*)
mixture in DMSO





2-5a (E/Z)
mixture in CDCl₃

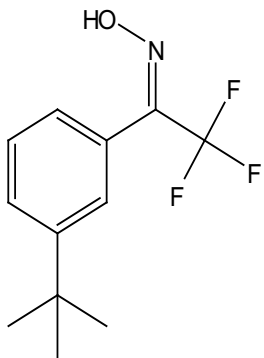
-65.4304

-69.3351

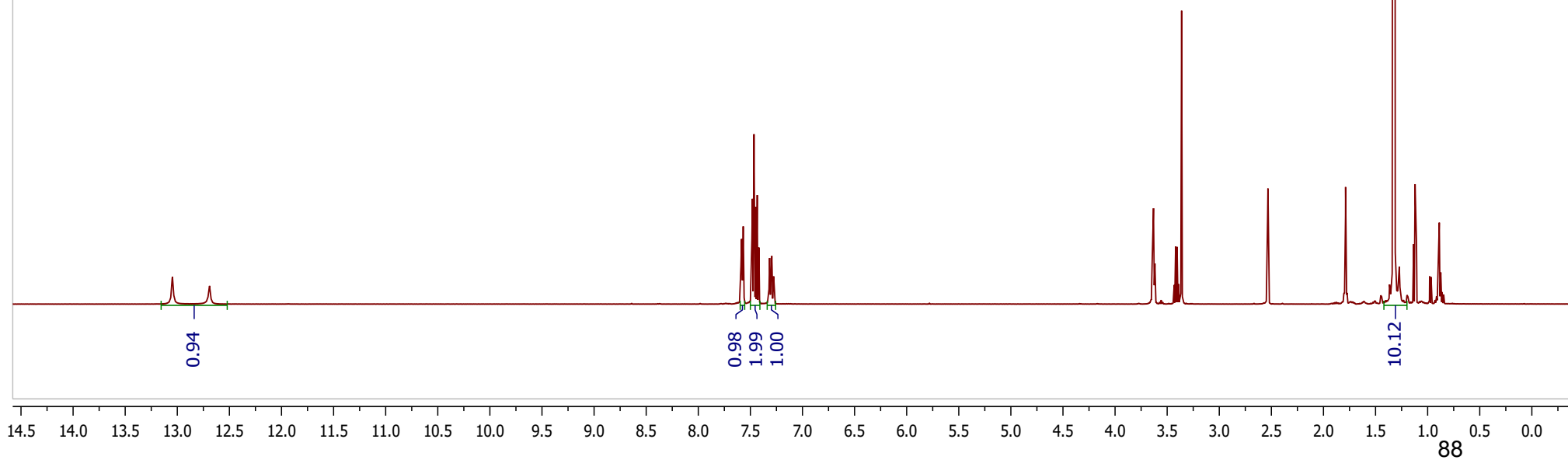
-164.9004

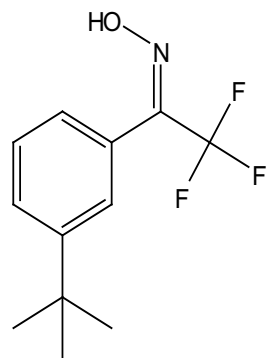
-55 -60 -65 -70 -75 -80 -85 -90 -95 -100 -105 -110 -115 -120 -125 -130 -135 -140 -145 -150 -155 -160 -165 -170 -175

87



2-6a in DMSO (E/Z)
mixture
Note purity <95%

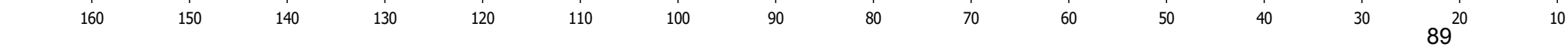


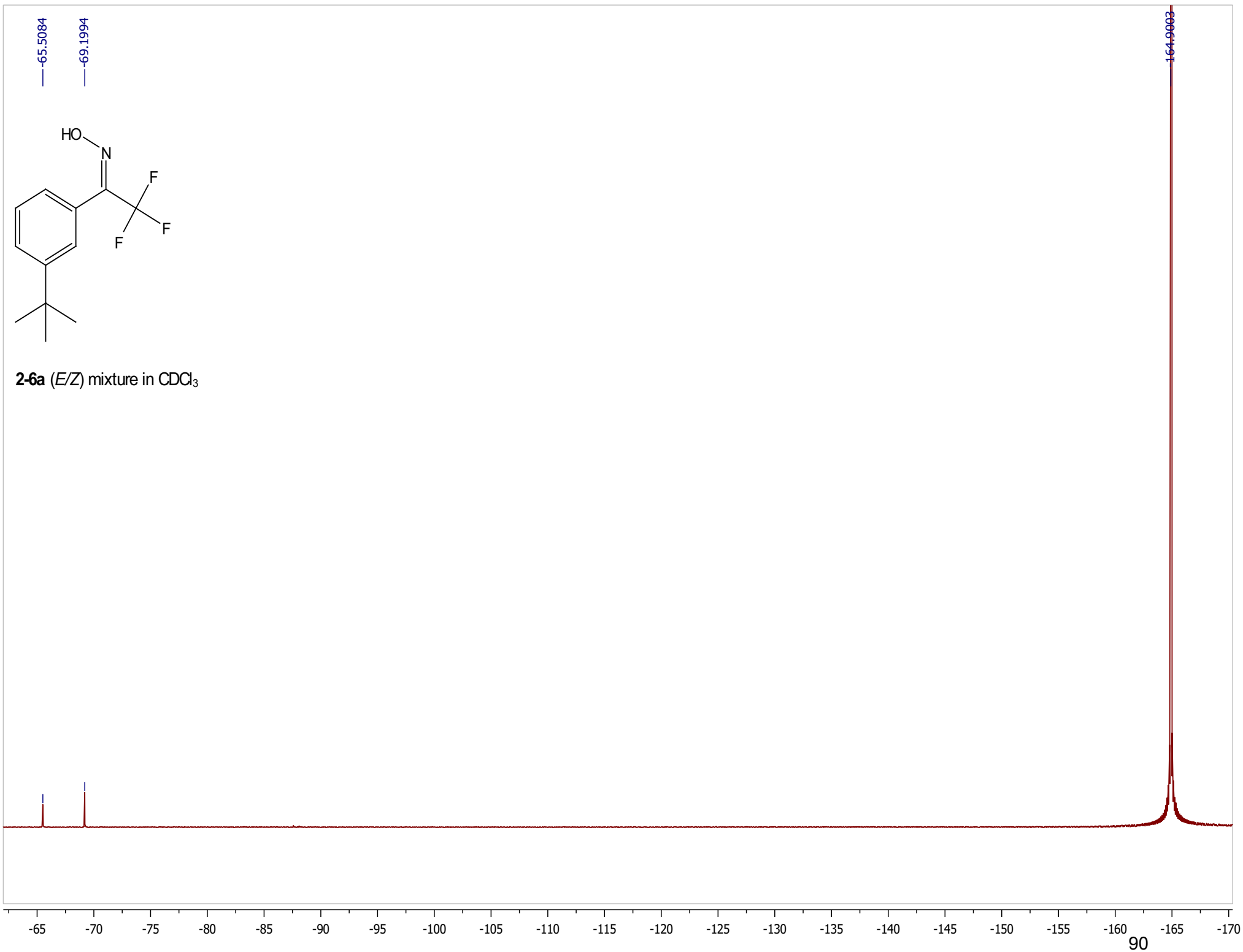


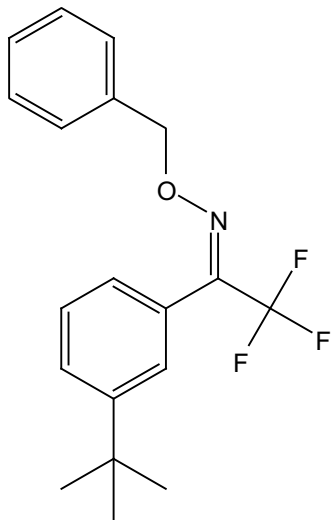
2-6a (*E/Z*) mixture in DMSO

150.9784
150.8991
145.1358
145.0659
144.8900
144.8404
130.1383
128.3159
128.2907
127.0505
126.8792
126.4443
125.6036
125.3030
124.9278
124.7785
122.2191
120.0416
119.5910
117.3402
115.0905

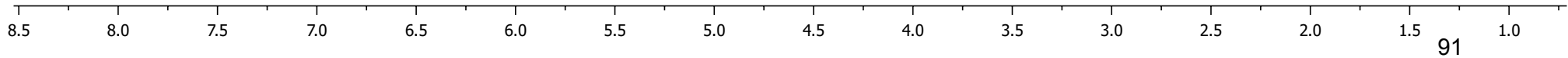
34.4158
30.9090

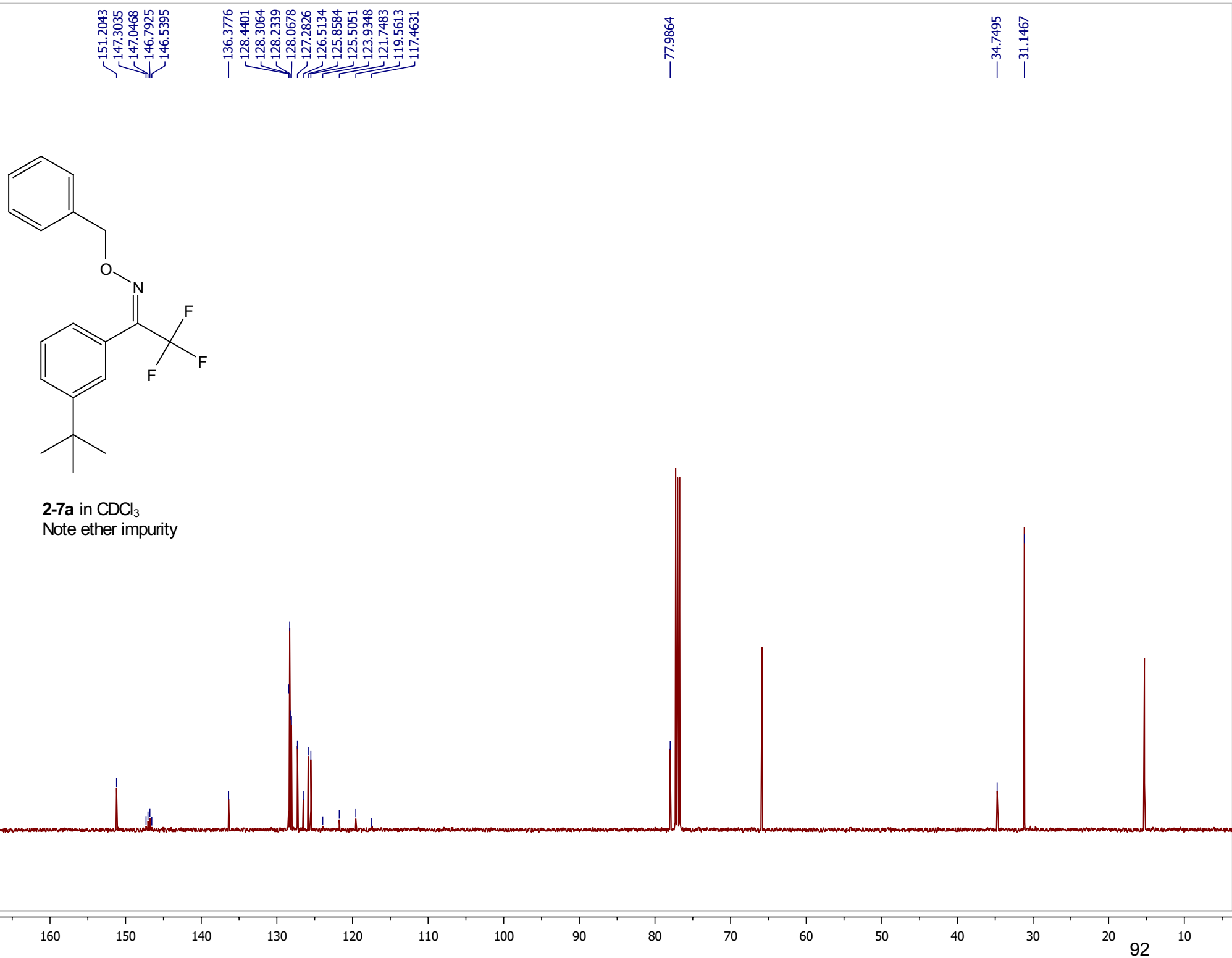


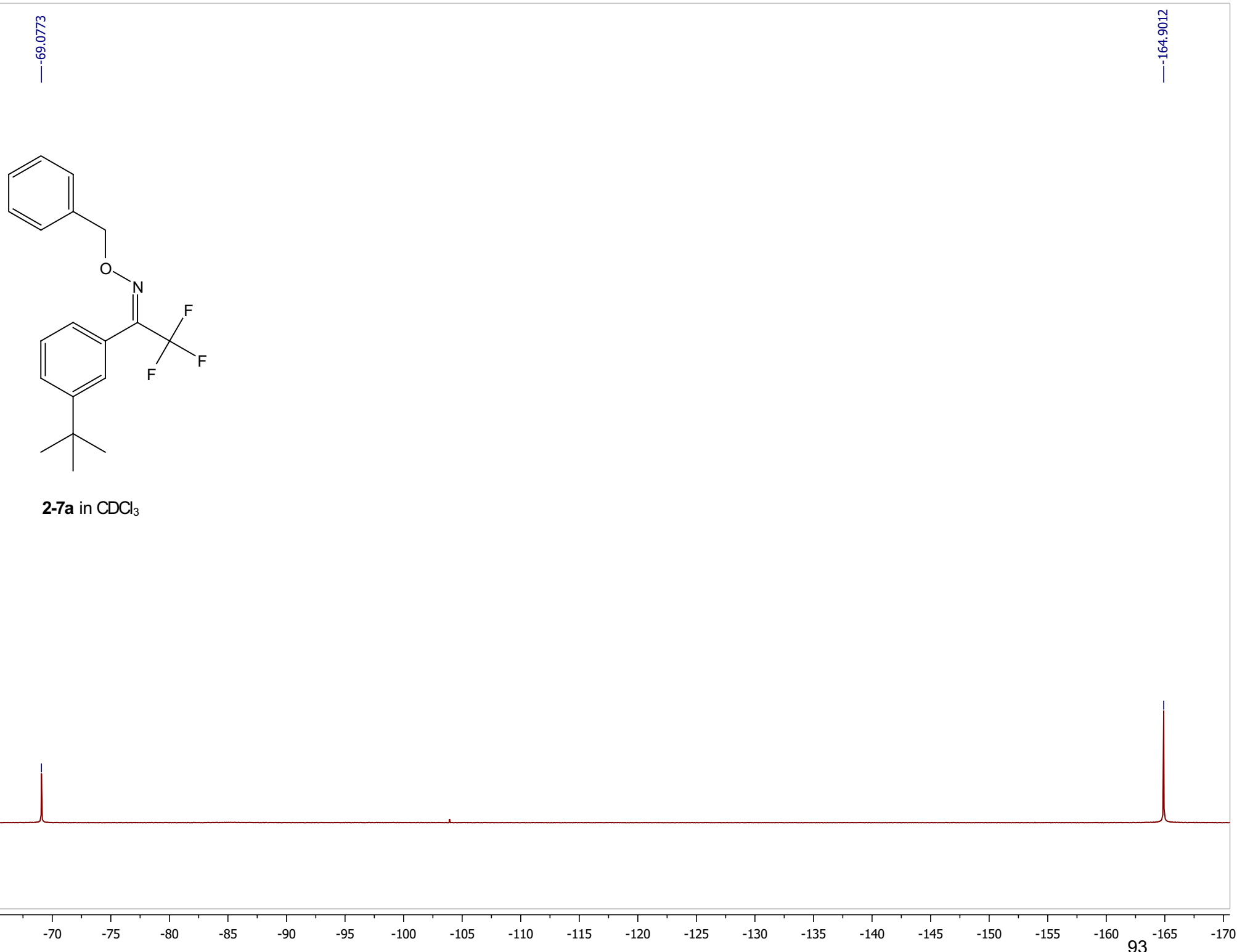


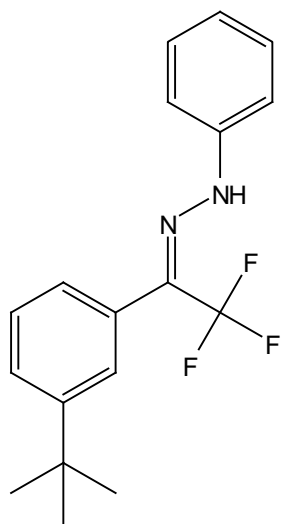


2-7a in CDCl₃
Note ether impurity

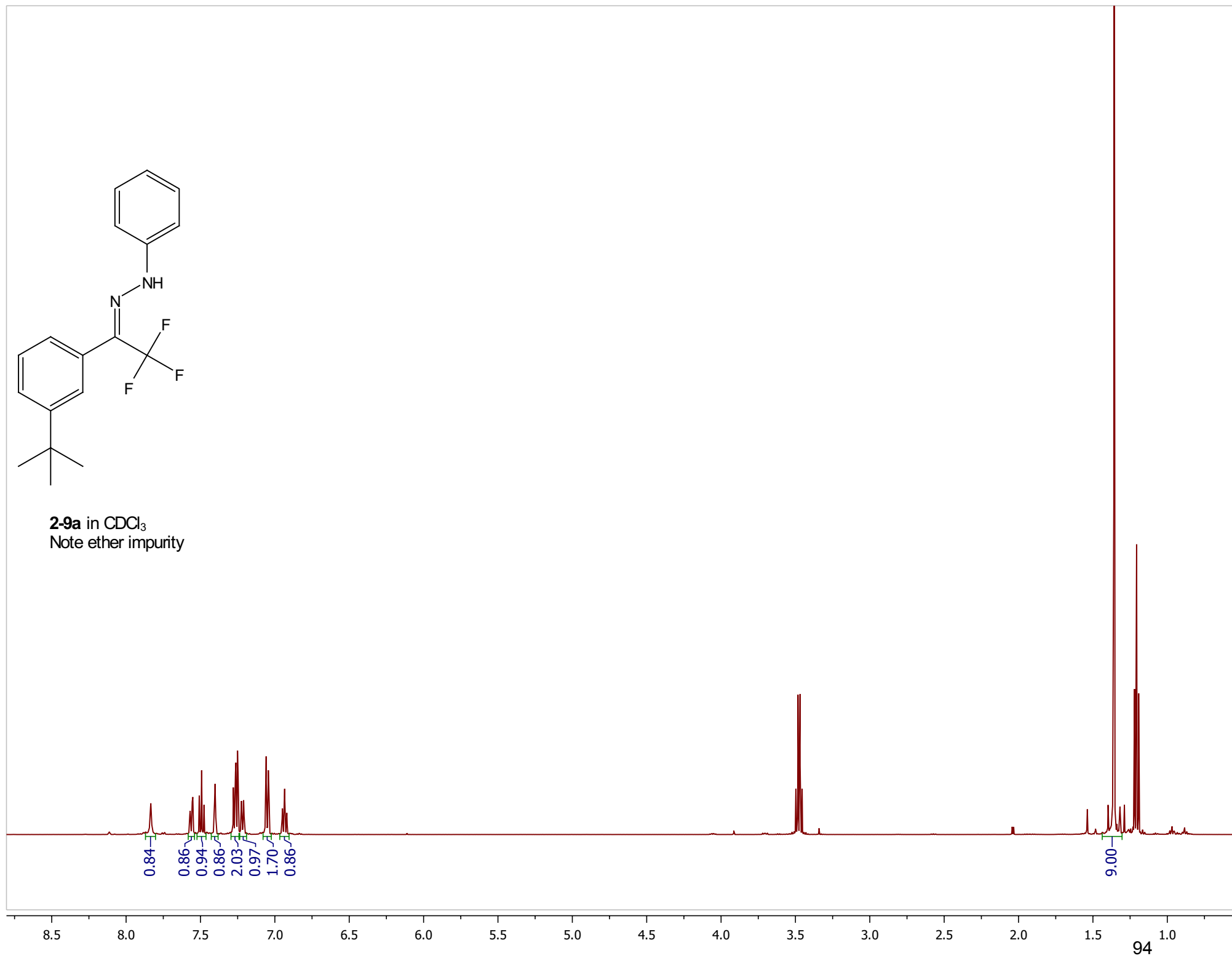


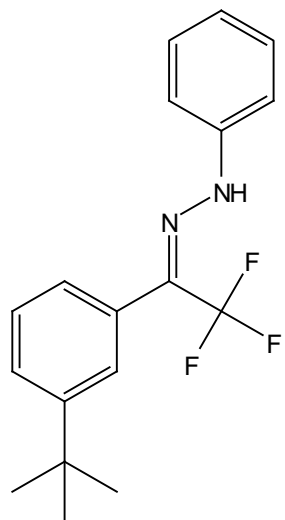




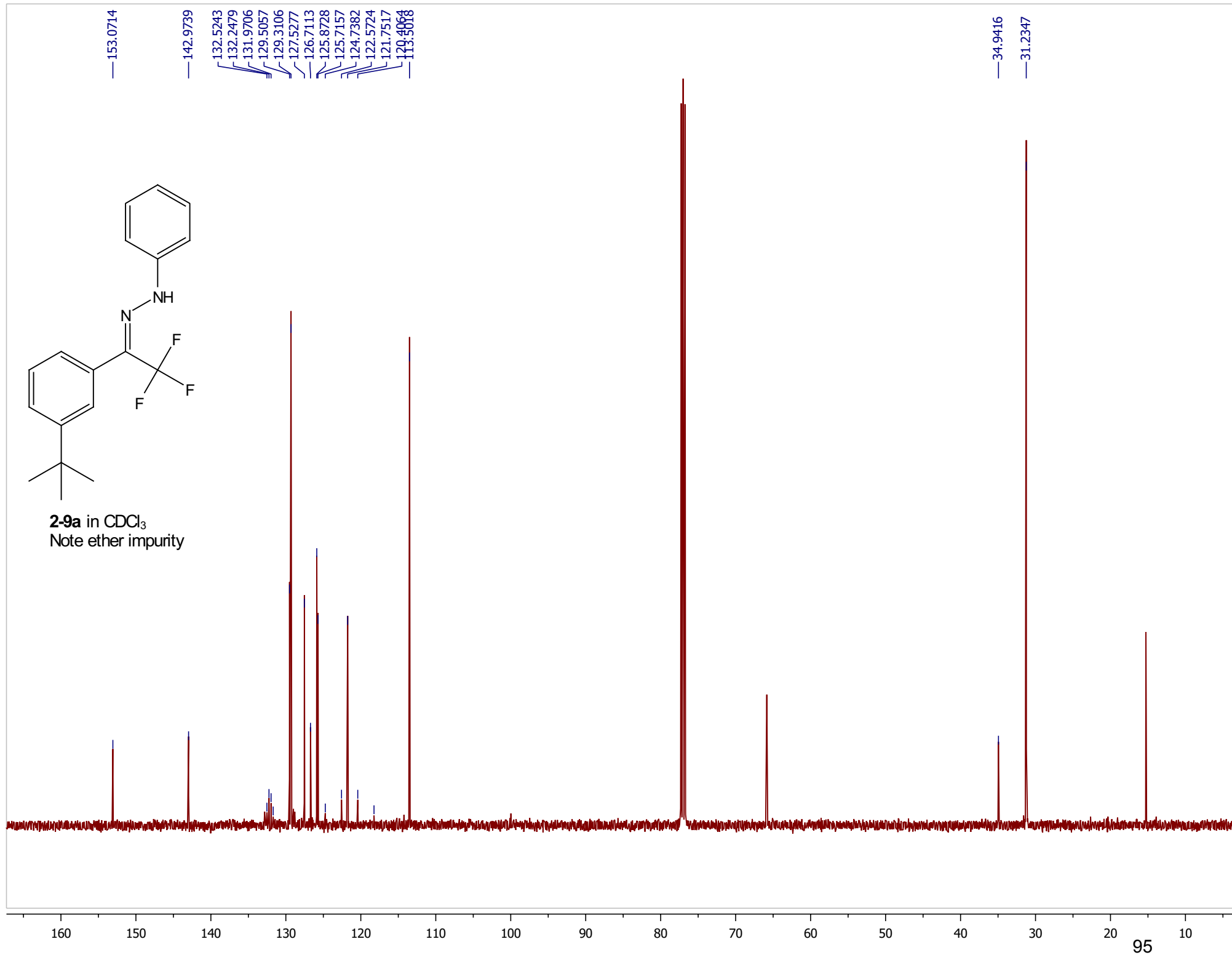


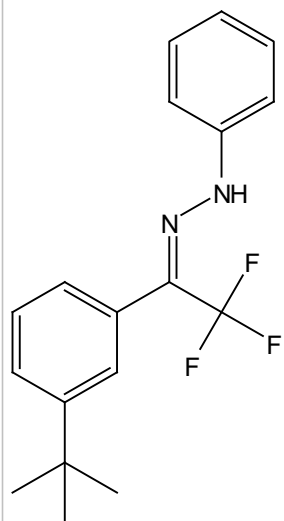
2-9a in CDCl₃
Note ether impurity



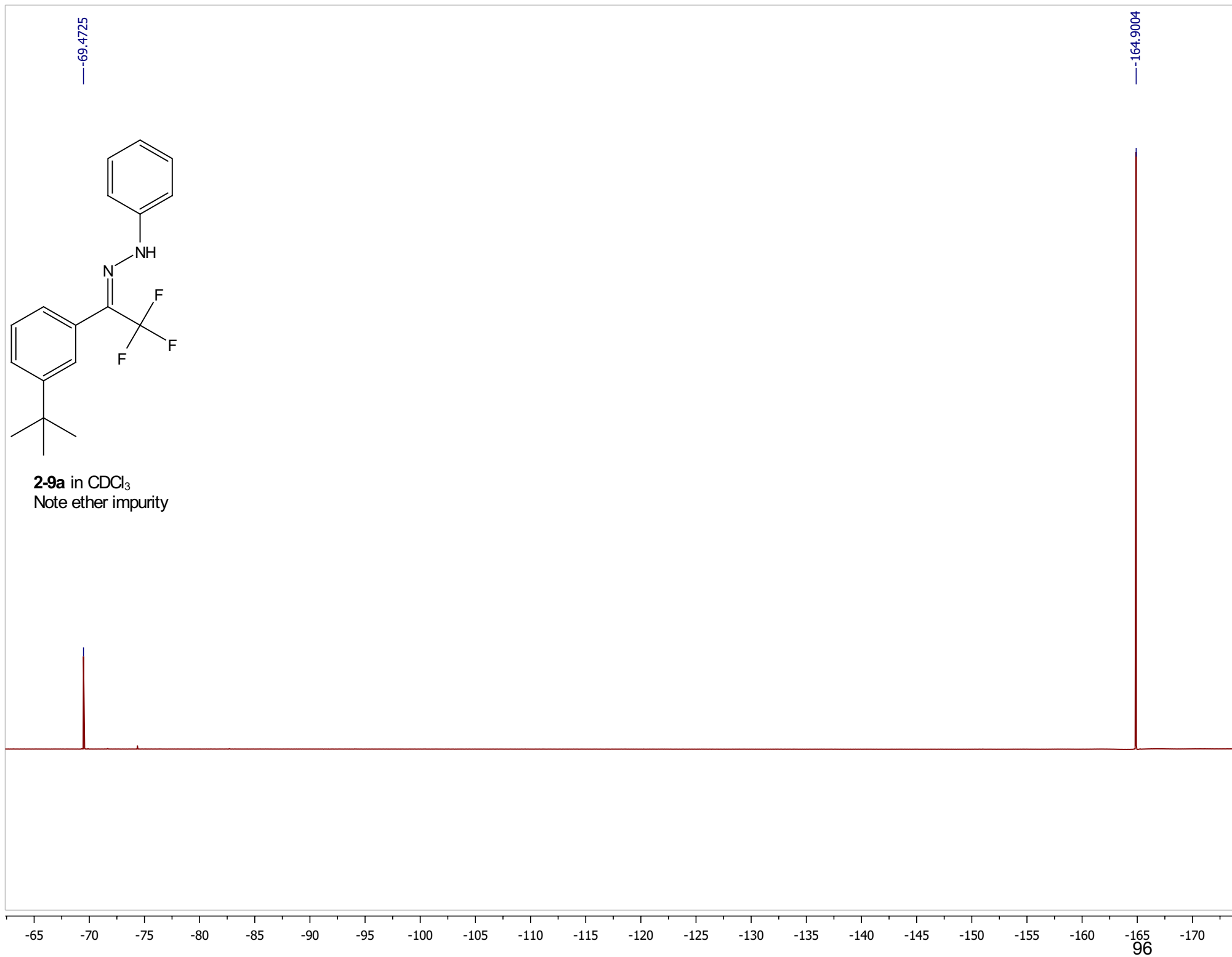


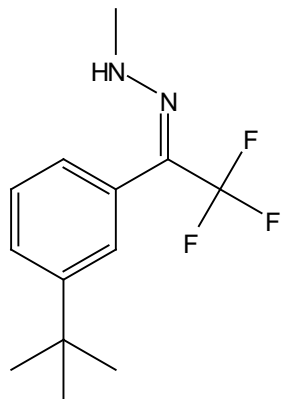
2-9a in CDCl₃
Note ether impurity



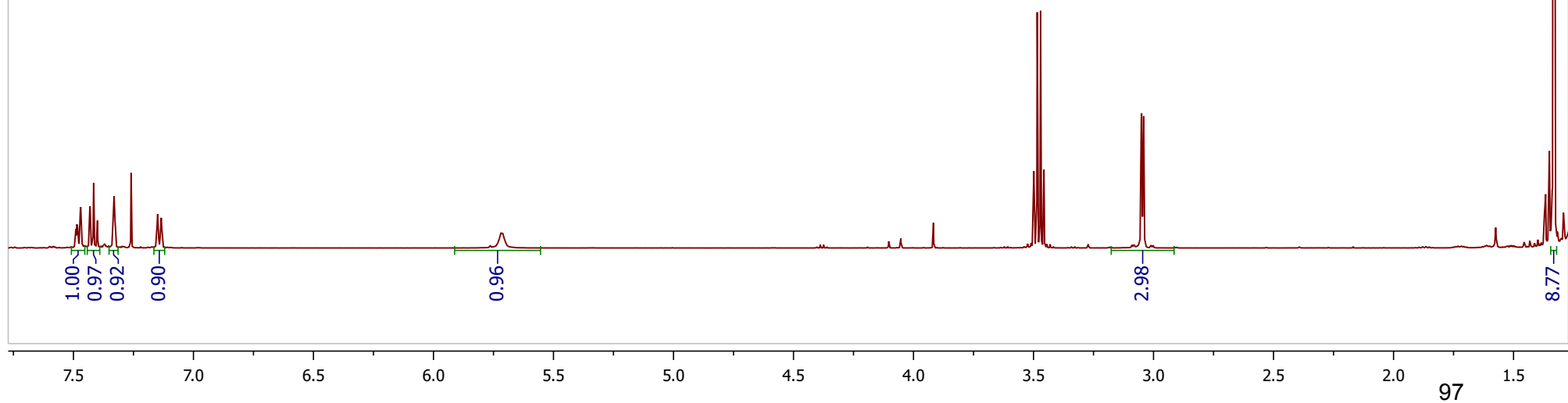


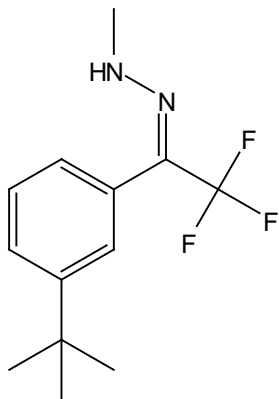
2-9a in CDCl₃
Note ether impurity



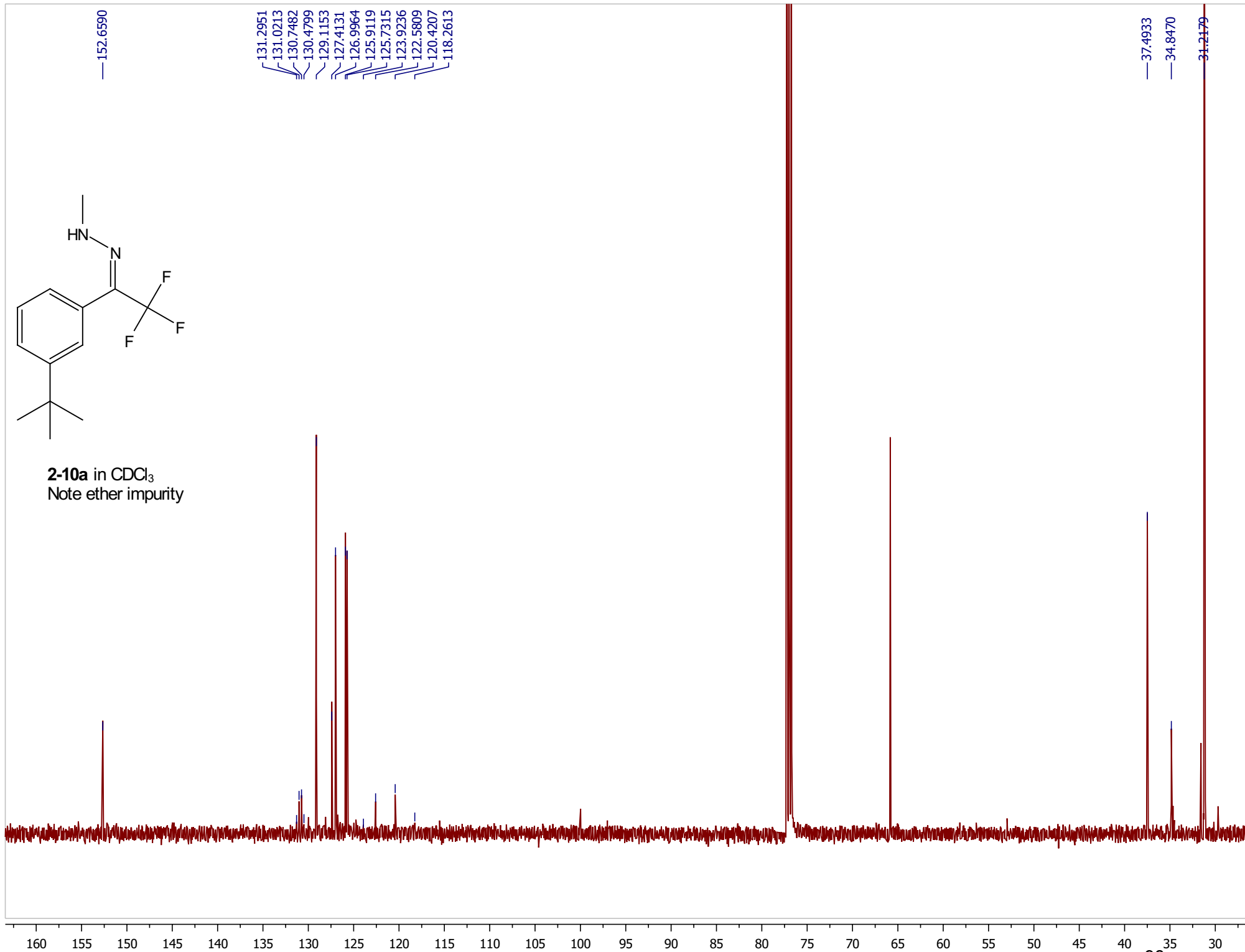


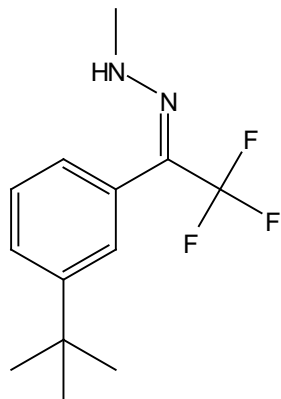
2-10a in CDCl₃
Note ether impurity





2-10a in CDCl₃
Note ether impurity

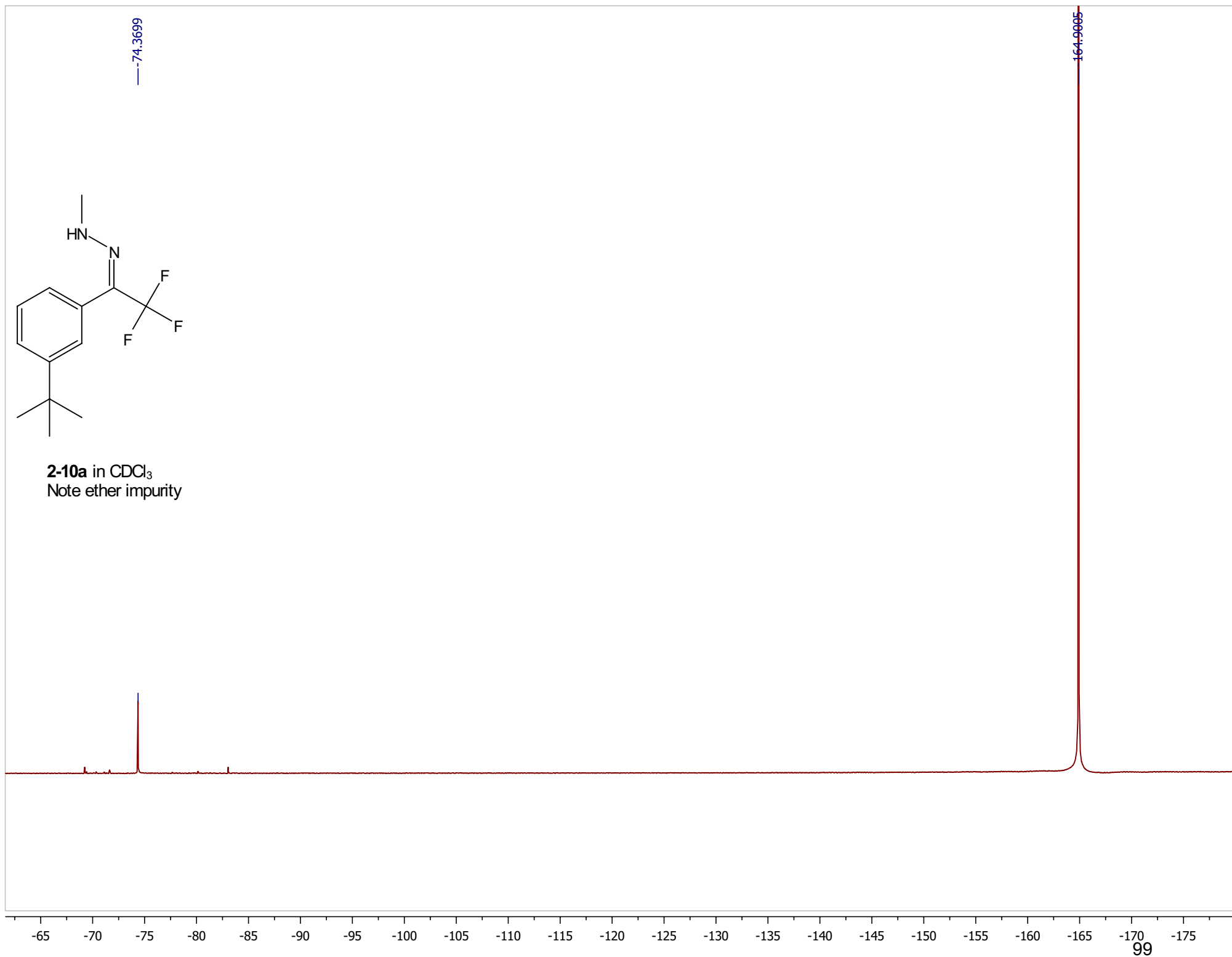


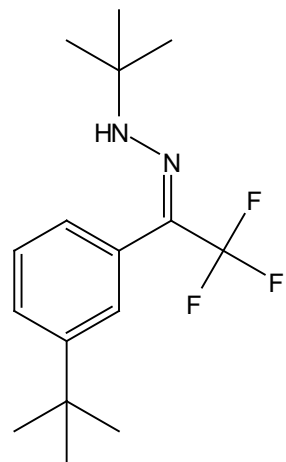


2-10a in CDCl₃
Note ether impurity

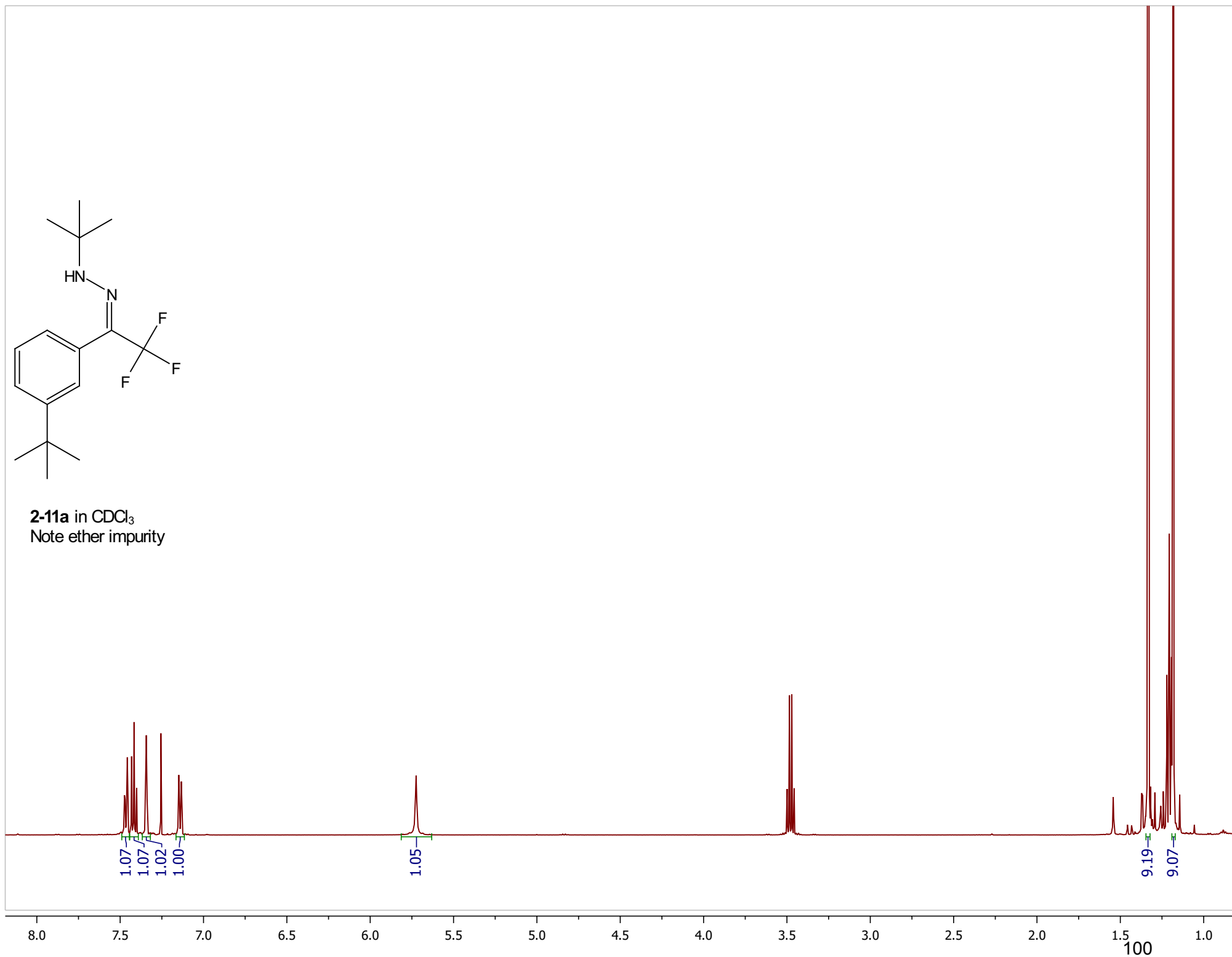
74.3699

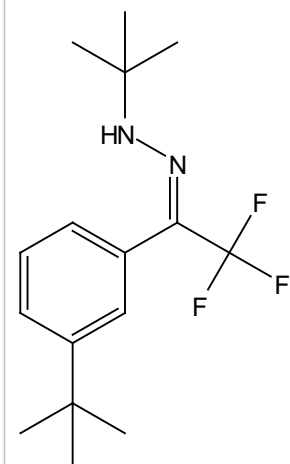
164.9095



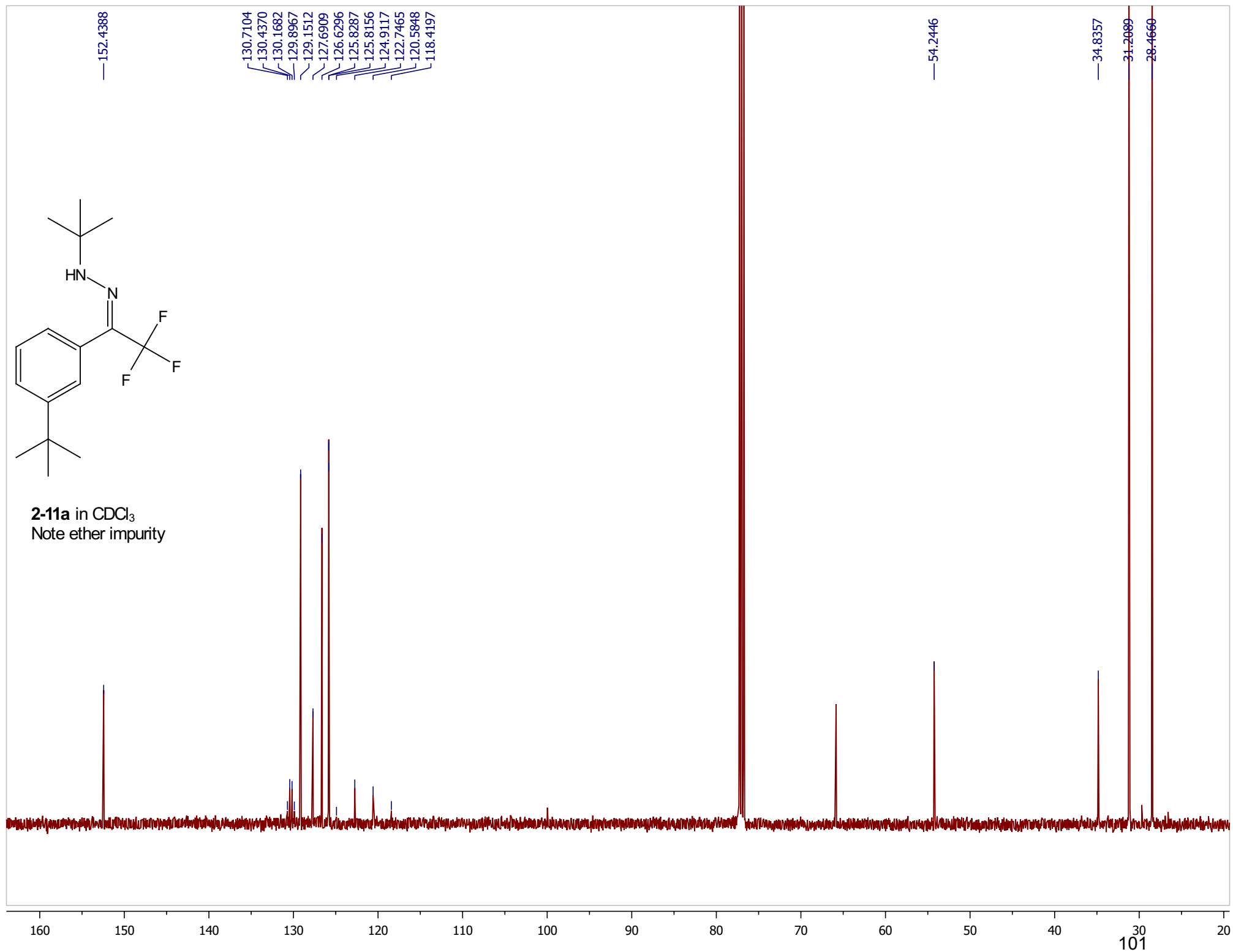


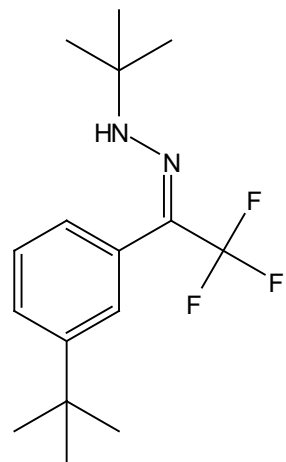
2-11a in CDCl₃
Note ether impurity





2-11a in CDCl₃
Note ether impurity



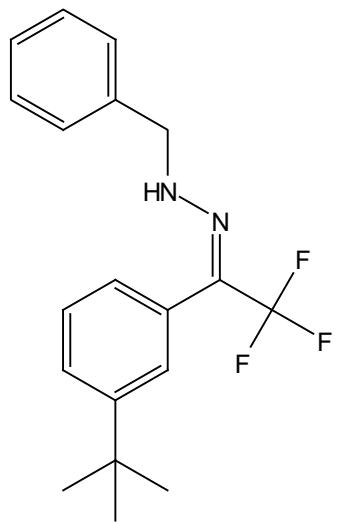


2-11a in CDCl₃
Note ether impurity

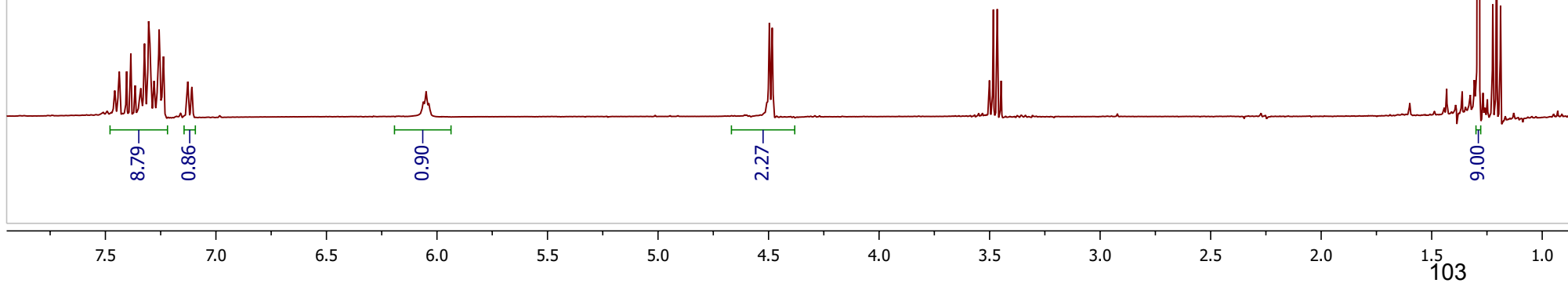
-69.0672

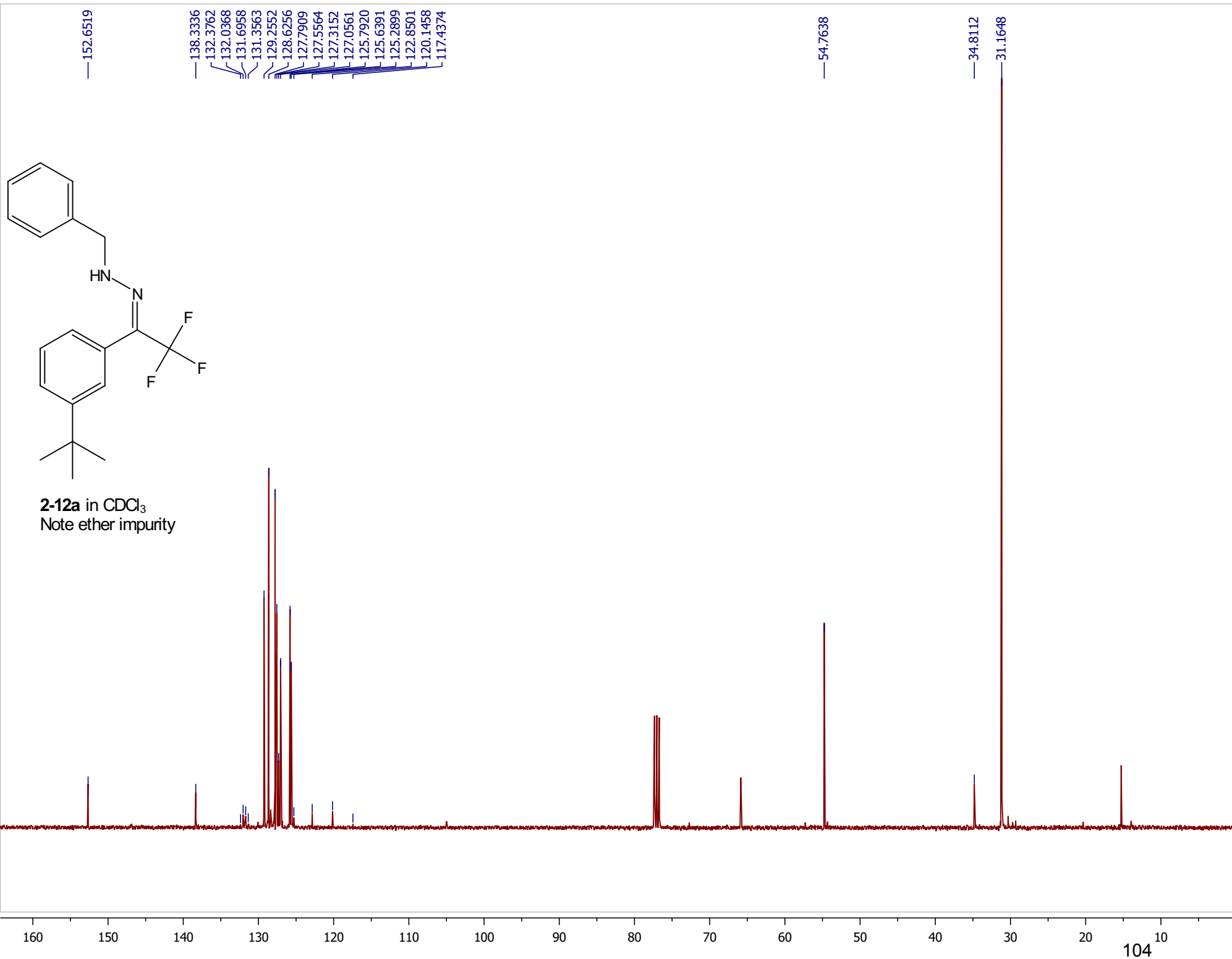
-164.9005

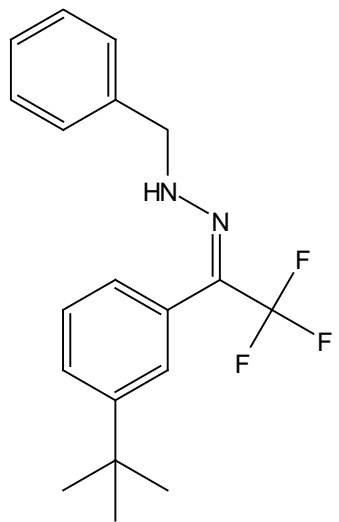
-40 -50 -60 -70 -80 -90 -100 -110 -120 -130 -140 -150 -160 -170 -180



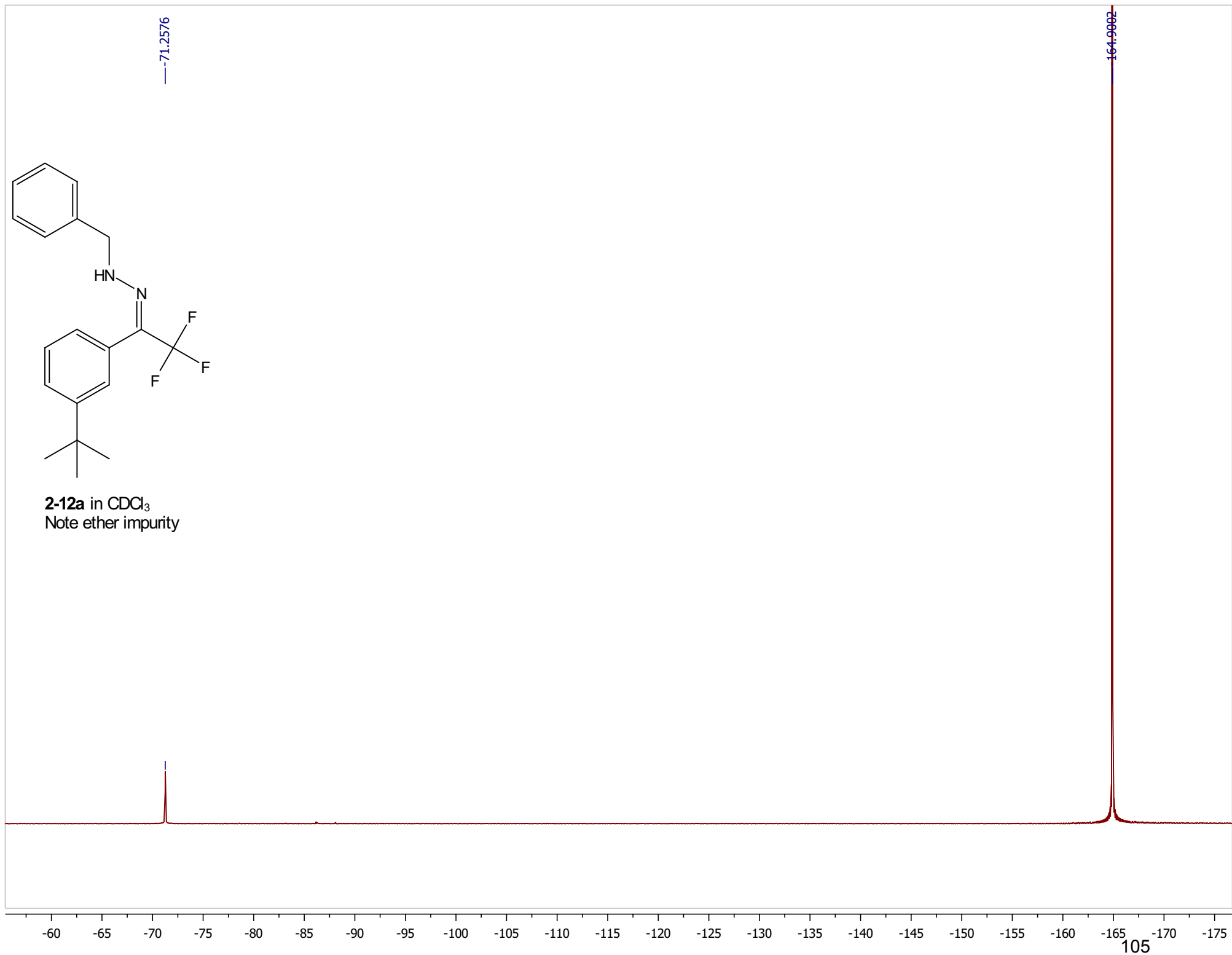
2-12a in CDCl₃
Note ether impurity

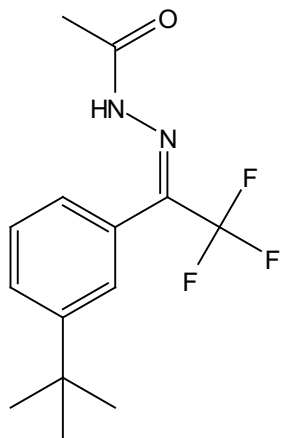




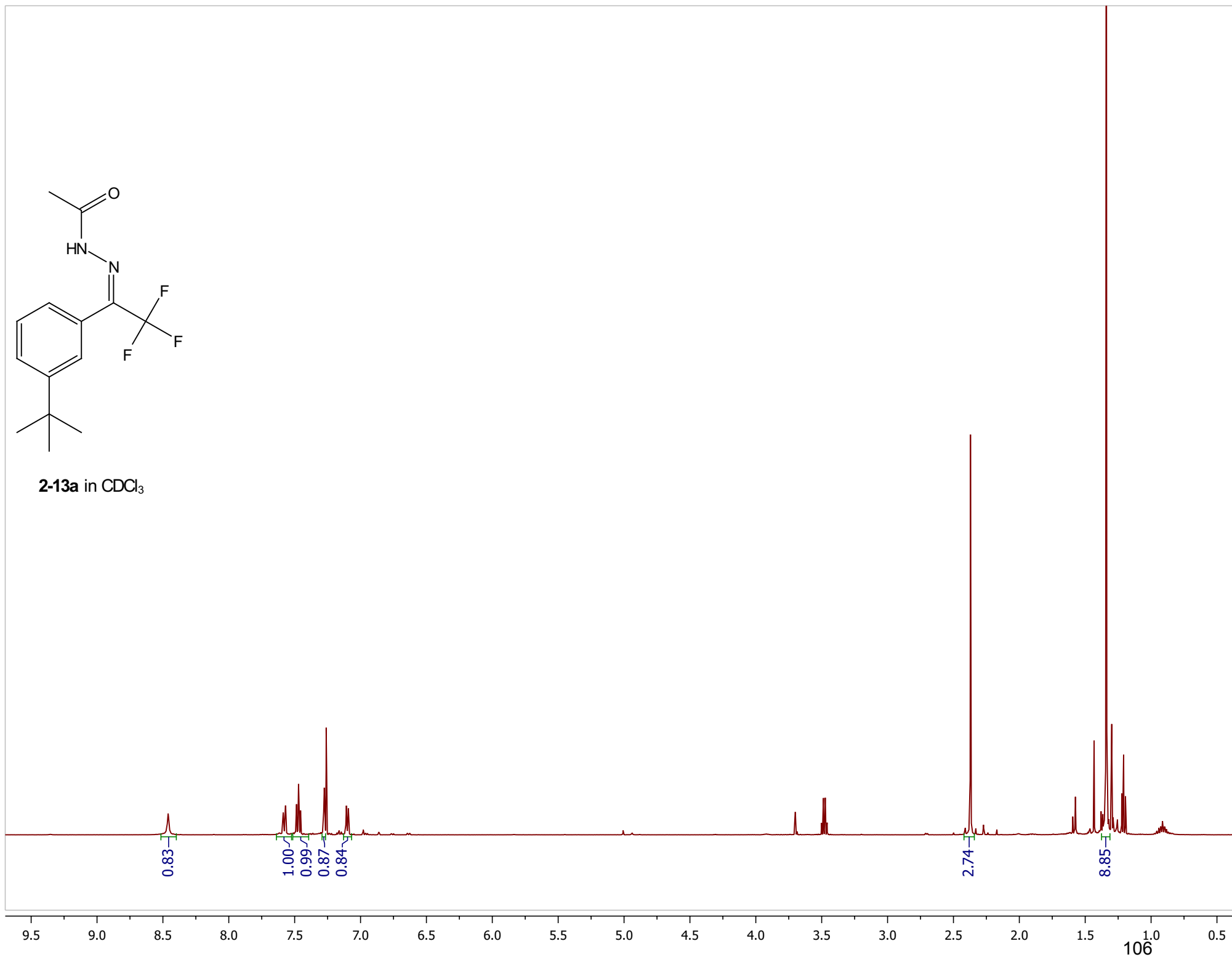


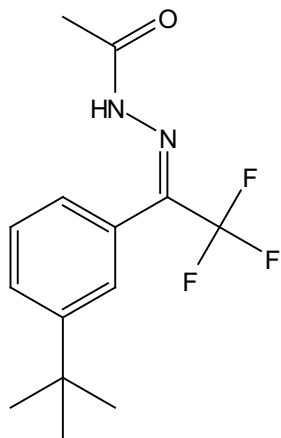
2-12a in CDCl₃
Note ether impurity



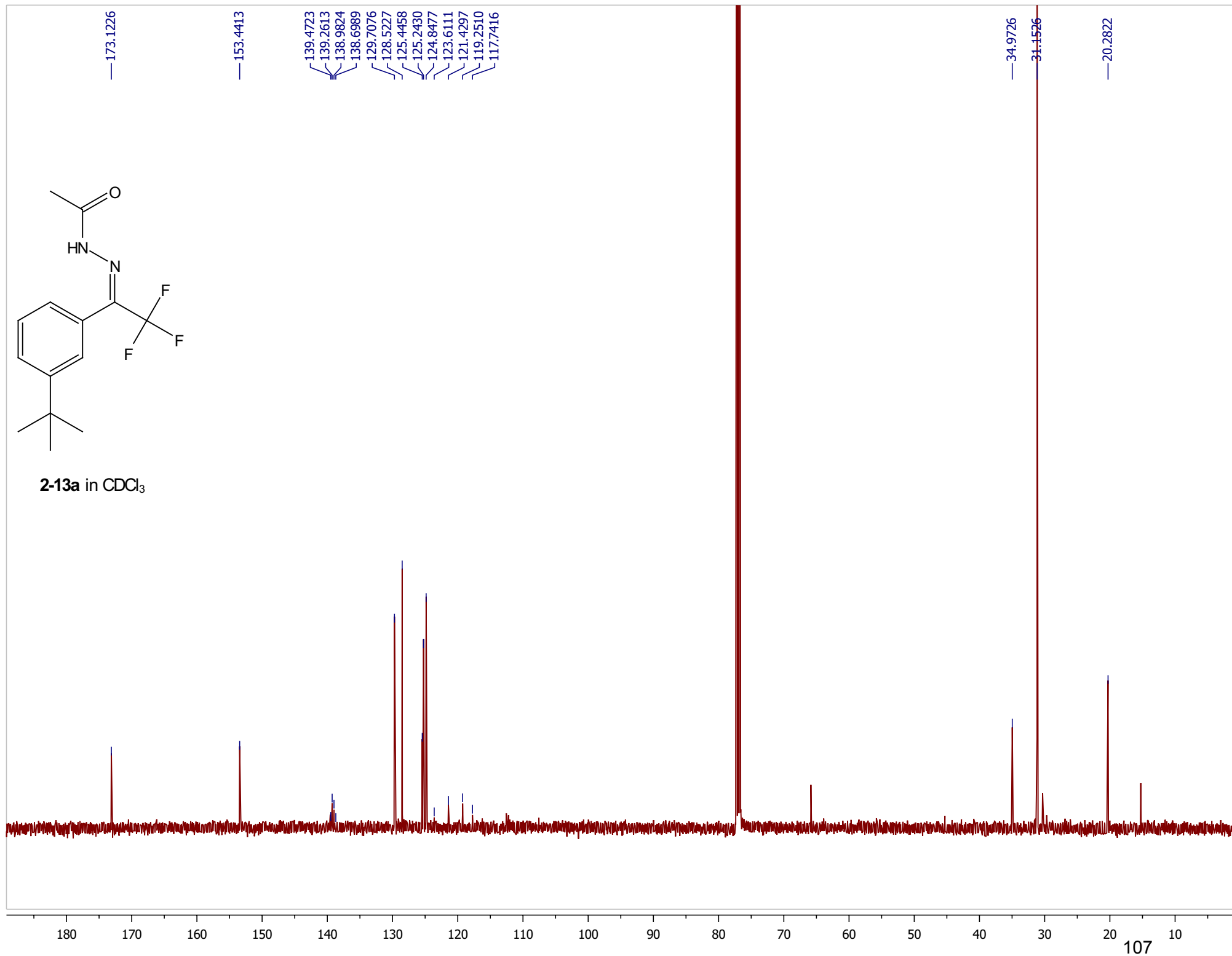


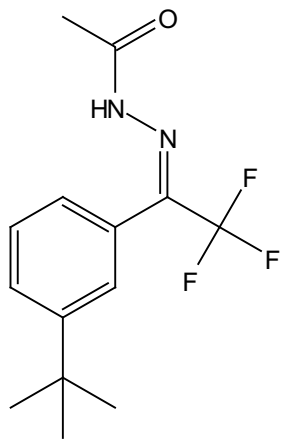
2-13a in CDCl₃





2-13a in CDCl₃

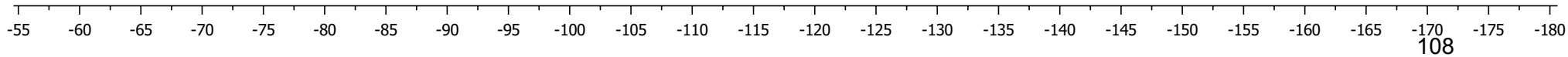


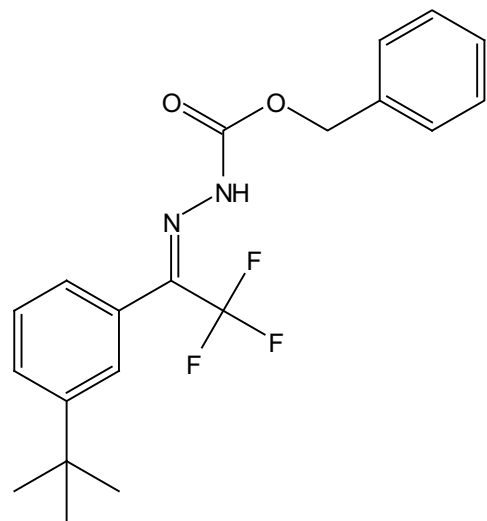


2-13a in CDCl₃

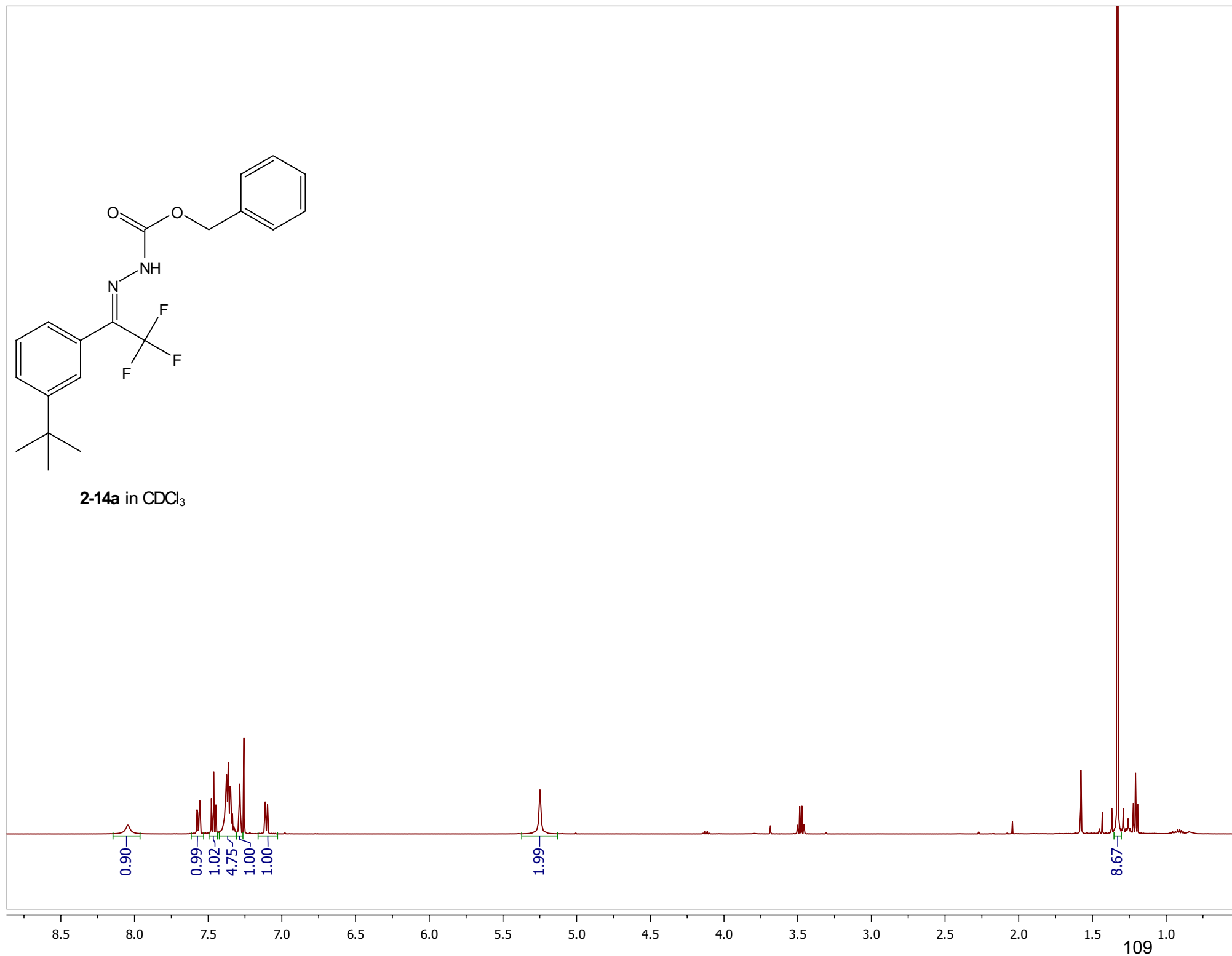
71.4463

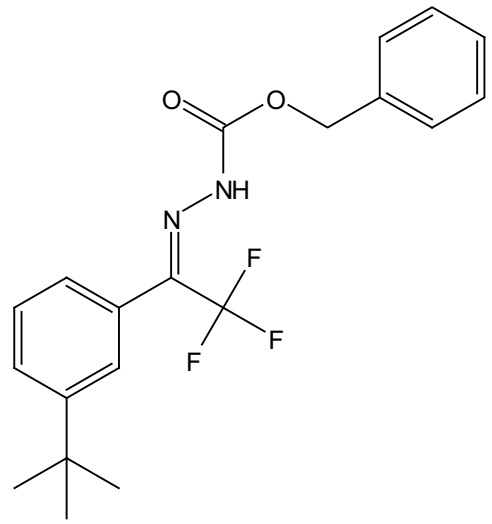
164.9802



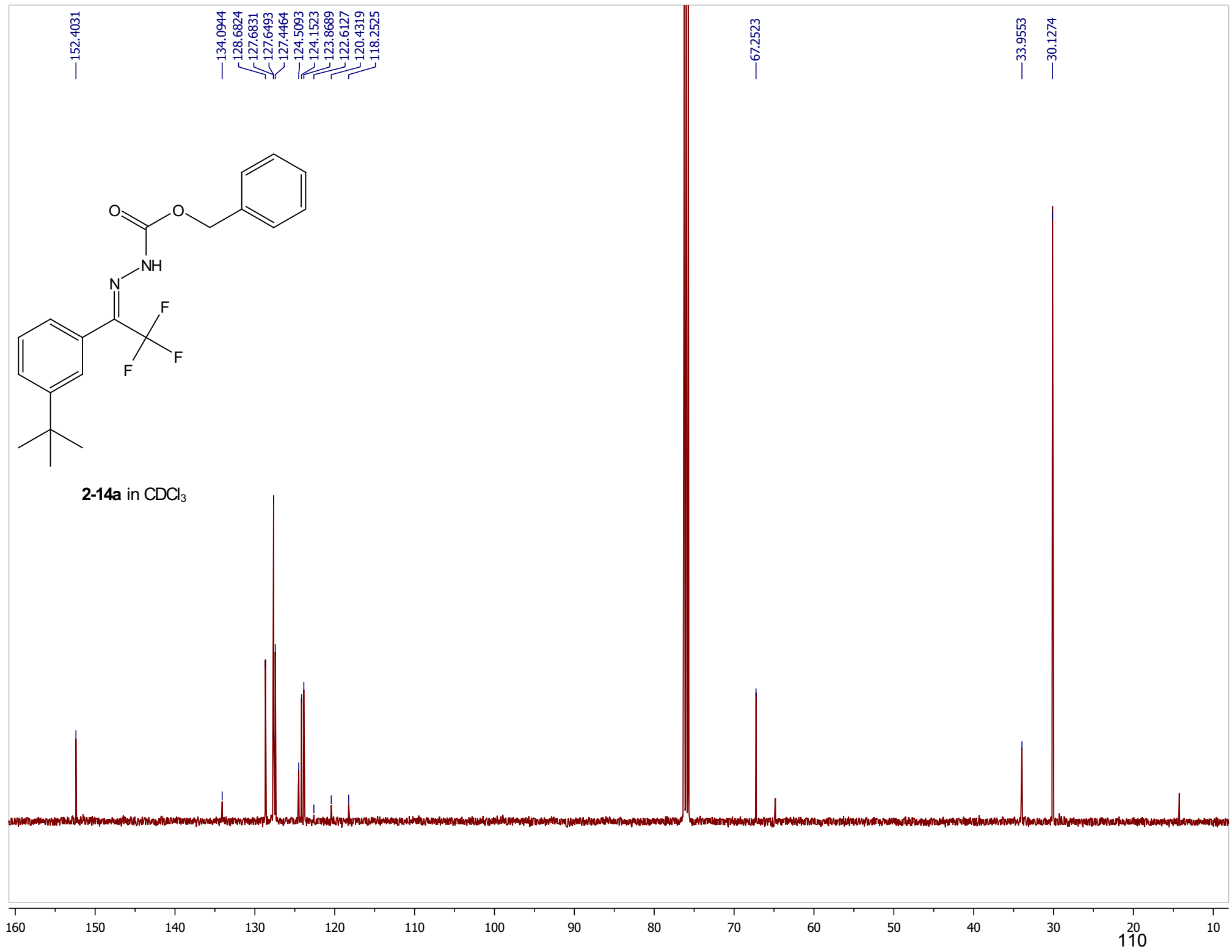


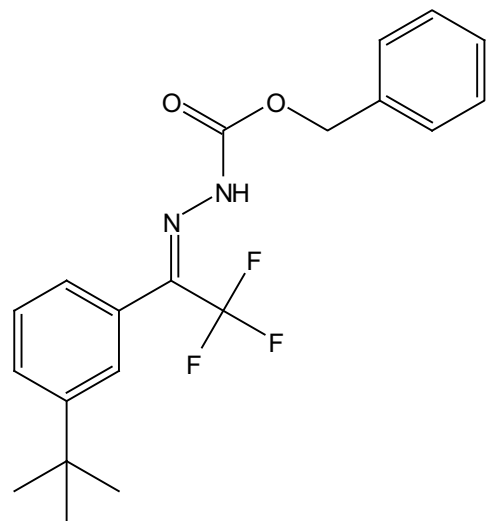
2-14a in CDCl₃





2-14a in CDCl₃

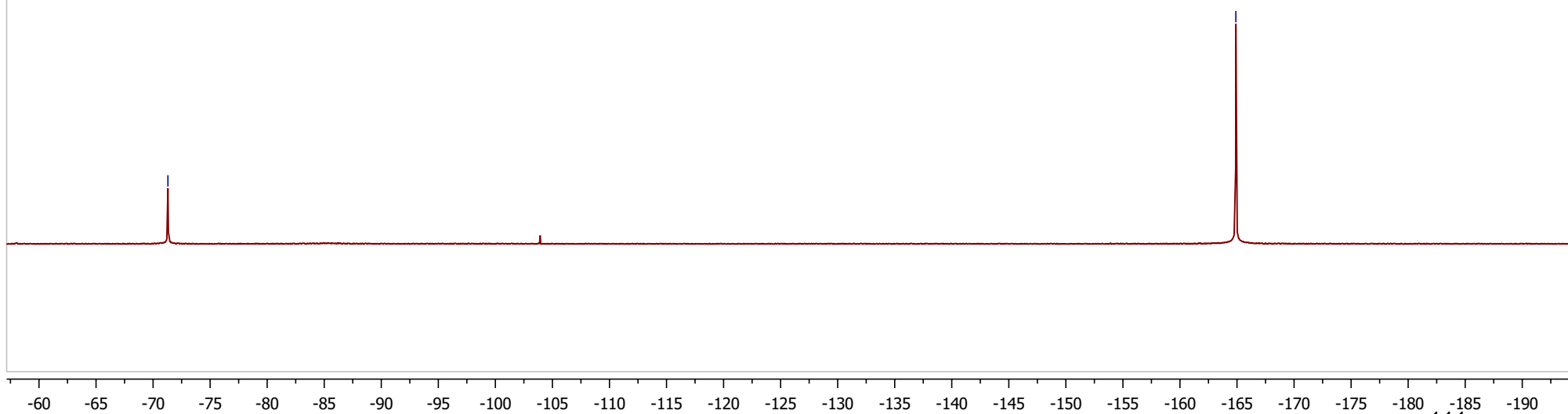


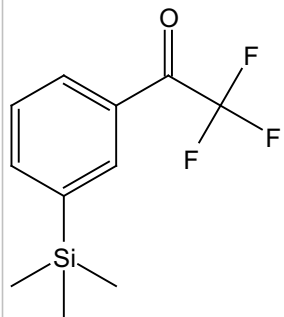


2-14a in CDCl₃

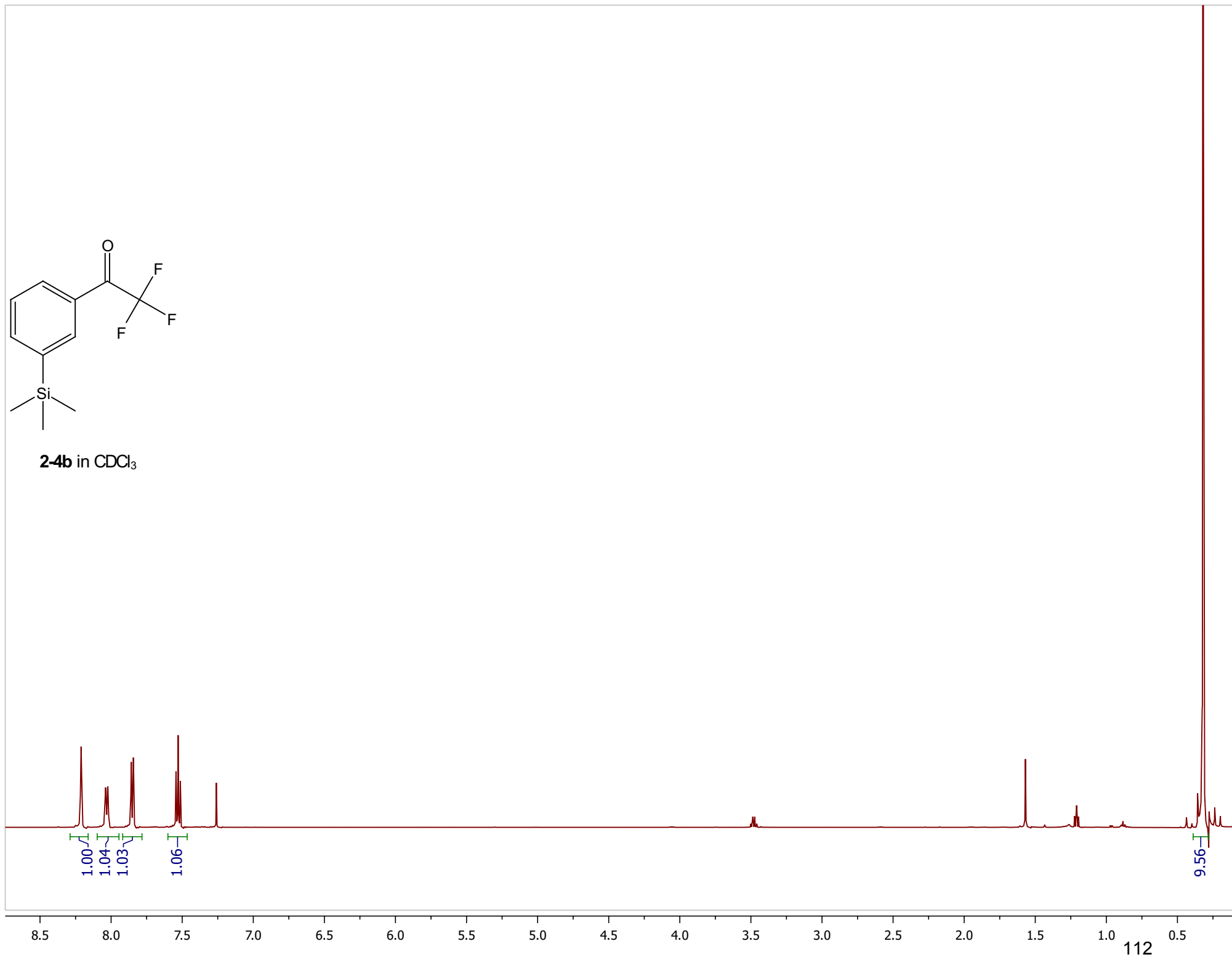
-71.3006

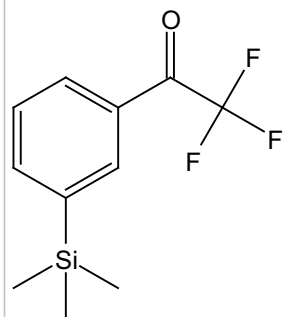
-164.8978



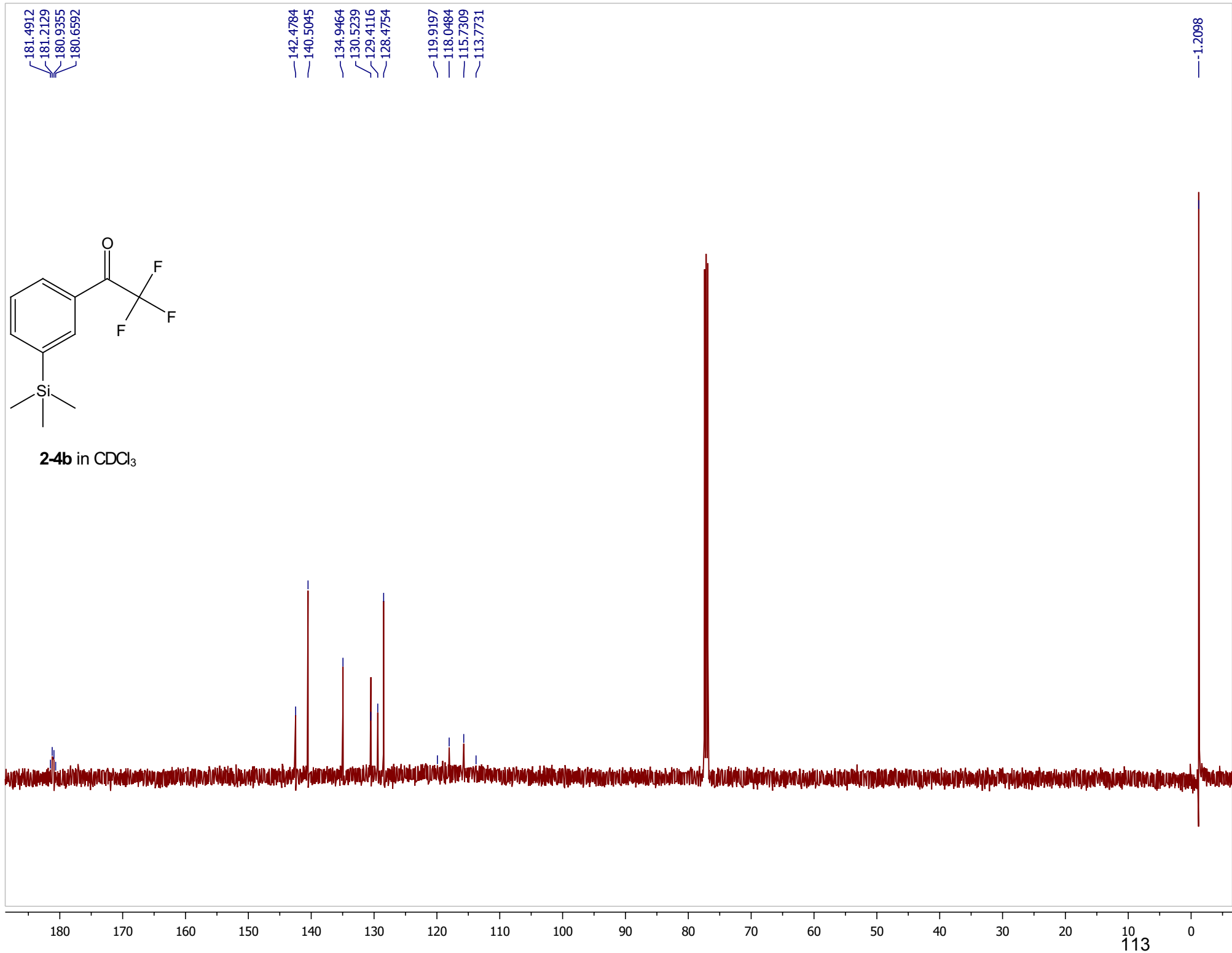


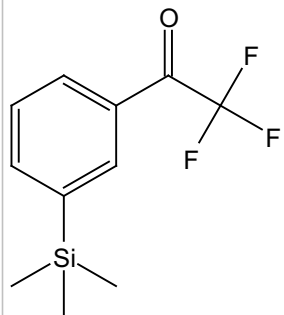
2-4b in CDCl₃





2-4b in CDCl₃

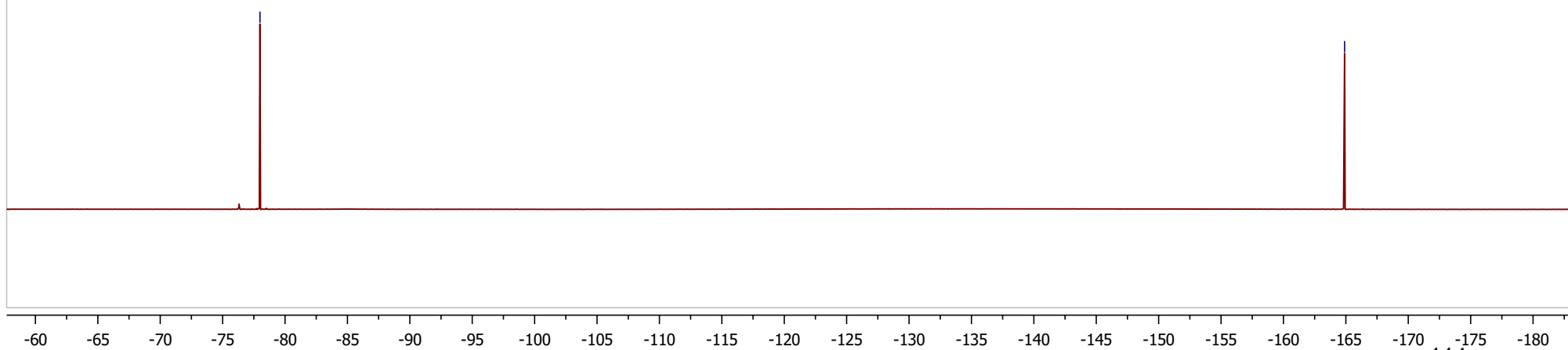


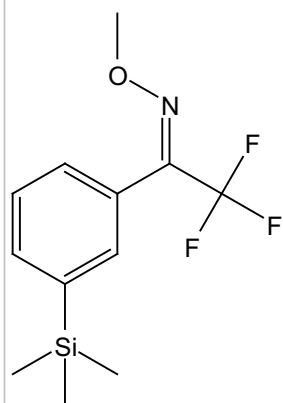


2-4b in CDCl₃

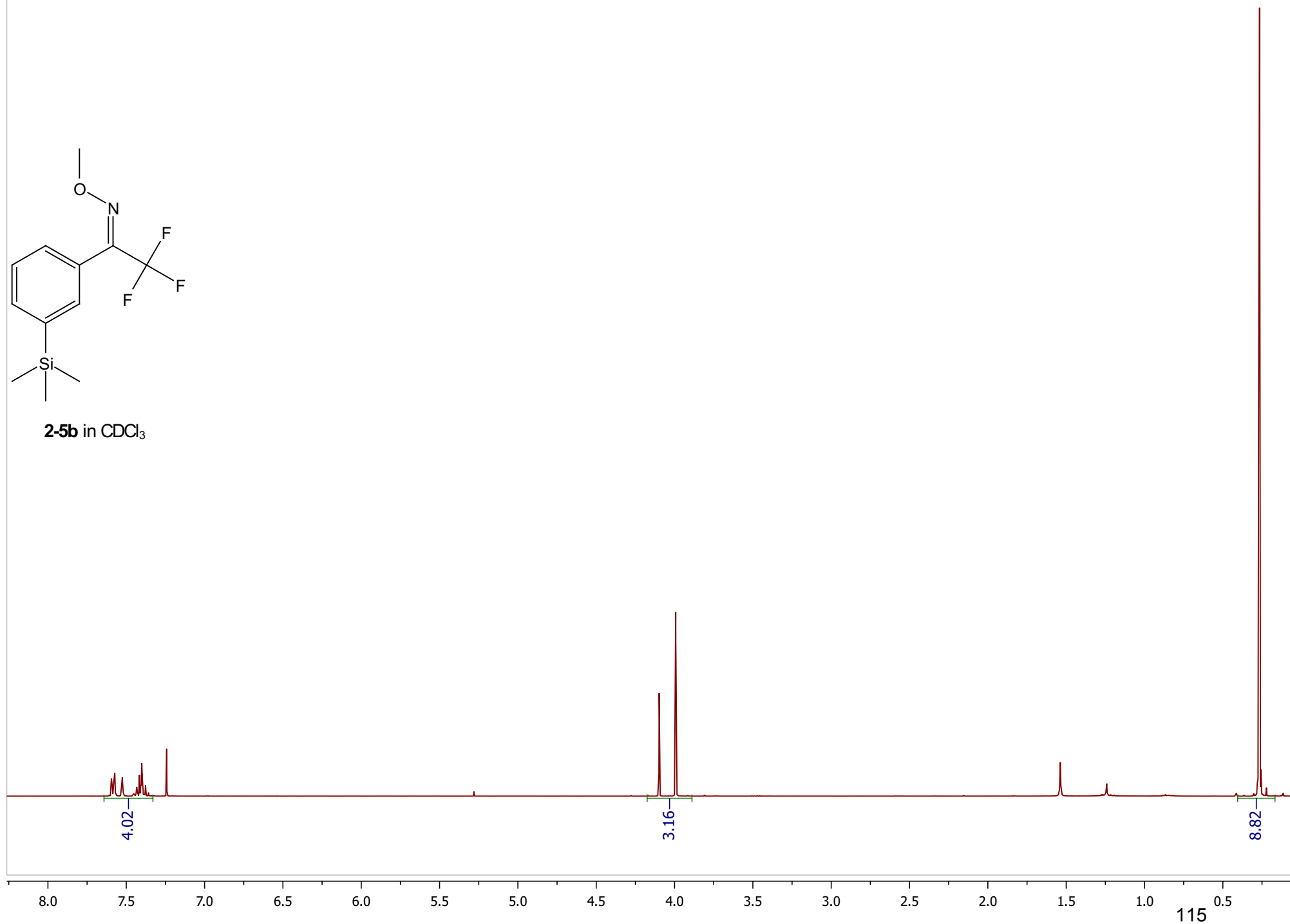
—77.9916

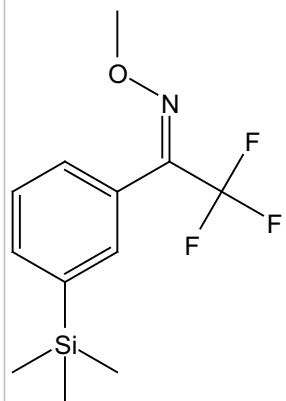
—164.8998



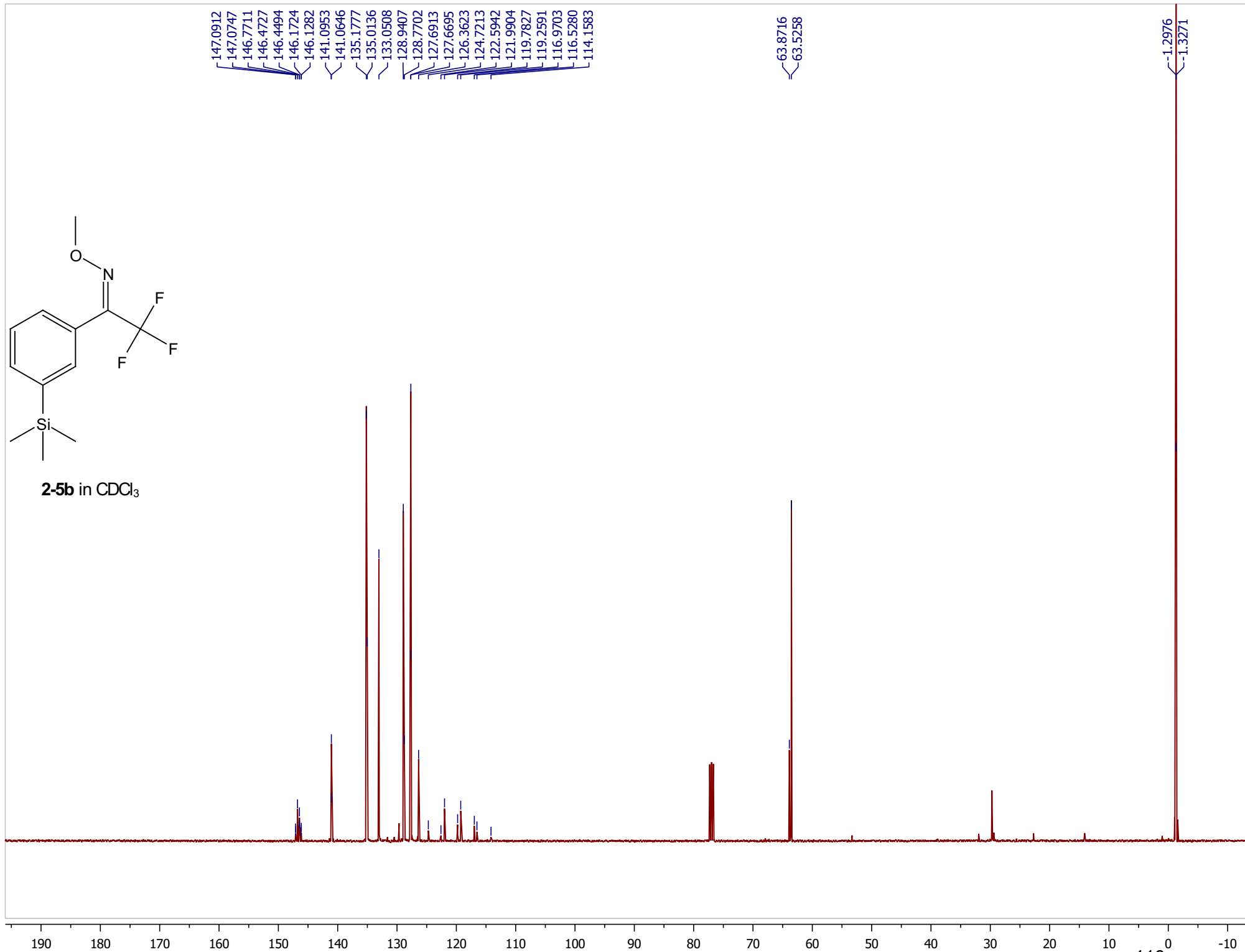


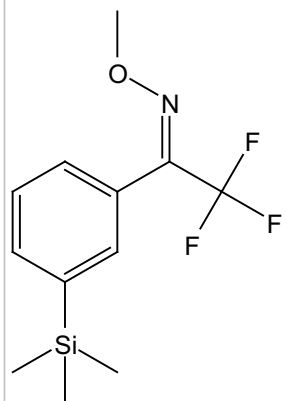
2-5b in CDCl₃





2-5b in CDCl₃





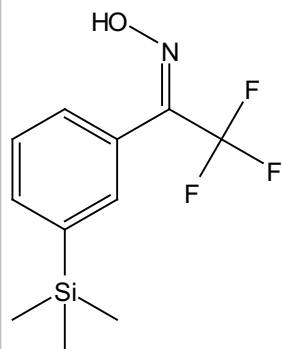
2-5b in CDCl₃

65.4610

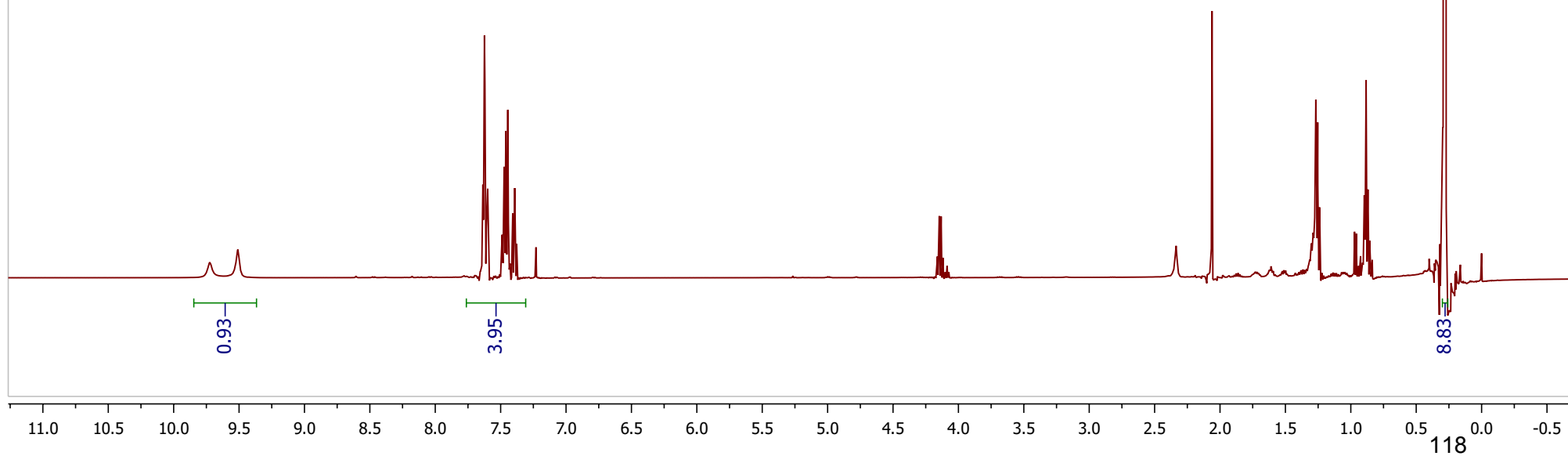
69.4201

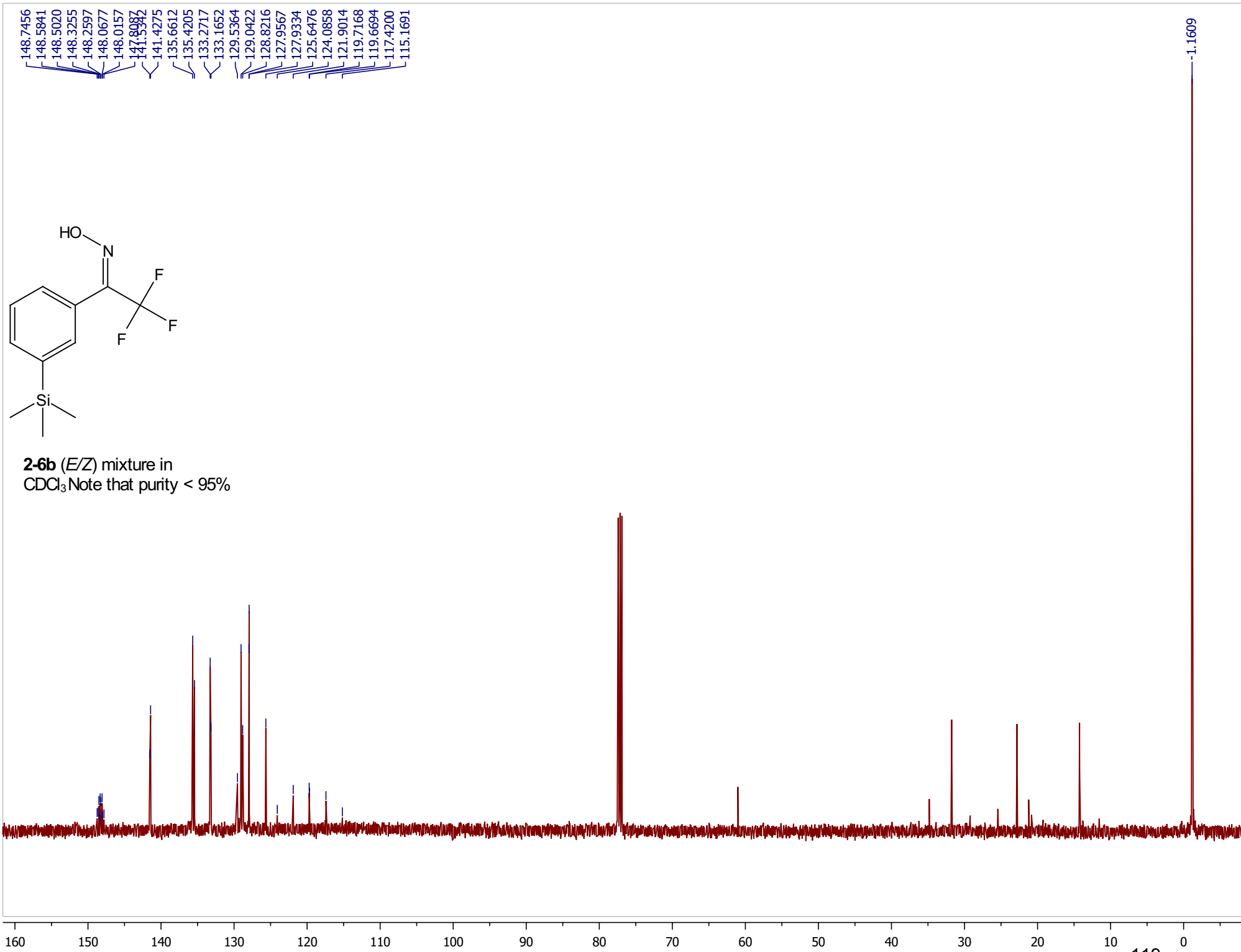
164.9000

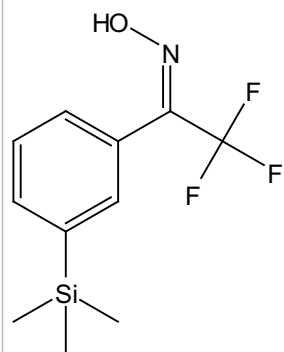
-50 -60 -70 -80 -90 -100 -110 -120 -130 -140 -150 -160 -170 -180



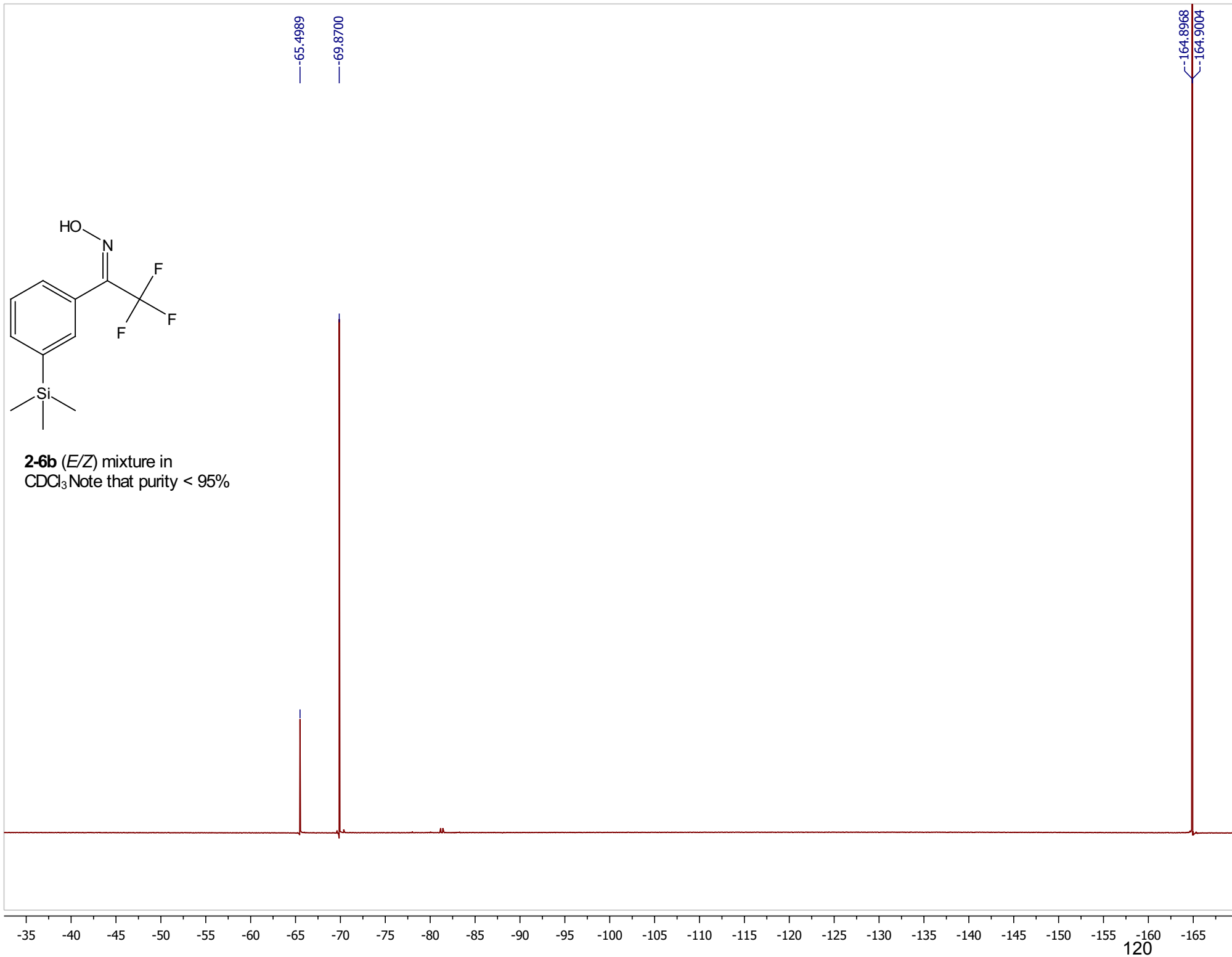
2-6b (*E/Z*) mixture in
CDCl₃ Note that purity < 95%

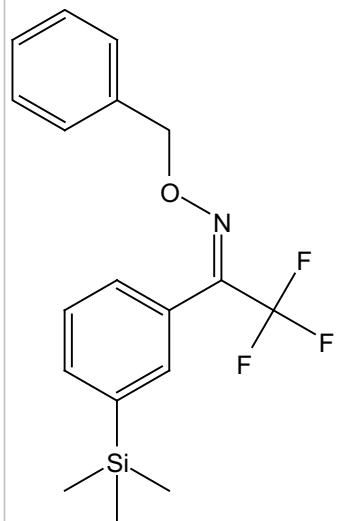




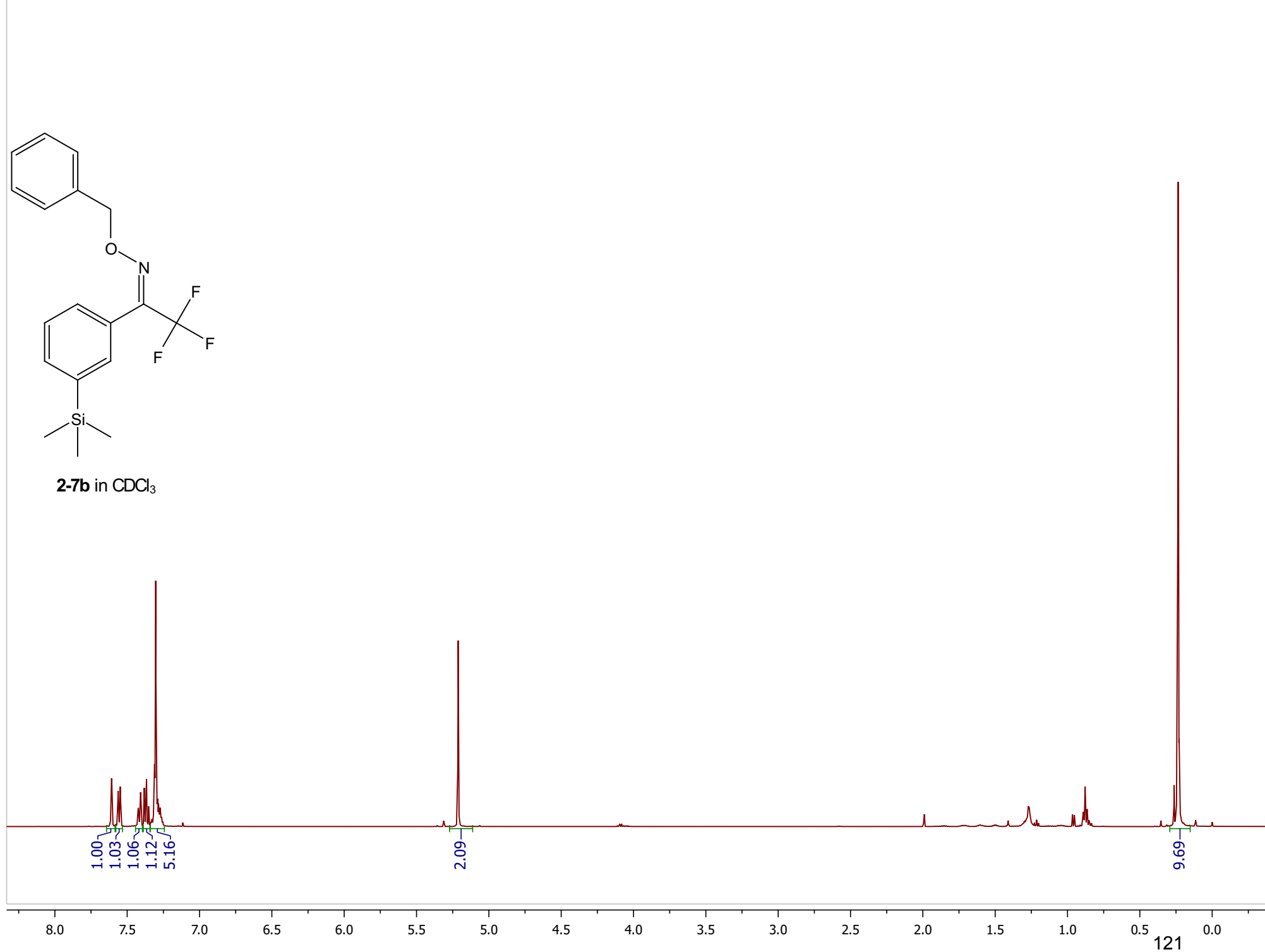


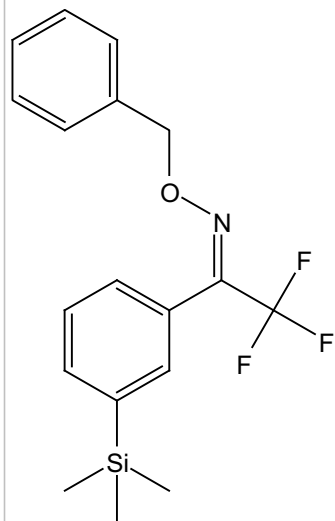
2-6b (*E/Z*) mixture in CDCl_3 Note that purity < 95%



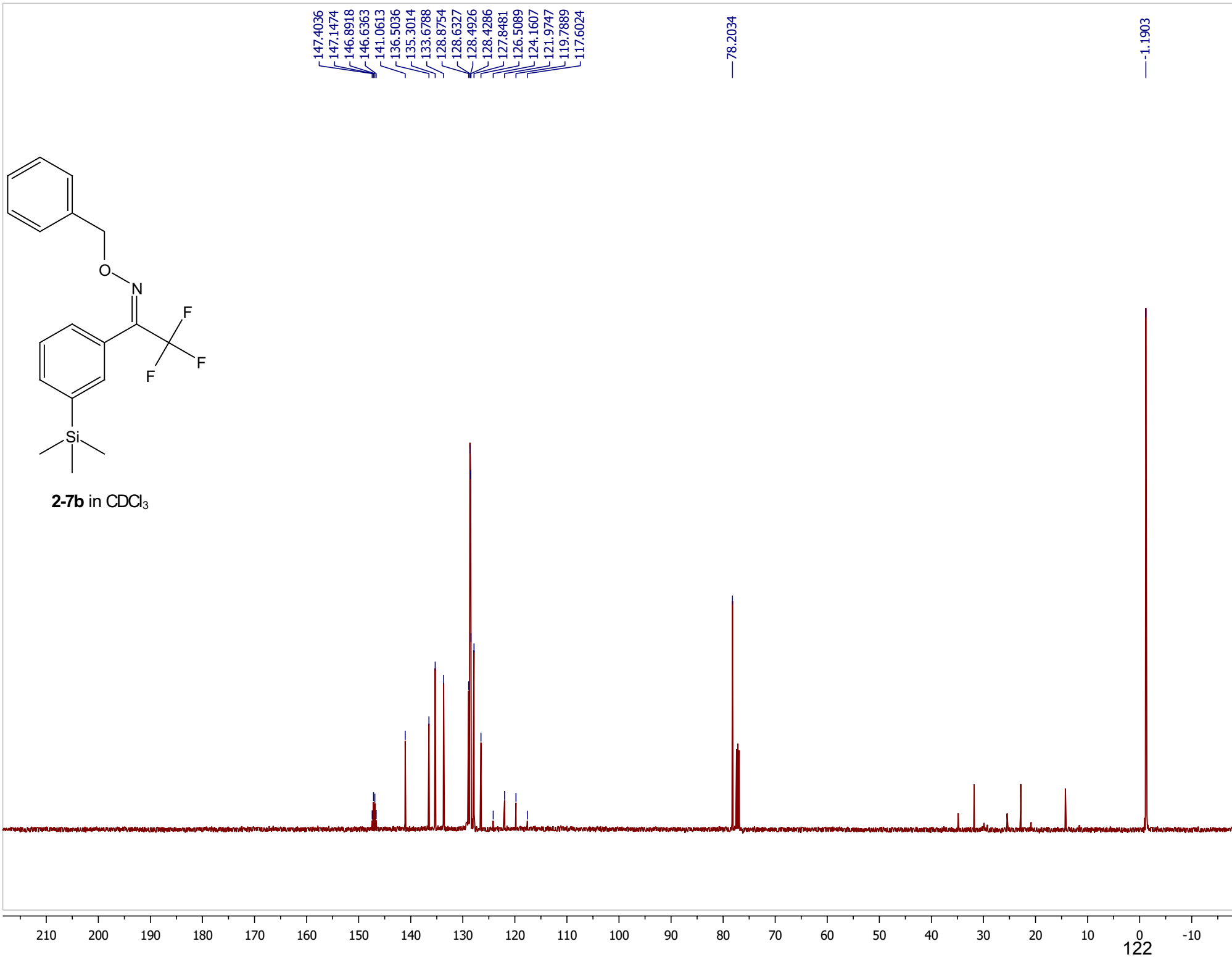


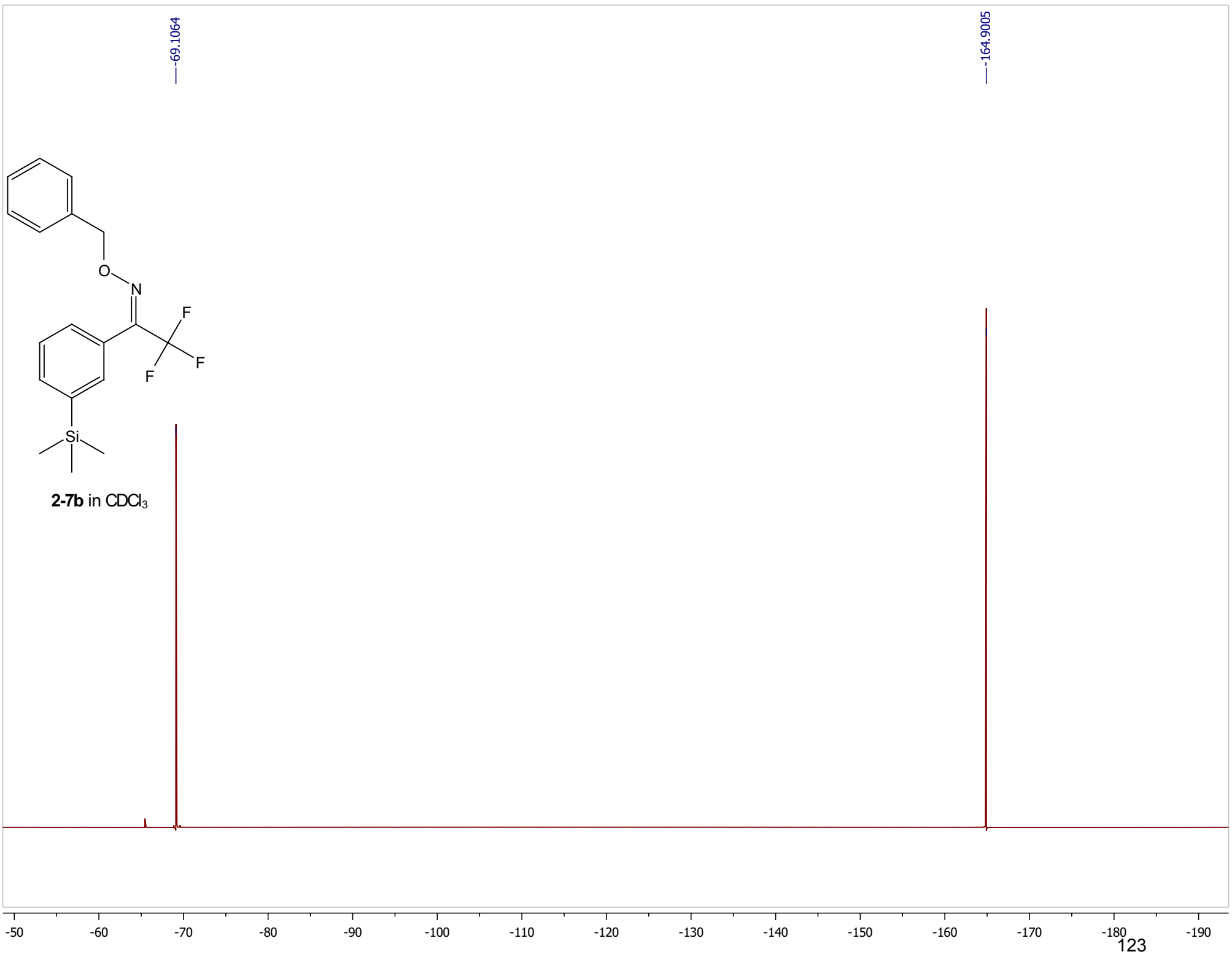
2-7b in CDCl₃



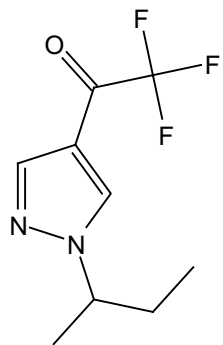


2-7b in CDCl₃

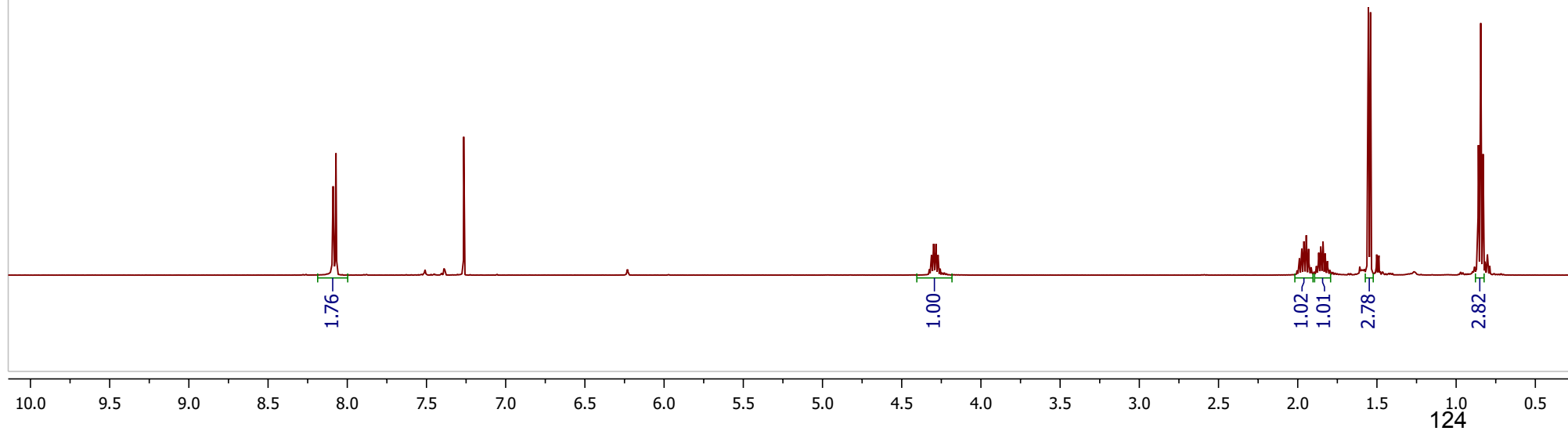




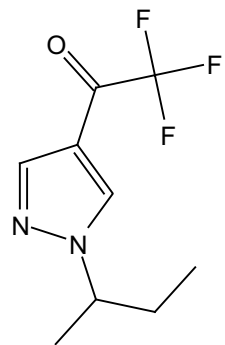
2-7b in CDCl_3



2-4c in CDCl₃



Carbon01



2-4c in CDCl₃

175.1229
174.7626
174.3974
174.1347

141.6510

132.5593

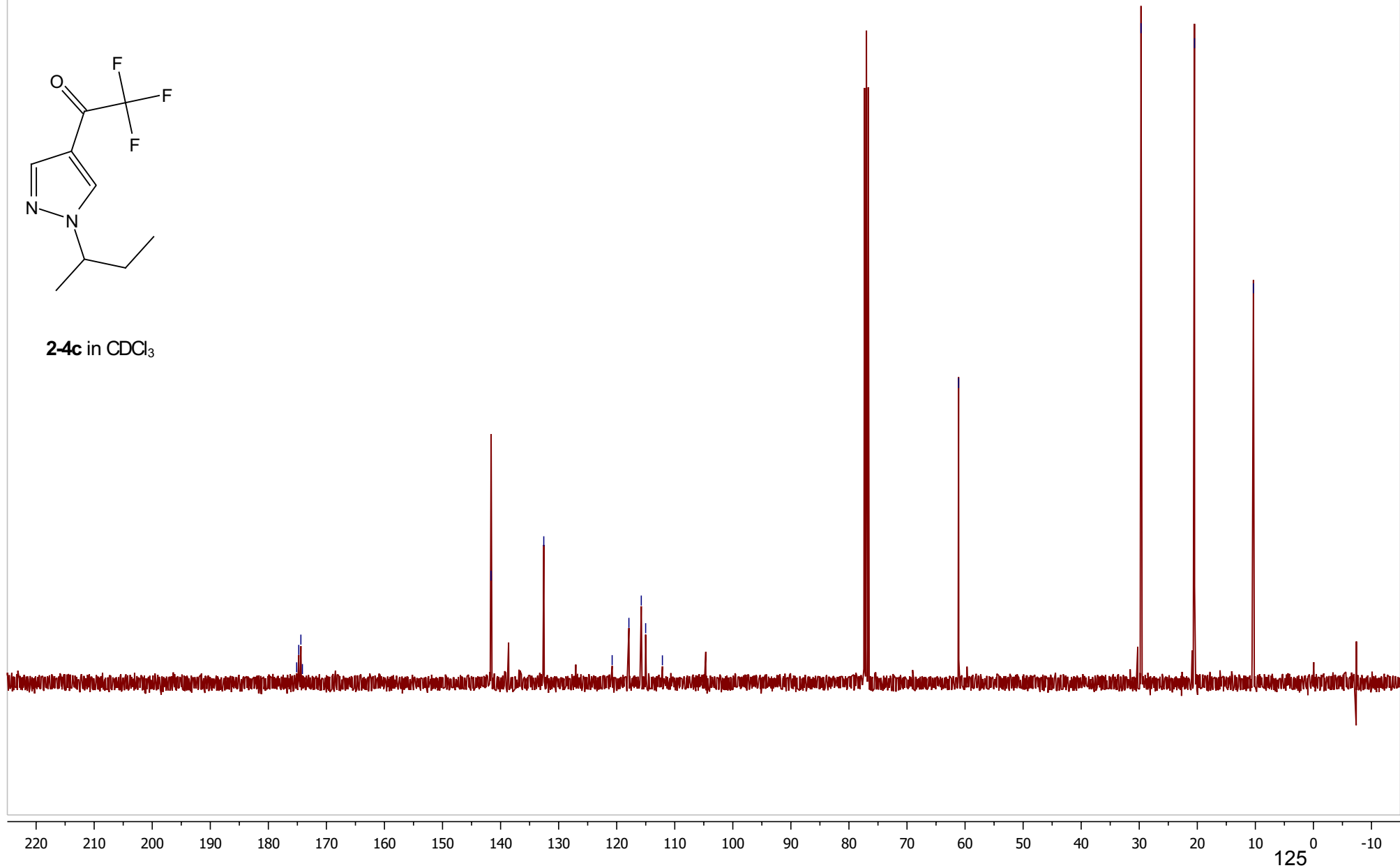
120.7836
117.8984
115.7672
115.0131
112.1278

61.1112

29.6937

20.4811

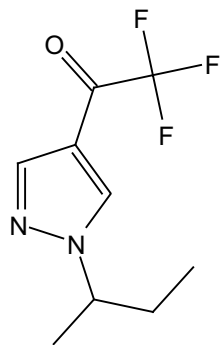
10.3355



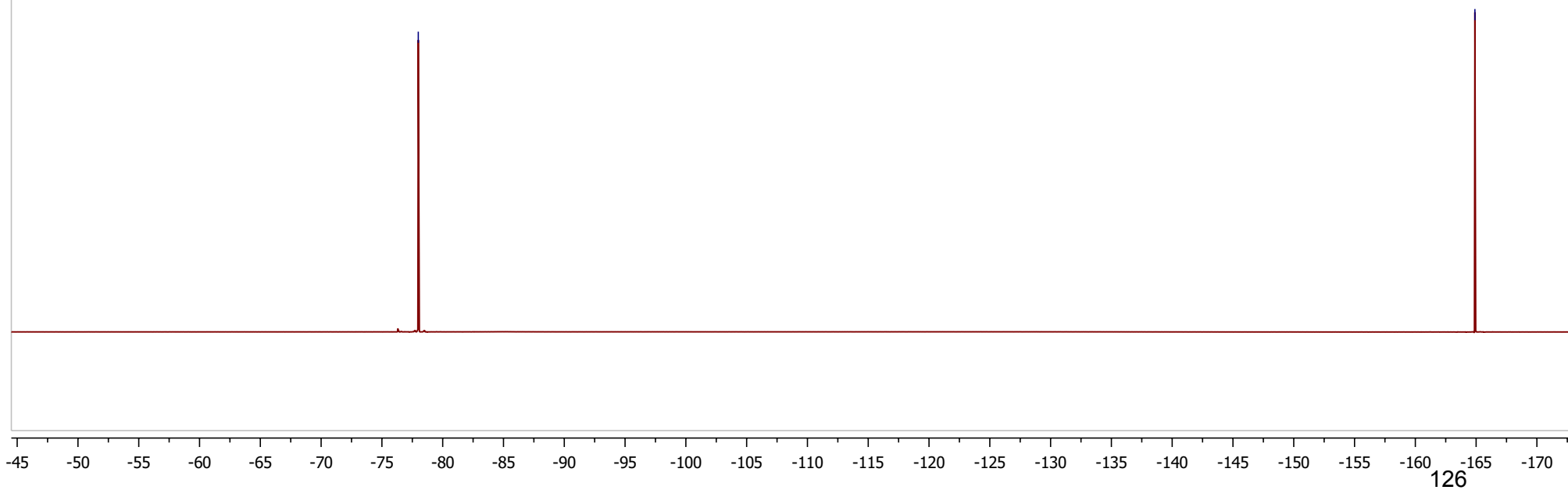
Fluorine01

-77.9912

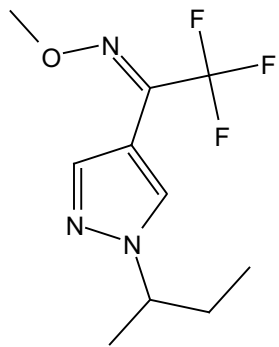
-164.9004



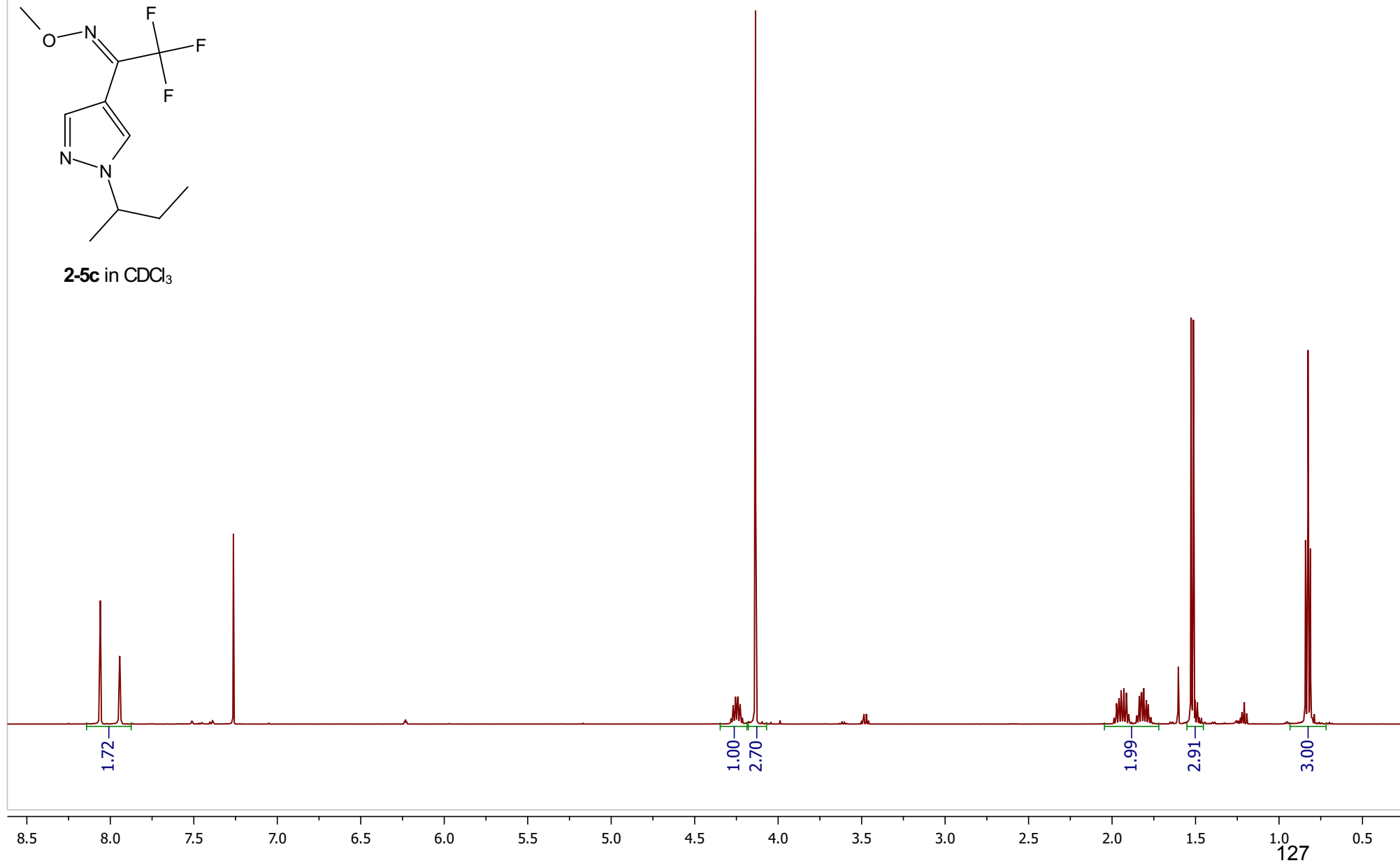
2-4c in CDCl₃



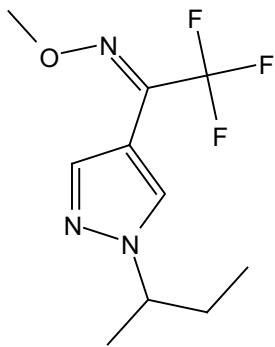
EXC-1-96 1H take 2 Jan15-2012
PROTONRO CDCl3 /opt/topspin3.0/icon-data carlie-1 2



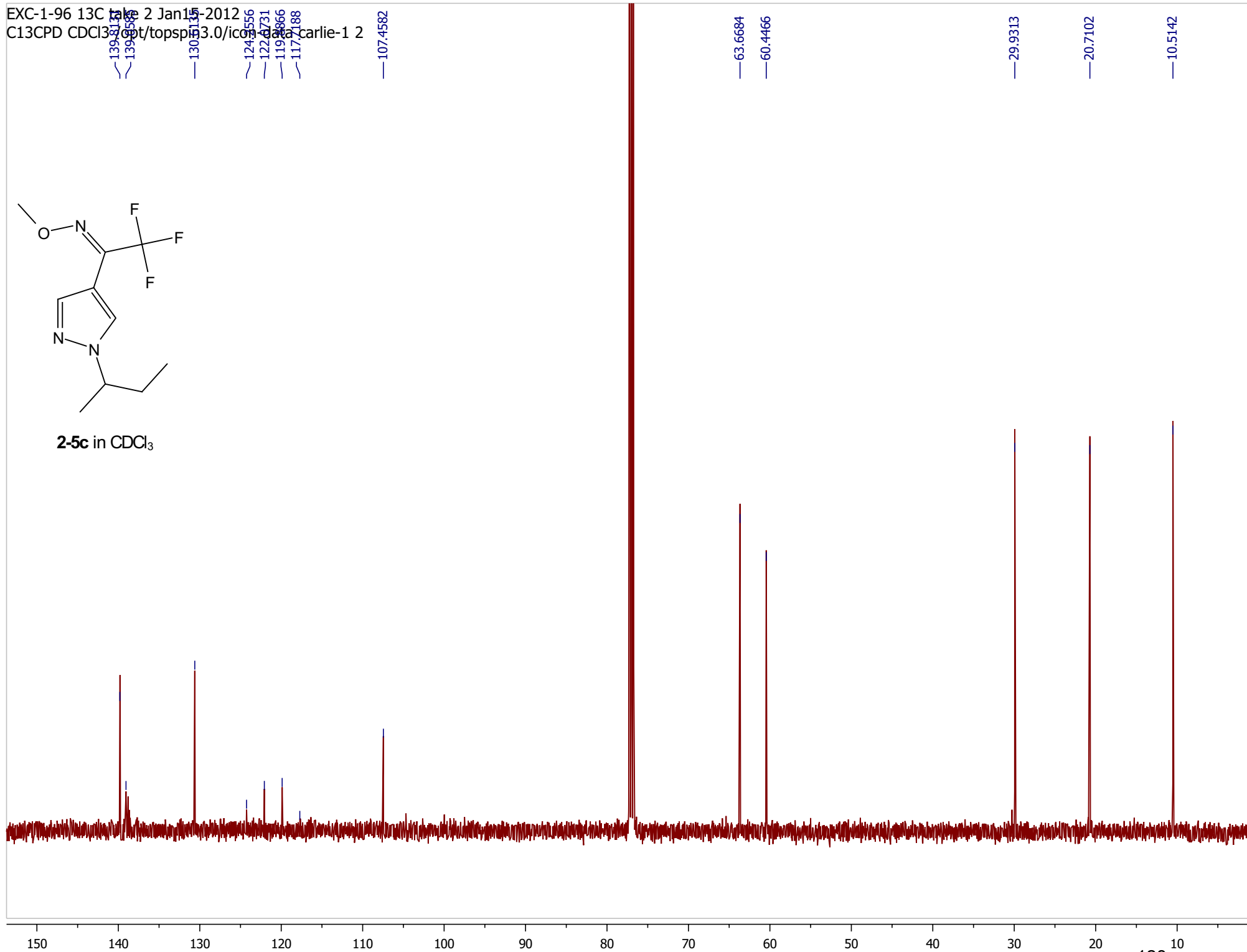
2-5c in CDCl₃

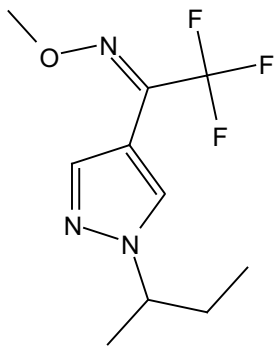


EXC-1-96 13C take 2 Jan 15-2012
C13CPD CDC13 opt/topspin3.0/icon data carlie-1 2



2-5c in CDCl₃





2-5c in CDCl₃

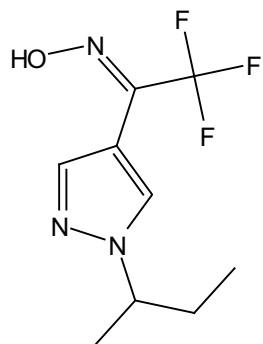
-68.9460

-164.8996

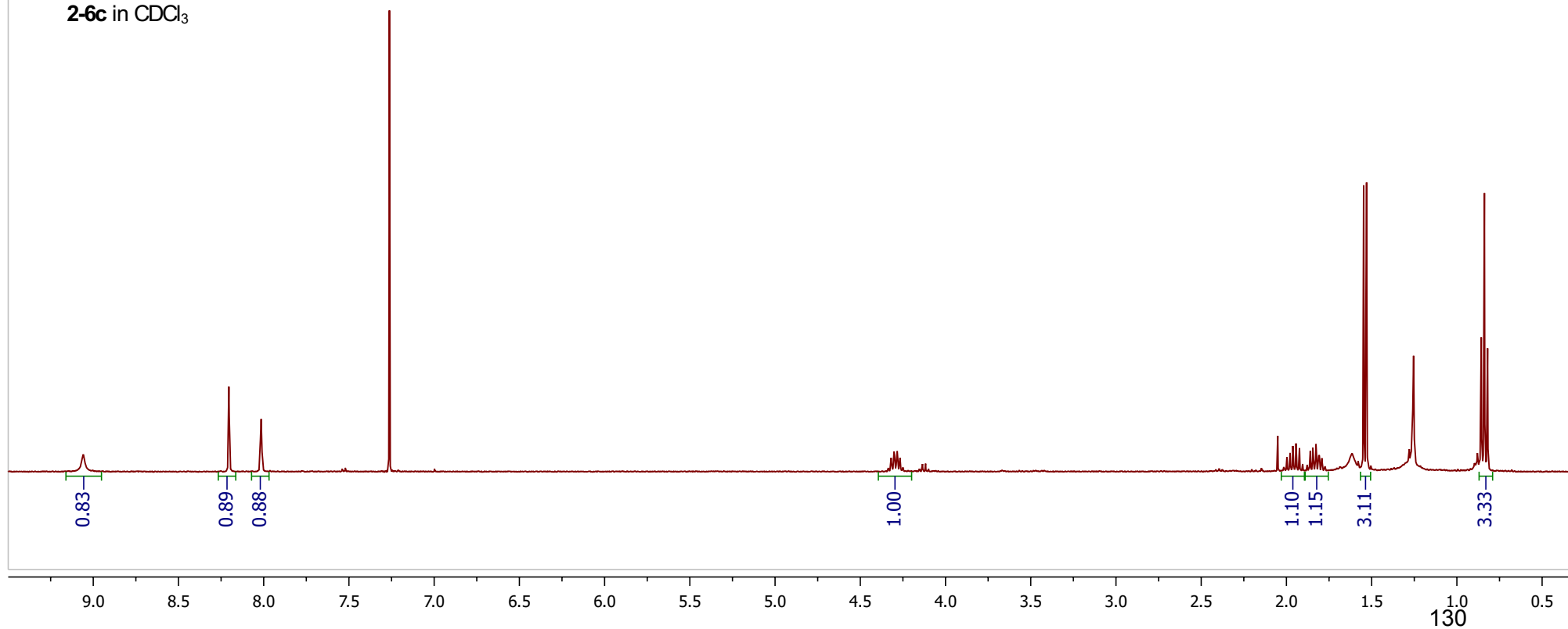
-60 -65 -70 -75 -80 -85 -90 -95 -100 -105 -110 -115 -120 -125 -130 -135 -140 -145 -150 -155 -160 -165 -170 -175

129

Proton01

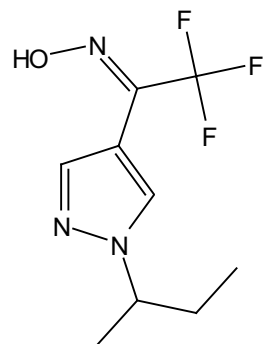


2-6c in CDCl₃



130

Carbon01



2-6c in CDCl₃

—139.7604

—131.0102

—122.3942

—119.6632

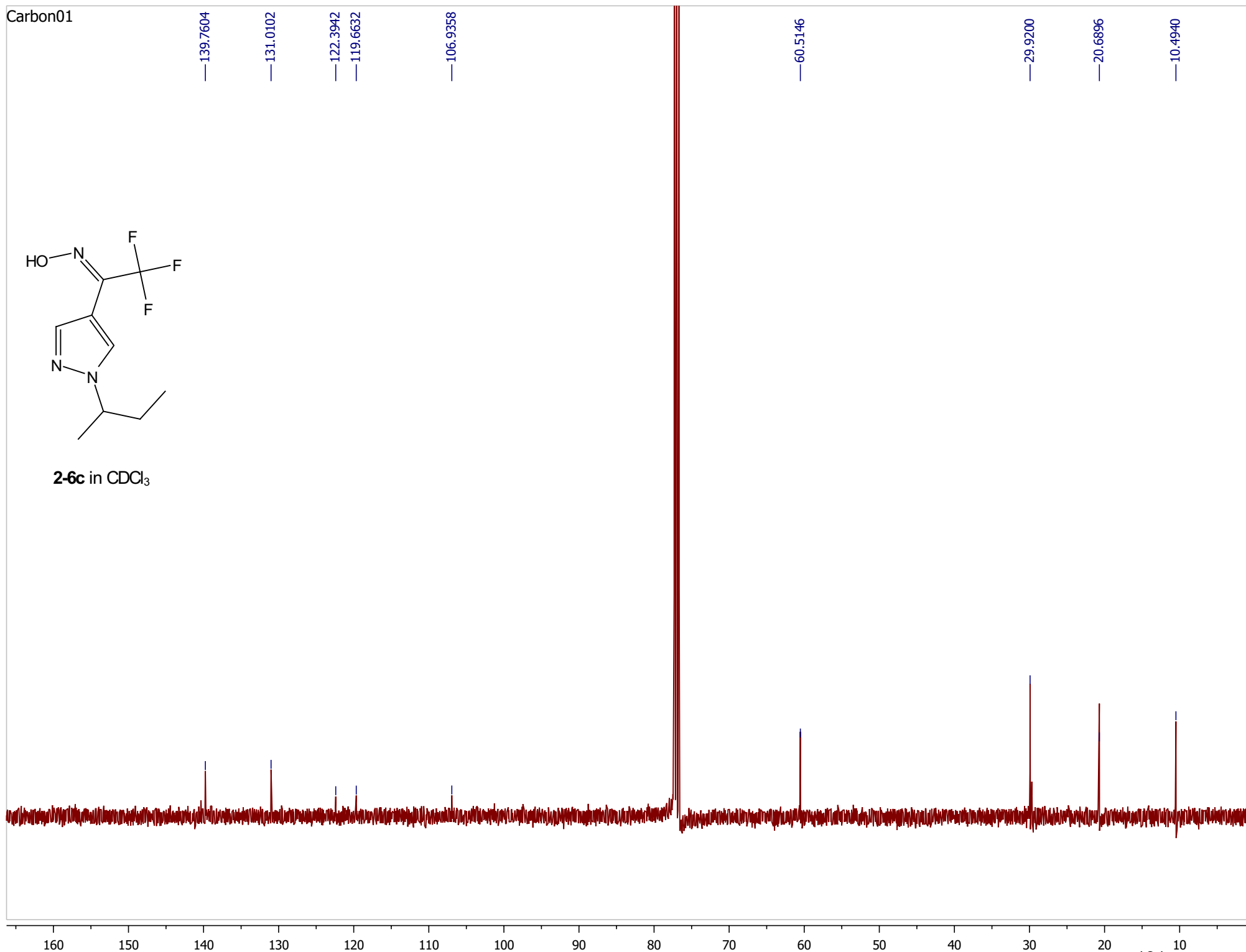
—106.9358

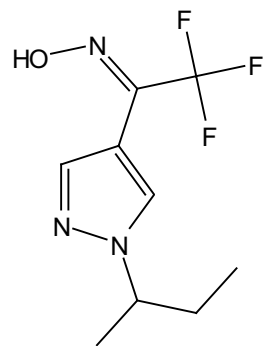
—60.5146

—29.9200

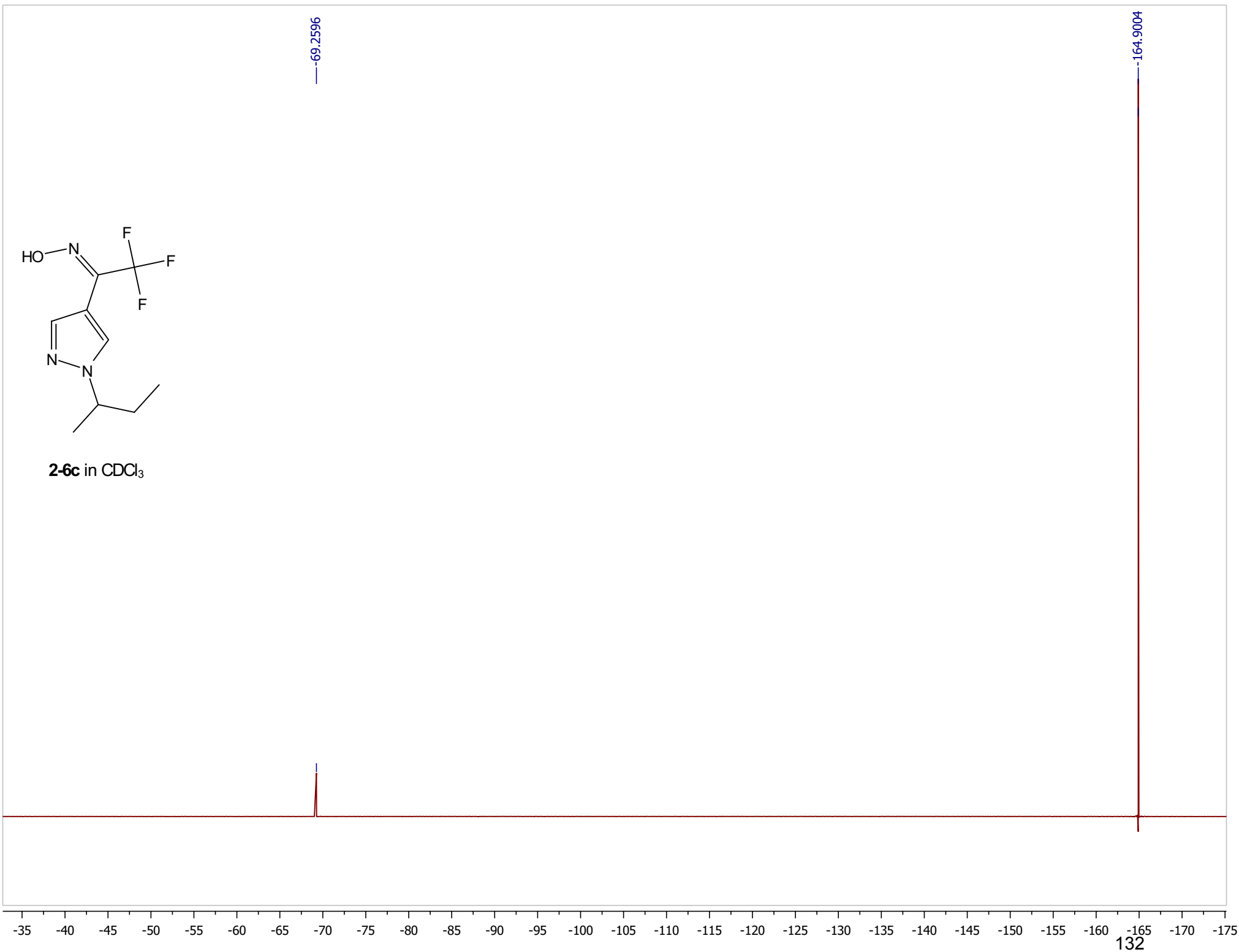
—20.6896

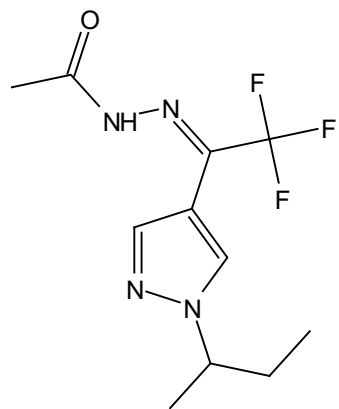
—10.4940



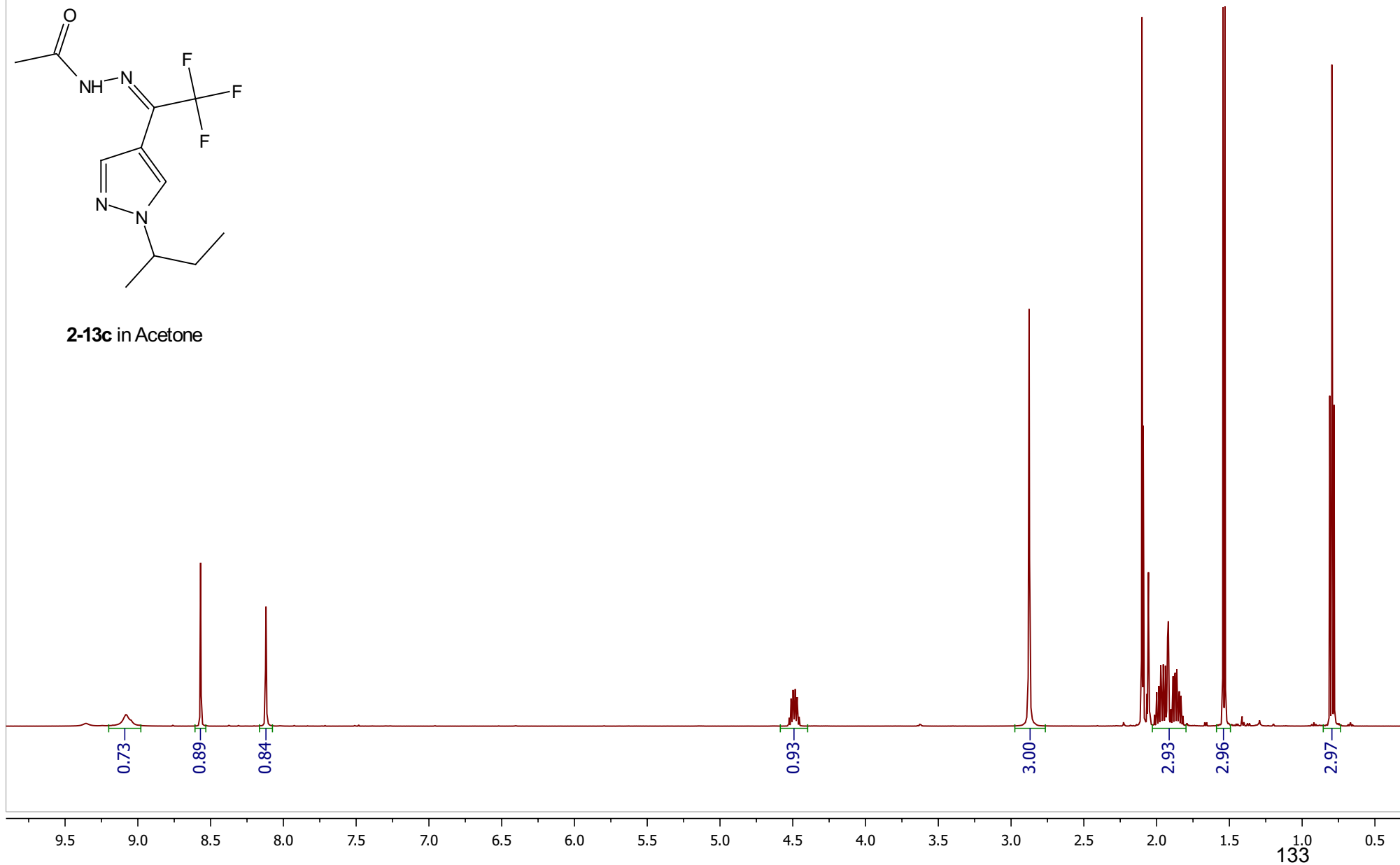


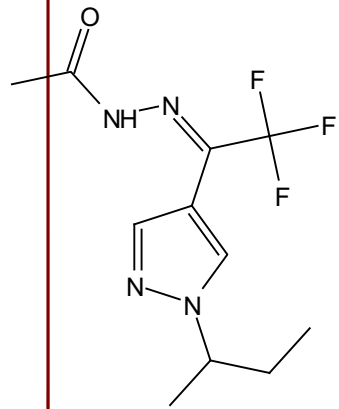
2-6c in CDCl₃



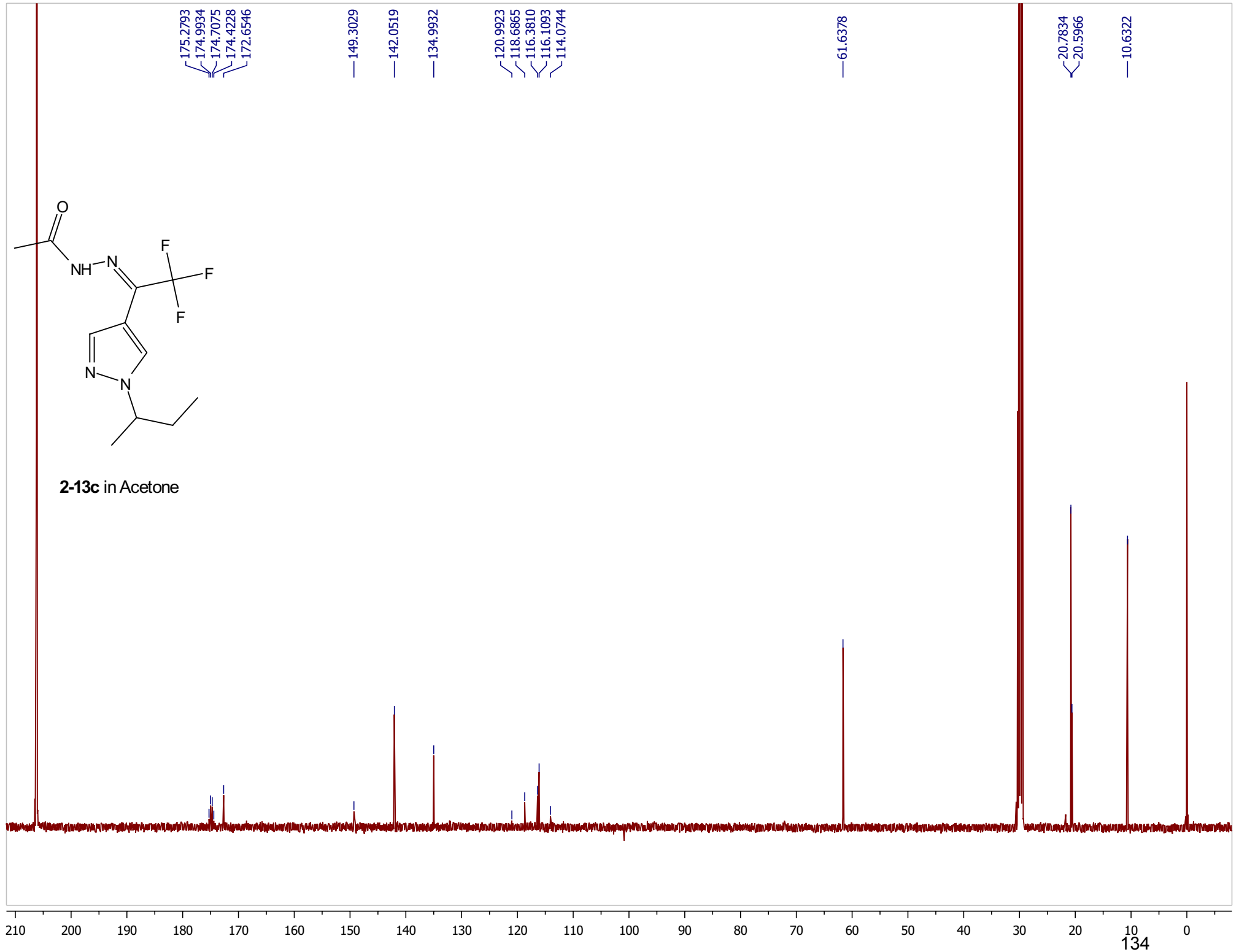


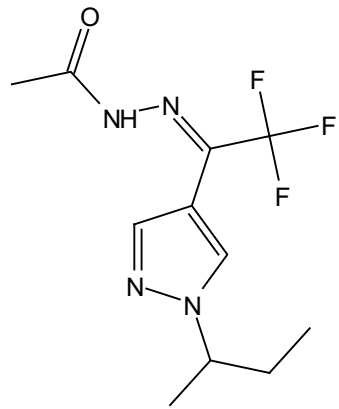
2-13c in Acetone





2-13c in Acetone

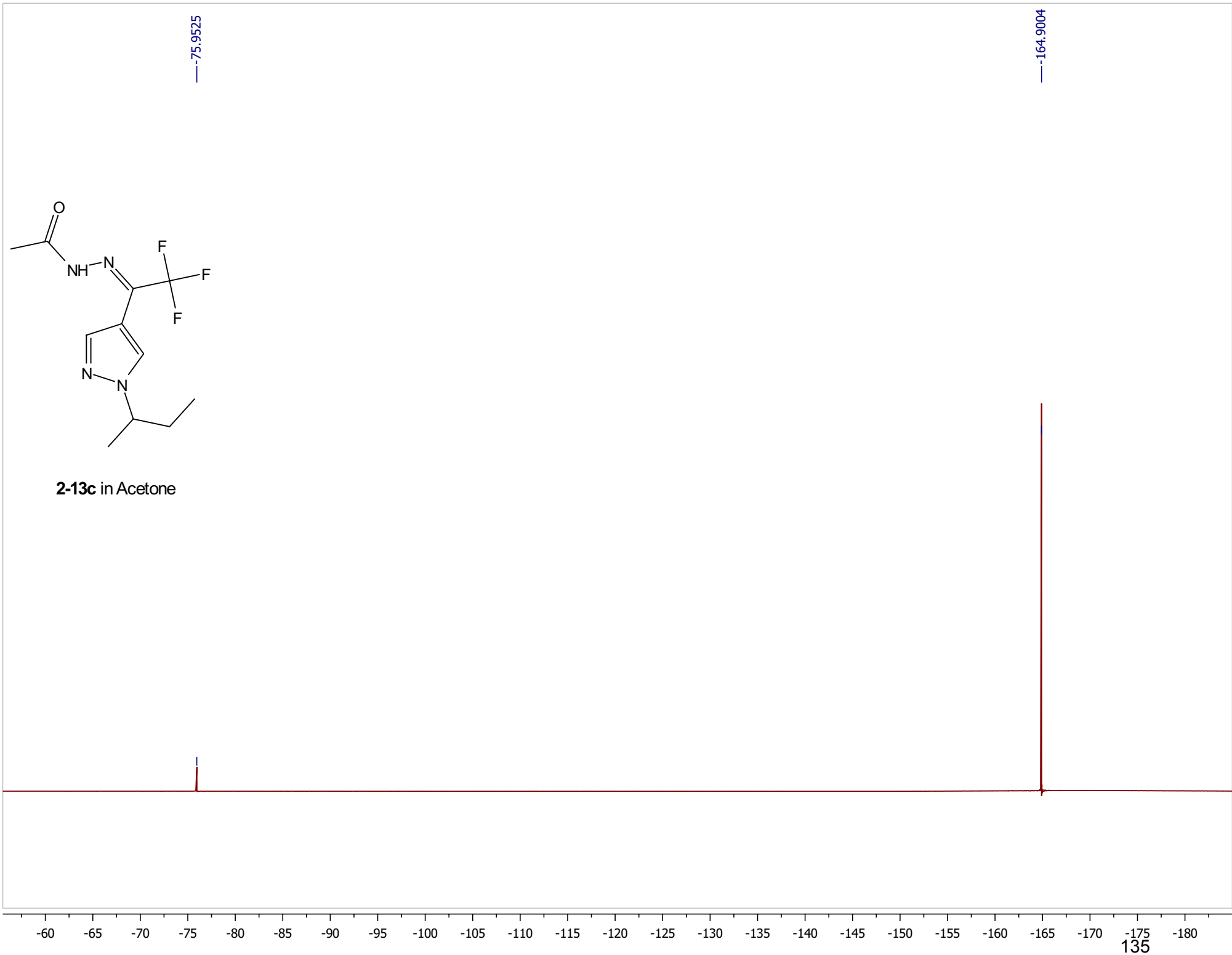


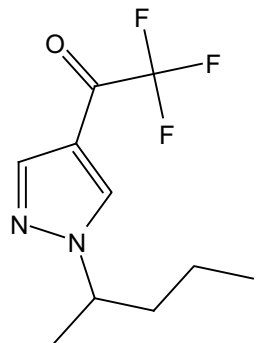


2-13c in Acetone

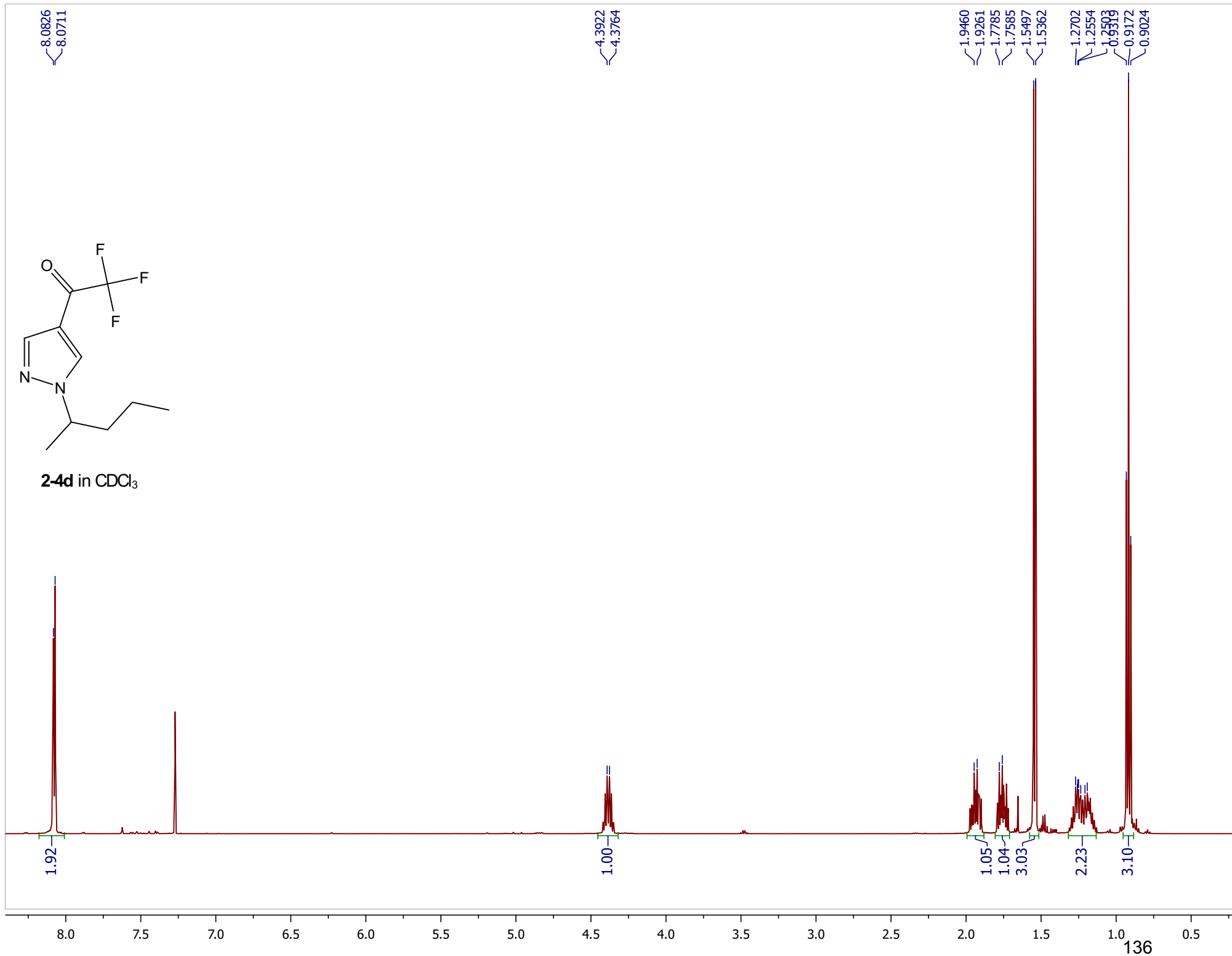
—75.9525

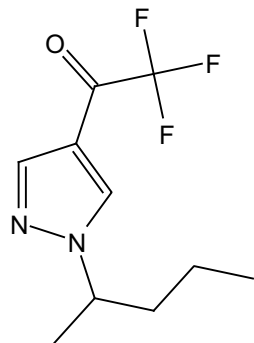
—164.9004



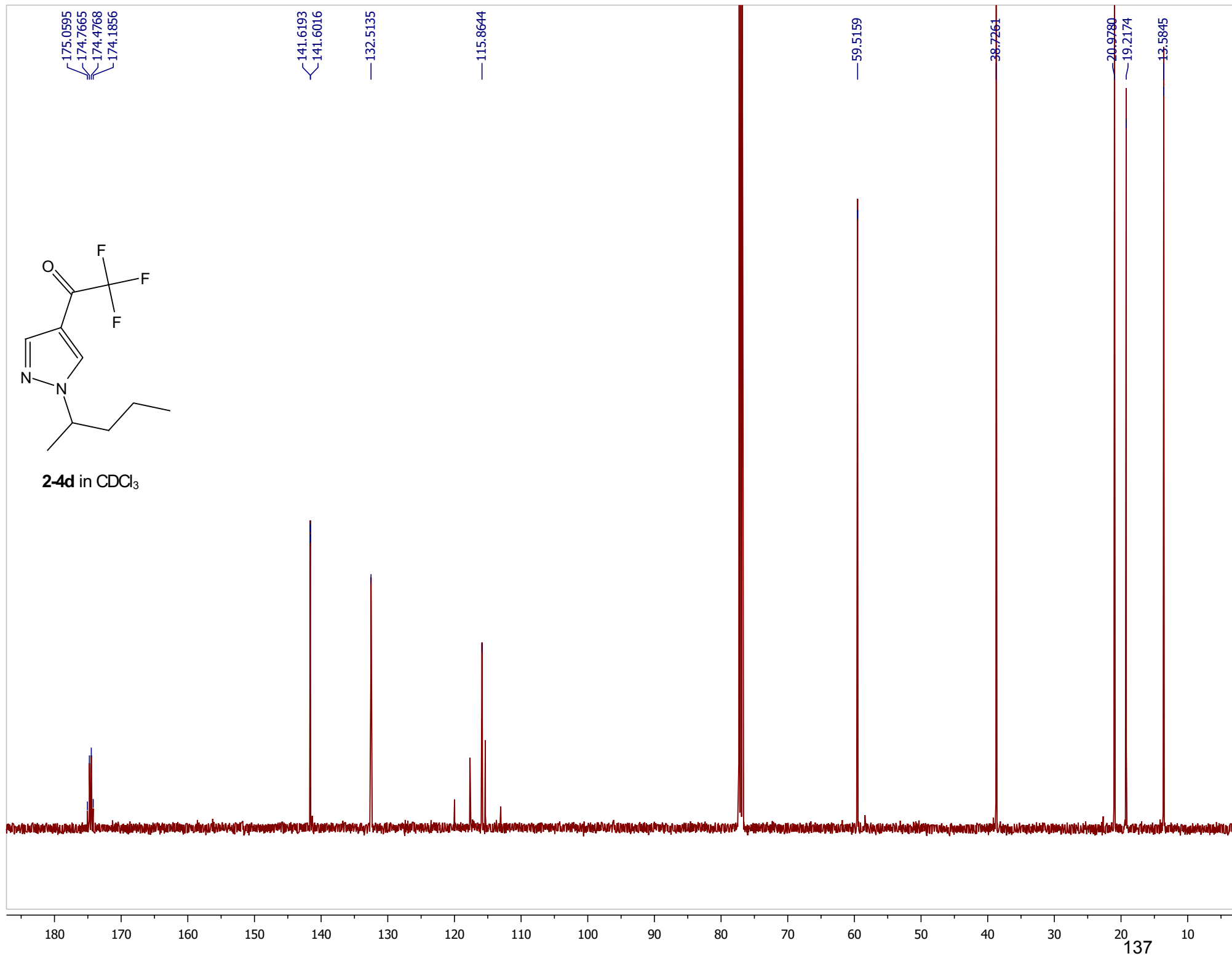


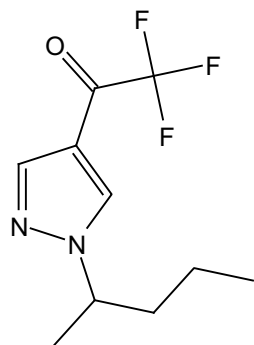
2-4d in CDCl₃



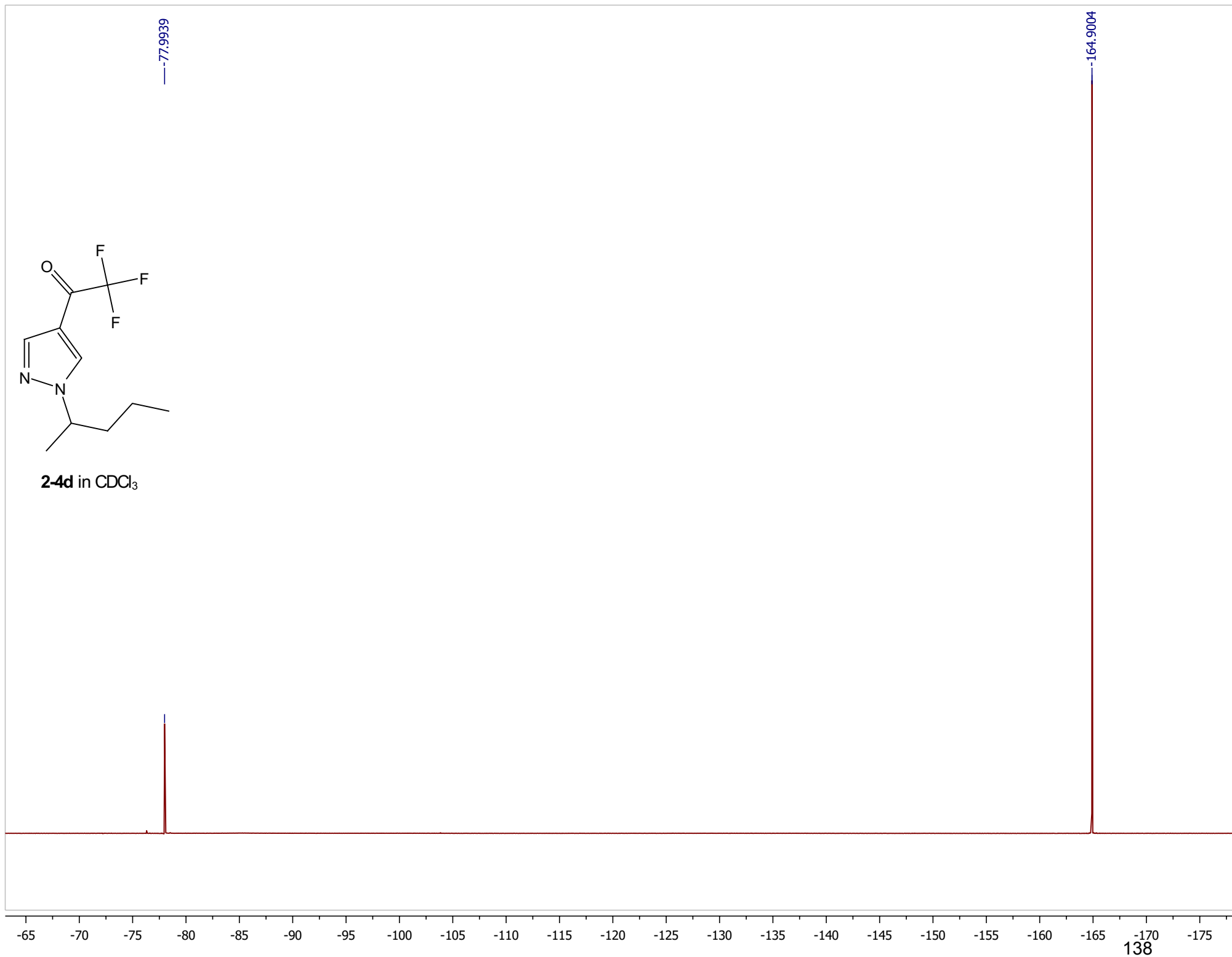


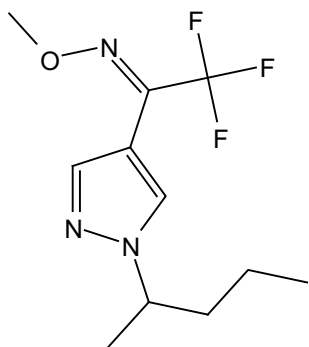
2-4d in CDCl₃



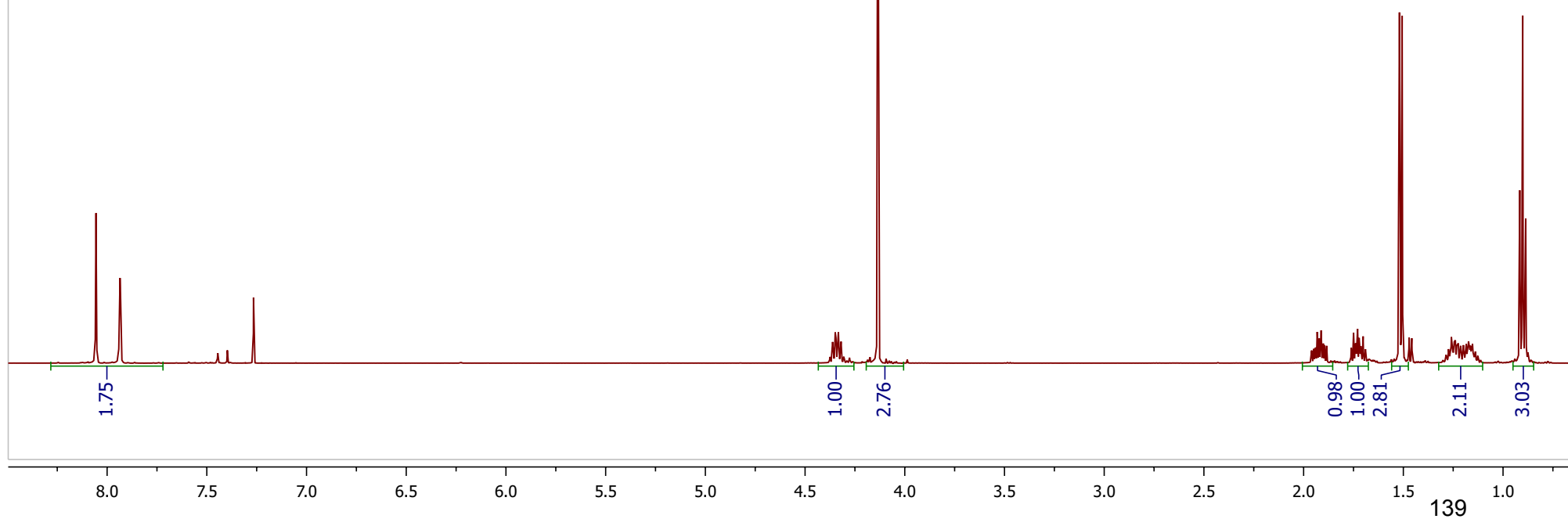


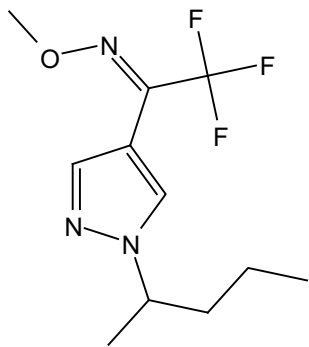
2-4d in CDCl₃



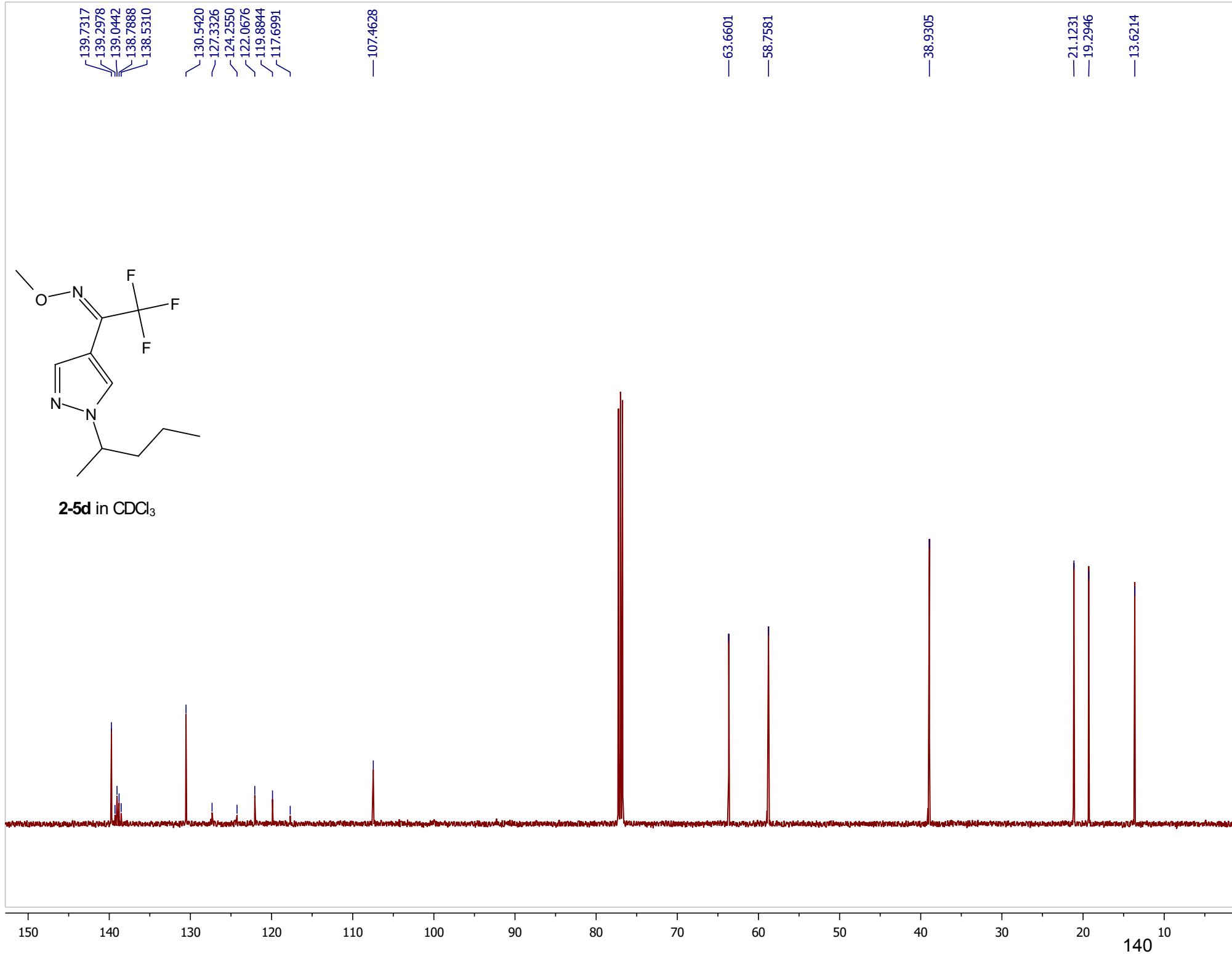


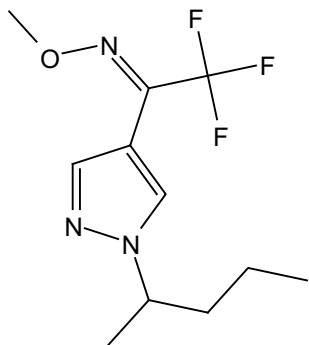
2-5d in CDCl₃



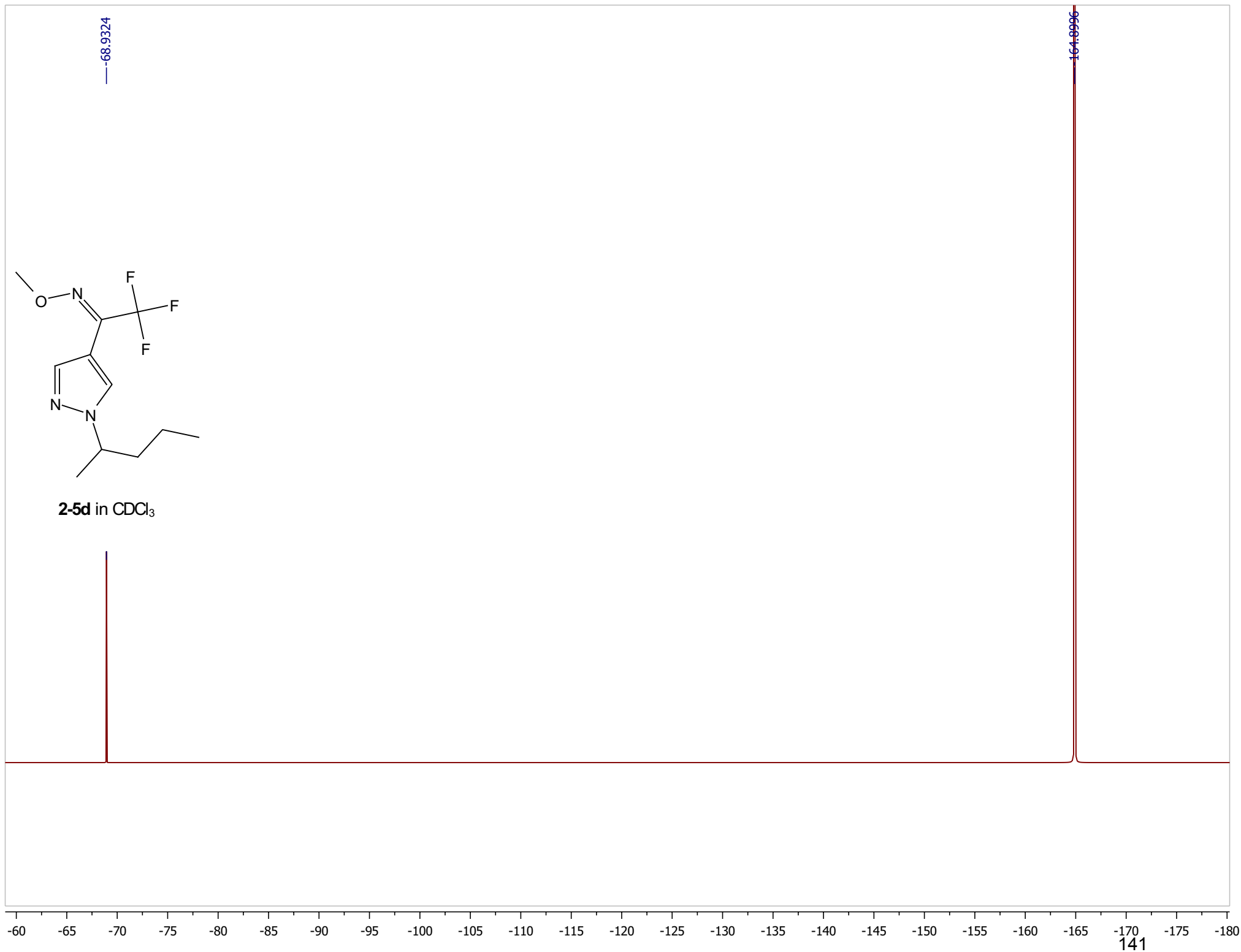


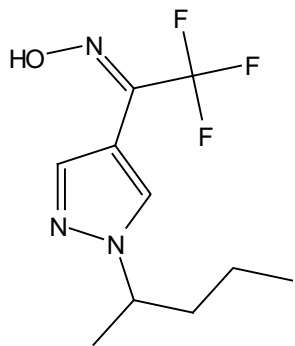
2-5d in CDCl₃



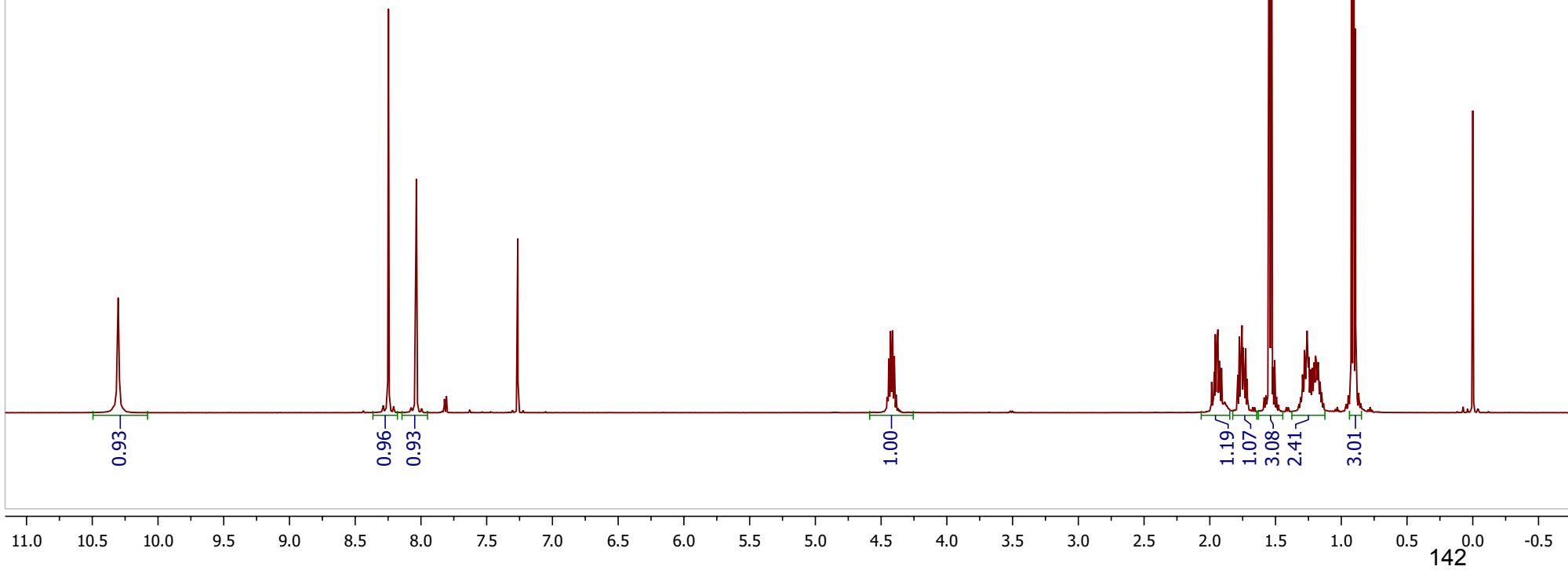


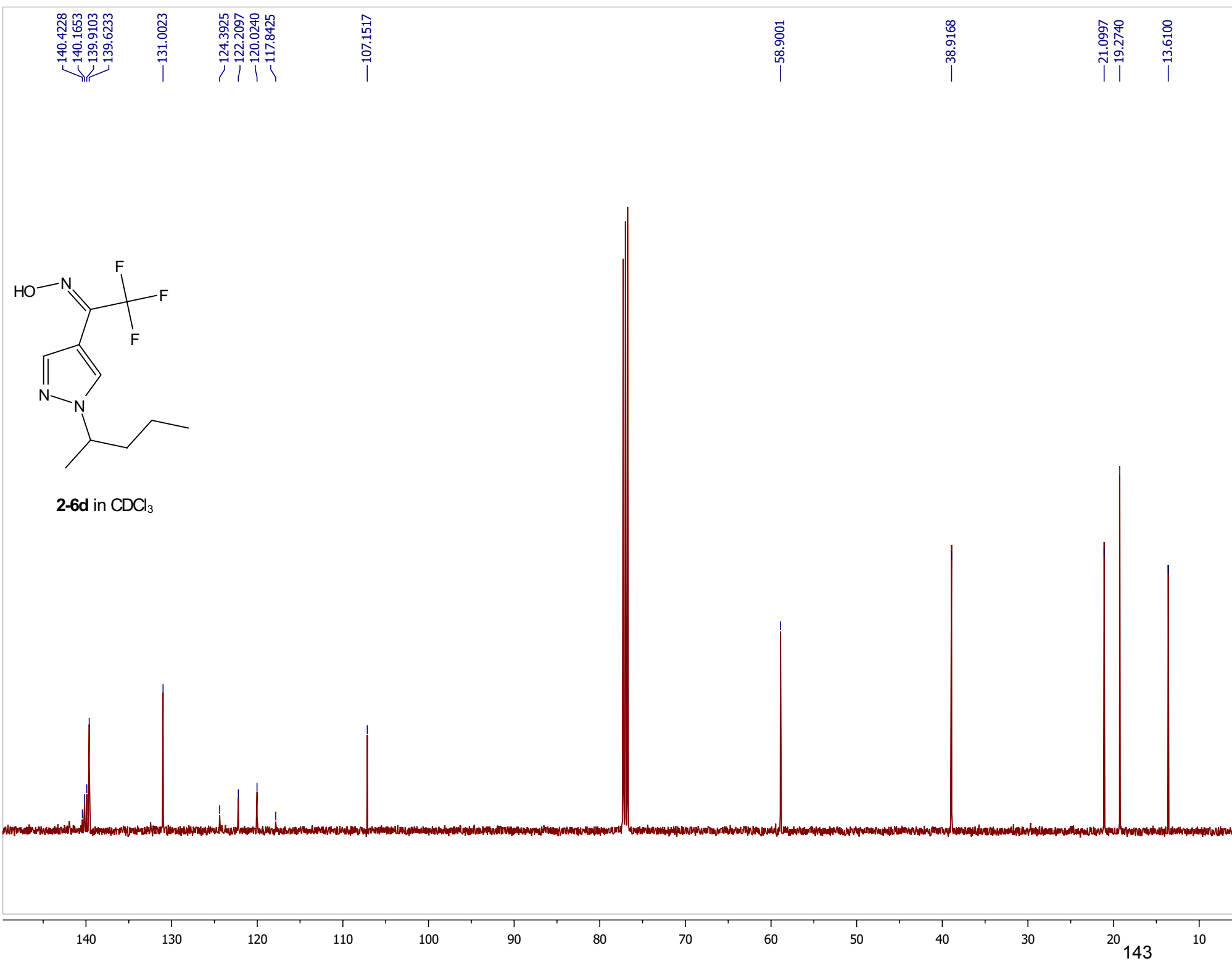
2-5d in CDCl₃

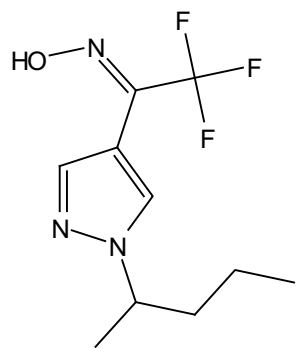




2-6d in CDCl₃



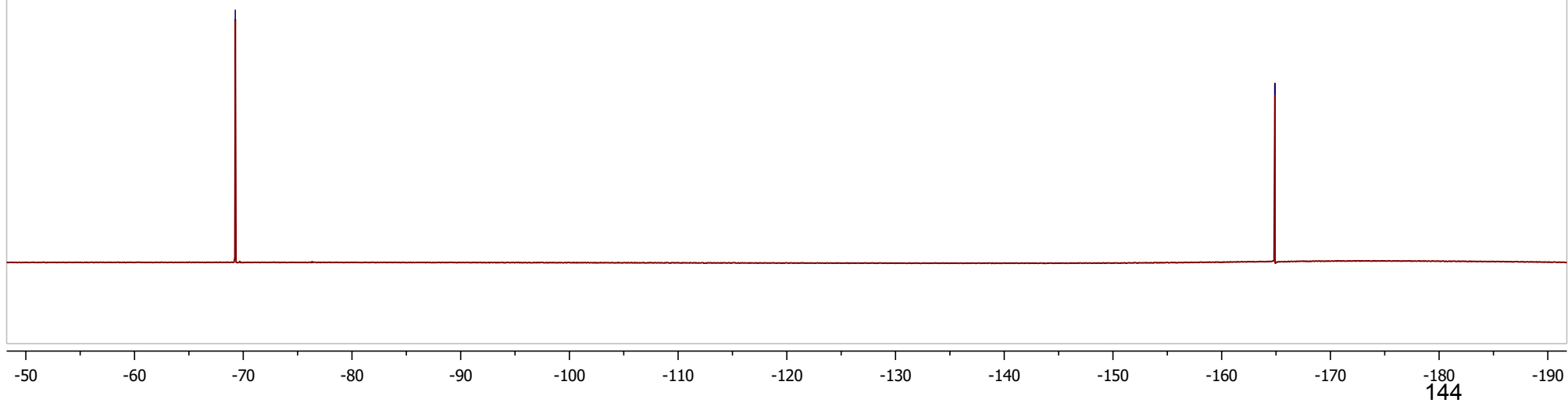


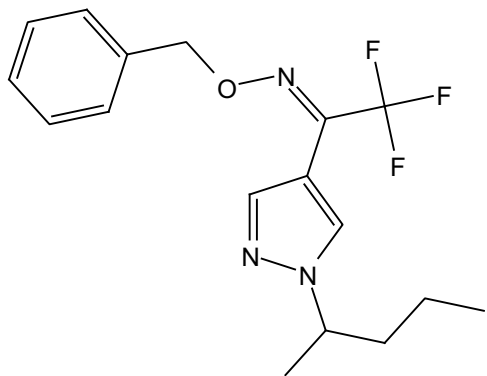


2-6d in CDCl₃

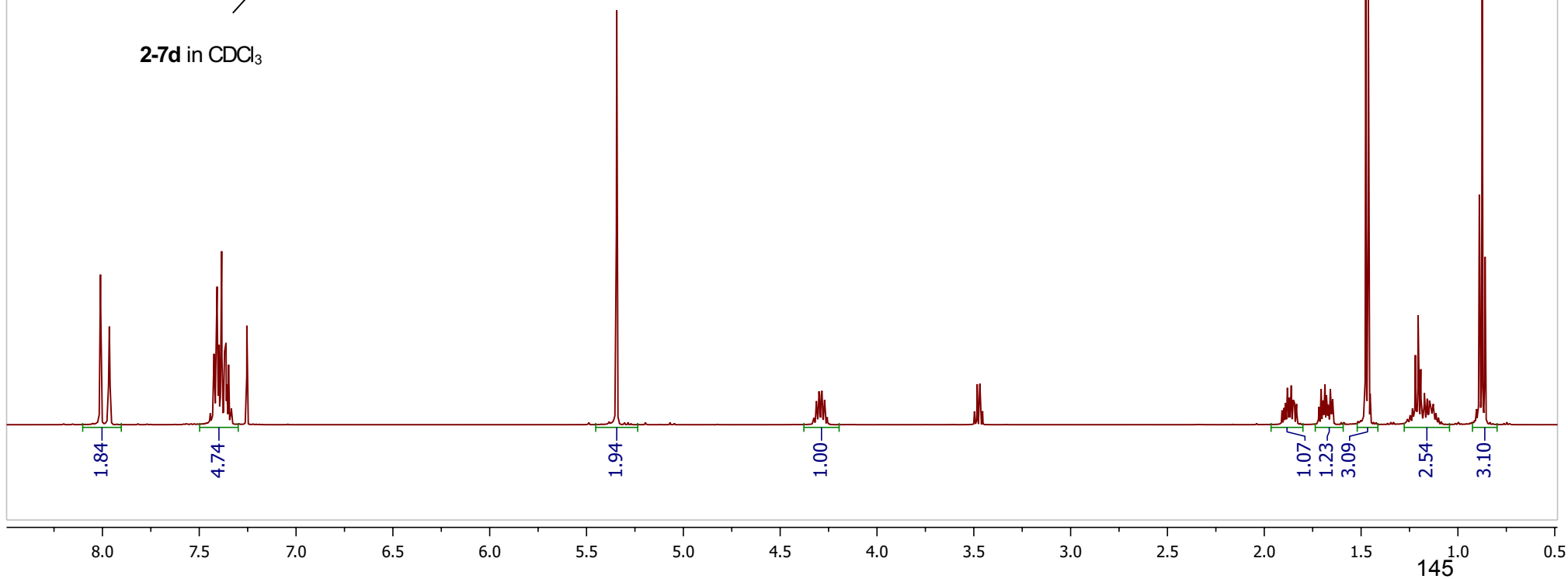
—69.2674

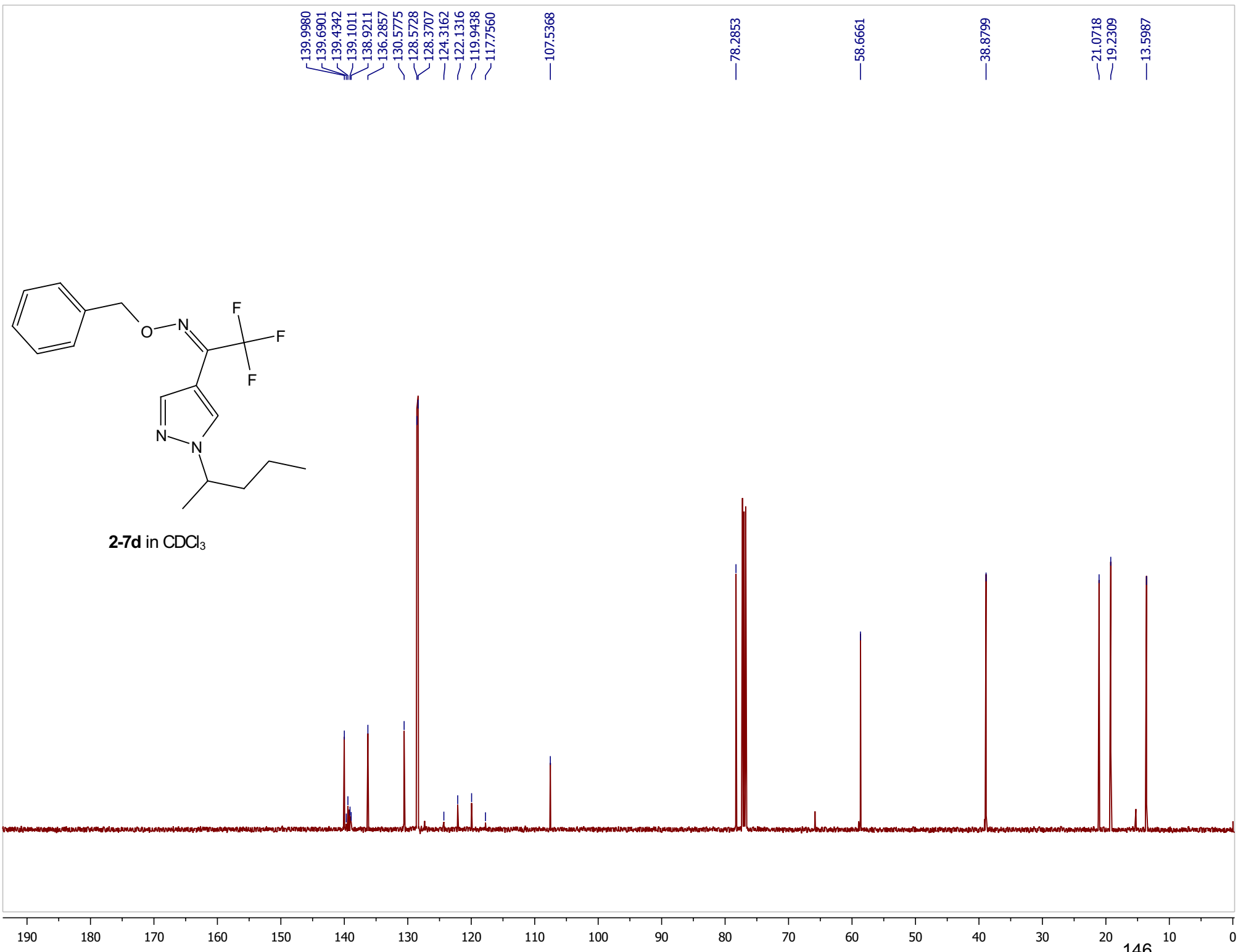
—164.9004

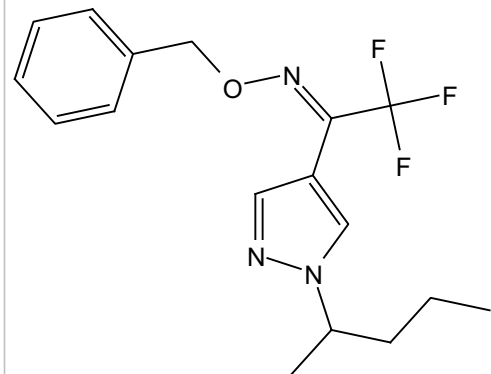




2-7d in CDCl₃







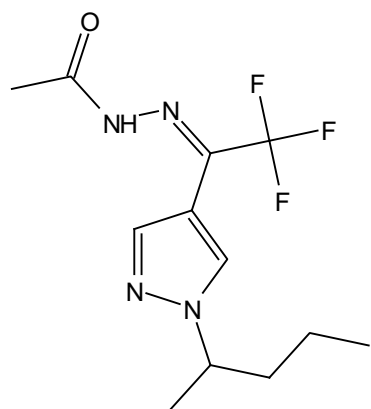
2-7d in CDCl₃

-68.8365

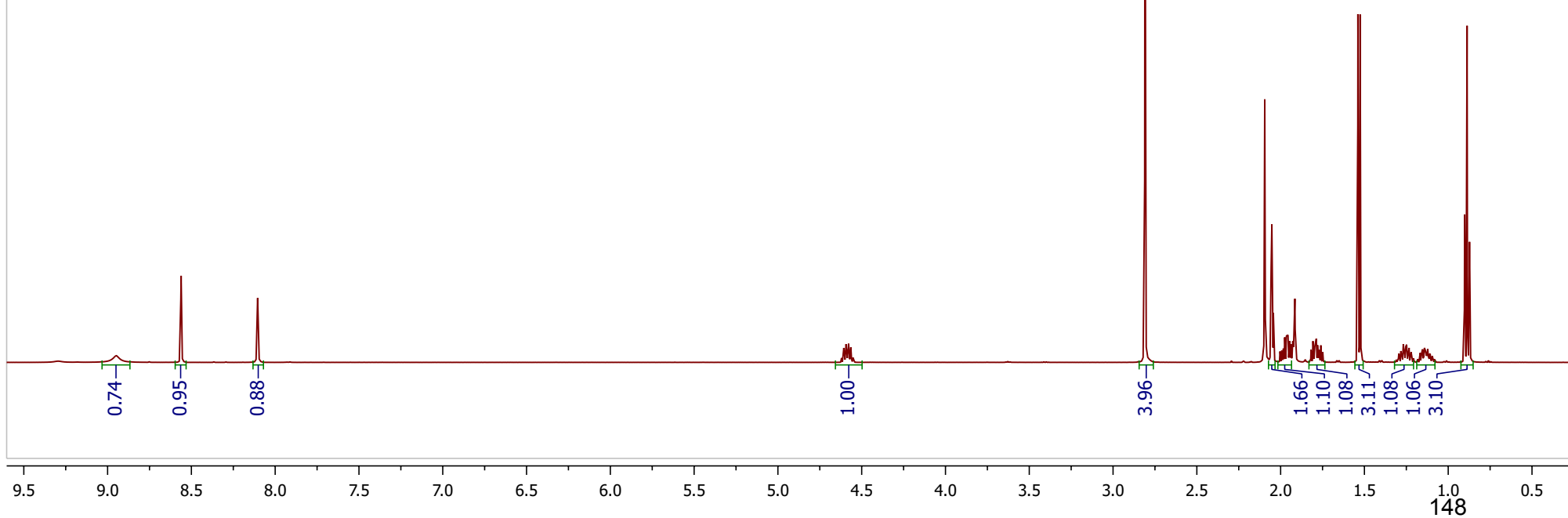


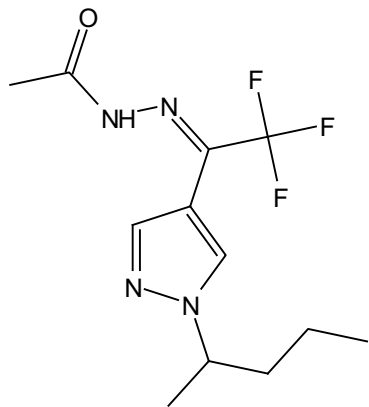
-60 -65 -70 -75 -80 -85 -90 -95 -100 -105 -110 -115 -120 -125 -130 -135 -140 -145 -150 -155 -160 -165 -170 -175 -180

147

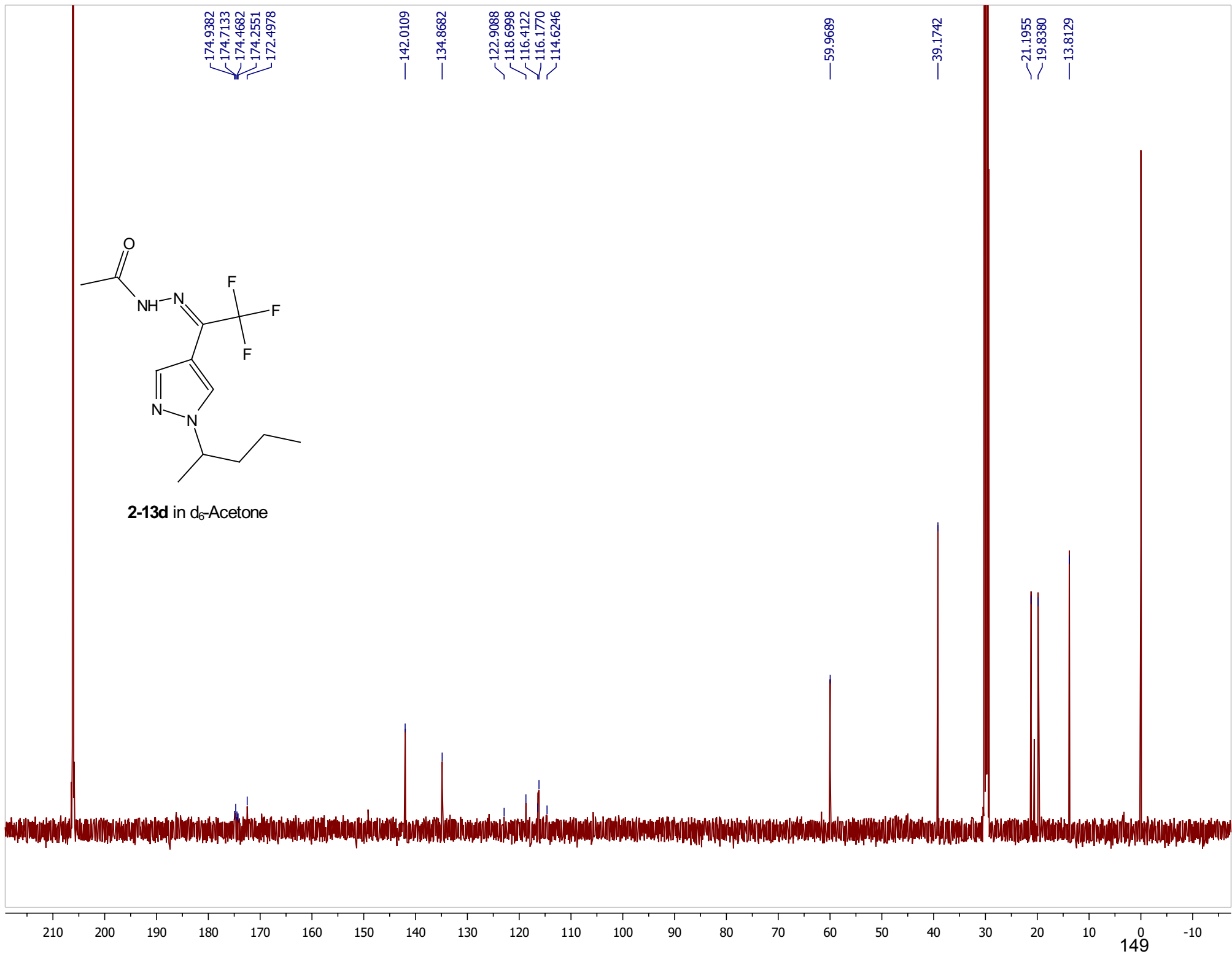


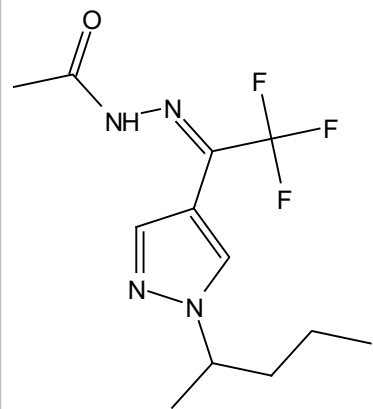
2-13d in d₆-Acetone



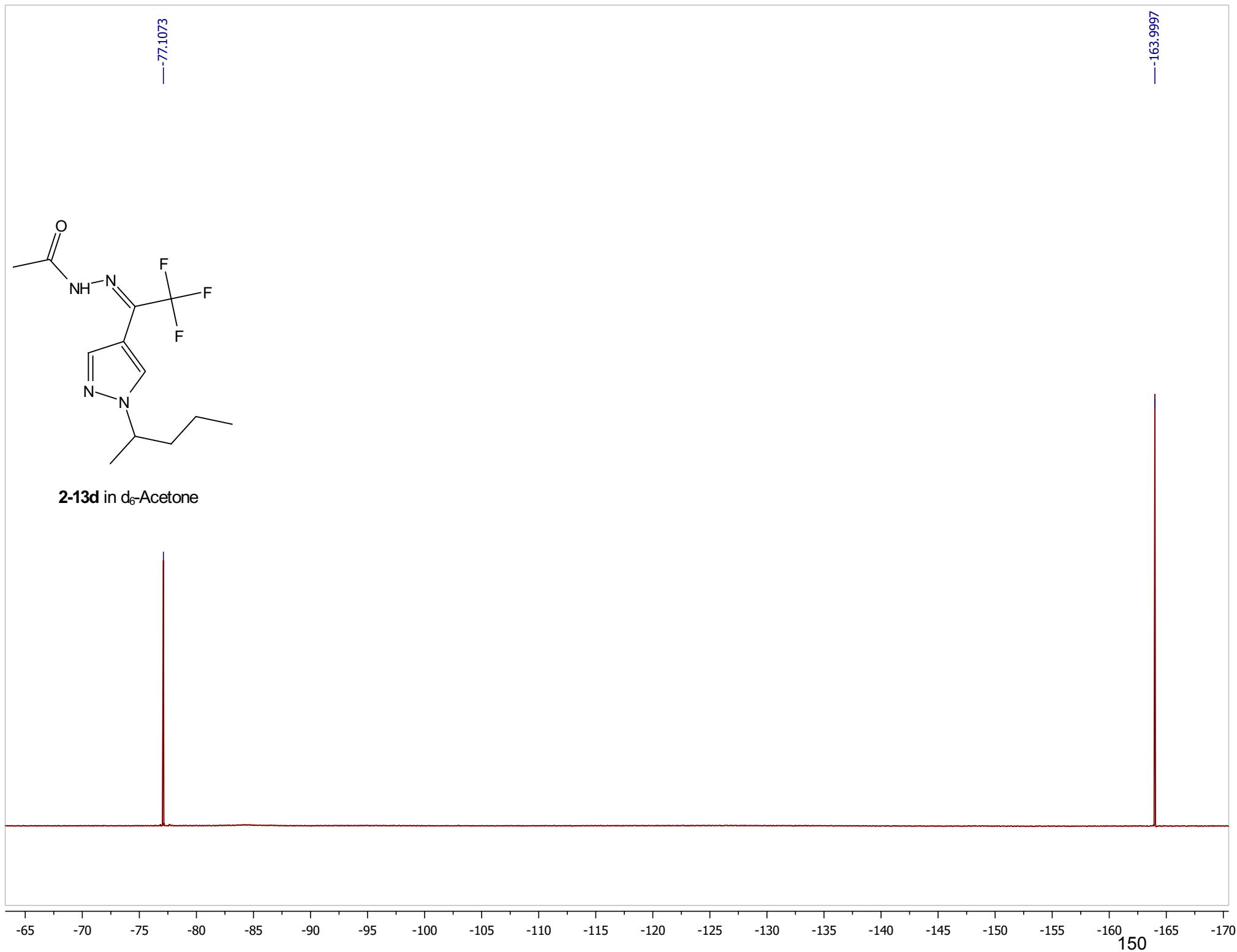


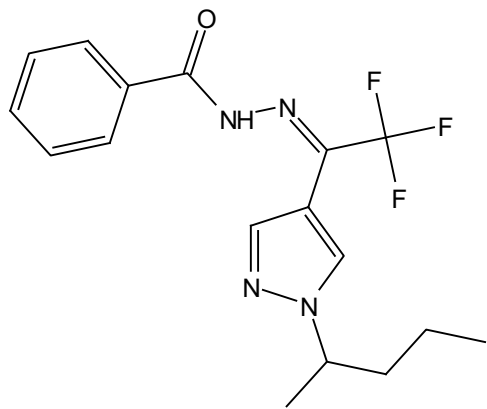
2-13d in d₆-Acetone



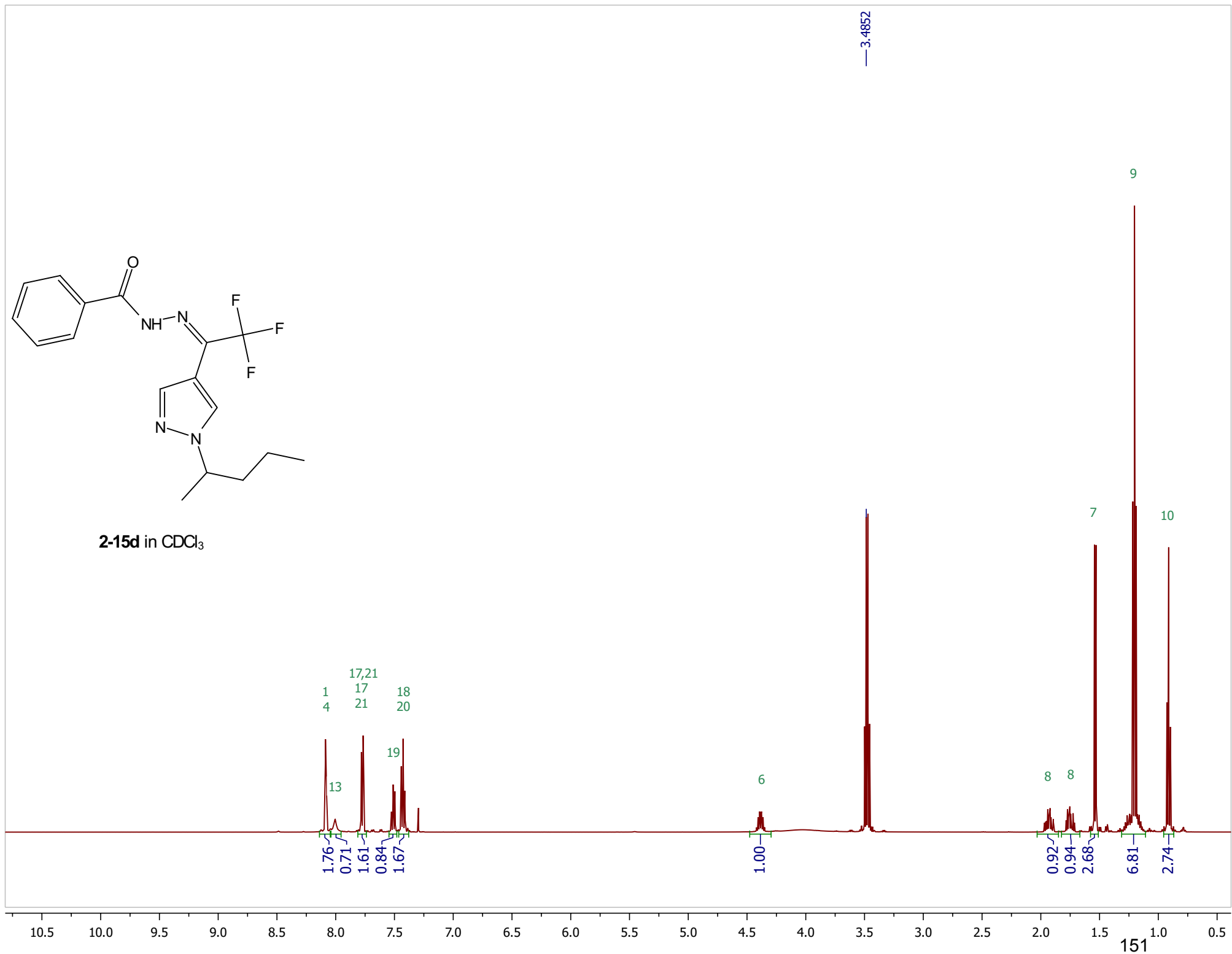


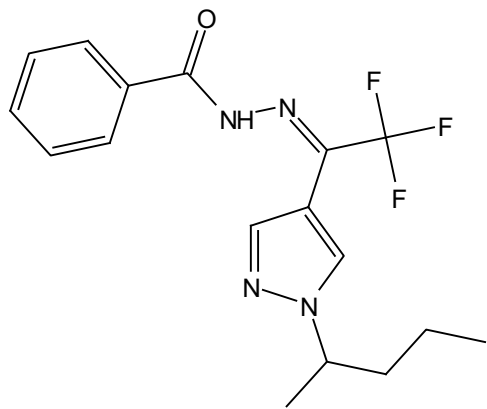
2-13d in d_6 -Acetone



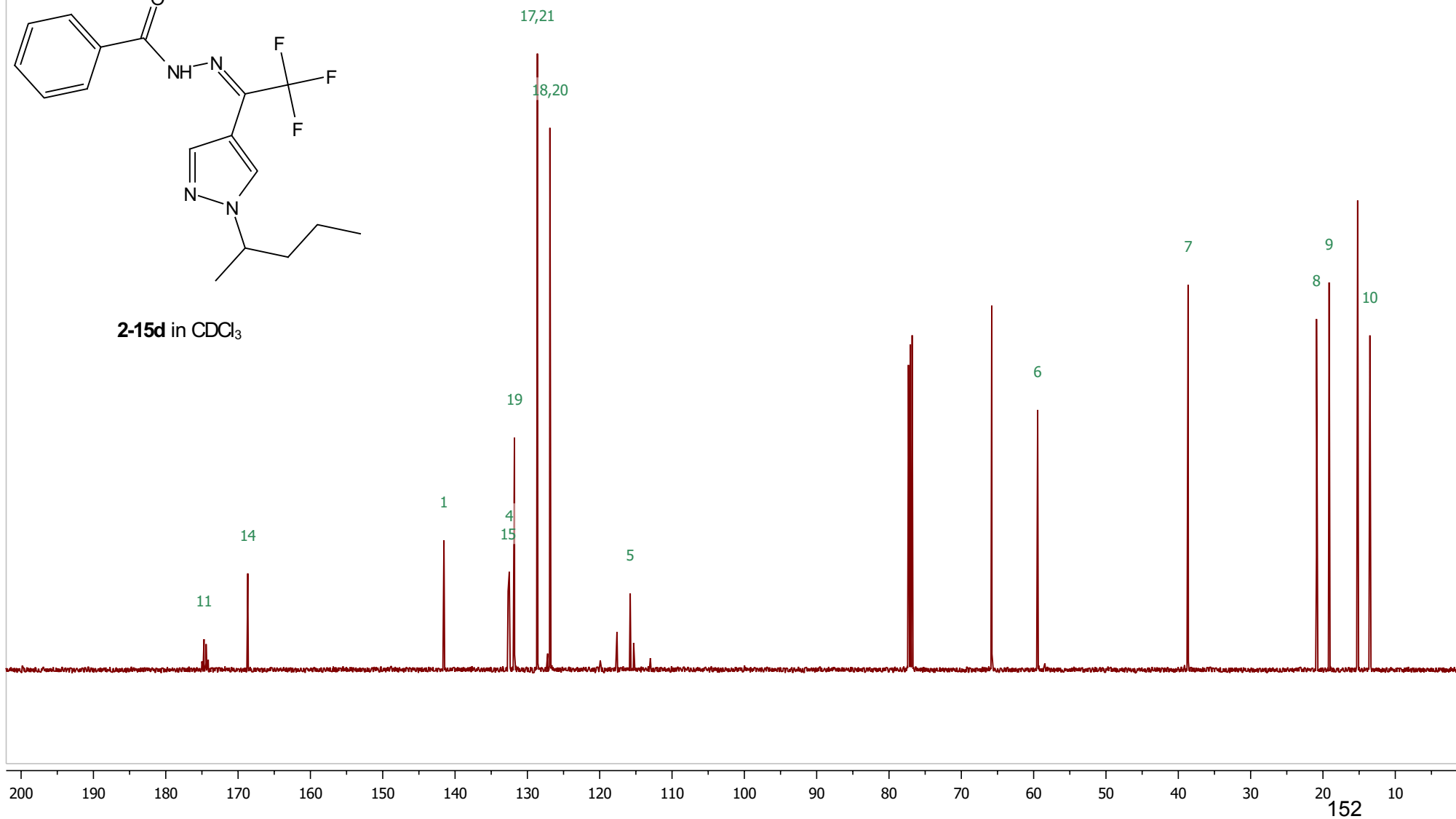


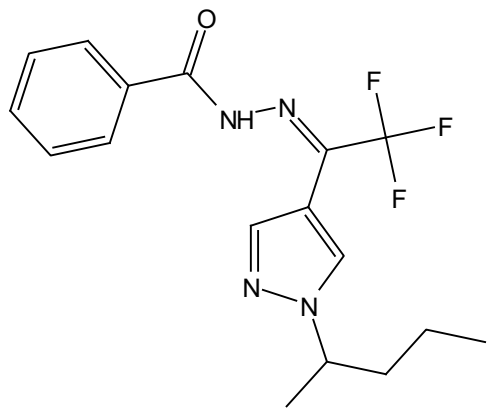
2-15d in CDCl₃





2-15d in CDCl₃

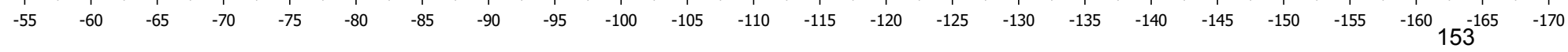




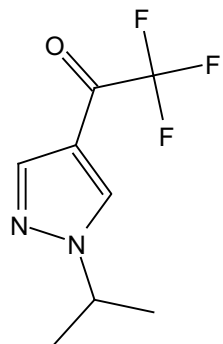
2-15d in CDCl₃

-78.0064

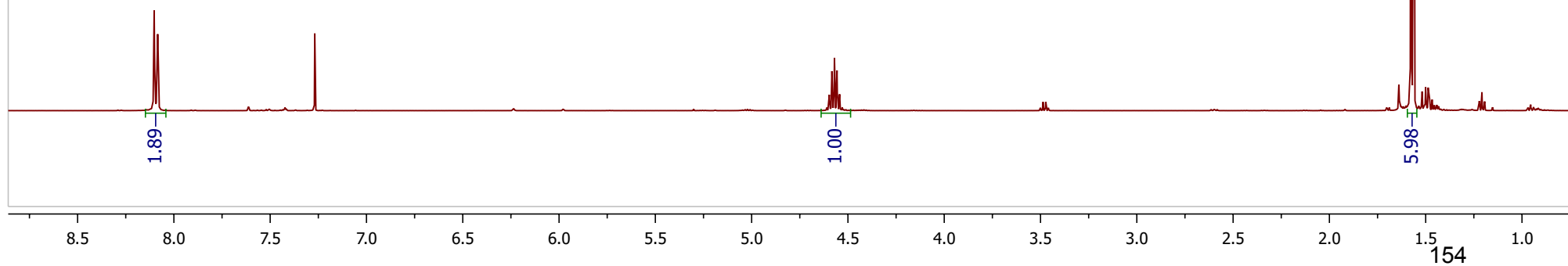
-164.9863

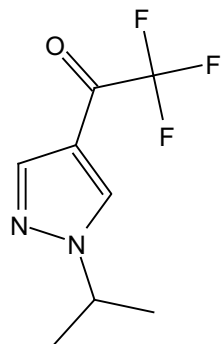


153



2-4e in CDCl₃





2-4e in CDCl₃

—174.4211

—141.5652

—131.6518

—119.9382

—117.6324

—115.9432

—115.3235

—113.0181

—55.0376

—22.5531

7,8

6

1

4

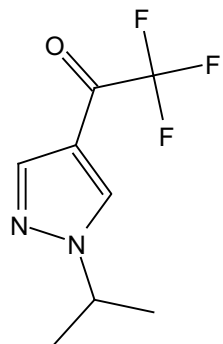
11

5

9

210 200 190 180 170 160 150 140 130 120 110 100 90 80 70 60 50 40 30 20 10 0 -10

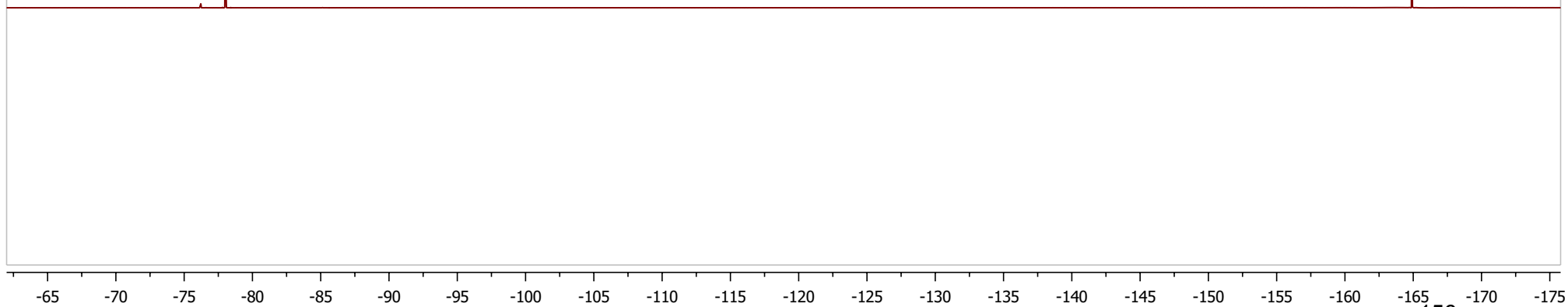
155

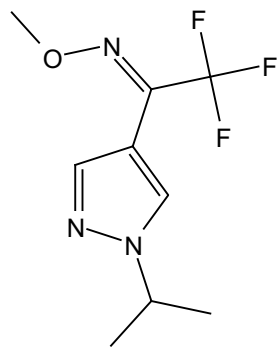


2-4e in CDCl₃

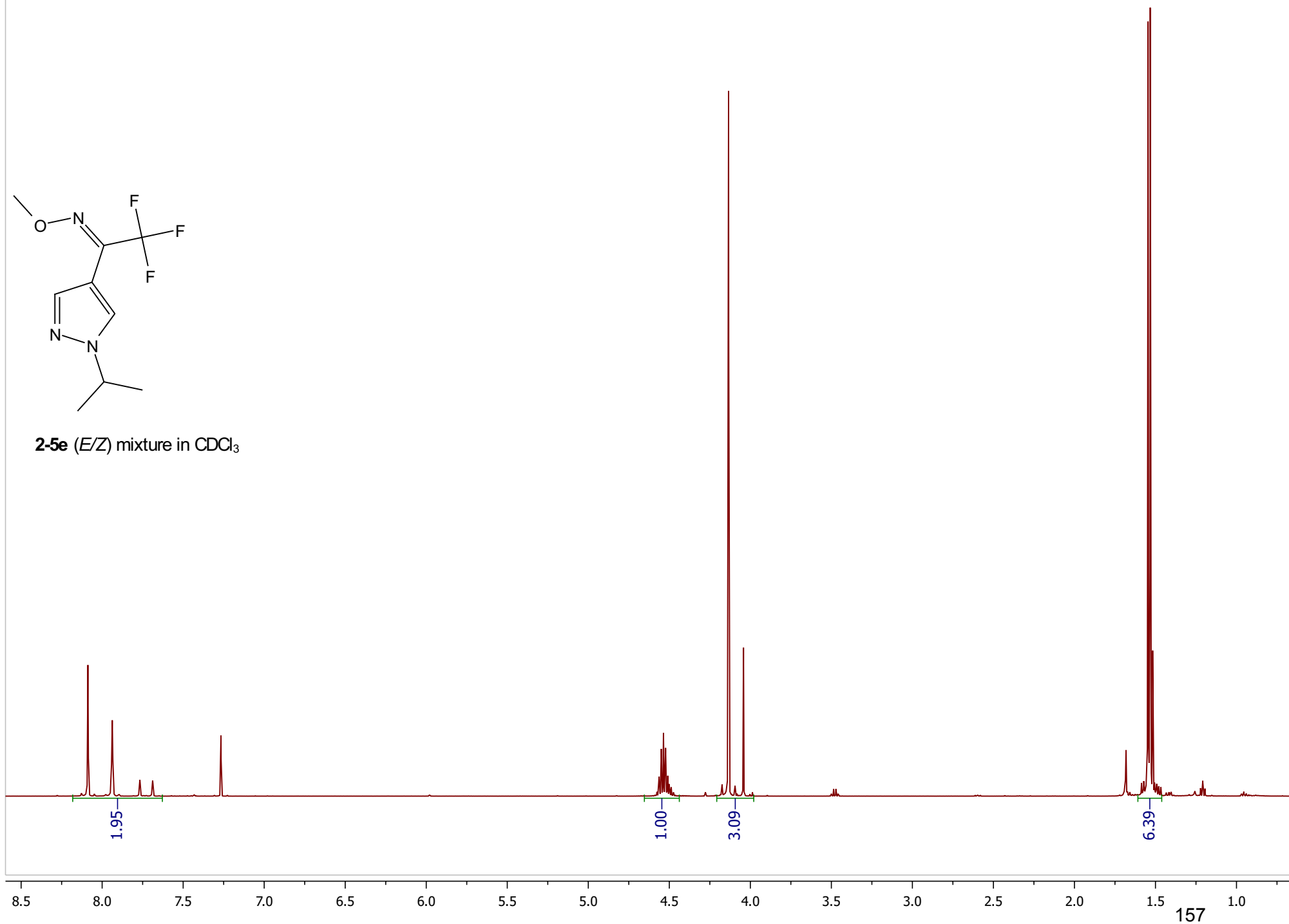
—77.9988

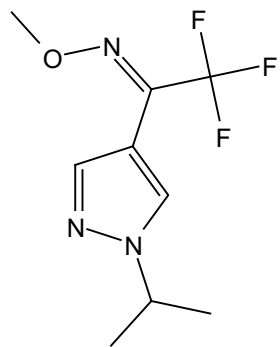
—164.8999





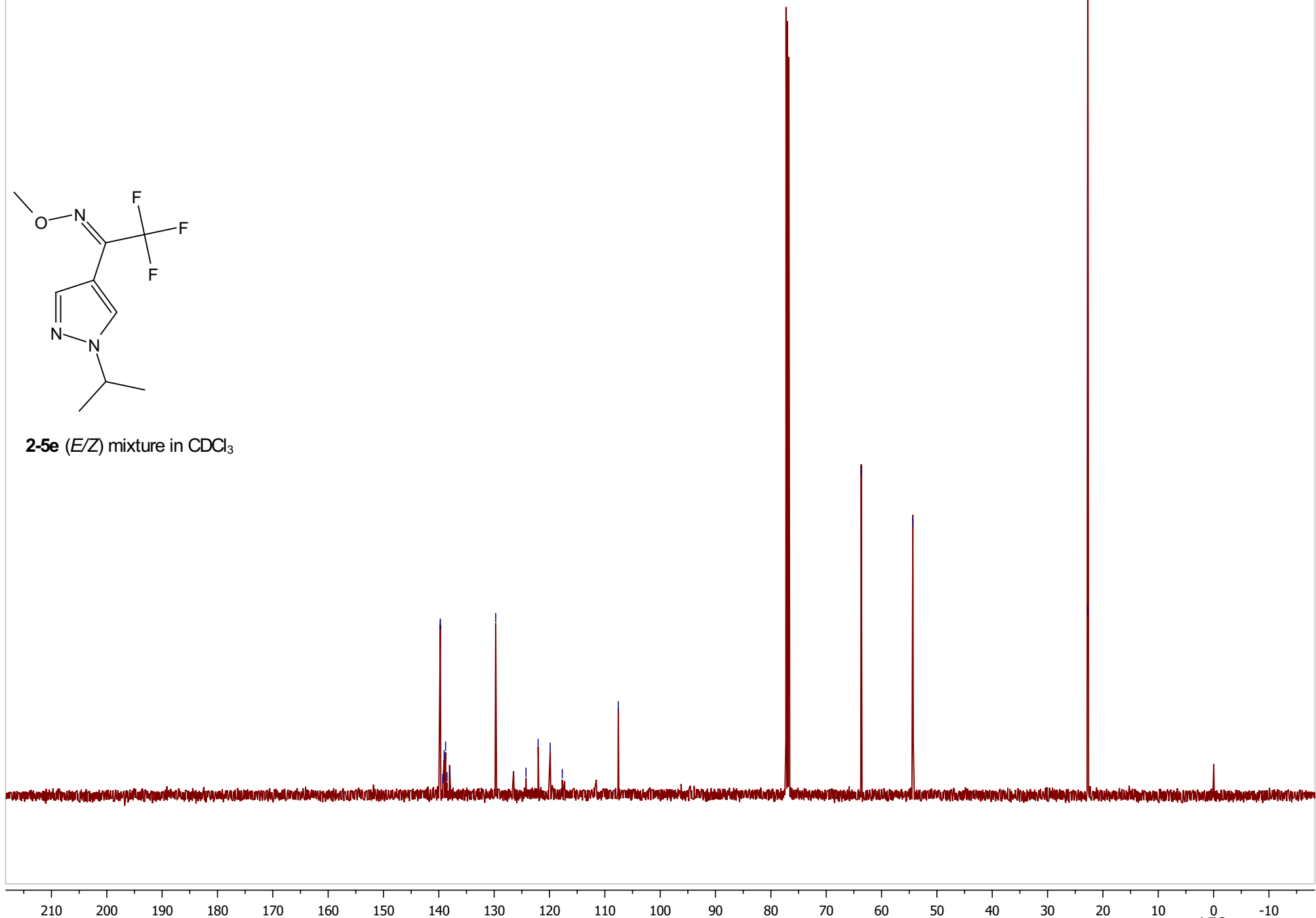
2-5e (*E/Z*) mixture in CDCl_3

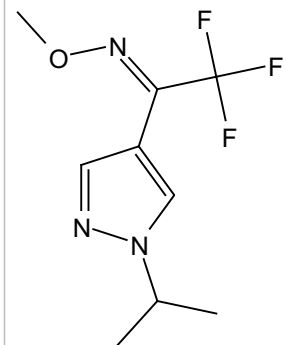




2-5e (*E/Z*) mixture in CDCl₃

139.7449
139.7306
139.2893
139.0322
138.7769
138.5197
138.0180
129.7182
124.2475
122.0607
119.8782
117.6911
107.5769
63.6671
54.3419
22.7613
22.7254

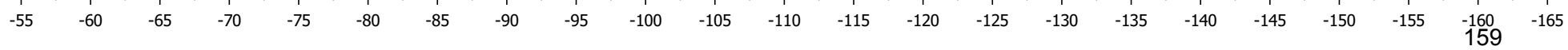


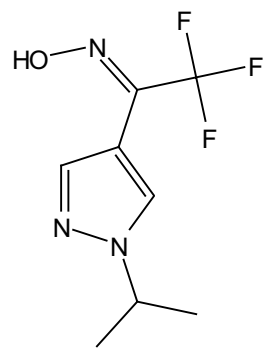


2-5e (*E/Z*) mixture in CDCl₃

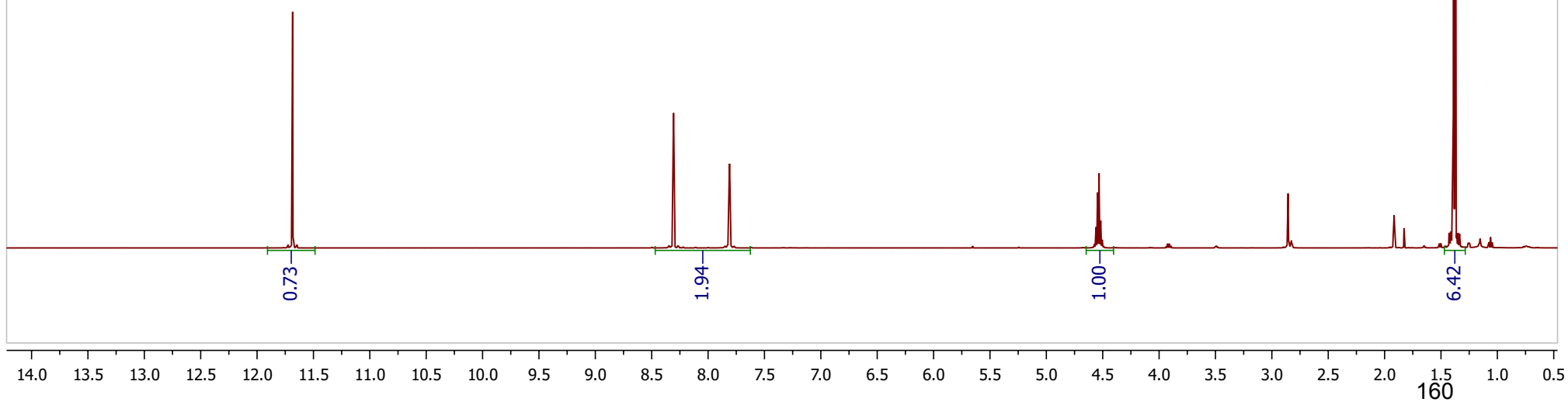
—67.1179
—68.9613

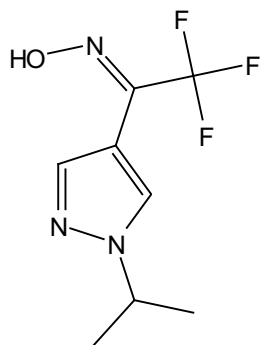
—164.8998



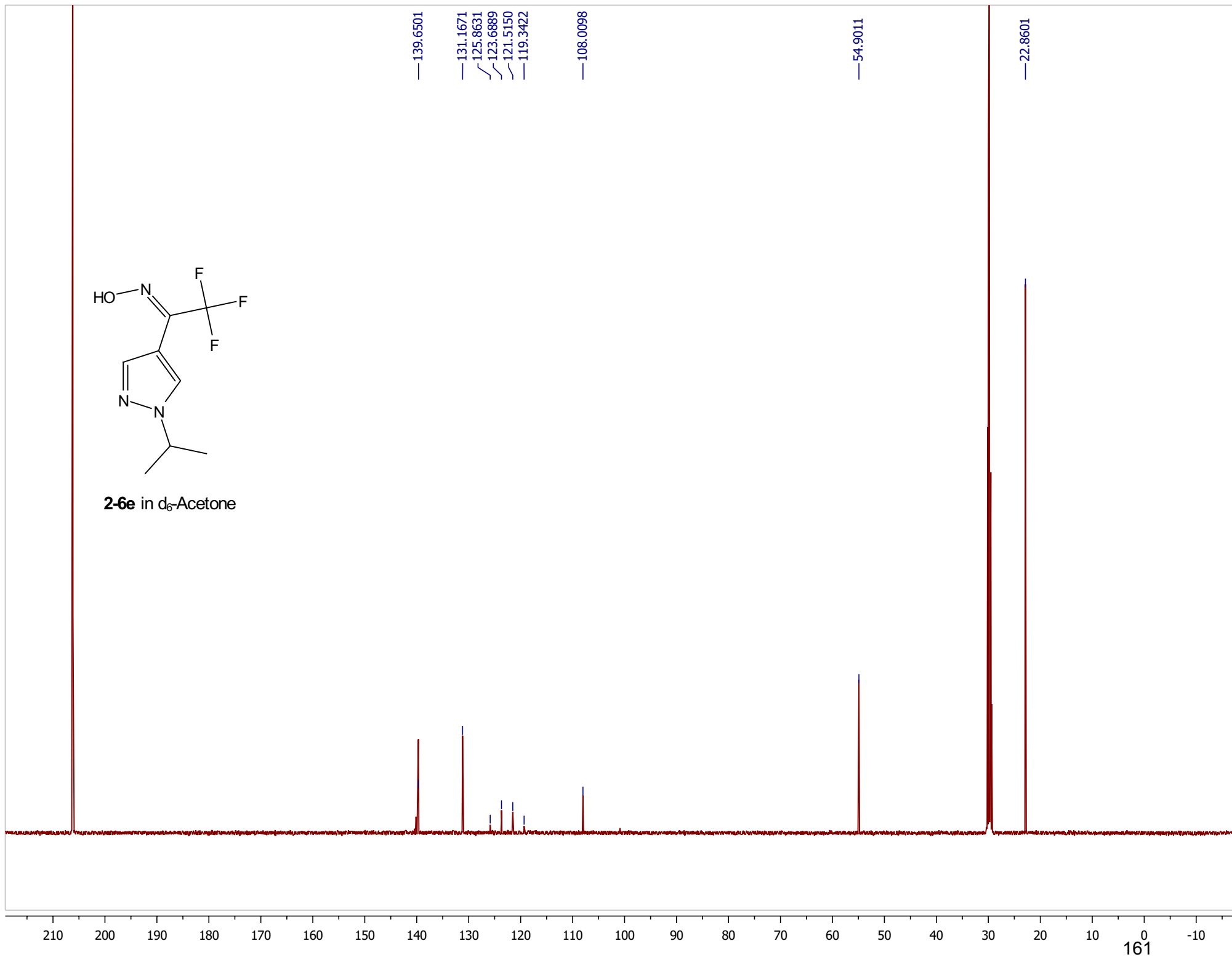


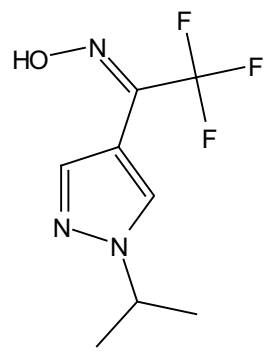
2-6e in d₆-Acetone



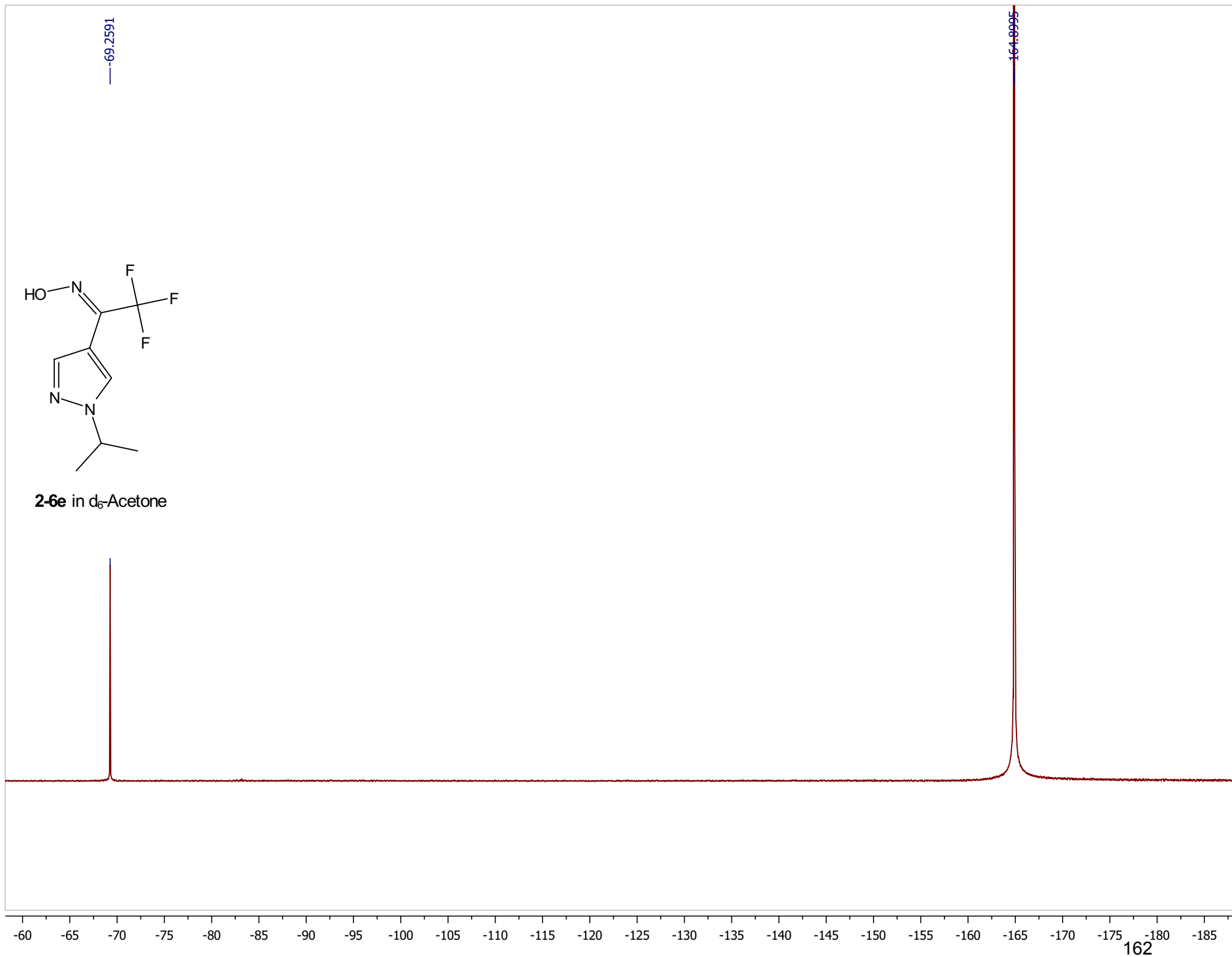


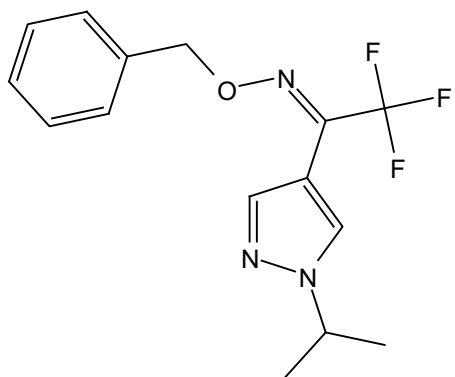
2-6e in d_6 -Acetone



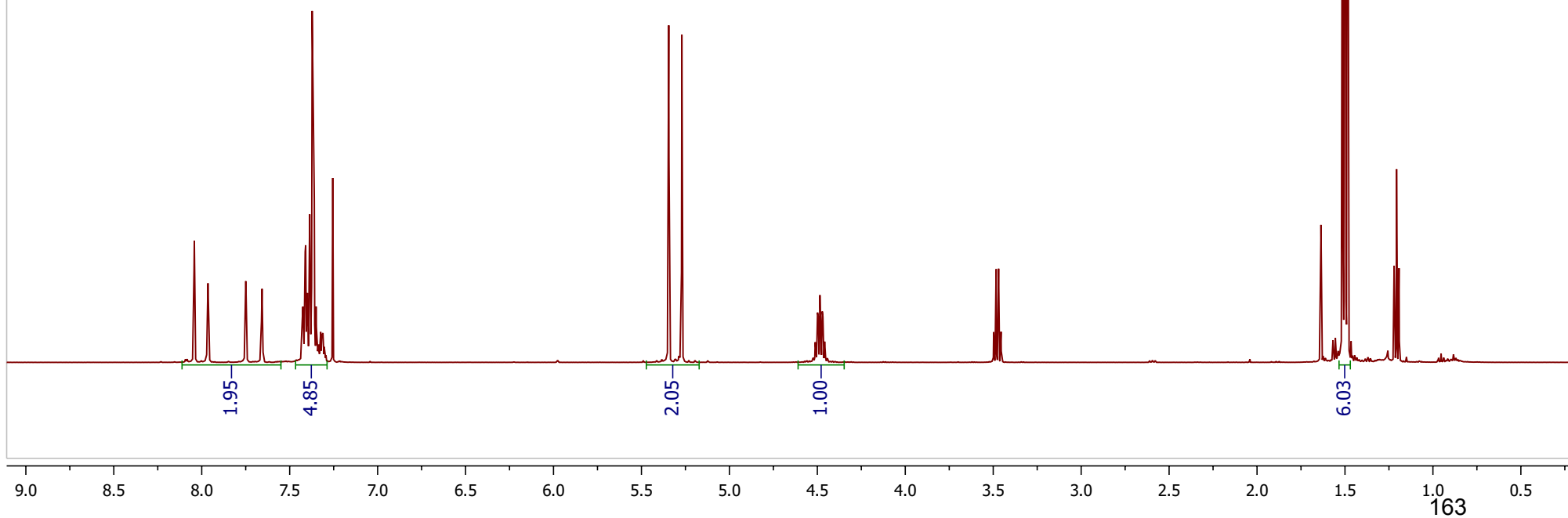


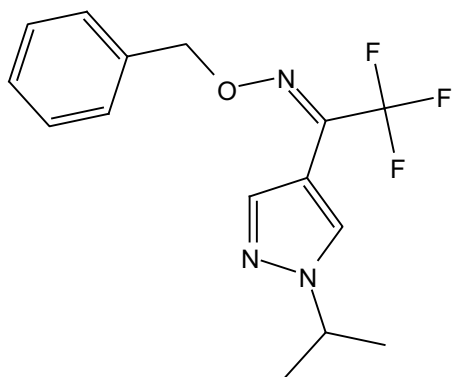
2-6e in d₆-Acetone



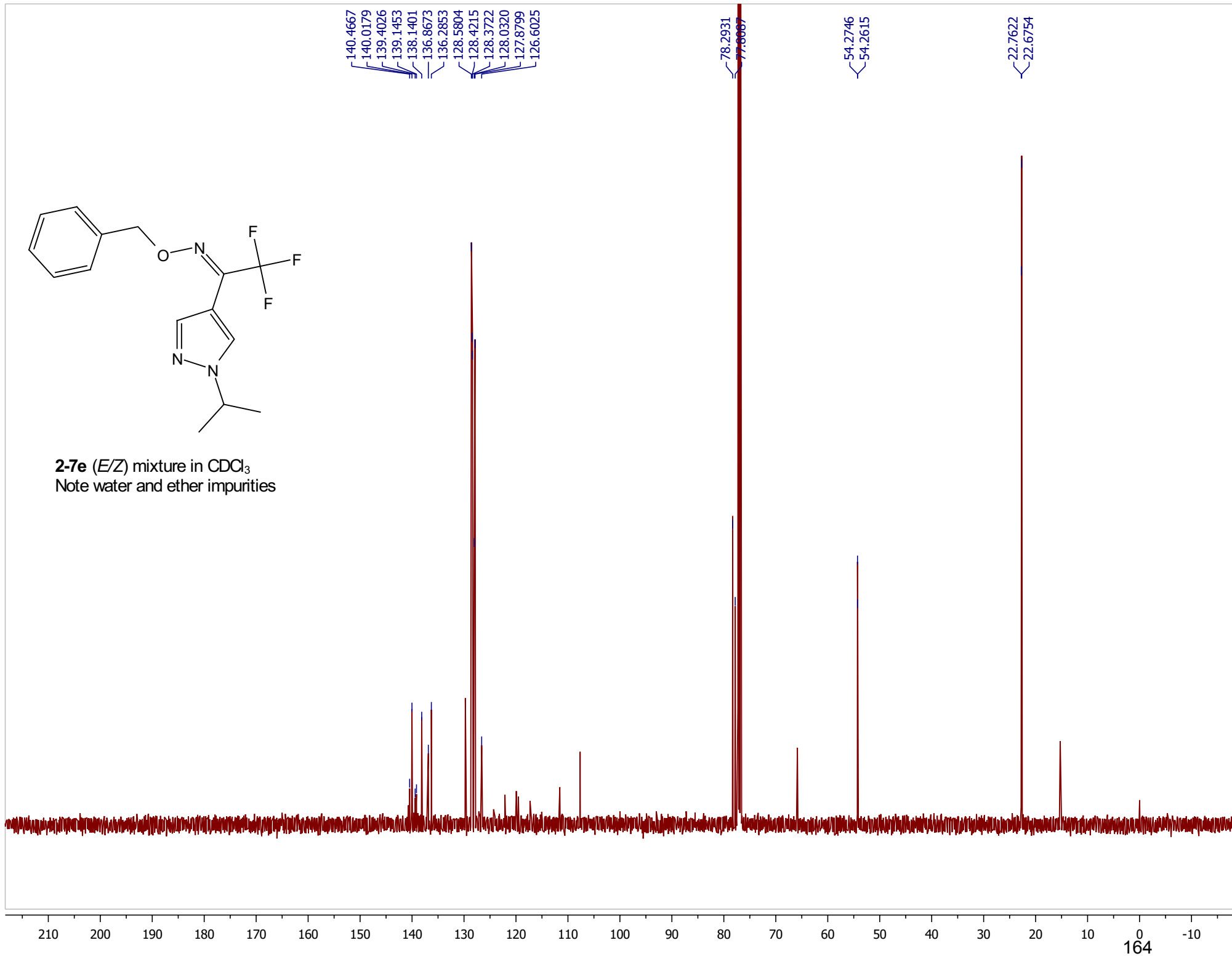


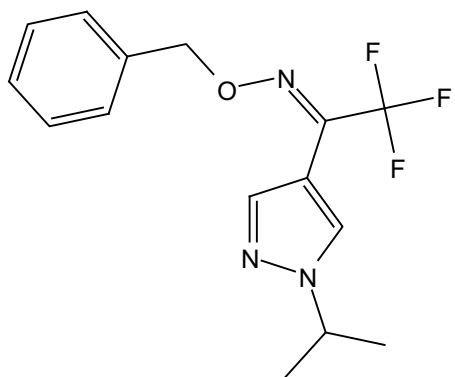
2-7e (*E/Z*) mixture in CDCl₃
Note water and ether impurities





2-7e (*E/Z*) mixture in CDCl₃
Note water and ether impurities



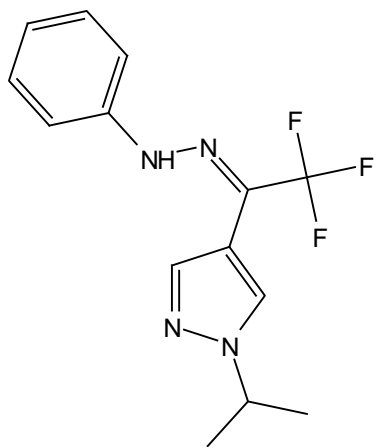


2-7e (*E/Z*) mixture in CDCl₃
Note water and ether impurities

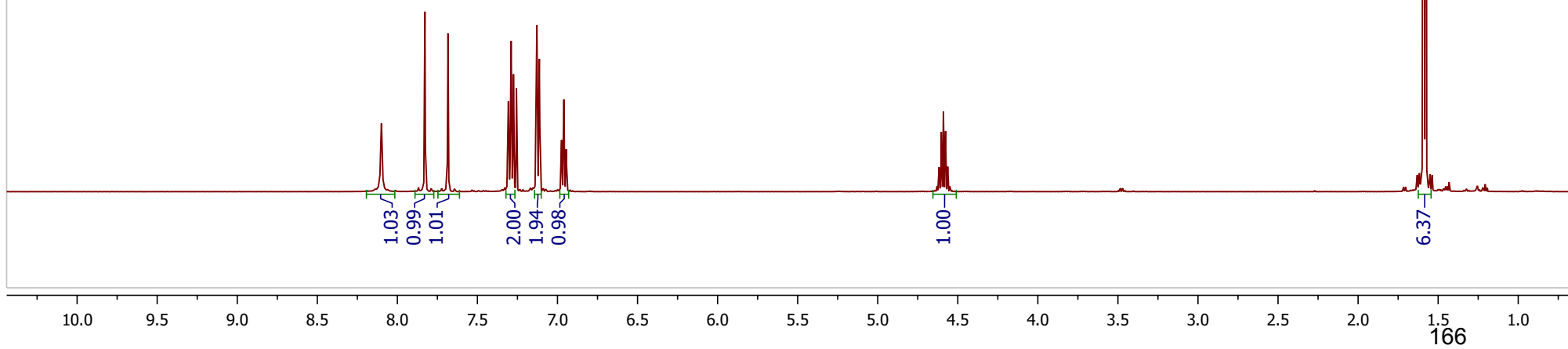
—67.1063
—68.8508

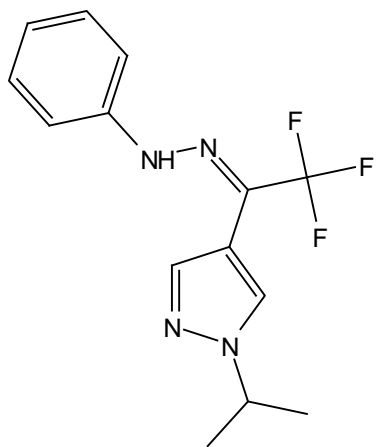
—164.9005

-55 -60 -65 -70 -75 -80 -85 -90 -95 -100 -105 -110 -115 -120 -125 -130 -135 -140 -145 -150 -155 -160 -165 -170 -175 -180 -185

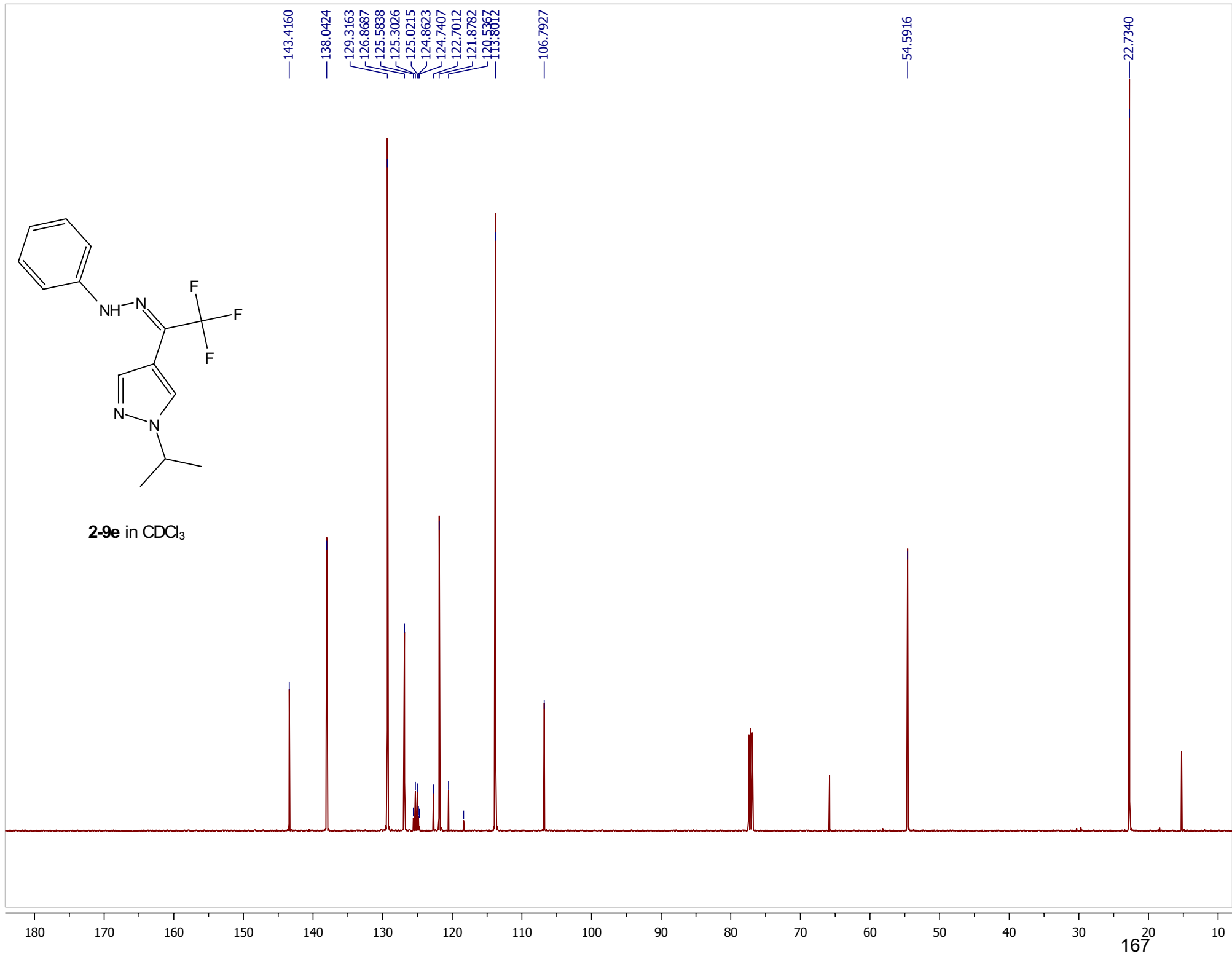


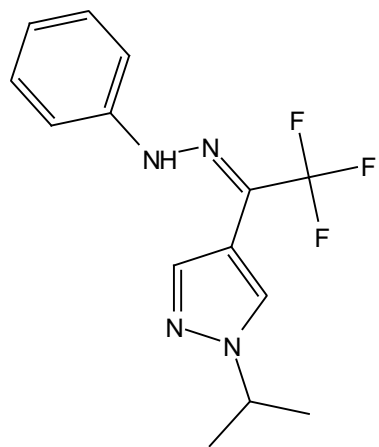
2-9e in CDCl₃





2-9e in CDCl₃

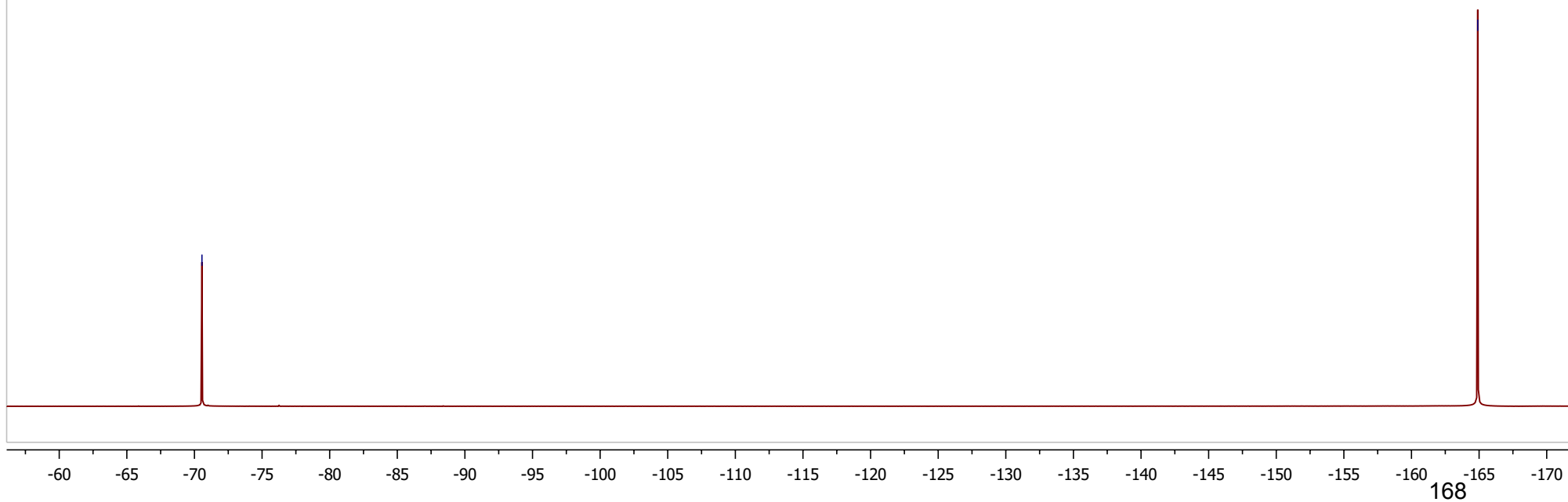


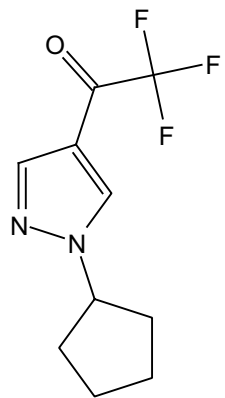


2-9e in CDCl₃

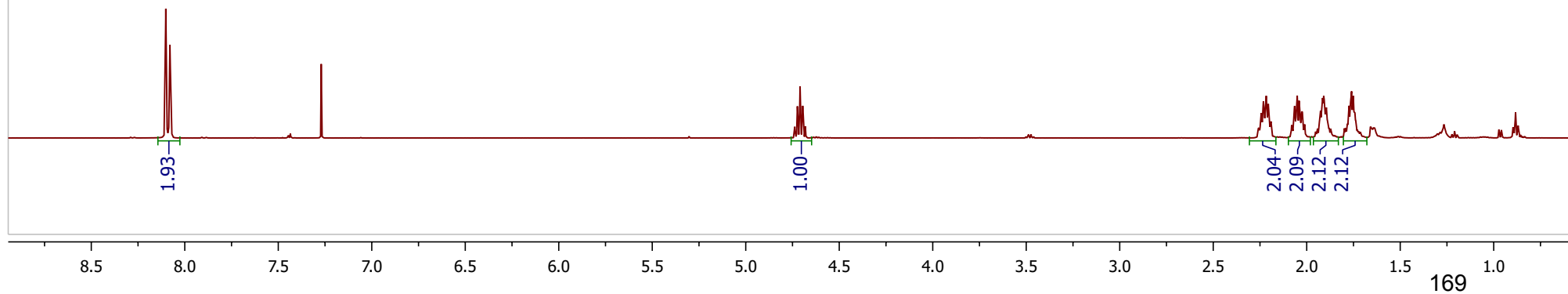
—70.5547

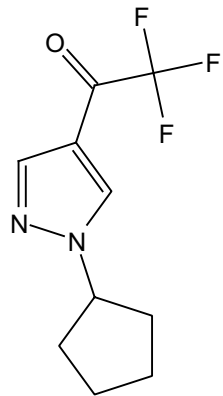
—164.9005



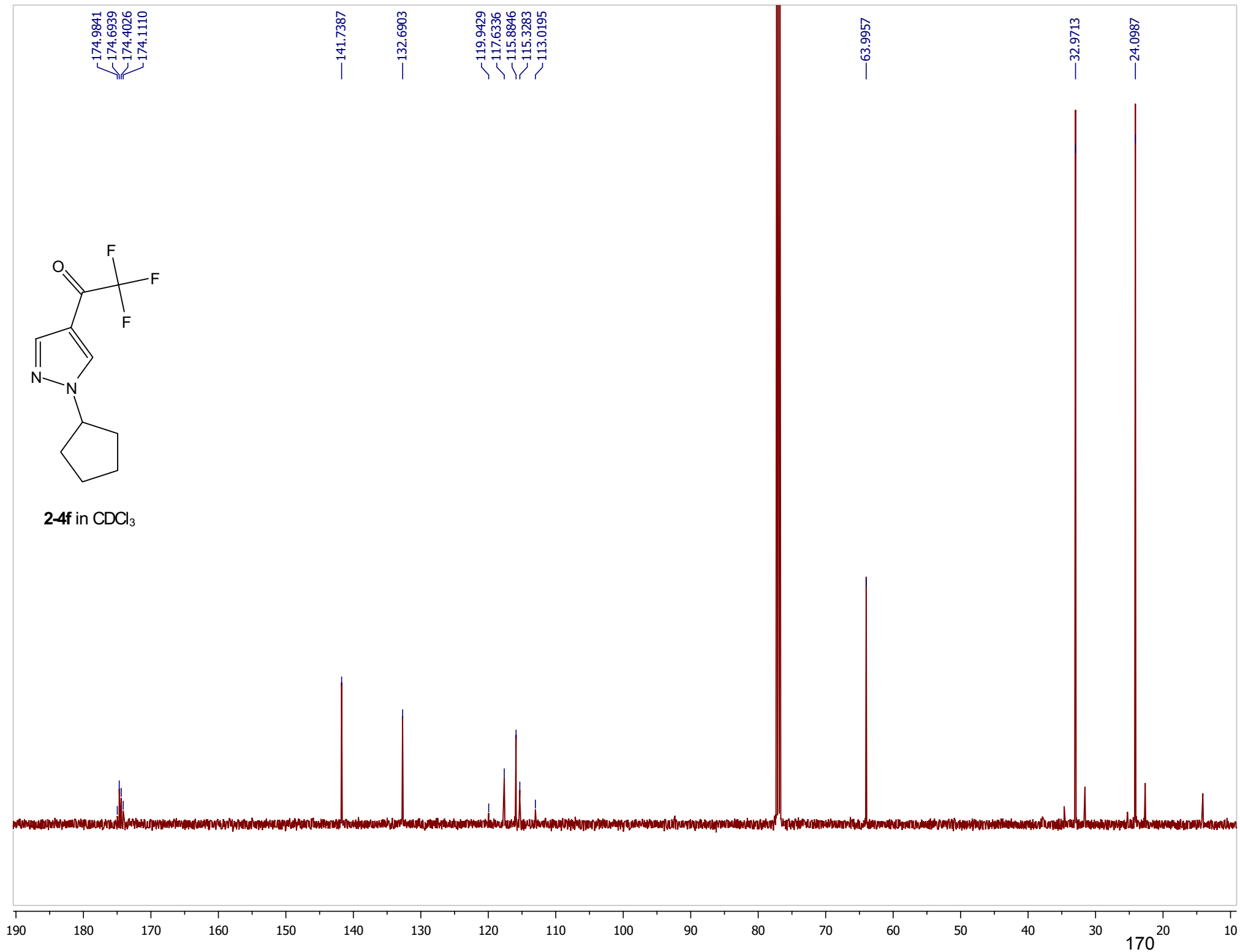


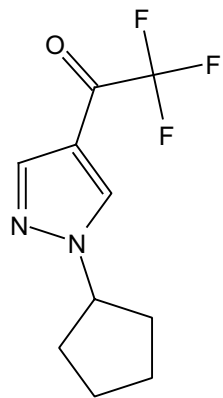
2-4f in CDCl₃





2-4f in CDCl₃





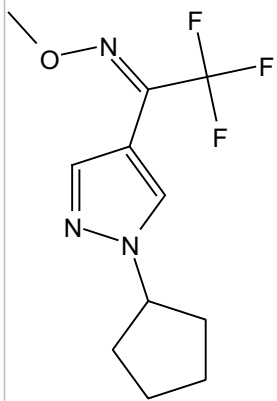
2-4f in CDCl₃

-77.1073

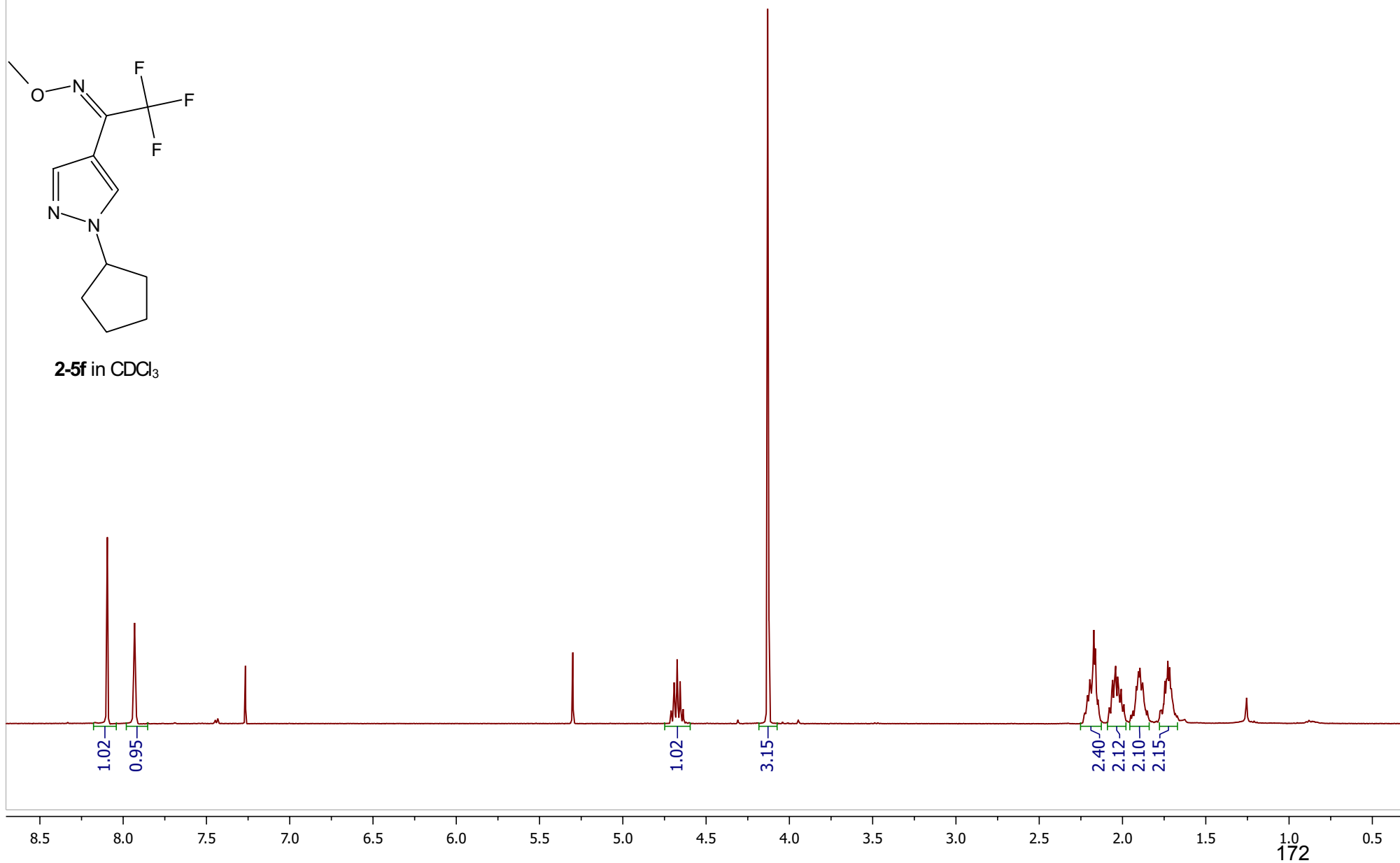
-163.9997

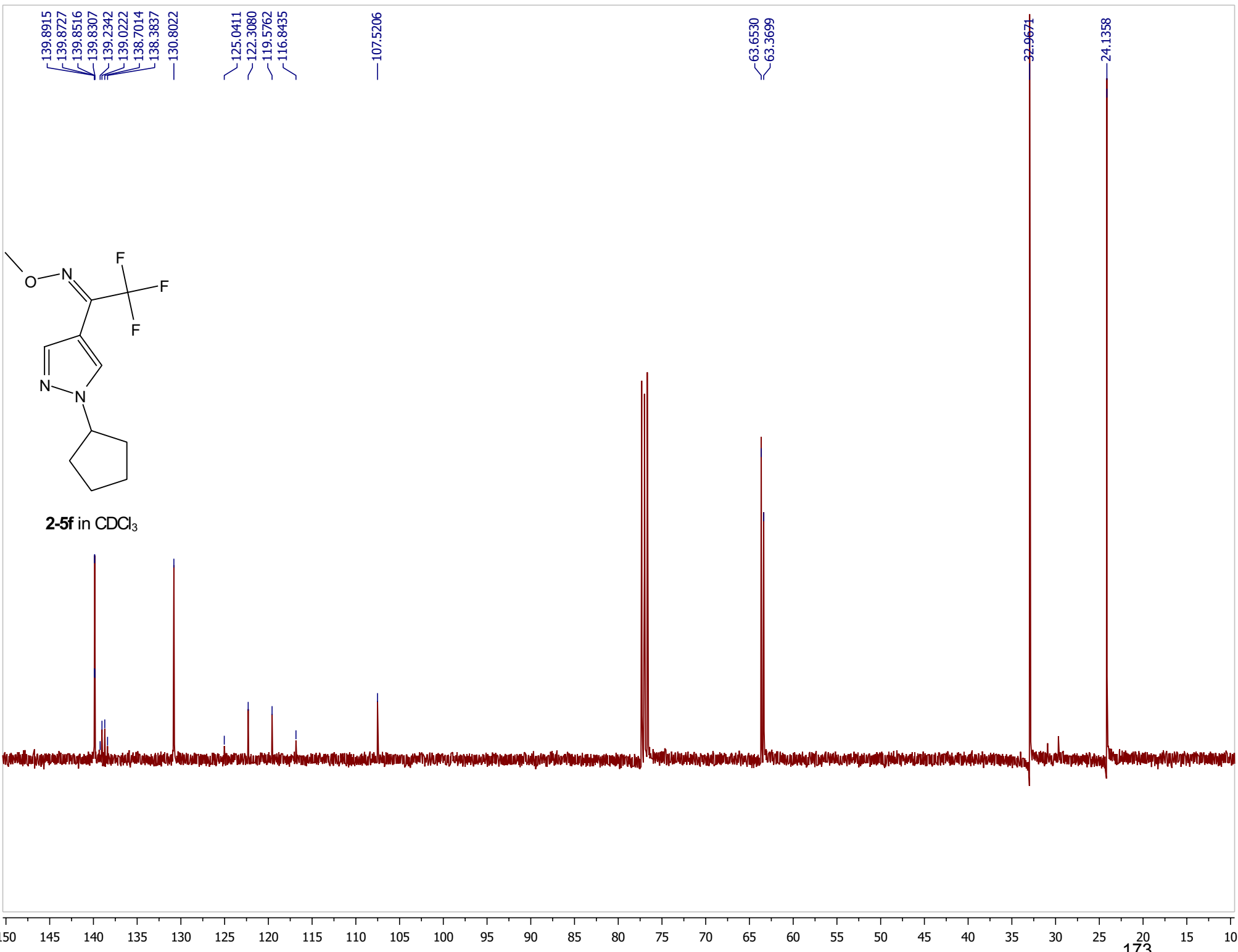


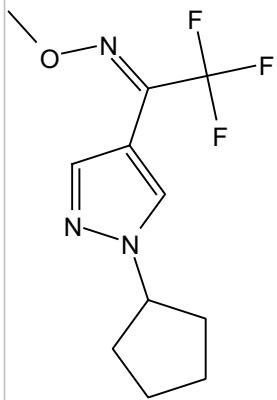
-40 -50 -60 -70 -80 -90 -100 -110 -120 -130 -140 -150 -160 -170 -180 -190 -200 -210 -220 -230



2-5f in CDCl₃







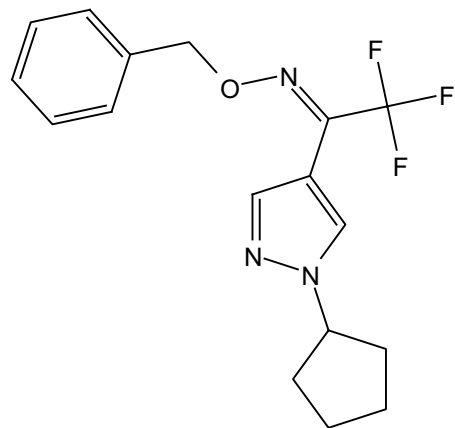
2-5f in CDCl₃

-68.9854

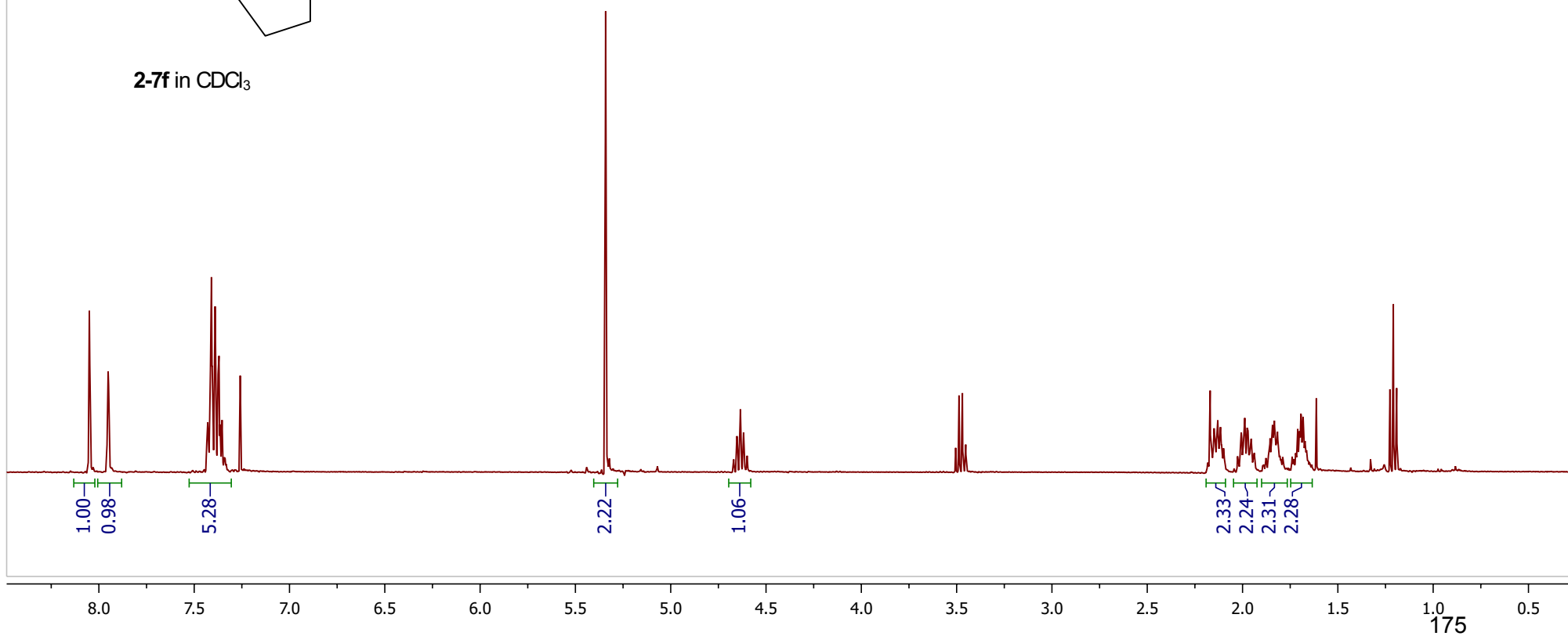
-164.8999

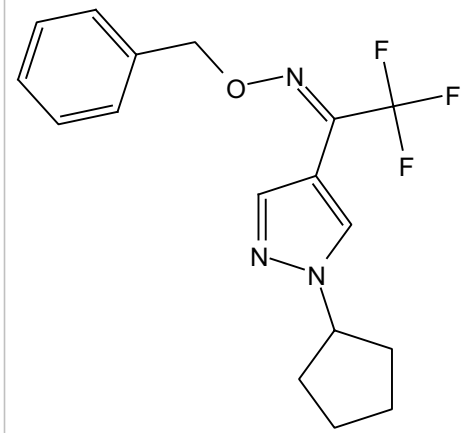
-50 -55 -60 -65 -70 -75 -80 -85 -90 -95 -100 -105 -110 -115 -120 -125 -130 -135 -140 -145 -150 -155 -160 -165 -170 -175

174

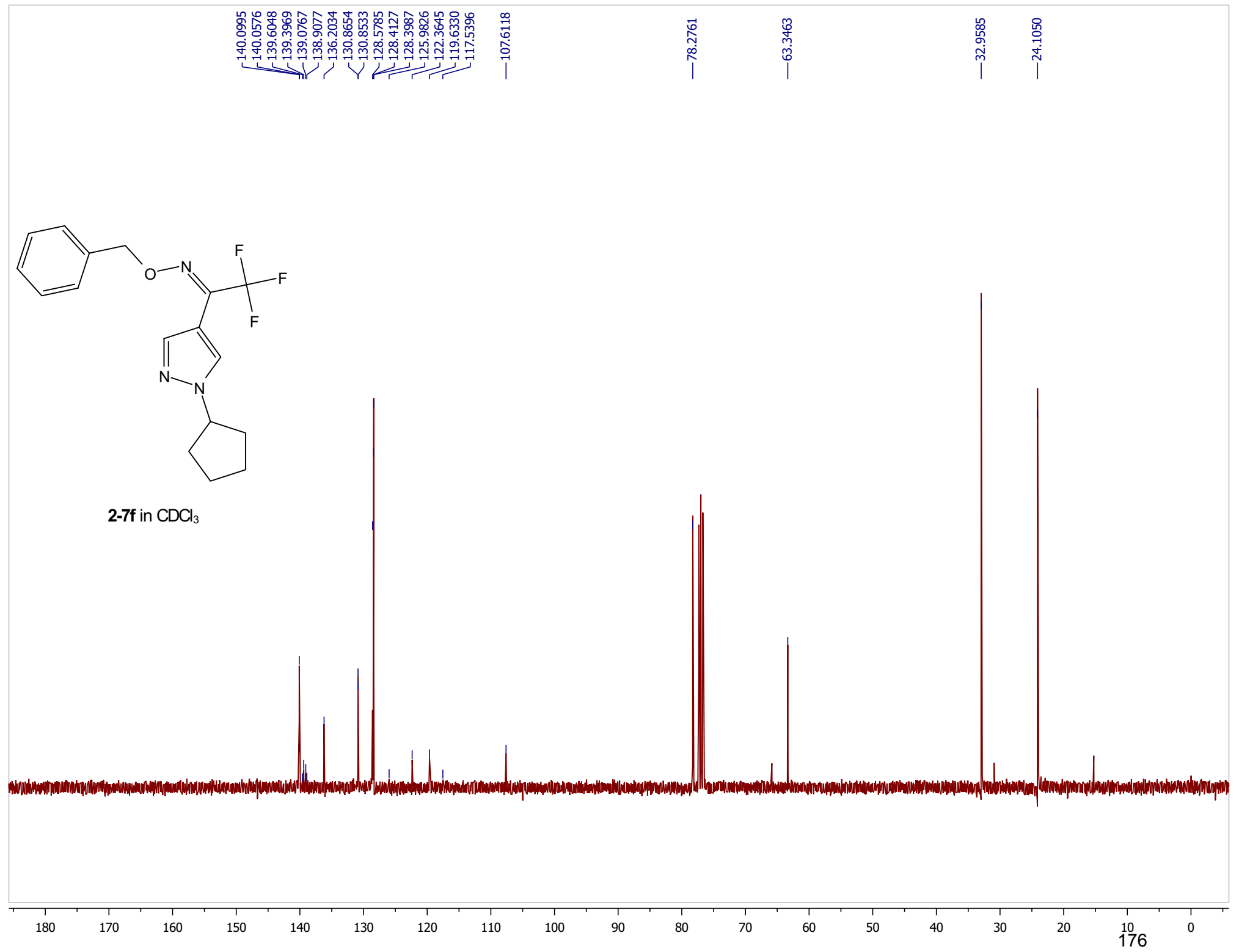


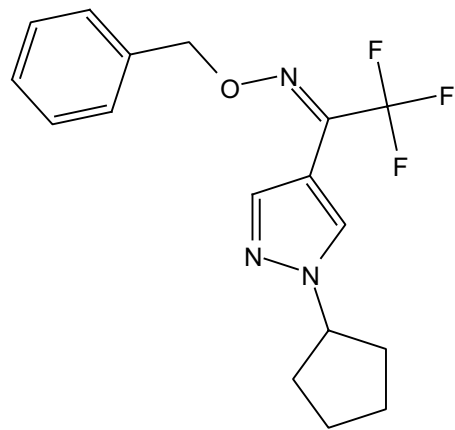
2-7f in CDCl₃



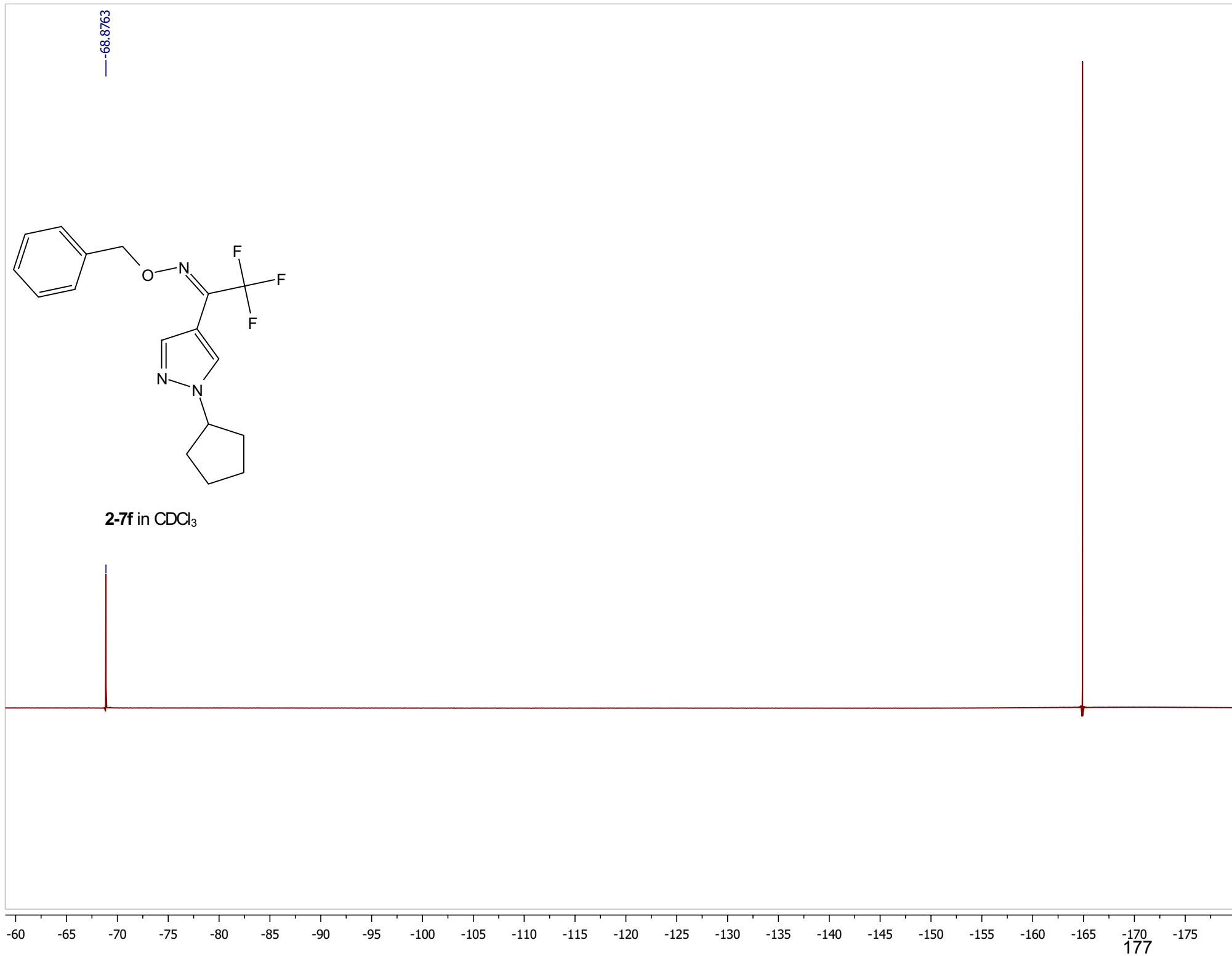


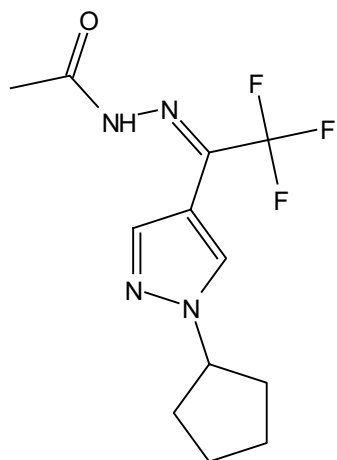
2-7f in CDCl₃



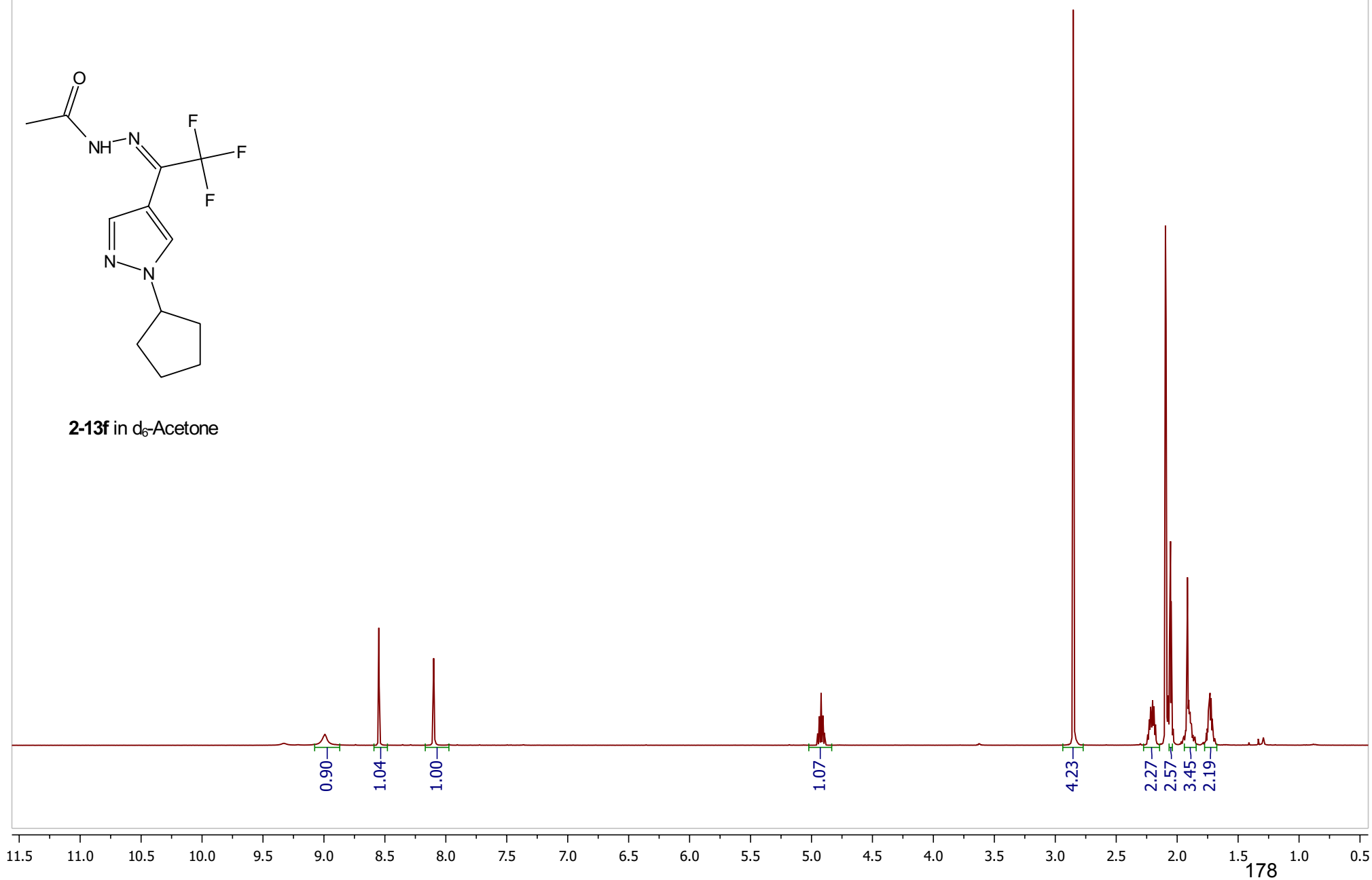


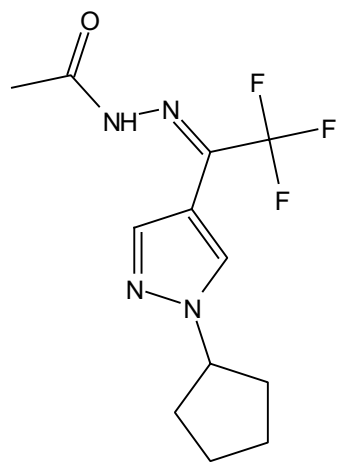
2-7f in CDCl₃



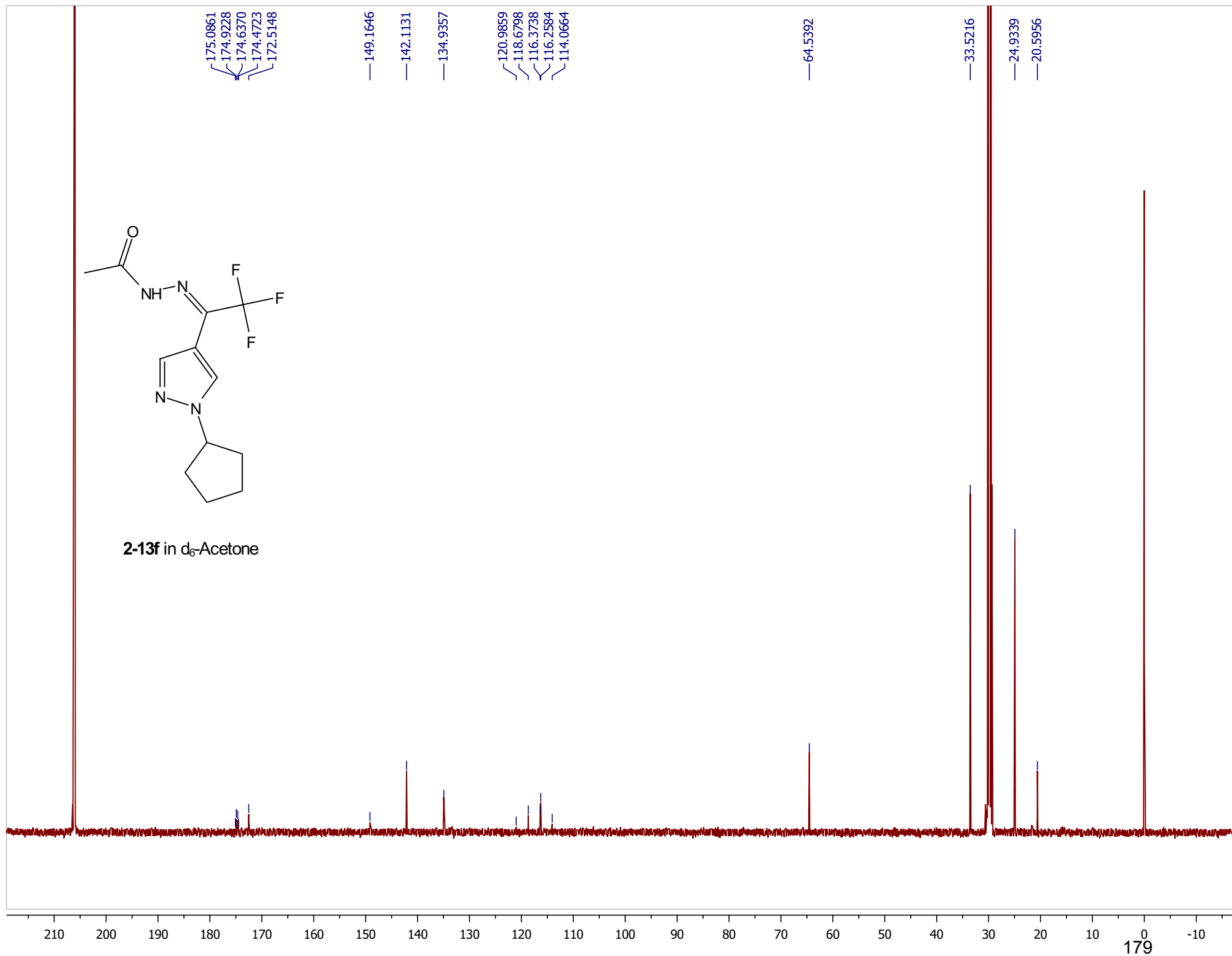


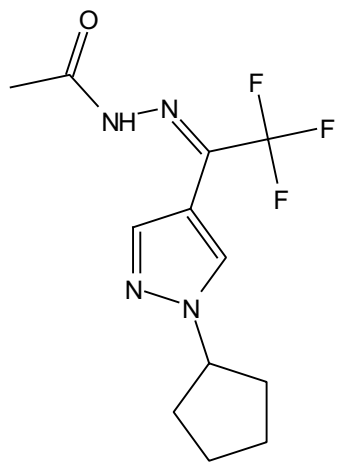
2-13f in d₆-Acetone





2-13f in d₆-Acetone

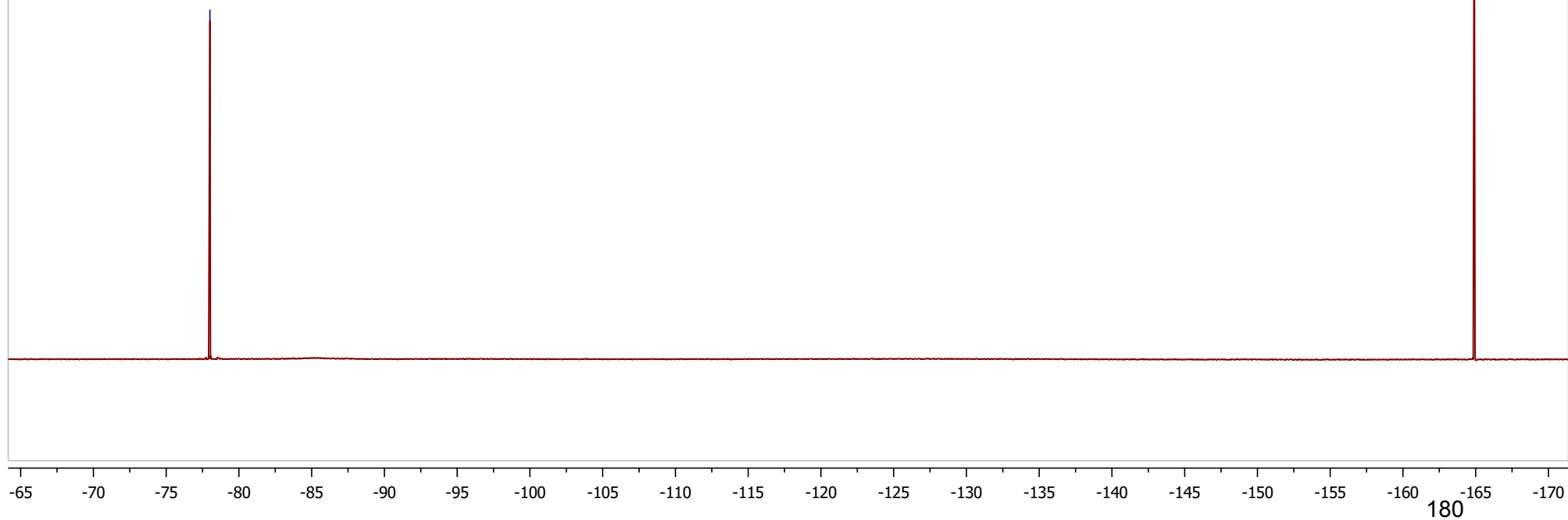


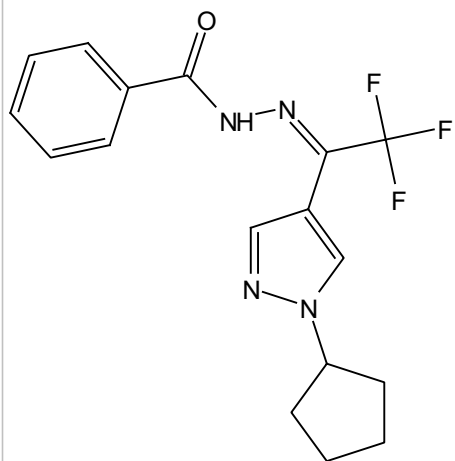


2-13f in d₆-Acetone

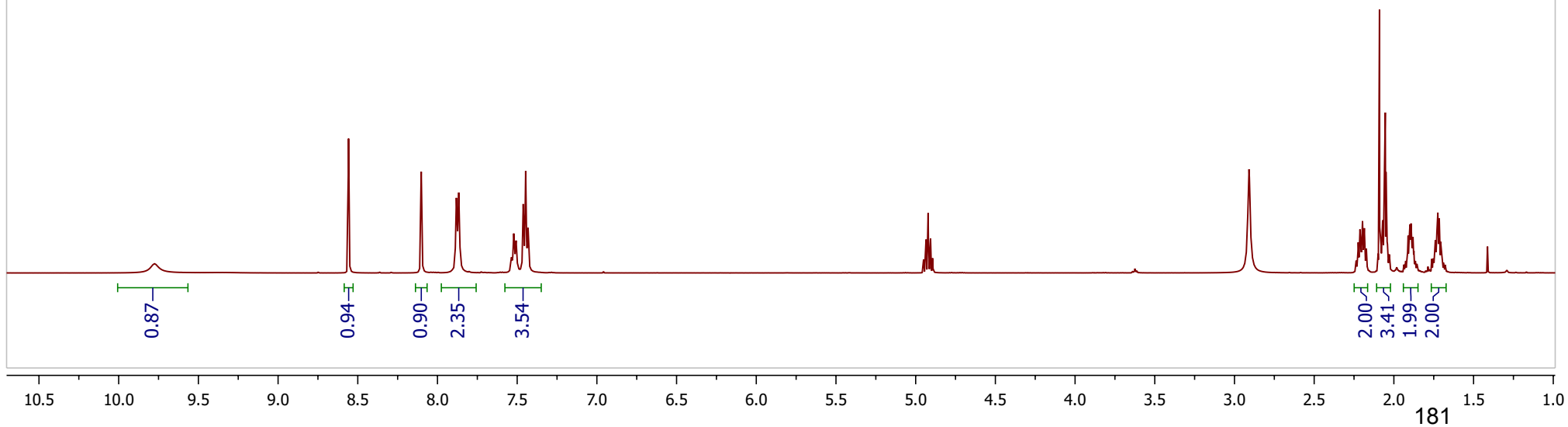
-78.0073

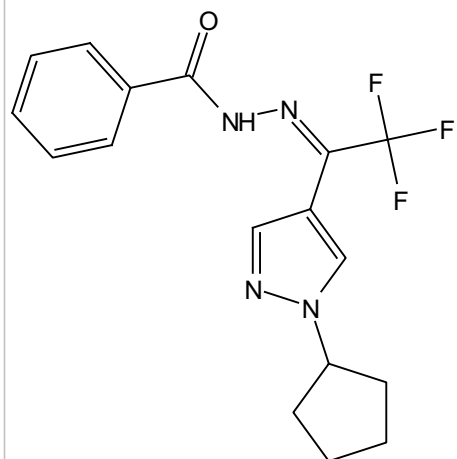
-164.8997



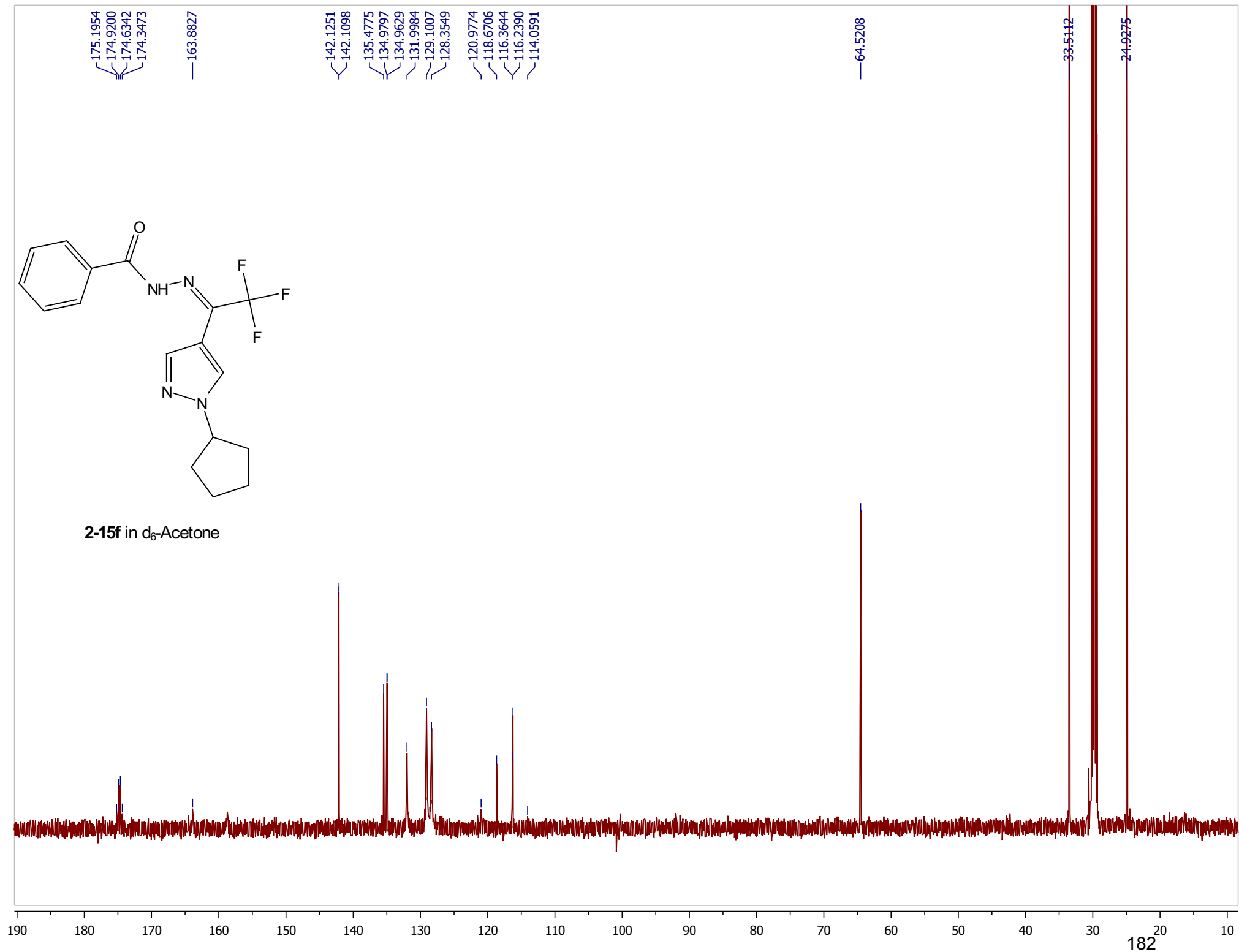


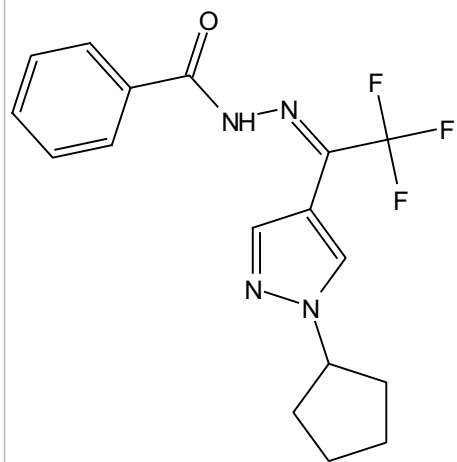
2-15f in d₆-Acetone





2-15f in d₆-Acetone





2-15f in d_6 -Acetone

